Development of Modified Vaccinia Virus Ankara-based Influenza Vaccines

Arwen F. Altenburg

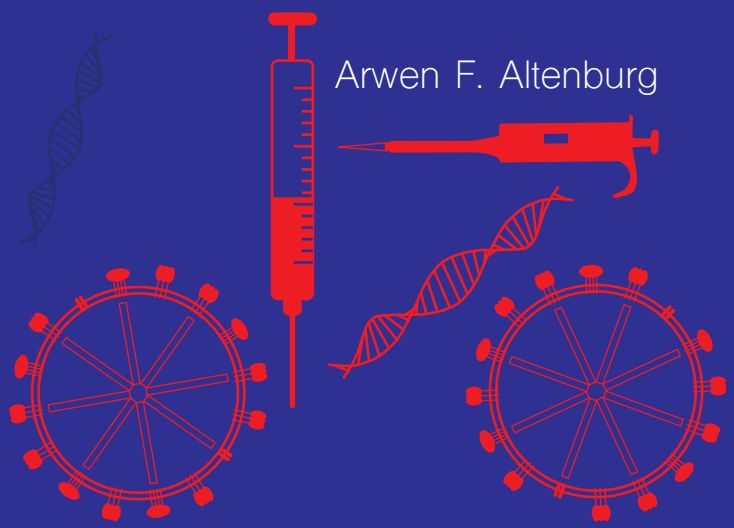

Development of Modified Vaccinia Virus Ankara-based Influenza Vaccines

Arwen F. Altenburg

Colofon
The studies presented in this thesis were financially supported by the European Commission FP7 project FLUNIVAC (602604) and the ERC grant FLUPLAN (250136). The studies were performed within the framework of the Erasmus Molecular Medicine Post Graduate School.

Printing of this thesis was financially supported by Novavax, Aerogen, Cirion Foundation, Eurogentec & Greiner Bio-One.

Cover design: Arwen F. Altenburg & Nynke J. Altenburg
Photograph p187: Nynke J. Altenburg
Print: ProefschriftMaken || www.proefschriftmaken.nl
ISBN: 978-94-6295-796-1

This thesis was printed on FCS paper.

Development of Modified Vaccinia Virus Ankara-based Influenza Vaccines

Ontwikkeling van op Modified Vaccinia virus Ankara-gebaseerde influenzavaccines

Proefschrift

ter verkrijging van de graad van doctor aan de
Erasmus Universiteit Rotterdam
op gezag van de
rector magnificus

Prof.dr. H.A.P. Pols

en volgens besluit van het College voor Promoties.

De openbare verdediging zal plaatsvinden op

woensdag 31 januari 2018 om 11:30 uur

Arwen Fieke Altenburg
geboren te Buren

Erasmus University Rotterdam

Promotiecommissie

Promotor:	Prof.dr. G.F. Rimmelzwaan
Overige leden:	Prof.dr. R.A.M. Fouchier
	Prof.dr. R.W. Hendriks
	Prof.dr. G. Sutter
Co-promotor:	Dr. R.D. de Vries

‘There is a theory which states that if ever anyone discovers exactly what the Universe is for and why it is here, it will instantly disappear and be replaced by something even more bizarre and inexplicable. There is another theory mentioned, which states that this has already happened.’

Douglas Adams
The Hitchhiker’s Guide to the Galaxy

Table of contents

Chapter 1
General introduction

Partially based on:

1. RD de Vries, **AF Altenburg** & GF Rimmelzwaan. Universal influenza vaccines: a realistic option? *Clinical Microbiology and Infection, 2016; 22: S120-S124.*
2. RD de Vries, **AF Altenburg** & GF Rimmelzwaan. Universal influenza vaccines, science fiction or soon reality? *Expert Review Vaccines, 2015; 14(10): 1299-1301.*
3. **AF Altenburg**, GF Rimmelzwaan & RD de Vries. Virus-specific T cells as correlate of (cross-) protective immunity against influenza. *Vaccine, 2015; 33(4): 500-506.*
4. **AF Altenburg** *et al*. Modified Vaccinia virus Ankara (MVA) as production platform for vaccines against influenza and other viral respiratory diseases. *Viruses, 2014; 6(7): 2735-2761.*

1.1 Influenza virus

Influenza viruses are infectious pathogens (~100nm) that belong to the family of *orthomyxoviridae*. This family consists of seven genera, including influenza A and B viruses[1,2]. Influenza viruses are distinguished based on genome size and surface (glyco)proteins[3]. The nomenclature of influenza viruses is based on serotype/host species (if not human)/geographical location of isolation/strain number/year of isolation, e.g. A/Mallard/Netherlands/12/00 or A/Netherlands/602/09. Influenza A viruses are further classified based on the two major surface proteins hemagglutinin (HA) and neuraminidase (NA). Thus far, 18 types of HA (H1-18) and 11 types of NA (N1-11) have been described[4-6]. The subtypes of influenza A virus are based on the types of their HA and NA, for example H1N1 or H3N2. Influenza B viruses are not divided into subtypes but are discriminated into two lineages: B/Yamagata/16/88-like and B/Victoria/2/87-like[4].

Influenza A, endemic in aquatic birds and swine, and B viruses cause seasonal epidemics in the human population[4]. In humans, most infections are self-limiting and restricted to the upper respiratory tract. Complications leading to morbidity and mortality following infection are predominantly observed in high risk groups, such as immunocompromised individuals and the elderly. Therefore, annual vaccination of these risk groups is recommended. It is estimated that influenza virus epidemics annually cause 3-5 million cases of severe respiratory illness worldwide, resulting in 250.000-500.000 fatal cases[7]. Furthermore, if an antigenically distinct influenza virus, often of a novel subtype originating from animal reservoirs, is introduced into the human population, the population at large is at risk due to the lack of strain-specific neutralizing antibodies[4].

Structure of influenza A viruses

An influenza virus particle possesses an envelope derived from the plasma membrane of the infected host cell from which the particle has budded. There are three different virus proteins present on the surface of the virus particle: two major membrane glycoproteins HA and NA, and the Matrix protein 2 ion channel (M2). The envelop encapsulates a layer of Matrix protein 1 (M1) that contains the viral ribonucleoproteins (vRNPs) comprised of eight negative-sense RNA strands[1] (**Fig. 1**). These RNA strands are each folded into a helical hairpin coated with nucleoprotein (NP) and have a polymerase complex comprised of PA, PB1 and PB2 subunits attached to the terminus[8]. In addition to the proteins that are essential for the structure of the virus particle, the viral RNA genome encodes non-structural proteins such as nuclear export protein (NEP) and non-structural protein 2 (NS2)[1].

Influenza A viruses increase the coding capacity of the eight RNA segments by the use of alternative open reading frames and splicing. For example, M1 and M2 proteins are derived from the same RNA segment and the PB1 gene segment is known to encode several non-structural proteins in addition to the PB1 polymerase subunit. These PB1-F2 and PB1-N40 proteins are involved in immune evasion and induction of apoptosis in the infected cell, thereby allowing for more efficient virus replication[1,9,10].

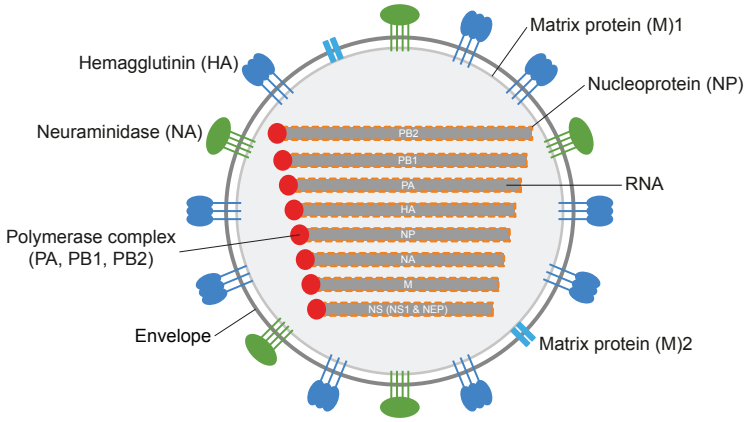

Figure 1. Schematic overview of the structure and gene segments of an influenza A virus*. There are two surface glycoproteins present in the lipid bilayer of a virion: HA and NA. The third surface protein is M2. Below the lipid bilayer resides a capsid of M1, which contains eight negative-sense RNA strands encoding the indicated influenza virus proteins. The RNA is coated by NP with the polymerase complex consisting of PA, PB1 and PB2 subunits at the terminus.*

Replication cycle

Influenza viruses infect cells through attachment of the receptor binding site in the head-domain of the viral HA protein to sialic acids on the host's cell surface. HA from human influenza viruses preferentially binds to sialic acid attached to galactose by an α2,6 linkage, which is predominantly present on cells in the upper respiratory tract. In contrast, avian influenza viruses mostly bind α2,3 sialic acids that are mainly present in the human lower respiratory tract. The receptor binding preference partially explains why some avian influenza viruses can cause severe lung disease in humans but are not efficiently transmitted between individuals without adaptive mutations[11,12].

After attachment, the influenza virus particle is internalized through receptor-mediated endocytosis. The low pH in the endosome induces conformational changes in HA, thereby exposing the fusion peptide required for interaction with the endosomal membrane. The M2 ion channel allows for influx of H^+ molecules into the virus particle, leading to disruption of protein interactions between M1 and the vRNP[1,13]. Combined, these mechanisms result in the release of the viral genome into the cytoplasm of the cell. The nuclear localization signal (NLS) in NP leads to translocation of the vRNP from the cytoplasm to the nucleus where the polymerase complex attached to each RNA strand starts transcription of the negative-sense RNA genome into positive-sense RNA[1]. New genomic RNA is synthesised in the nucleus using positive-sense complementary (c)RNA as a template. Furthermore, positive-sense messenger (m)RNA is transported to the cytoplasm for translation of new viral proteins (**Fig. 2**).

Before the viral mRNA can be exported from the nucleus, the RNA needs to be stabilized by addition of a 5' cap and a 3' poly-A-tail to the transcripts. The 5' cap on viral transcripts is obtained from host RNA transcripts through 'cap-snatching' by the

polymerase subunits[14,15], thereby efficiently inhibiting translation of host transcripts. The 3' poly-A-tail is automatically included in the transcript through a conserved U-stretch in the viral template RNA[15,16]. With these modifications, viral mRNA can be transported to the cytoplasm where the 5' cap allows for recognition of viral mRNA by the host's translational machinery.

After translation, the transmembrane proteins HA, NA and M2 are transported through the Golgi system to the plasma membrane. Newly synthesised NP, PA, PB1 and PB2 molecules return to the nucleus where new vRNP complexes are assembled. Nuclear export of vRNP is mediated by M1, most likely in combination with NEP/NS2, after which the vRNP complex translocates to the plasma membrane for assembly into new virus particles. The plasma membrane forms an outward curvature until the virus core is completely enveloped by the lipid bilayer. Membrane fusion is initiated and the progeny virus particle is formed. Newly formed virus particles remain attached to the infected cell surface through the interaction of sialic acid with HA. Enzymatic activity of NA is required for the destruction of sialic acid and the release of progeny virions from the cell, allowing further spread of the virus infection[1] (**Fig. 2**).

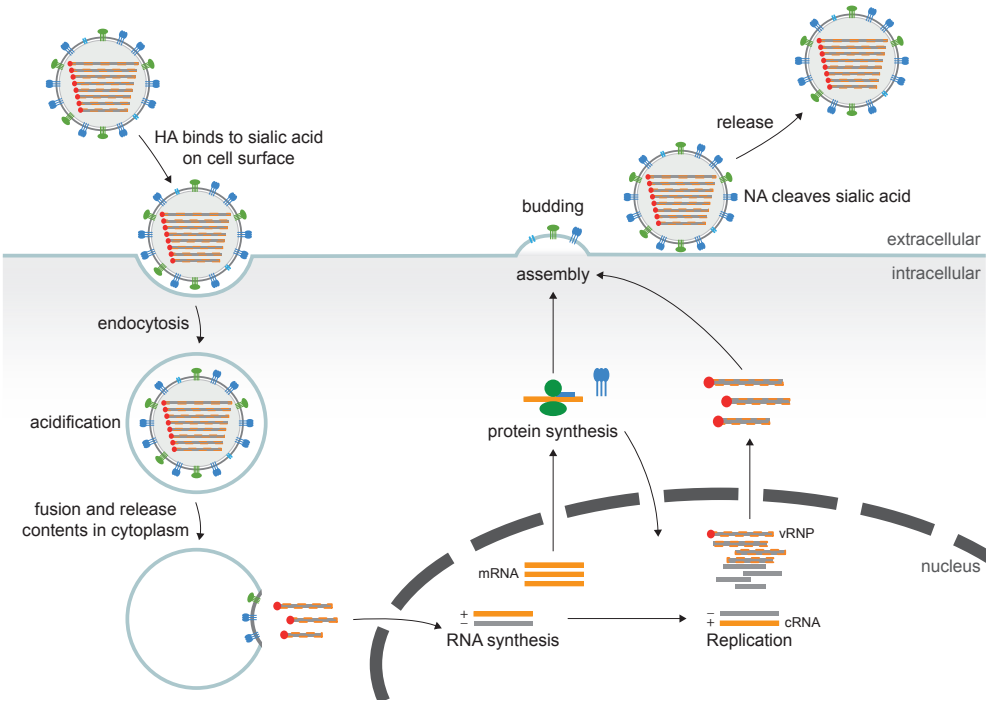

Figure 2. Influenza virus replication cycle. *HA binds to sialic acid on the host's cell surface, thereby initializing internalization of the virus particle. Due to the low pH in the endosome, conformational changes in HA are induced leading to the fusion of the viral and endosomal membranes. vRNP is released into the cytoplasm and translocated to the nucleus. Genomic, negative-sense RNA is translated into mRNA – for the synthesis of virus proteins – and cRNA, which serves as a template for the production of new genomic RNA. Viral proteins and vRNP assemble at the plasma membrane where a new virion buds from the cell. NA releases progeny virus particles from the cell through cleavage of sialic acids on the host cell surface.*

Seasonal and pandemic influenza

Influenza viruses are able to perpetuate in the human population through evasion of recognition by virus neutralizing antibodies due to the continuous accumulation of mutations in the surface glycoproteins HA and NA, *i.e.* antigenic drift[4,17,18]. This results in seasonal influenza epidemics that are caused by influenza A(H1N1), A(H3N2) or B viruses.

In addition to infections caused by antigenic drift variants, antigenically distinct influenza viruses originating from animal reservoirs are occasionally introduced into the human population. This antigenic shift can occur in animal reservoirs through re-assortment of gene segments derived from two or more different influenza viruses, often resulting in a virus with new subtypes of HA and NA proteins. These novel influenza viruses have the potential to cause serious pandemics when they acquire the ability to be transmitted efficiently from human-to-human because antibodies against these viruses are virtually absent in the population at large. The last four pandemics have been caused by influenza A viruses of the H1N1 (1918 and 2009), H2N2 (1957) and H3N2 (1968) subtypes.

During the last decades, zoonotic transmission of highly pathogenic avian influenza A viruses, in particular those of the A(H5N1) subtype, has been reported regularly. In order to monitor viral adaptations to acquire the ability to efficiently spread between individuals, transmission experiments have been performed in ferrets. Since distribution of sialic acids with an α2,6 and α2,3 linkage in the ferret respiratory tract is similar to the human respiratory tract, influenza virus pathogenesis and transmission is expected to be similar in ferrets and humans. Therefore, this animal model is the best proxy to gain insight in viral adaptations required for human-to-human transmission. Interestingly, it has been demonstrated that only a few mutations in HA and proteins of the polymerase complex were sufficient for A(H5N1) viruses to become airborne transmissible between ferrets[19-21], and some of these mutations have already been detected in naturally circulating A(H5N1) viruses[22]. Human infections with avian viruses from other subtypes have been reported as well, including infections with viruses of the A(H5N6)[23], A(H6N1)[24], A(H7N3)[25], A(H7N7)[26], A(H7N9)[27], A(H9N2)[28] and A(H10N8)[29] subtypes. With the correct adaptations, any one of these viruses could potentially become transmissible from human-to-human and cause a widespread outbreak and eventual pandemic with considerable morbidity and mortality.

1.2 Immune response against influenza viruses

To study the immune response against influenza viruses different animal models are used, including mice, ferrets and non-human primates. The mouse model is the most attractive, because specific-pathogen free mice are readily available, mice are easily housed in groups at relatively low cost and genetically modified mouse models are available. Furthermore, the immune response can be studied in detail due to a complete understanding of the mouse immune system in combination with an extensive, well characterized set of mouse-specific reagents. However, influenza viruses sometimes require adaptation to cause substantial disease in mice. Furthermore, the pathogenesis in and transmission between mice is different compared to humans. Therefore, the ferret model is favoured for these studies as they accurately reflect human disease and are usually susceptible to human influenza viruses. Disadvantages of the ferret model include the costs, the size of the animal, which requires larger housing, and the lack of available species-specific reagents. The latter particularly complicates assessment of the immune response against influenza viruses. Non-human primates are also susceptible to most human influenza viruses and in contrast to ferrets, there is an extensive toolset available for studies on the immune system in this species. However, this animal model is more expensive than the ferret model and ethical issues complicate the use of non-human primates[30]. Taken together, the mouse model is considered an appropriate model for preliminary assessment of intervention strategies and fundamental research of the immune response against influenza viruses.

Innate immune response

The innate immune system is hallmarked by a rapid response (within hours) upon an infection. This response is aspecific, *i.e.* responds similar to a primary or re-infection with the same pathogen, and involves chemical as well as cellular components.

An influenza virus infection is first detected by pattern recognition receptors (PRRs). These molecules are expressed on most cells, including non-hematopoietic cells, and are sensors activated by evolutionary conserved pathogen associated molecular patterns (PAMPs). There are different families of PRRs capable of specifically detecting an intracellular or extracellular pathogen. First, extracellular virions can be detected by Toll-like receptors (TLRs) and C-type lectin receptors (CLRs), which recognize viral nucleic acids and leucine-rich repeats on transmembrane proteins. In addition, TLRs present in the endolysosome can be activated by single- or double-stranded RNA present in cell debris from influenza virus-infected cells or single-stranded genomic viral RNA in phagocytosed and degraded virions. Second, once an infection has been established, intrinsic cellular PRRs such as retinoic acid-inducible gene I (RIG-I)-like receptors and nucleotide oligomerization domain (NOD)-like receptors detect nucleic acid structures in the cytosol of infected cells. Furthermore, specific intracellular viral protein structures and stress signals, including signals from neighbouring dying cells, can activate intrinsic PRRs. Recognition of an influenza virus infection by PRRs induces a series of events generally starting with the production of type I interferons (IFN) and other anti-viral cytokines and chemokines. These signalling molecules are involved in the induction of an antiviral state in cells

in the vicinity of the infection, activation of the complement system, recruitment and/or activation of innate immune cells and regulation of induction of the adaptive immune response[31-33].

The innate immune response is multifaceted and comprises many components that are often interlaced. The complement system consists of soluble proteins that are activated in a cascade-like manner. Studies in mice have shown that complement factors may play an important role in early control of an influenza virus infection before the adaptive immune system has responded[34,35]. Complement factors can directly bind to virions thereby inducing phagocytosis (opsonisation) or virolysis. Furthermore, complement factors can initiate lysis of influenza virus-infected cells and act as signalling molecules by binding to specific complement receptors on leukocytes[31,36]. Natural killer (NK) cells are another important first line of defence against influenza virus infections. Activation of NK cells requires signalling from the activation receptors after they have bound their ligand on virally infected cells, in combination with downregulation of inhibitory receptor ligands. Many viruses have developed mechanisms interfering with the major histocompatibility complex (MHC) class I pathway, leading to reduced inhibitory signalling in NK cells. Activated NK cells have cytolytic capacities and produce cytokines to induce other anti-viral immune responses[31,32,37].

Other innate immune cells involved in the influenza virus-specific innate immune response include monocytes, present in the blood stream and peripheral tissues, which are the precursor of macrophages and dendritic cells (DCs). Macrophages are professional phagocytes that can engulf and degrade influenza virions, and patrol most organs and barriers, including mucosal tissues. Specialized macrophages present in the alveoli of the lung (alveolar macrophages) can become infected with influenza viruses and subsequently produce high levels of type I IFNs to prevent infection of other, perhaps more vulnerable, cells[32]. In addition, immature DCs are also present in all barriers throughout the body. DCs are characterized as professional antigen presenting cells (APC) that orchestrate both innate and adaptive immune responses. Immature DCs possess a specific set of PRRs to recognize an incoming pathogen and can be can be activated by direct influenza virus infection, uptake of a virus or soluble antigen (most likely to be remnants of apoptotic infected cells) or by signalling molecules. Mature DCs can travel to secondary lymphoid tissues, such as lymph nodes (LN), for activation of adaptive immune cells. DCs are key players in deciding between an anti-bacterial (extracellular) and anti-viral (intracellular) immune response through the secretion of a variety of inflammatory cytokines[31,32,38].

Influenza viruses have developed the capacity to evade different components of the innate immune system. For example, M1 was shown to interact with complement protein C1qA, thereby inhibiting virus neutralization[39]. Furthermore, influenza virus non-structural proteins can act as IFN antagonist and the PB1-F2 protein has pro-apoptotic properties and is thought to induce apoptosis of immune cells specifically[1,9]. These properties contribute to suppression of the innate response and are critical for influenza virus while establishing a productive infection.

Adaptive immune response

Hallmarks of the adaptive immune response are its specificity and formation of immunological memory. This response is slow compared to the innate immune response and may take days to develop upon the first encounter with a pathogen. After the first exposure, immunological memory is formed which allows a rapid and pathogen-specific response upon the second encounter. The adaptive immune response can be divided into two main components: humoral and cellular immunity.

Humoral immunity

Naïve B cells circulate in the blood and reside in secondary lymphoid organs, such as the LN and the spleen. Given the short half-life, between 3 days and 8 weeks, only a small number of B cells produced in the bone marrow transitions to a mature state. B cell maturation takes place in the LN and requires specific recognition of an antigen – a virion or viral antigen carried by APCs – by the B cell receptor (BCR). The BCR-antigen complex is internalized into endosomes where the antigen is degraded for presentation on MHC class II molecules to $CD4^+$ T cells. Co-stimulation by $CD4^+$ T cells is required for subsequent B cell proliferation and differentiation. During the maturation process, binding to the antigen is optimized (affinity maturation) and immunoglobulin (Ig) isotype class switching takes place from IgM to predominantly IgG or IgA. Subsequently, mature B cells proliferate and differentiate into plasma cells, which produce soluble Ig (*i.e.* antibodies), or memory B cells[40].

Antibodies are capable of recognizing structures on the surface of a virus particle or transmembrane proteins on a virus-infected cell and have several effector functions, partially dependent on epitope specificity. First, antibodies can have influenza virus neutralizing capacities, achieved by blocking the receptor-binding pocket on HA or by preventing conformational changes necessary for endosomal membrane fusion and uncoating[38]. Second, the fragment crystallisable (Fc) tail of antibodies bound to influenza virus particles or influenza virus-infected cells can induce complement activation leading to direct virolysis, inhibition of virus attachment to the host cell, induction of phagocytosis (antibody-dependent phagocytosis, ADP)[41], complement-dependent cytotoxicity (CDC)[42] or antibody-dependent cellular cytotoxicity (ADCC)[43-45]. Finally, antibodies can prevent the release of progeny virions from an infected cell by inhibition of NA activity[46]. Since neutralizing antibodies can directly interfere with the initial infection of a host, whereas non-neutralizing antibodies mainly interfere after establishment of infection, neutralizing antibodies are considered to be more effective[38].

Influenza virus-specific serum antibodies can initially be detected 7-12 days after a primary infection, but memory B cells remain and can be maintained for decades. These cells reside in the spleen and other secondary lymphoid tissues in a resting state, not secreting antibodies. Re-exposure to viral antigens induces rapid proliferation and differentiation of the memory B cells into plasma cells. This leads to production of higher antibody concentrations compared to the primary infection to rapidly clear the infection[38,40].

The influenza virus-specific antibody response is mainly directed against the two surface glycoproteins HA and NA, which corresponds well with protection from infection with homologous influenza virus strains[47]. Influenza viruses are capable of efficiently evading the humoral response by accumulating antigenic changes in the surface proteins, leading to evasion of HA- and NA-specific antibodies[17,18,48]. Furthermore, glycosylation of HA is thought to modulate the immunogenicity of certain epitopes[49-51]. It has even been suggested that the stalk-domain of HA from an A(H7N9) influenza virus can inhibit formation of antibodies against the HA head-domain[52]. Thus, virus-specific antibodies have the capacity to efficiently neutralize an influenza virus infection, but in general do not provide protection against the wide range of influenza virus subtypes.

Cellular immunity

In addition to humoral immunity, infection with (seasonal) influenza virus also induces T cell responses[53-57]. T cells are activated during an infection by recognition of MHC – human leukocyte antigens (HLA) in humans – class I or II molecules presenting virus peptides generally obtained from different origins. Viral peptides presented on MHC class I molecules are released from proteins though proteasomal degradation in the cytosol of infected cells. These peptides are transported into the endoplasmatic reticulum (ER) by the protein 'transporter associated with antigen processing' (TAP) where the peptides are loaded onto MHC class I molecules. Subsequently, the MHC-peptide complex is transported to the cell surface for presentation to $CD8^+$ T cells[58]. MHC class I molecules are present on virtually all nucleated cells. In contrast, MHC class II is only present on professional APC such as DCs. APCs engulf antigens, such as influenza virus-infected apoptotic cells, from their environment into endosomes that subsequently fuse with lysosomes where the contents are degraded. MHC class II molecules are transported to the endolysosomes, allowing peptides to be loaded on the MHC class II molecules. Subsequently, these complexes are transported to the cell surface for presentation to $CD4^+$ T cells[59] (**Fig. 3**). Of note, antigens of extracellular origin can also be presented on MHC class I molecules by DCs, a process defined as cross-presentation[60,61].

Since influenza viruses infect epithelial cells of the respiratory tract, sentinel lung-resident $CD103^+$ DC present in the immediate proximity of respiratory epithelial cells are in a unique position to capture antigens from virus-infected cells, mature and migrate to LN, and exert their function as professional APC by activating naïve T cells[62-64]. After the T cell receptor (TCR) recognizes a MHC-peptide complex, there is clonal expansion of virus-specific naïve T cells into effector cells. Co-stimulatory signals are required to prevent abortive clonal expansion and stimulate differentiation[65]. In the course of an influenza virus infection, primed T cells migrate from LN to the lungs where they exert their antiviral effects by eliminating influenza virus-infected epithelial cells.

After clearance of infection, immunological memory is established. There are various memory T cell subsets, however, the role of each subset during a secondary

infection is incompletely understood. In general, the memory T cells can be divided into long-lived central memory T cells (T_{CM}) and effector memory T cells (T_{EM})[66]. Because there is less variability in the internal influenza virus proteins it has been hypothesized that heterosubtypic immunity, *i.e.* virus-specific T cells that respond to a secondary infection with an antigenically different virus, is mainly conferred by immune responses against these conserved internal epitopes. Similar to HA and NA, the internal epitopes that are mainly recognized by T cells are subject to selective pressure. It has been shown that small sequence variations in an epitope can significantly impact the immune response against a virus[67-70]. However, mutations in conserved regions of the internal influenza virus proteins, such as NP, M1 and the polymerase subunits, seem to be hampered by functional constraints[71]. Therefore, influenza virus-specific T cells are mainly targeted against the more conserved internal proteins and, because of their cross-reactive nature, contribute significantly to heterosubtypic immunity[72-75].

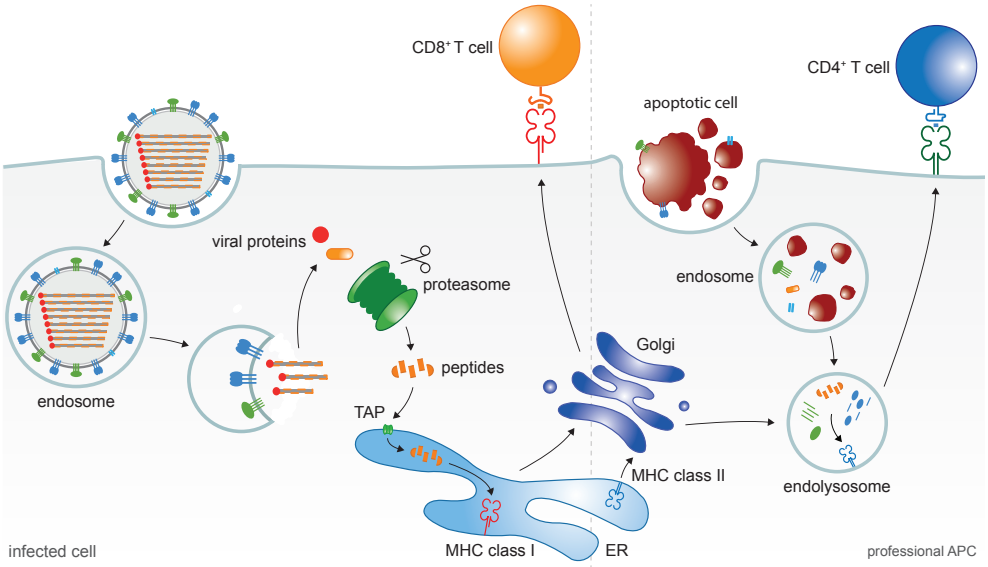

Figure 3. MHC class I and II antigen presentation pathways. *Viral proteins are degraded by the proteasome in the cytosol of an influenza virus-infected cell. The peptides released from the proteins are transported to the ER by TAP. Subsequently, peptides are loaded onto MHC class I molecules, followed by transportation to the cell surface. CD8⁺ T cells with a T cell receptor (TCR) specific for the peptide-MHC class I complex will recognize the complex and become activated to subsequently exert effector functions. Virtually all nucleated cells are capable of antigen presentation via the MHC class I pathway. In contrast, only professional APC can obtain antigens from exogenous origin, e.g. cell debris from influenza virus-infected cells. Antigens are degraded in the endolysosome and loaded onto MHC class II molecules, which are derived from the ER. The peptide-MHC class II complex is transported to the cell surface for presentation to CD4⁺ T cells.*

CD8⁺ T cells

Decades ago it was already recognized that influenza virus infections in mice lacking MHC class I-restricted CD8⁺ T cells resulted in delayed virus clearance and more severe diseases upon re-infection[76]. However, depletion of CD8⁺ T cells from influenza virus-infected mice still led to viral clearance[76-79], indicating that other

branches of the immune system were also involved. In experimentally infected humans an inverse correlation between $CD8^+$ cytotoxic T lymphocytes (CTL) present in peripheral blood and virus shedding has been observed[72]. Over the years, the role of $CD8^+$ T cells in clearing influenza virus infections has been confirmed in various animal models[73,76,80,81]. More recently, it was demonstrated that pre-existing virus-specific $CD8^+$ T cells in humans correlated with protection against disease severity caused by infection with 2009 pandemic A(H1N1) influenza viruses[82].

CTL responses are often directed at only a fraction of all potential antigenic epitopes, which are defined as immunodominant epitopes[83]. Several factors have been implicated to influence immunodominance, for example in mice the prevalence of high avidity T cells in a starting population predominantly determines the hierarchy in the T cell response[84]. After primary activation by APC, T cells migrate to the lung to exert their effector functions. Classically, $CD8^+$ T cells exert their effects via cytolytic contact-dependent pathways[85], however, CTL have also been shown to have suppressor functions in mice and humans by the secretion of cytokines or chemokines[86,87]. Furthermore, in the mouse model $CD8^+$ T cells have been shown to produce chemokines upon antigen-specific interaction with epithelial cells[88] and promote chemokine production by epithelial cells themselves[89] (**Fig. 4**).

$CD8^+$ T cells can be divided in Tc1, Tc2 and Tc17 subgroups depending on the cytokine production profile. Tc1 and Tc2 have direct cytolytic capacity in mice, whereas this is not the case for the Tc17 subset[90,91]. Direct cytolytic capacity is exerted via either release of perforin and granzymes, or via apoptosis triggered by Fas/FasLigand (FasL) or tumor necrosis factor (TNF) receptor 1 interaction[85,92]. Tc17 can efficiently recruit B cells, neutrophils, NK cells, macrophages and T cells by the production of cytokines and chemokines[81]. By themselves, each of the Tc1, Tc2 and Tc17 subgroups was able to confer protection from infection with a lethal dose of influenza virus in mice[90,91], suggesting that there is a redundancy in the effector mechanisms of $CD8^+$ T cells[81]. Although the secretion of chemokines and cytokines is important to establish solid anti-viral immunity, the contact-dependent pathway is still considered to be the major effector mechanism by which $CD8^+$ T cells exert their protective effects[92].

Immunological memory is established after resolution of an influenza virus infection. It has been hypothesized that antigen presentation by distinct DC subsets orchestrates the $CD8^+$ T cell memory response by determining whether responding $CD8^+$ T cells differentiate into cells with either an effector or a memory phenotype. $CD103^+CD11b^{+/-}$ migratory respiratory DC support the generation of $CD8^+$ effector cells that migrate to the infected mouse lungs. In contrast, $CD103^-CD11b^{high}$ DC support the generation of $CD8^+$ T_{CM} that remain within the draining LN[64]. Furthermore, the infectious dose during initial infection might have an effect on the phenotype distribution of the developing $CD8^+$ memory response[93].

As with other respiratory virus infections, influenza virus-specific effector and memory $CD8^+$ T cells following infection are not only found in the secondary lymphoid organs of mice and humans, but a relatively large pool also persists locally[94-98]. This lung

resident memory population in mice is comprised of circulating memory T cells, which are continuously recruited to the lung through CXCR3, and tissue resident memory T (T_{RM}) cells that are retained in the lung by the collagen-binding integrin VLA-1[99,100]. Furthermore, the maintenance of $CD8^+$ memory T cells in the lungs of mice has been attributed to persistent antigen presentation in the draining LN of the lung[96]. Although in mice the number of antigen-specific $CD8^+$ T cells in the draining LN remains stable[101], over time the functionality of the $CD8^+$ T cell recall response wanes[102]. This waning correlated with the loss of high avidity memory $CD8^+$ T cells[103].

$CD4^+$ T cells

Compared to $CD8^+$ T cells, the importance of $CD4^+$ T cells during the immune response against an influenza virus infection was only recognized more recently. Although $CD4^+$ T cells by themselves are unable to efficiently clear an influenza virus infection in mice, their helper effects to $CD8^+$ T cells and B cells indicate an important role in the defence against influenza virus infections[104,105]. Furthermore, the transfer of influenza virus-specific $CD4^+$ T cells into naïve mice protected them from challenge, even in the absence of $CD8^+$ T cells or B cells[106]. It was shown that $CD4^+$ T cell memory is generated after a primary infection[105] and responses to immunodominant epitopes in Matrix protein and NP are predominantly mediated by $CD4^+$ T cells[107,108]. Furthermore, pre-existing $CD4^+$ T cells specific for influenza virus internal proteins were associated with lower virus shedding and less severe illness in experimentally infected humans[108]. However, in these experiments individuals were intranasally inoculated with a high dose (10^6 $TCID_{50}$) of virus, which does not mimic a natural human infection. As a limitation to this study, peripheral blood is not the optimal site to assess cellular immunity and recall responses, since virus-specific memory lymphocytes may not circulate to a high extent but rather reside in mucosal or peripheral tissues[109].

Similar to $CD8^+$ T cells, $CD4^+$ T cells can be divided into several subgroups depending on the cytokine secretion profiles during infection[110]. These subgroups of $CD4^+$ T cells have distinct functions and, as with $CD8^+$ T cells, several redundant $CD4^+$ T cell mechanisms to protect against influenza virus infections have been described for mice[106]. The main functions of $CD4^+$ T cells include activation of APC and, most importantly, providing help in the activation of $CD8^+$ T cells and B cells[77,110-113] (**Fig. 4**). Mouse studies suggest that optimal $CD4^+$ T cell help to B cells is induced when the respective epitopes that activate the $CD4^+$ T cell or B cell lies physically within same viral protein[114,115]. Crucially, $CD4^+$ T cell help to B cells was the limiting factor for the kinetics and the magnitude of the virus-specific antibody response[115], which emphasises the importance of the induction of efficient $CD4^+$ T cell help during an influenza virus infection as well as for vaccination strategies. Additional functions of $CD4^+$ T cells include direct lysis of virus-infected cells in a perforin-dependent manner[116]. It was recently shown, in both explanted lung tissue and in human cell cultures, that primary bronchial epithelial cells can be MHC class II positive, allowing a direct role for cytotoxic $CD4^+$ T cells within the infected lung[108]. Furthermore, memory $CD4^+$ T cells play a role in the induction of an antiviral state of cells in the vicinity of virus-infected cells[110] and rapid initiation of the innate antiviral response in the lung[111] (**Fig. 4**).

Following influenza virus infection, virus-specific CD4⁺ memory T cells with the ability to rapidly expand upon re-infection with influenza virus are generated[111,117]. Using a mouse model, it was shown that CD4⁺ T cells induced during primary infection indirectly contribute to viral clearance by providing help to CTL. However, upon secondary infection, influenza virus-specific memory CD4⁺ T cells can also induce direct protective responses through helper-independent mechanisms via the production of INF-ɣ in the lungs[118]. Repeated re-infection of the host can lead to the exhaustion of the memory CD4⁺ T cell pool, resulting in reduced cytokine production and help to antibody producing B cells[119].

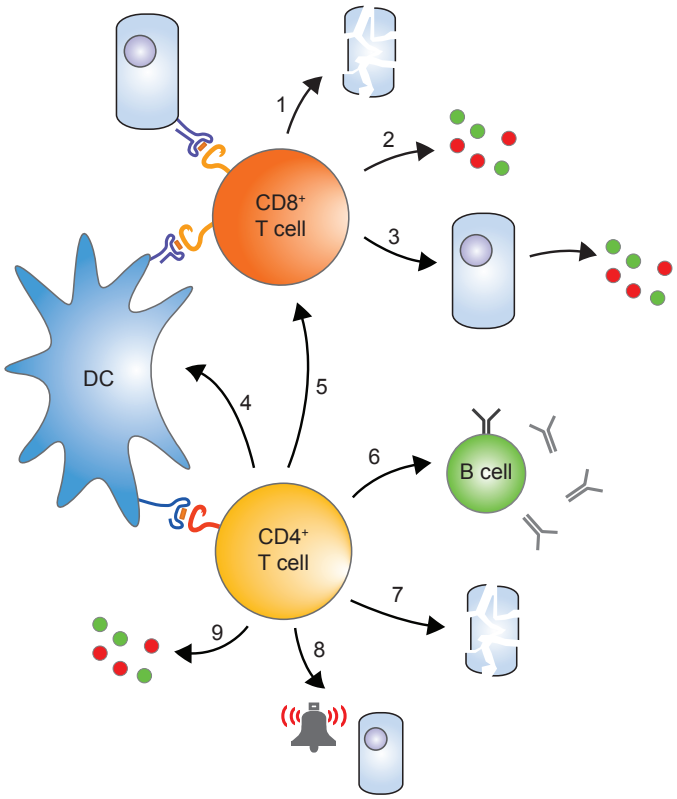

Figure 4. T cell immunity against influenza virus. *CD4⁺ and CD8⁺ T cells contribute to immunity against influenza virus through several mechanisms. After activation of T cells via MHC-restricted influenza virus antigen presentation, the main function of virus-specific CD8⁺ T cells is direct lysis of influenza virus-infected cells (**1**). In addition, virus-specific CD8⁺ T cells produce (antiviral) chemokines and cytokines (**2**) and stimulate epithelial cells to produce these molecules (**3**). Influenza virus-specific CD4⁺ T cells aid in the activation of APC (**4**), CD8⁺ T cells (**5**) and B cells (**6**). Furthermore, CD4⁺ T cells can have direct cytotoxic effects (**7**), induce an antiviral state in cells in the vicinity (**8**) and activate the innate immune system through production of chemokines and cytokines (**9**).*

1.3 Influenza vaccines

Antigenic drift of influenza viruses, requires almost annual updates of the seasonal influenza vaccine composition. The World Health Organization (WHO) makes a recommendation for vaccine strains twice a year based on the strains that are most likely to circulate next season[120]. Complications leading to morbidity and mortality following seasonal influenza virus infections are predominantly observed in high-risk groups, such as the elderly and immunocompromised. Therefore, annual vaccination of these high-risk groups against seasonal influenza viruses is recommended[121]. Furthermore, in case of an influenza virus pandemic a tailor-made vaccine needs to be developed momentarily. This is an unwanted and time-consuming process in the face of a pandemic. Currently, inactivated whole virus, split virion, subunit and live attenuated influenza vaccines are available.

Inactivated/recombinant influenza vaccines

Inactivated and recombinant protein influenza vaccines are used to prevent both seasonal and pandemic influenza virus infections, and to reduce influenza-related morbidity and mortality. Trivalent inactivated vaccines (TIV) are most commonly used, particularly in high-risk groups such as the elderly, against seasonal influenza virus infections. These vaccines contain components of three influenza viruses responsible for epidemic outbreaks: A(H1N1) and A(H3N2) influenza viruses and an influenza B virus. More recently, quadrivalent vaccines have become available that contain an additional, antigenically different influenza B virus[120]. Using the annual WHO prediction of influenza viruses that are likely to circulate in the next season whole-inactivated, split virion (virus particles disrupted by a detergent) or subunit (purified protein) vaccines are prepared[121]. All these vaccines aim at the induction of virus-neutralizing antibodies against HA, and to a lesser extent NA.

In case of a pandemic outbreak, procedures are in place to rapidly develop an inactivated vaccine that antigenically matches the pandemic influenza virus. For the highly pathogenic avian influenza viruses of the A(H5N1) subtype pre-pandemic inactivated influenza vaccines have been stockpiled in some countries[122]. Similar to TIV, the pre-pandemic A(H5N1) vaccine also induces neutralizing antibody responses predominantly against HA and poorly induce a heterosubtypic immune response. Thus, due to the continuous antigenic changes in HA of H5 influenza viruses, the stockpiled vaccine may be a poor antigenic match with eventual pandemic influenza viruses.

Traditionally inactivated influenza vaccine components are grown on embryonated chicken eggs[121]. Reassortant viruses with the HA and NA gene segment from the influenza A virus of interest in the A/Puerto Rico/8/34 backbone are generated to produce vaccine components, because these reassortant viruses generally replicate better in eggs than the wild-type virus. In contrast, reassortant influenza B viruses generally do not replicate better than the wild-type virus on chicken cells and therefore have to be adapted to replicate in eggs, which could lead to unwanted antigenic changes in HA. In general, growing influenza viruses for vaccine production in chicken eggs is a slow and labour-intensive process[123]. In order to expand production capacities, influenza vaccines produced in mammalian

cell lines have been approved in the United States and Europe[123-125]. Furthermore, recombinant influenza vaccines are now commercially available that are prepared using a baculovirus expression system. This system uses recombinant baculoviruses containing the HA gene segment of the influenza virus of interest and are grown on insect cells. Since the HA protein is not significant for the baculovirus replication cycle, adaptation of these proteins to the cell line does not occur frequently. Thus, potential antigenic changes in the HA protein during the manufacturing process are limited. The HA protein produced using the baculovirus expression system is purified and can be used as influenza vaccine preparation[126].

In general, inactivated vaccines are poorly immunogenic, but immunogenicity can be improved by the addition of an adjuvant to the vaccine preparation. Currently, MF59 and adjuvant system (AS)03 adjuvants (both oil-in-water emulsions) have been approved for the use in conjunction with human influenza vaccines. These adjuvants recruit and activate innate immune cells, and increase antigen uptake and subsequent transport to the draining LN. The use of MF59 or AS03 adjuvants in influenza vaccine preparations results in antigen dose sparing and/or induction of broader immune responses[127-130].

For decades, the use of inactivated influenza vaccines has helped to reduce influenza-related morbidity and mortality[131]. However, the preparation and use of current inactivated influenza vaccines has limitations. First, if the vaccine strains do not match the epidemic influenza strains antigenically, vaccine effectiveness will be reduced. In addition, the seasonal influenza vaccine will offer little or no protection against influenza viruses of a novel subtype with pandemic potential. Second, the vaccine production capacity, even of all manufacturers combined, is limited. This is especially problematic in the case of a pandemic outbreak, which was illustrated during the 2009 pandemic caused by swine-origin influenza virus of the A(H1N1) subtype. In some countries, tailor-made vaccines, in which the HA matched the pandemic strain antigenically, only became available after the peak of the pandemic[132-135]. Third, subjects in the high-risk groups may not respond optimally to vaccination and therefore the vaccine is least effective in the people who need it most. Finally, inactivated influenza vaccines inefficiently induce virus-specific $CD8^+$ T cells, which substantially contribute to enhanced viral clearance and have the ability to provide cross-protective immunity[136,137]. Moreover, these vaccines may even hamper the induction of $CD8^+$ T cell responses otherwise induced by for example natural infections[138-141].

Live attenuated influenza vaccines

In addition to inactivated influenza vaccines, live-attenuated influenza vaccines (LAIV) are available in some countries and are especially used to vaccinate children[121]. Attenuated viruses are prepared by reverse genetics, thereby introducing HA (and NA) RNA segments into the backbone of an influenza virus adapted to replicate at 25°C. The attenuated vaccine viruses containing HA and NA gene segments of influenza viruses recommended by the WHO are grown on embryonated chicken eggs[142,143]. The vaccine is administered as a spray intranasally and has been shown capable to induce antibodies, including mucosal IgA, $CD4^+$ and $CD8^+$ T cells[143].

Vaccination with LAIV has been proven safe without any serious adverse events, although with the use of attenuated viruses potentially similar symptoms as observed with a natural infection can arise. Furthermore, when using live-attenuated vaccines there is always a risk of reversion of the attenuated virus to the virulent form. Virus shedding has been observed for several days after vaccination in children, but transmission of the attenuated virus seems to be rare[121].

Recently, there has been debate about the effectiveness of LAIV following reports of studies unable to show significant LAIV effectiveness. Other studies showed significant LAIV effectiveness, however, the vaccine did not perform better than the inactivated influenza vaccines[144,145]. Thus far, the WHO has not changed the influenza vaccine recommendations, but further investigation into LAIV effectiveness is warranted[144].

1.4 Novel (universal) influenza vaccines

In order to develop vaccines that induce immunity against different influenza viruses within the same subtype (intrasubtypic immunity) or against influenza viruses of different subtypes (intersubtypic immunity), different viral components are currently evaluated as novel vaccine targets (**Fig. 5**). These targets should be immunogenic, accessible during infection and conserved across several subtypes of influenza virus. In addition, novel delivery strategies and vaccine production platforms are evaluated to develop long-lasting and broadly reactive influenza virus-specific immune responses.

Novel vaccine targets

HA stalk-specific antibodies

Broadly neutralizing antibodies specific for the head-domain of HA have been described[146-151]. However, considering the high mutation rate of the head-domain, eliciting an antibody response specific for the relatively conserved stalk-domain is believed to have more potential to induce heterosubtypic immunity. It has been shown that passive immunization with stalk-specific antibodies affords protection against infection with a heterologous influenza virus in mice and ferrets[146,150,152-158]. Human stalk-specific antibodies induced by influenza virus infection or vaccination have been identified and are specific for epitopes shared by either group I subtypes of HA (including H1, H2, H5, H6 and H9), group II HA subtypes (H3, H4, H7, H10, H14 and H15) or even both[146,152,159-161]. However, upon natural infection the HA stalk-specific antibody response is subdominant compared with the response to the globular head region and the magnitude of the stalk-specific antibody response varies considerably between individuals. Given the low frequency of stalk-specific B cells it is unlikely that the antibody levels induced upon influenza virus infection can afford protection[146,161].

In the context of the development of a universal influenza vaccine, various designs of stalk-based immunogens have been proposed. First, the globular head of HA has been removed to avoid the immunodominant antibody response to this variable region[162-165]. However, to retain the correct conformation of the stalk-domain without the head has been a challenge. Therefore, extra stabilizing mutations have been introduced and synthetic HA stalk molecules have been constructed[164,165]. Second, modifications have been made to the head-domain by the introduction of extra glycosylation sites. Glycosylation shields the head-domain from recognition by virus-specific B cells in favour of an antibody response to the stalk-domain[166]. A third approach to induce stalk-specific antibodies is to sequentially immunize with chimeric HA molecules carrying a (irrelevant) head-domain of different HA subtypes but the same stalk-domain in order to boost the stalk- and not the head-specific immune response. This approach has resulted in substantial antibody responses to the stalk, which afforded protection against challenge infection with heterosubtypic viruses[158,167-171] (**Fig. 5**).

In contrast to virus-neutralizing antibodies specific for the head-domain, stalk-specific antibodies do not inhibit agglutination of erythrocytes in a hemagglutination inhibition (HI) assay. Therefore, alternative mechanisms than interference with receptor

binding have been proposed for their protective effect. These include prevention of conformational changes of HA in the endosomes and subsequent fusion of the virus membrane with the endosomal membrane[159], effects on virus egress from the infected cells[150] and interference with maturation of HA by preventing cleavage of HA by host proteases[168]. Furthermore, recently it was shown that interactions between the Fc region of broadly neutralizing HA stalk-specific antibodies and Fc-ɣ receptors were essential in protecting mice from lethal influenza virus challenge. This suggests that ADCC or ADP mediated by HA stalk-specific antibodies contributed to protection[45].

Antibodies against NA

Upon an influenza virus infection NA-specific antibodies are induced, which can be boosted by vaccination with TIV[172]. Because antibodies to NA have been shown to cross-react with different NAs of the same subtype, these antibodies may afford a degree of cross-protection in the absence of a matching HA, e.g. A(H1N1) versus A(H5N1)[173-175]. In contrast to HA head-domain antibodies, NA-specific antibodies do not prevent virus infection but rather prevent release of newly formed virus particles[46] (**Fig. 5**).

Not only NA-specific antibodies elicited through natural infection, but also NA antibodies induced by vaccination have been shown to provide intrasubtypic protection. Vaccination of mice with a DNA plasmid expressing NA provided protection against infection with a influenza virus containing a structurally similar NA protein[173,176]. Given the narrow range of protection of this NA-specific antibody response, a stand-alone NA-based vaccine is not the most attractive candidate for universal influenza vaccine development. However, the addition of NA to an HA component can improve the virus-specific antibody response[177].

Antibodies against M2

The ectodomain of M2 (M2e) is considered a good candidate for universal influenza vaccine development because it is relatively conserved among influenza A viruses[178]. The protective effect of M2-specific antibodies has been demonstrated after hyperimmunization and passive administration[179]. Antibodies specific for M2 are unable to neutralize influenza virus due to their inability to bind the protein on the virion surface, however, antibodies can bind to M2e when it is exposed on the surface of infected host cells. These antibodies mediate killing of the infected cells by ADCC, most likely by NK cells[180] (**Fig. 5**). Furthermore, M2-specific antibodies may also opsonize infected cells for phagocytosis by macrophages[43,181].

Due to its poor immunogenicity, vaccine development based on M2 protein is challenging. However, if the M2-based peptide vaccine is adjuvanted, a robust antibody response can be induced[182]. Several M2-based influenza vaccine candidates have been described and validated in various animal models, including DNA constructs[183], virus-like particles (VLPs)[43,180,181,184] and viral vectors[185]. It has been shown in mice that M2-based vaccines can provide protection against infection with a heterologous virus[181,185,186]. Moreover, even six months after vaccination mice were protected from a homologous challenge infection[181], indicating that an M2-based vaccine can provide long-term protection. Currently, M2-based vaccines

are evaluated in clinical trials[187]. M2-specific antibodies alone cannot provide sterile immunity[178], therefore, combining M2 with another influenza antigen might induce a better protective immune response[179].

Antibodies against NP

Protective effects of NP-specific antibodies have been demonstrated in mouse models[188,189] and was shown to be dependent on Fc receptors and $CD8^+$ T cells. Therefore, it has been suggested that formation of NP immune complexes and opsonisation plays a role in conferring protection[188,189], although this could not be confirmed *in vitro*[190]. More recently, it has been shown that NP-specific antibodies inducing ADCC could be detected in children and adults. These antibody responses cross-reacted with NP from seasonal A(H1N1) and A(H3N2) influenza viruses, A(H1N1)pandemic(pdm)09 and A(H7N9) influenza viruses[191]. Thus, although NP-specific antibodies may not induce virus neutralization, they could be an important component to establish heterosubtypic immunity.

Broadly reactive T cell responses

It was already recognized over 30 years ago that conserved internal influenza virus proteins, such as NP and M1, are targets for CTL that consequently cross-react with influenza viruses of different subtypes[72-75,107]. Indeed, CTL induced after infection with seasonal A(H1N1) and A(H3N2) influenza viruses cross-react with A(H5N1)[53,55,107], A(H1N1)pdm09[56,192,193], variant A(H3N2)[56] and A(H7N9)[57] influenza viruses. During the pandemic of 2009, it was demonstrated that the frequency of pre-existing cross-reactive $CD8^+$ T cells was inversely associated with disease severity in individuals infected with the A(H1N1)pdm09 virus[82,194]. In acutely infected patients a rapid anamnestic cross-reactive virus-specific $CD8^+$ CTL response was observed, which may have contributed to accelerated clearance of the virus[195]. Furthermore, in patients infected with the avian A(H7N9) virus that emerged in China, disease outcome correlated with the virus-specific $CD8^+$ T cell response[196]. This indicates that vaccines capable of inducing influenza virus-specific $CD8^+$ T cell responses may afford broadly protective immunity (**Fig. 5**).

It is now generally accepted that virus-specific $CD8^+$ T cells play an important role in cross-protective immunity[197]. More recently, it has been demonstrated both in animal models and humans that $CD4^+$ T helper cells contribute to cross-protective immunity as well[105,106,108,116,118]. Upon infection with heterologous influenza viruses, cross-reactive anamnestic T cell responses contribute to accelerated clearance of infection and reduction of clinical symptoms[82,195].

Various studies attempted to define the relative contribution of $CD4^+$ and/or $CD8^+$ T cells to heterosubtypic immunity, and it has been suggested that $CD8^+$ T cells are the major mediators[82,197]. It has been shown in mice that $CD8^+$ T cells in combination with non-neutralizing antibodies directed against internal influenza virus proteins were capable of providing complete protection against a lethal influenza virus challenge. This process was, at least in part, dependent on alveolar macrophages[198]. In contrast, there are also mouse studies showing that $CD4^+$ T cells[199,200] and/or B cells[201,202] contribute to heterosubtypic immunity. Clearly, the immune response to

influenza virus is multifactorial[203] and therefore it is difficult to attribute heterosubtypic immunity to a single effector mechanism. Although T cell mediated immunity induced by either vaccination or natural infection may not induce sterile immunity, it could afford a significant degree of clinical protection against both seasonal and pandemic influenza viruses.

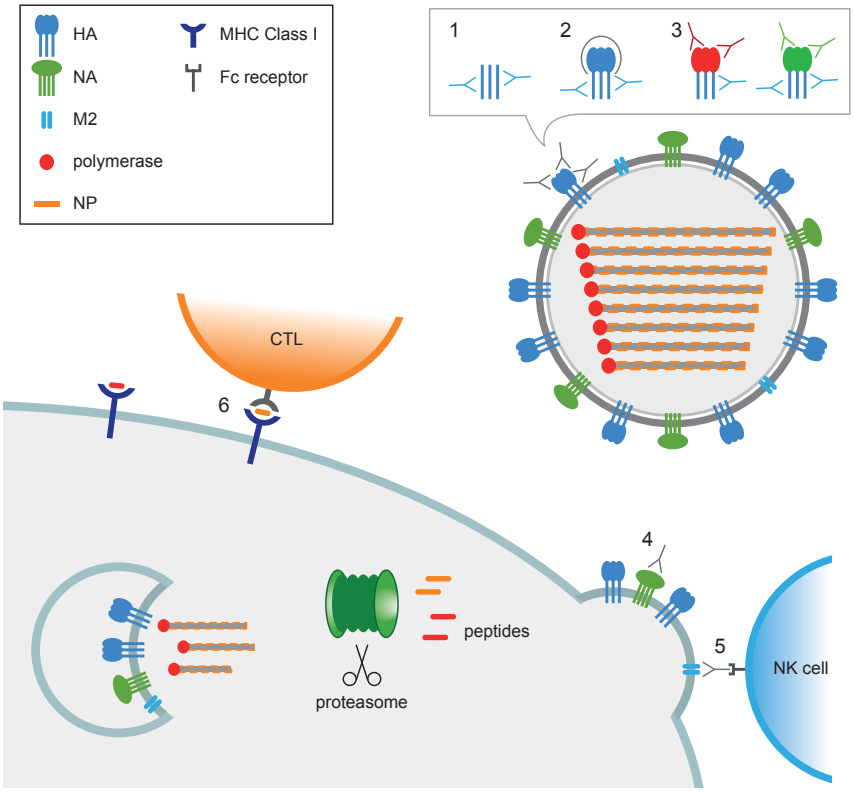

Figure 5. Design approaches for novel universal influenza vaccines. *Different approaches are currently investigated for the design of novel universal influenza vaccines. Vaccines can be designed to induce HA stalk-specific antibody responses (**1-3**), non-neutralizing antibody responses (**4-5**) or CD8⁺ T cell responses (**6**). In order to redirect antibody responses towards the conserved HA stalk-domain, several modifications have been made to HA. These include headless HA molecules (**1**), 'shielded' head HA molecules through introduction of glycosylation sites (**2**) and chimeric HA molecules (**3**). The latter boost the stalk-specific antibody response through repeated vaccinations with molecules expressing similar a stalk-domain but different head-domains. Furthermore, non-neutralizing antibodies (antibodies-specific for NP, M2, NA and HA stalk) can be important in protection from influenza virus, in particular antibodies that prevent virus egress from cells (**4**) or are capable of inducing ADCC/ADP (**5**). Finally, conserved internal proteins such as NP or polymerase complex can be used as antigens to induce virus-specific CTL response (**6**).*

Respiratory vaccine administration

In addition to the identification of novel vaccine target proteins, alternative vaccination strategies are currently under investigation. Most vaccines, including TIV, are administered intramuscularly and therefore induce a systemic immune response. However, influenza virus mainly causes infection of the respiratory tract and induction

of local immunity by respiratory vaccination may be more effective. An added benefit of respiratory vaccine administration is that no needles are required. This would facilitate large-scale vaccination campaigns without the need for professional health care workers and destruction of potentially contaminated needles.

Currently, LAIV is already administered as a nasal spray to children and has been shown to induce local mucosal IgA antibody responses[204,205]. In addition, LAIV vaccination has also been shown capable of inducing a mucosal immune response in adults, however, the number of individuals that seroconverted was low. Of note, the majority of the volunteers in this study previously received TIV, which induced antibodies that can neutralize the attenuated vaccine virus resulting in reduced LAIV effeciveness[206]. Furthermore, intranasal instillation of a vaccine candidate comprised of a cocktail of VLPs displaying four subtypes of HA protected mice from infection with influenza viruses of eight different HA subtypes. Since sterile immunity against heterosubtypic viruses was not achieved, factors other than neutralizing antibodies were considered to mediate the observed protection[207].

Vaccine vectors

For the efficient induction of virus-specific $CD8^+$ T cells, vaccine delivery systems are required that allow *de novo* synthesis of viral proteins. In this respect, the use of viral vectors for the delivery of viral proteins holds promise, because it allows for synthesis of viral proteins in the cytosol of infected cells and thus facilitates antigen processing and presentation to virus-specific $CD8^+$ T cells. Furthermore, the antigens of interest are (over-)expressed in their native conformation, thus are also able to induce antibodies of the proper specificity.

Viral vector-based influenza vaccine candidates that are currently under development include baculovirus, parainfluenza virus 5, alphavirus and Newcastle disease virus vaccine vectors[208,209]. However, efficacy/safety in humans has not been extensively tested for these vectors. In addition, recombinant adenoviruses (rAd) are investigated, forming a stable vector system that allows for easy insertion of an antigen of interest. There are many serotypes of adenoviruses of which several have been tested as a vaccine vector, either as a replication competent vector or modified to become replication-deficient[209]. These vectors readily express the antigen of interest and are capable of inducing innate, cellular and humoral immune responses. Drawbacks of the use of rAd vaccine vectors include two clinical trial failures with rAd5[210,211] and potential interference of pre-existing adenovirus-specific immunity in humans[212,213]. The use of a non-human, low-prevalent and/or genetically altered rAd vectors is investigated as an alternative[214-218]. In addition to adenovirus vectors, several poxvirus-based vaccine vectors have been investigated for the development of vaccines. First, the replication competent vaccinia virus (VACV), used in vaccination campaigns to eradicate smallpox, was used as a recombinant vaccine vector expressing various influenza virus antigens. However, substantial reactogenicity against the VACV vector was observed in various animal models, which propelled development of attenuated VACV-derived virus vectors. This includes NYVACV, created by the deletion of 18 open reading frames from the VACV genome, and Modified Vaccinia virus Ankara (MVA)[209].

Modified Vaccinia virus Ankara

MVA is derived from Chorioallantois Vaccinia virus Ankara through serial passaging in chicken embryo fibroblasts (CEF)[219,220], which resulted in major deletions in the viral genome and many mutations that affected most known VACV virulence and immune evasion factors[221-223]. Consequently, efficient MVA replication is restricted to avian cells and the virus is unable to produce infectious progeny in most cells of mammalian origin[224-226]. The host cell restriction of MVA is associated with a late block in the assembly of viral particles in non-permissive cells. This phenotype is rather exceptional among poxviruses with host range deficiencies, which are usually blocked prior to this stage during the abortive infection in mammalian cells[227-229]. Non-replicating MVA allows for unimpaired synthesis of viral early, intermediate and abundant late gene products, which supported its development as safe and particularly efficient viral vector[226]. Moreover, the biological safety and replication deficiency of MVA has been confirmed in various *in vivo* models, including avian species and animal models with severe immunodeficiencies[230-233], and immunocompromised humans[234]. Therefore, recombinant (r)MVA viruses as genetically modified organisms can be used under conditions of biosafety level (BSL-)1 in most countries, provided that innocuous heterologous gene sequences are expressed. The latter attribute is an important advantage compared to replication competent poxvirus vectors (BSL-2 organisms) and other viral vectors, and has certainly contributed to the increasing use of rMVA in clinical testing.

Antigens encoded by target gene sequences inserted into the MVA genome are transcribed under the highly specific control of poxviral promoters that are only recognized and activated by virus encoded enzymes and transcription factors. Since there is no survival of MVA infected host cells it can be assumed that full clearance of recombinant virus and DNA occurs within days after vaccine administration, ensuring only transient expression of proteins. Despite this transient production, MVA vector vaccines are able to elicit high levels of antigen-specific humoral and cellular immune responses, as was demonstrated with the first MVA candidate vaccine delivering influenza antigens[235,236].

Another characteristic of MVA vaccines is their level of immunogenicity and protective capacity when compared to replicating VACV vaccines, expressing an identical transgene[235,237,238]. Replication competent vectors are expected produce more antigen per vaccination than non-replicating vectors because of their capacity to amplify and spread to new cells *in vivo*. Nevertheless, the efficacy of MVA-based vaccines was as good as or even better than the vaccinations with replication competent VACV vectors in mice and non-human primates. These observations are explained by the capacity of MVA to activate various components of the host innate immune system, probably because of the lack of immune evasion factors encoded by wild-type VACV[239-246]. Unlike other VACV strains, MVA does not produce the soluble viral proteins that function as receptor-like inhibitors of type I and type II IFN, TNF and chemokines[241]. Moreover, MVA infection can be sensed by multiple intracellular host detection mechanisms resulting in the production of IFN, inflammatory cytokines and chemokines[243]. In addition, MVA has lost several of the VACV inhibitors targeting intracellular signalling pathways, e.g. host NF-κB

activation. As a consequence, *in vivo* administration of MVA, but not other VACV strains, can trigger the rapid immigration of monocytes, neutrophils and $CD4^+$ T cells to the site of inoculation[245]. These intrinsic immunostimulatory activities suggest that the use of additional adjuvant systems together with MVA might be dispensable for most vaccine applications.

MVA has potential as a rapid response vaccine platform for newly emerging and potentially pandemic viruses. Established standard protocols allow rapid generation of rMVAs that are suitable for clinical evaluation[247]. This is done by simultaneous infection of CEF with fully characterized non-recombinant MVA seed virus and subsequent transfection of vector plasmid DNA containing the target gene of interest. Through homologous recombination, the heterologous gene sequences are inserted in the viral genome. The rMVA is clonally selected and amplified by serial passaging on CEF derived from certified embryonated eggs of specific pathogen free (SPF) chickens. The ideal process from a human case of infection with a novel respiratory virus to the construction and isolation of a candidate rMVA would takes 6-12 weeks (**Fig. 6**).

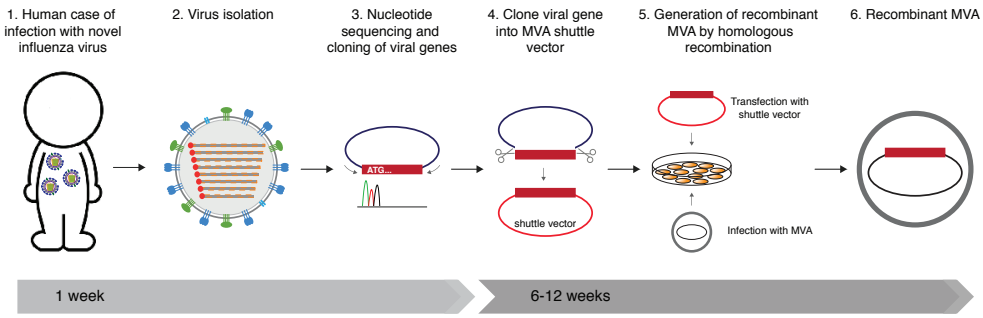

Figure 6. Ideal timeline for construction of an MVA-based vaccine after a human case of infection with a novel respiratory virus. *Influenza virus is used as an example. After the emergence of a novel respiratory virus with the ability of infecting humans (**1**), the virus is isolated (**2**) and the sequence of a target gene of interest can be obtained within a week (**3**). Subsequently, the gene of interest is cloned or synthesized and subcloned into an MVA shuttle vector plasmid (**4**). This plasmid is then transfected in cells infected with wild-type (wt)MVA. Through homologous recombination the gene of interest is inserted into the MVA genome (**5**). By serial plaque passaging on CEF a good laboratory practice (GLP) compliant rMVA is clonally isolated (**6**). The process from cloning to obtaining the rMVA takes about 6-12 weeks.*

In order to produce enough vaccine doses for a large-scale vaccination campaign, bulks of tissue culture are required. Primary CEFs are readily prepared from embryonated eggs without need for further amplification and, as known from the production of seasonal influenza vaccines, millions of eggs can be obtained and handled within days. CEF can be produced at a large scale and cryopreserved for a later time point, however, this negatively impacts the quality of the cells. Therefore, especially in the context of pandemic preparedness, continuous cell lines that allow for efficient MVA propagation, such as the duck cell lines AGE1.CR and AGE1.CR.pIX[248], would be more beneficial.

After generation of rMVA, the vector vaccine needs to be validated *in vitro* to verify genetic stability, antigen expression and unimpaired growth capacity. Subsequently, *in vivo* experiments in pre-clinical models (e.g. mice, ferrets and/or macaques) are performed to determine vaccine immunogenicity and efficacy, usually testing various dosages and routes of administration. If successful in the pre-clinical phase, the vaccine can be tested in humans. Thus far, no MVA-based vaccine is registered and marketed for human use, but numerous vaccines have been tested in clinical trials[249,250]. If the vaccine is successful during the incrementing phases of the clinical trials, it can be registered for common use. Currently, this process is too long for rapid rMVA validation in the face of a pandemic (**Fig. 7**).

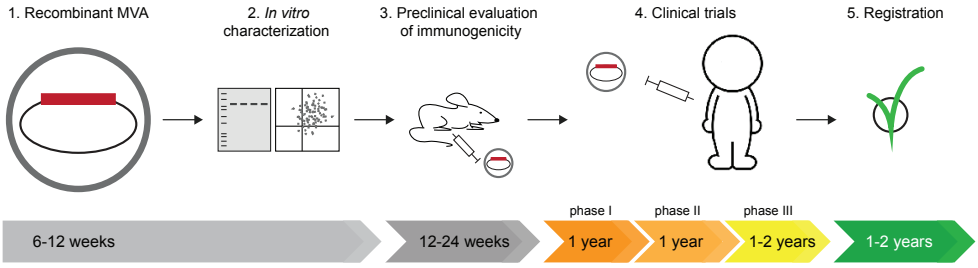

Figure 7. Timeline for evaluation of a novel MVA-based vaccine. *A newly developed rMVA vaccine (**1**) is tested* in vitro *to assess correct gene insertion and protein expression in rMVA infected cells, e.g. by western blot or flow cytometry (**2**). Subsequently, vaccine immunogenicity and efficacy is tested in an appropriate animal model (**3**). If the MVA-based vaccine is successful in the pre-clinical tests, the vaccine is tested in phase I, II and III clinical trials (**4**). Finally, when the vaccine has proven safe and effective, it can be filed for market authorization (**5**).*

1.5 Modified Vaccinia virus Ankara–based influenza vaccines

Antigen expression from MVA allows for efficient induction of immune responses involving both the humoral and cellular component of the immune system. Therefore, the MVA virus vector is of considerable interest for the development of novel influenza vaccines. Many MVA-based influenza vaccines have been generated and are currently at different stages of development.

rMVA-H1

In order to evaluate an MVA-based vaccine against A(H1N1)pdm09 influenza virus, the HA gene of the prototypic A/California/7/09 influenza virus was cloned into rMVA (rMVA-H1). Mice vaccinated with rMVA-H1 were protected from a challenge infection with A(H1N1)pdm09 influenza virus. Protection correlated with the induction of virus-specific neutralizing antibodies and T cells[251]. Furthermore, vaccination with rMVA-H1 induced cross-protective immunity against some but not all swine A(H1N1) influenza viruses[252].

The rMVA-H1 vaccine candidate was also evaluated in ferrets and non-human primates. One vaccination afforded only modest protection in ferrets, but a second vaccination induced robust antibody titres that reduced virus replication after challenge infection with A(H1N1)pdm09 influenza virus. However, full sterile immunity was not achieved in this study, possibly related to the route of administration and/or dose of challenge virus[253]. Furthermore, rMVA expressing HA from A/California/04/07 was assessed in macaques and provided full protection against an antigenically similar A(H1N1)pdm09 virus[254]. Taken together, these data indicate that an rMVA-H1 vaccine would have been able to induce protective immunity against the influenza virus responsible for the 2009 pandemic, although the extent of cross-protection against unrelated A(H1N1) influenza viruses may have been limited.

rMVA-H5

The development of efficacious A(H5N1) vaccines is complicated by the co-circulation of different H5 influenza viruses that belong to antigenically distinct clades. Ideally, a novel vaccine induces antibodies that cross-react with A(H5N1) influenza viruses from multiple clades. Several rMVA vaccines expressing the HA gene of different A(H5N1) influenza viruses have been constructed and tested in animal models[255]. rMVA expressing the HA gene of influenza virus A/Vietnam/1194/04 (rMVA-H5) induced strong antibody responses that cross-reacted with other viruses to some extent and protected mice from infection with homologous and heterologous A(H5N1) viruses[256,257]. rMVA-H5 induced superior protective immunity against homologous and heterologous A(H5N1) viruses in mice compared to rMVA expressing HA genes of A/Hong Kong/156/97, A/Indonesia/5/05, A/turkey/Turkey/1/05, A/Chicken/Egypt/3/06 or A/Anhui/1/05 H5N1 influenza viruses[257]. Furthermore, this rMVA-H5 vaccine candidate has been evaluated in non-human primates. Two vaccinations with rMVA-H5 protected cynomolgus macaques against infection with influenza viruses A/Vietnam/1194/04 or A/Indonesia/5/05[258,259]. rMVA-H5 also proved to be immunogenic in chickens and afforded protection against infection with A(H5N1)[233]. The favourable outcome of pre-clinical testing of rMVA-H5 prompted the further clinical testing of this vaccine candidate in a phase I/IIa trial. The vaccine was shown

to be immunogenic in humans and induced cross-reactive antibody responses against antigenically diverse H5 influenza viruses[260,261].

The minimal dose of rMVA-H5 required to induce protection from a lethal infection A(H5N1) influenza virus has been investigated in mice. Interestingly, a single dose of 10^5 plaque-forming units (PFU) was sufficient for the induction of sterile immunity against a challenge infection with the homologous influenza virus. However, two vaccinations with ≥10^4 PFU rMVA-H5 were required for induction of protective immunity against challenge infections with either the homologous or a heterologous influenza virus[262]. These data indicate that in case of a pandemic, when large numbers of vaccine doses need to be produced in a short period of time, protective immunity against A(H5N1) viruses can be induced with one or two relatively low doses of MVA.

In addition to MVA-based H5 influenza vaccines expressing a wild-type HA gene, rational design approaches have been taken to induce broadly reactive immune responses. To that end, potential B and T cell epitopes in HA derived from A(H5N1) viruses were selected and recombined into a mosaic proteins using an *in silico* approach. This mosaic H5 (H5M) was expressed by MVA (rMVA-H5M) and was shown to induce broader T cell responses than MVA expressing wild-type HA. Vaccine-induced antibody responses were long lived and vaccination provided protection against both A(H5N1) and A(H1N1) influenza viruses[263].

Other rMVA-HA vaccines

rMVA expressing HA from H3N8 A/Equine/Kentucky/1/81 (rMVA-H3) has been evaluated in ponies as standalone vaccine or in combination with a DNA HA vaccine. Vaccination with rMVA-H3 was shown to induce antigen-specific antibody and T cell responses, and protected from disease caused by a challenge infection with the homologous influenza virus[264]. Furthermore, rMVA expressing HA from A/Shanghai/2/13 (rMVA-H7) has been constructed and tested in ferrets. The vaccine significantly reduced viral loads in the trachea and lungs after a challenge with A(H7N9) influenza virus[265].

rMVA-NP

In order to induce virus-specific T cell responses with an MVA-based vaccine, MVA expressing NP derived from H3N8 A/Equine/Kentucky/1/81 was assessed in ponies in combination with a DNA NP vaccine. This vaccine regimen was shown to induce both humoral and cellular immunity against influenza virus. However, full protection from a challenge infection with the homologous virus was not observed although disease severity was reduced[264]. In addition, rMVA expressing NP from influenza virus A(H5N1) was constructed. Vaccination with this rMVA-NP vaccine induced humoral and cellular NP-specific immune responses in mice and provided partial protection from a lethal challenge with the homologous A(H5N1) influenza virus. In contrast, mice primed with a sub-lethal A(H1N1)pdm09 infection followed by rMVA-NP vaccination were fully protected from the challenge. Sub-lethal infection with A(H1N1)pdm09 was not enough to achieve this level of protection, indicating that vaccination with rMVA-NP can boost cross-reactive immune responses. Cross-reactive immune responses induced by vaccination with rMVA-NP were shown

to (partially) protect from a lethal A(H9N2) or A(H7N1) influenza virus infection in mice[266]. In contrast, in macaques vaccination with a similar rMVA-NP vaccine did not afford cross-reactive protection against a challenge with the heterologous A(H1N1) pdm09 influenza virus[254].

rMVA-HA+NP

In order to elicit both virus-specific antibodies and T cell responses with a single vaccine, multivalent rMVA vaccines expressing both the HA and NP genes have been constructed and tested in mice. rMVA expressing HA and NP genes derived from influenza virus A/Puerto Rico/8/34 (H1N1) induced protective antibody and CTL responses against a homologous or heterologous infection in mice[235,267].

Other rMVA-HA+NP vaccines expressing NP derived from A/Vietnam/1203/04 (H5N1) and HA from either the same A(H5N1) influenza virus (rMVA-H5+NP) or H1N1pdm09 (rMVA-H1+NP) have been constructed. Vaccination with rMVA-H1+NP induced cross-protective immunity against infection with the homologous A(H1N1) pdm09 influenza virus, an unrelated A(H1N1) influenza virus and an A(H5N1) influenza virus in mice. Furthermore, this vaccine afforded partial protection against a challenge with A(H3N2) influenza viruses. In contrast, rMVA-H5+NP only induced only protection against A(H5N1) and A(H1N1)pdm09 influenza viruses in mice[268]. In concordance with these results, vaccination of macaques with rMVA-H1+NP provided protection from an A(H1N1)pdm09 influenza virus challenge, whereas rMVA-H5+NP induced only partial protection[254].

rMVA-NP+M1

Multivalent rMVAs expressing genes encoding the relatively conserved internal structural proteins NP and M1, aiming exclusively at the induction of virus-specific T cell responses, have been constructed. The rMVA-NP+M1 vaccine was tested in phase I and phase IIa clinical trials and mainly induced virus-specific $CD8^+$ T cells, which were detected one week after intramuscular (IM) injection and induced protective immunity against an experimental infection one month after vaccination[269,270]. Furthermore, the vaccine was assessed in people over 60 years of age and shown to be safe and immunogenic[271].

Different vaccination strategies have been investigated for the rMVA-NP+M1 vaccine[272-274]. Priming with an adenovirus vector expressing NP and M1 and a subsequent boost with MVA expressing the same antigens induced higher levels of protective T cells than vaccination with either of the vectors alone in mice. The strongest T cell responses were obtained after IM injection (adenovirus vector) and intranasal (IN) instillation or IM injection (MVA) compared to intradermal (ID) injection[273]. In addition, rMVA-NP+M1 vaccination has been tested in combination with TIV as a cocktail, heterologous prime-boost regimen or as simultaneous adjacent vaccinations in mice and humans. Priming with rMVA-NP+M1 and subsequent boosting with TIV resulted in higher levels of total IgG but did not affect the number of IFN-γ-producing T cells when compared to vaccination with rMVA alone[275,276]. The heterologous prime-boost strategy protected mice from a heterologous challenge infection six months after vaccination[275].

MVA expressing other (combinations of) influenza virus proteins

To develop a universal influenza vaccine, different rMVAs expressing a variety of conserved antigens derived from A(H5N1) influenza virus were constructed. These antigens included PB1, M1, M2, the HA stalk-domain, HA-stalk combined with NP, HA-stalk in combination with four repeats of M2e – derived from A(H5N1), A(H9N2), A(H7N2) and A(H1N1) viruses – and HA-stalk+4xM2e+NP. Mice were immunized twice with the respective rMVA vaccines and subsequently challenged with A(H5N1), A(H7N1) or mouse adapted A(H9N2) influenza virus. Both rMVA expressing HA-stalk+NP and HA-stalk+4xM2e+NP induced heterosubtypic immunity. Co-expression of NP seemed essential since expression of NP induced virus-specific $CD4^+$ and $CD8^+$ T cells[266]. All the other rMVA vaccines tested (rMVA-HA-stalk, rMVA-HA-stalk+M2e, rMVA-M1, rMVA-M2, rMVA-PB1) failed to induce protective immunity. Interestingly, vaccination with rMVA-M1 predisposed for more severe disease upon challenge infection of the mice, although the difference in survival rates with the naïve control group was not statistically significant[266]. Furthermore, rMVA expressing NA derived from A(H1N1)pdm09 was constructed. After two vaccinations with either 10^6 or 10^7 PFU, partial protection against a A/California/7/2009 H1N1 influenza virus challenge was observed[251]. Taken together, rMVA is widely used for the development of influenza vaccines and encouraging results have been obtained.

1.6 Outline of the thesis

This thesis discusses the development and evaluation of novel MVA-based influenza vaccine candidates that aim at the induction of broadly protective immune responses. Chapter 2 describes studies performed to validate MVA as a vaccine vector. In chapter 2.1 the *in vivo* tropism of rMVA in mice, ferrets and macaques is described and delivery of rMVA by IM injection is compared to administration via the respiratory tract. The results of this study advance our understanding of the tropism and immunogenicity of MVA-based vaccines, and aid in the development of novel vaccines and delivery systems. Chapter 2.2 discusses the effect of pre-existing MVA-specific immunity, induced by either smallpox vaccination or repeated rMVA-based vaccination, on the performance of rMVA-based vaccines. Since pre-existing vector-specific immunity is known to have a detrimental effect on for example adenovirus vector-based vaccines, it is essential to understand the implications of pre-existing immunity to MVA on vaccine immunogenicity and efficacy.

In chapter 3, novel MVA-based influenza vaccine candidates were tested in pre-clinical studies. Chapter 3.1 and 3.2 describe rMVA-based influenza vaccine candidates designed to optimize influenza virus-specific T cell responses. Modifications to NP aiming at enhanced proteasomal protein degradation to increase subsequent release of peptides for presentation on MHC class I molecules were investigated. The immunogenicity and protective capacity of rMVA vaccines expressing (modified) NP was addressed in C57BL/6 mice (chapter 3.1) and BALB/c mice (chapter 3.2). Furthermore, the immunogenicity of rMVA-based vaccines expressing the NP (chapter 3.2) or HA (chapter 3.3) gene was compared to vaccination with corresponding protein-based vaccines with and without Matrix-M™ adjuvant. These studies provide insight in optimization of induction of influenza virus-specific immune responses using MVA-based vaccines and the added value of using MVA-based vaccines over protein-based vaccines. In addition, chapter 3.3 addresses the effect of supplementing either protein- or MVA-based vaccines with Matrix-M™ adjuvant. Recruitment, proliferation and activation of different immune cell populations in the draining LN shortly after vaccination was described. The results of this study highlight the immune potentiating effects of Matrix-M™ adjuvant with both protein- and MVA-based HA vaccines.

Finally, in chapter 4 the immunogenicity of an rMVA-based vaccine candidate expressing the HA gene from avian influenza A(H5N1) virus was assessed in a phase 1/2a clinical trial. The breadth and functionality of the vaccine-induced antibody and T cell response was analysed. This study further validates the rMVA-H5 vaccine candidate for human use in the event of a pandemic outbreak with influenza viruses of the H5 subtype.

Collectively, the studies described in chapters 2-4 fill gaps in the current understanding of the MVA vaccine vector in general and as an influenza vaccine in particular, and provide essential information for licencing of MVA as a vaccine vector. Furthermore, novel MVA-based influenza vaccine candidates have been constructed and tested. The implications of the results obtained in these studies are discussed in chapter 5.

Chapter 2

Validation of MVA as vaccine vector

CHAPTER 2.1

Modified Vaccinia virus Ankara preferentially targets antigen presenting cells *in vitro, ex vivo* and *in vivo*

AF Altenburg*, CE van de Sandt*, BWS Li, RJ MacLoughlin, RAM Fouchier, G van Amerongen, A Volz, RW Hendriks, RL de Swart, G Sutter, GF Rimmelzwaan & RD de Vries
*Authors contributed equally

Scientific Reports, 2017; 7(1)8580: 1–14

Modified Vaccinia virus Ankara (MVA) is a promising vaccine vector with an excellent safety profile. However, despite extensive pre-clinical and clinical testing, surprisingly little is known about the cellular tropism of MVA, especially in relevant animal species. Here, we performed *in vitro*, *ex vivo* and *in vivo* experiments with recombinant MVA expressing green fluorescent protein (rMVA-GFP). In both human peripheral blood mononuclear cells and mouse lung explants, rMVA-GFP predominantly infected antigen presenting cells. Subsequent *in vivo* experiments performed in mice, ferrets and non-human primates indicated that preferential targeting of dendritic cells and alveolar macrophages was observed after respiratory administration, although subtle differences were observed between the respective animal species. Following intramuscular injection, rMVA-GFP was detected in interdigitating cells between myocytes, but also in myocytes themselves. These data are important in advancing our understanding of the basis for the immunogenicity of MVA-based vaccines and aid rational vaccine design and delivery strategies.

Introduction

Modified Vaccinia virus Ankara (MVA) is an attenuated poxvirus that is frequently used as viral vector. MVA is derived from the chorioallantois vaccinia virus strain Ankara by serial passaging in chicken embryo fibroblasts (CEF) over 500 times. This resulted in major deletions in the viral genome and rendered MVA replication-deficient in mammalian cells[223]. MVA was used in smallpox vaccination regimens and has been tested in numerous clinical trials, resulting in the immunization of >100.000 study subjects without serious adverse events[277,278]. Moreover, MVA-based vaccines also proved safe in immunocompromised non-human primates[279]. Given this impressive safety record, combined with the capacity to encode genes of interest of up to 10 kb in size, MVA holds promise as a vaccine vector. Vaccination with recombinant (r)MVA leads to efficient induction of both humoral and cellular immune responses targeting proteins encoded by the inserted transgene (reviewed by de Vries *et al*.[209] & Altenburg *et al*.[280]). Because of these favourable properties, there has been considerable interest in developing rMVA-based vaccines against various infectious diseases and cancer, reflected by the steady increase in the number of clinical trials that have been performed with rMVA in recent years[250].

Despite frequent testing in clinical trials, the cellular tropism of MVA, particularly in relevant animal models, has been studied only to a limited extent. Even though the poxvirus lifecycle is complicated, in general poxviruses enter target cells via direct fusion with the cell membrane or endocytosis[281], but the cellular receptor enabling either process has not been identified. Because MVA promiscuously infects almost any cell type, a putative cellular receptor is expected to be a ubiquitously expressed protein shared by different cell types[282]. Extensive research has been performed with vaccinia virus (VACV), the parental pathogenic and replication-competent poxvirus closely related to MVA, which implicated an important role for cell surface proteoglycans in VACV attachment[283,284]. Identical or similar proteins could be involved in attachment and entry of MVA into target cells.

Recombinant viruses expressing fluorescent reporter proteins that can be sensitively traced *in vitro* and *in vivo* have been instrumental in improving our understanding of the tropism of different viruses[285-288]. Previous *in vitro* studies with human peripheral blood mononuclear cells (PBMC), performed to determine the cellular tropism of VACV, showed that recombinant VACV expressing green fluorescent protein (GFP) preferentially infected professional antigen-presenting cells (APC)[282,289,290]. In accordance with these results, similar *in vitro* infection studies with rMVA expressing GFP (rMVA-GFP) also demonstrated that APC were preferentially infected, directly followed by apoptosis of these target cells[245,291,292]. Furthermore, to determine the tissue tropism of MVA *in vivo*, mice were previously inoculated via the intranasal (IN), intraperitoneal (IP) or subcutaneous (SC) route with rMVA expressing luciferase[231,293]. In these studies, it was shown that following IN instillation rMVA-infected cells could be detected in nasal-associated lymphoid tissue (NALT), lungs and draining lymph nodes (LN) of the lungs. Following IP and SC injection, rMVA-encoded luciferase was detected in all lymphoid organs, lungs, liver and ovaries. A mouse study with rMVA-GFP demonstrated predominant infection of $CD11c^+$ dendritic cells (DC) in the spleen at 9 hour post-administration (HPA), however, in this study rMVA-GFP was administered intravenously[292], which is not a standard immunization route. These studies focused on tissue tropism in mice, but the nature and phenotype of cells targeted by MVA *in vivo* in this and other, more relevant, animal models after administration via routes commonly used for vaccination, remain largely unknown.

In order to extensively elucidate the tissue and cell tropism of MVA, we performed *in vitro*, *ex vivo* and *in vivo* infection studies with rMVA-GFP. In addition, we compared the *in vivo* cell tropism of MVA after IM injection with tropism after direct delivery to the respiratory tract. We demonstrated predominant infection of $CD11c^+$ MHC class II^+ DC by rMVA-GFP *in vitro* in human PBMC and *ex vivo* in mouse lung explants. *In vivo*, rMVA-GFP was detected in both interdigitating cells in between myocytes and myocytes themselves after IM injection, whereas direct administration of rMVA-GFP to the respiratory tract led to preferential targeting of alveolar macrophages (AM) in mice and DC in non-human primates, respectively. Since GFP^+ cells were subsequently detected in the LN draining the site of administration, we concluded that rMVA-GFP-infected cells migrated to secondary lymphoid tissues and that direct targeting of professional APC is involved in the shaping of the immune response.

Results

rMVA-GFP predominantly infects professional APC *in vitro* and *ex vivo*

To determine the cellular tropism of MVA *in vitro*, human PBMC were inoculated with rMVA-GFP at incrementing multiplicity of infection (MOI), ranging from 0.01 to 100. The percentage GFP$^+$ cells within different cell populations was determined by flow cytometry 24h post-inoculation. CD11c$^+$ HLA-DR^{high} DC and CD14$^+$ monocytes were readily infected by rMVA-GFP, even at low MOI. CD20$^+$ HLA-DR$^+$ B-lymphocytes were also easily infected by rMVA-GFP, followed by CD56$^+$ NK cells. In contrast, CD3$^+$ T-lymphocytes were refractory to infection with rMVA-GFP (**Fig. 1A**).

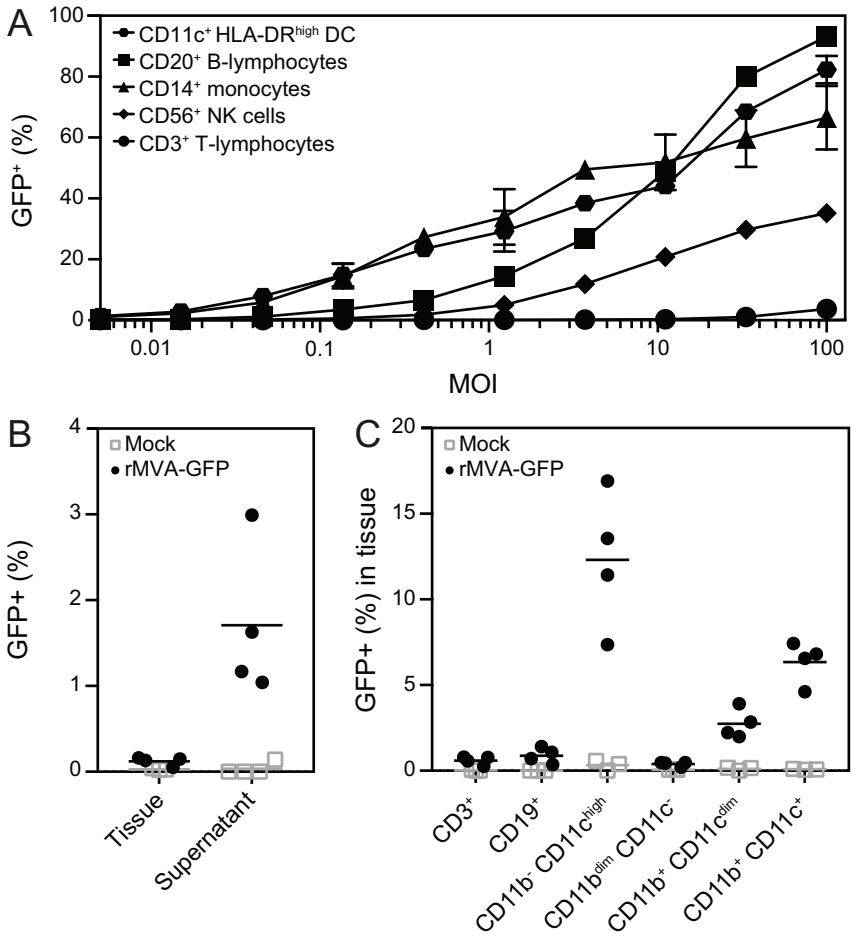

Figure 1. Populations infected by rMVA-GFP* in vitro *in human PBMC and* ex vivo *in mouse lung slices. *(**A**) Human PBMC were inoculated with rMVA-GFP at various MOI. Percentage of GFP$^+$ live cells within DC, B-lymphocyte, monocyte, NK cell and T-lymphocyte populations were determined by flow cytometry at 24h post-infection. Mean of duplicates and standard deviation are indicated. (**B**) Lung slices were inoculated with rMVA-GFP and analysed by flow cytometry after 24h. GFP$^+$ cells in single cell suspensions of lung tissue and culture supernatant were detected. (**C**) GFP$^+$ cells in single cell suspensions of lung slices were phenotyped by flow cytometry. Populations were defined as CD3$^+$, CD19$^+$, CD11b$^-$ CD11c^{high}, CD11b^{dim} CD11c$^-$, CD11b$^+$ CD11c^{dim} or CD11b$^+$ CD11c$^+$. Mean percentage of infection per population of four lung slice cultures is indicated.*

To determine MVA tropism in the respiratory tract, mouse lung slices were prepared and inoculated *ex vivo* with rMVA-GFP. At 24h post-inoculation, both the emigrant cells in the lung slice culture supernatant and single cells suspensions of the lung tissue were analysed for the presence of GFP^+ cells using flow cytometry. Interestingly, GFP^+ cells were mainly present in the supernatant of inoculated lung slice cultures, however, could also be detected in the single cell suspensions (**Fig. 1B**). Phenotyping of GFP^+ tissue-resident lung cells showed predominant rMVA-GFP infection of $CD11b^-$ $CD11c^{high}$ myeloid cells, commonly identified as AM or $CD103^+$ DC^{294}. However, $CD11c^+$ and $CD11c^{dim}$ myeloid cells double positive for $CD11b^+$ were also infected (**Fig. 1C**). $CD19^+$ B-lymphocytes were infected to a limited extent, whereas $CD11b^{dim}$ $CD11c^-$ single positive cells and $CD3^+$ T-lymphocytes were found refractory to infection (**Fig. 1C**).

rMVA-GFP-infected tissues and cells after IM or respiratory administration *in vivo*

In order to determine the tissue and cell tropism of MVA *in vivo*, rMVA-GFP was administered IM and to the respiratory tract of three different animal species (mice, ferrets and non-human primates, **Fig. 2**). Respiratory tract administration was performed by IN instillation, intra-tracheal (IT) inoculation or aerosol (AER) inhalation, depending on the animal model. Importantly, all routes in the respective animal models allowed for rMVA-GFP deposition in the lower respiratory tract. First, 10^7, 10^8 or 10^9 plaque-forming units (PFU) rMVA-GFP was administered to C57BL/6 mice via the IM or IN route. 6, 24 or 48 HPA mice were sacrificed to determine the optimal dose and time-point for follow-up experiments in ferrets and non-human primates.

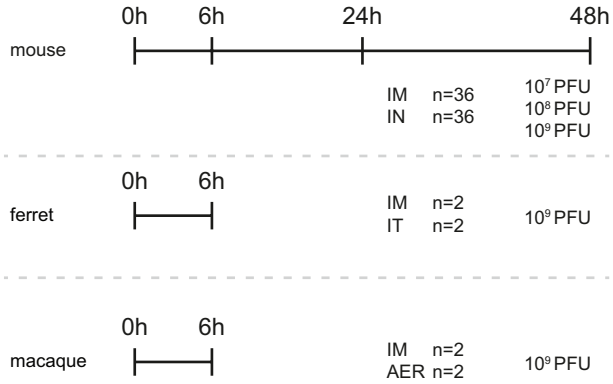

Figure 2. Experimental setup of rMVA-GFP* in vivo *studies. *Three different doses (10^7-10^9 PFU) of rMVA-GFP were administered to mice via IM injection or IN instillation. At 6, 24 or 48 HPA, mice were euthanized. Ferrets and macaques received 10^9 rMVA-GFP via IM injection or direct respiratory tract administration (IT inoculation for ferrets, AER inhalation for macaques) and were euthanized 6 HPA.*

rMVA-GFP targets myocytes and interdigitating cells after IM injection of mice

After IM injection of rMVA-GFP in mice, GFP^+ cells were consistently detected in the hind leg muscle in which rMVA-GFP was injected. Direct confocal laser scanning microscopy (CLSM) of muscle slices resulted in detection of GFP fluorescence in the muscle fibers (**Fig. 3A** & **Fig. S1**). Phenotypic characterization by dual staining and subsequent CLSM and immunohistochemistry (IHC) proved difficult for mouse

tissues, however, myocytes were clearly infected (**Fig. 3B**). GFP was never found in the isotype control staining of hind leg muscle (**Fig. 3B**). Furthermore, GFP$^+$ interdigitating cells were detected in the muscles and were identified as either having macrophage-/DC-like morphology or as part of the endomysium, the connective tissue that separates muscle fibers (**Fig. 3C**). Using IHC, GFP$^+$ cells were never found in the front leg muscle, which was used as a negative control (**Fig. 3C**).

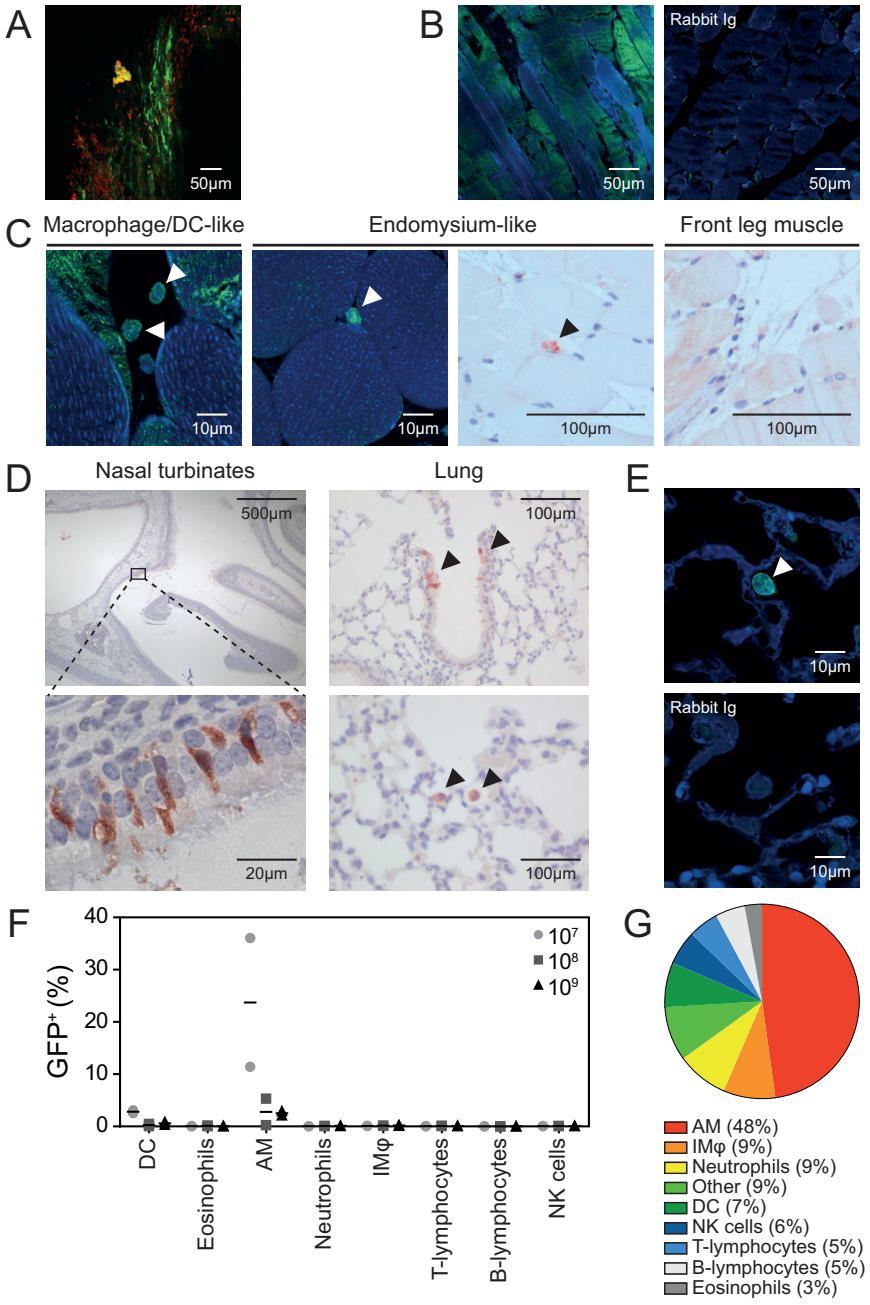

◄ ***Figure 3. GFP⁺ cells in muscle or respiratory tract after IM injection or IN instillation of rMVA-GFP to mice.*** *(**A**) Maximum intensity projection of a Z-stack of the hind leg muscle 24h after IM injection of rMVA-GFP. Green = GFP. Red = nucleus (stained by TO-PRO3). (**B**) Detection of GFP⁺ myocytes in hind leg muscle tissue after IM rMVA-GFP injection by staining with rabbit anti-GFP or rabbit Ig isotype (green) in combination with DAPI (blue). (**C**) Morphological characterization of GFP⁺ cells in hind leg muscle tissue after IM rMVA-GFP injection by CLSM (left two panels) or IHC (right two panels) showing hind leg muscle (24 HPA) or negative control front leg muscle (6 HPA). GFP⁺ interdigitating cells are indicated by arrows. CLSM: GFP = green, nucleus = blue (DAPI). IHC: GFP = red and counterstaining with haematoxylin. (**D**) Detection of GFP⁺ cells in the nasal turbinates and lungs 6 or 24h after IN instillation of rMVA-GFP. GFP⁺ cells are shown in red (indicated by arrows). Tissues were counterstained with haematoxylin. (**E**) Morphological characterization of GFP⁺ cells in lungs after IN instillation of rMVA-GFP by staining with rabbit anti-GFP or rabbit Ig isotype (green) in combination with DAPI (blue). GFP⁺ cell with macrophage-/DC-like morphology is indicated by arrow. (**F**) Percentage of GFP⁺ cells within different cell populations 6h after IN instillation of 10^7, 10^8 or 10^9 PFU rMVA-GFP determined by flow cytometry. Results are shown as mean of two mice. (**G**) Relative contribution of the different cellular subsets to the GFP⁺ population by reversed gating. The average percentages of all mice that received rMVA-GFP by IN instillation and were euthanized 6 HPA are shown. IMφ = interstitial macrophages. Contrast of some CLSM images has been linearly enhanced using Adobe Photoshop CC. Scale bars are indicated in each figure.*

rMVA-GFP targets predominantly AM in mice after IN instillation

At 6 or 24h after IN instillation of rMVA-GFP in mice, GFP⁺ cells were detected in both the nasal turbinates and the lungs. Mice were inoculated with a relatively large volume, directly exposing both the nasal cavity and the lungs. In the nasal turbinates, GFP⁺ cells were exclusively observed in the epithelial layer and had the morphology of epithelial cells. In the lungs, GFP⁺ cells were also detected in the epithelium of bronchioles, however, single GFP⁺ cells with an AM-like morphology were also observed in the lumen of the alveoli by IHC and CLSM (**Fig. 3D-E**). These data show that rMVA-GFP⁺ cells can consistently be detected at the anatomical site of administration and the infected cells morphologically resemble epithelial cells or AM.

Lungs of mice inoculated via the IN route were obtained during necropsy and single cell suspensions were prepared to determine the phenotype of GFP⁺ cells by multicolour flow cytometry (**Fig. S2**). GFP⁺ cells in the lungs were predominantly AM (defined as CD3⁻, CD19⁻, NK1.1⁻, Siglec-F⁺, CD11c⁺, F4/80⁺ and CD11b⁺), however, GFP⁺ DC (defined as CD3⁻, CD19⁻, NK1.1⁻, MHC class II⁺ and CD11c⁺) were also detected albeit to a lesser extent (**Fig. 3E**). Similar results were observed 24 HPA, whereas no GFP⁺ cells could be detected in the lungs 48 HPA (data not shown). Notably, when all GFP⁺ cells were selected at 6 HPA and subsequently characterized on basis of expression of various surface markers by reverse gating, it was found that AM constituted the largest proportion of GFP⁺ cells (48%, **Fig. 3F**).

rMVA-GFP-infected cells migrate to the draining LN and spread systemically in mice

To determine whether rMVA-GFP-infected cells migrated to the draining LN, the inguinal LN (ING-LN, draining the hind leg muscle) or mediastinal LN (MED-LN, draining the chest) was examined for presence of GFP⁺ cells after IM injection or IN instillation, respectively. As internal negative controls the axillary (AX-LN) draining the front leg muscle (after IM injection) or ING-LN (after IN instillation) were used. To determine whether rMVA-GFP could be detected systemically, blood and spleen samples were analysed for the presence of GFP⁺ cells.

After IM injection, GFP$^+$ cells were detected in single cell suspensions of the draining ING-LN as early as 6 HPA, mainly in mice that received the highest dose (10^9 PFU) rMVA-GFP. GFP$^+$ cells were hardly detected at later time-points and were never observed in the control AX-LN (**Fig. 4A**, left panel). Notably, GFP$^+$ cells were also detected systemically; in white blood cells (WBC) and single cell suspensions of the spleen at 6 and 24 HPA (**Fig. 4A**). After IN instillation of rMVA-GFP, low numbers of GFP$^+$ cells were detected in the MED-LN at all time-points, but not in the control ING-LN (**Fig. 4B**, left panel). Similar to IM rMVA-GFP injection, GFP$^+$ cells were detected systemically in WBC and spleen after IN instillation (**Fig. 4B**). Collectively, these data illustrate that both after IM injection and IN instillation, GFP$^+$ cells can be detected in the LN draining the site of inoculation and systemically.

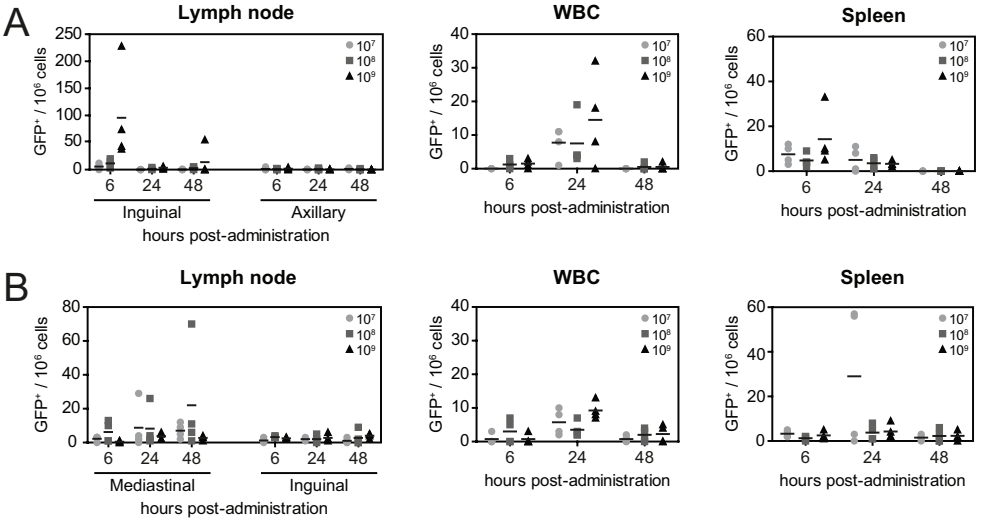

***Figure 4. Dissemination of GFP$^+$ cells after IM injection or IN instillation of rMVA-GFP to mice**. At 6, 24 or 48 HPA of 10^7, 10^8 or 10^9 PFU rMVA-GFP administration by IM injection (**A**) or IN instillation (**B**), GFP$^+$ cells were detected in LN, WBC and spleens using flow cytometry. Number of GFP$^+$ cells per 10^6 total cells is shown, mean of four mice is indicated.*

<u>rMVA-GFP-infected cells in ferrets are of DC- or macrophage-like morphology</u>

After determination of the optimal dose and kinetics of GFP expression in mice, ferrets received a high dose (10^9 PFU) of rMVA-GFP via either IM injection or IT inoculation and were sacrificed at 6 HPA. GFP$^+$ cells were detected in hind leg muscle slices after IM injection and lung slices and broncho-alveolar lavage (BAL) cells after IT inoculation, respectively (**Fig. 5A**). Although direct CLSM could not be used to determine the phenotype of GFP$^+$ cells, it demonstrated that rMVA-GFP infected cells were present at the site of administration at 6 HPA. BAL cells, WBC and single cells suspensions of lymphoid tissues obtained from ferrets were directly analysed for GFP expression by flow cytometry. By performing positive/negative scorings based on flow cytometry data (**Fig. 5B**), BAL cells were consistently positive after IT inoculation and GFP$^+$ cells disseminated from the site of administration and could be detected in the ING-LN draining the hind leg muscle and trachea-bronchial

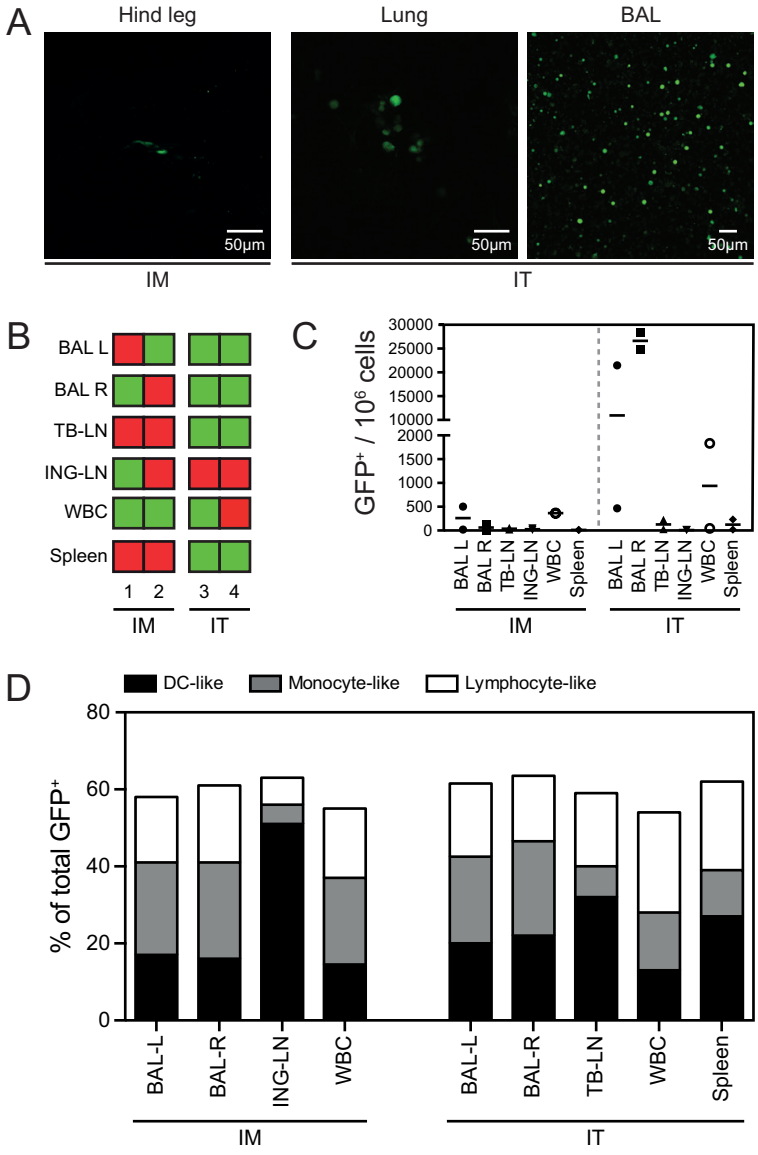

Figure 5. Detection of GFP⁺ cells in ferrets after IM injection and IT inoculation of rMVA-GFP. *(**A**) Direct detection of GFP⁺ cells using CLSM after IM injection (left panel) or IT inoculation (middle and right panel) of 10^9 PFU rMVA-GFP, 6 HPA. Middle panel shows direct CLSM of a lung slice, whereas the right panel shows cells recovered from the lungs by BAL. Contrast of certain images was linearly enhanced using Adobe Photoshop CC. (**B**) Overview of detection of GFP⁺ cells in BAL (left [L] or right [R] lung lobes), TB-LN, ING-LN, WBC or spleen in each individual ferret (n=2 per group) after IM injection or IT inoculation of rMVA-GFP. Green = GFP⁺. Red = GFP-negative. (**C**) Frequency of GFP⁺ cells in the respective tissues after IM injection or IT inoculation of rMVA-GFP. Number of GFP⁺ cells per 10^6 total cells is shown, mean of two ferrets is indicated. (**D**) GFP⁺ cells were phenotypically characterized as DC-like, monocyte-like or lymphocyte-like cells based on scatter properties of the different cell types.*

(TB-)LN draining the lungs after IM injection or IT inoculation, respectively (**Fig. 5B-C**). Systemic rMVA-GFP$^+$ cells were detected in both the spleen and WBC of multiple animals, however, the detection was not consistent. Low frequencies of GFP$^+$ cells were found in BAL after IM injection, potentially due to the circulation of GFP$^+$ cells in these animals (reflected by GFP$^+$ cells in PBMC). Of note, some tissues that scored positive in flow cytometry (**Fig. 5B**) appear negative in **Fig. 5C**, due to the low frequency of GFP$^+$ events. **Fig. S3** illustrates when tissues were scored positive using flow cytometry.

Phenotyping of GFP$^+$ cells in ferrets was experimentally challenging due to lack of the required ferret-specific antibodies directed against discriminative surface antigens. Therefore, we reversely gated the GFP$^+$ events observed in flow cytometry and discriminated between three different populations based on known scatter properties of different cell types: lymphocyte-like, monocyte-like and DC-like cells (**Fig. S3**). Notably, GFP$^+$ cells were equally distributed over the different populations for BAL, WBC and splenocytes, but there was a clear preference for DC-like cells in the draining LN of the hind leg muscle or lung after IM injection or IT inoculation, respectively. This suggests migration of rMVA-GFP-infected DC from the site of administration to the draining LN (**Fig. 5D**).

Validation of rMVA-GFP aerosol for administration to non-human primates

During aerosolization, an aerosol plume consisting of a droplet size distribution was generated. From within this plume, smaller droplets have a tendency towards deposition in the lower airways, whereas larger droplets most likely deposit in the nasal cavity and conducting airways. In order to fully characterize the aerosol and predict where in the respiratory tract rMVA-GFP may deposit, cascade impaction was performed during which the aerosol is fractioned into discrete droplet size ranges between 0.98 and 14.1µm. Each fraction was titrated in order to determine in what size aerosol droplets viable rMVA-GFP is present (**Fig. S4**). The Fine Particle Fraction (FPF) – the percentage of the rMVA particles contained in droplets under 5µm – was calculated as 96.75% with a mass median aerodynamic diameter (MMAD) of 1.70µm, predicting targeting of the lower airways of non-human primates. However, through the use of a facemask interface it was ensured that the nasal cavity/upper airways were exposed to aerosol as well. Collectively, these results confirm that rMVA-GFP can be delivered to the upper and lower respiratory tract of non-human primates via aerosol inhalation.

rMVA-GFP predominantly infects myocytes, DC and AM in non-human primates

After completion of ferret experiments, cynomolgus macaques were inoculated with 10^9 PFU rMVA-GFP by IM injection or aerosol (AER) inhalation[295-297]. Slices from either the hind leg muscle or lungs obtained from non-human primates at necropsy 6 HPA were analysed by direct CLSM, which revealed presence of GFP$^+$ cells after IM injection or AER inhalation, respectively (**Fig. 6A**). 3D reconstruction of a Z-stack obtained by CLSM of a non-human primate lung slice revealed that GFP$^+$ cells were predominantly detected in the lumen of the alveoli, and to a lesser extent directly in or connected to the epithelium lining the alveoli (**Fig. 6A** right panel, **Fig. S5**).

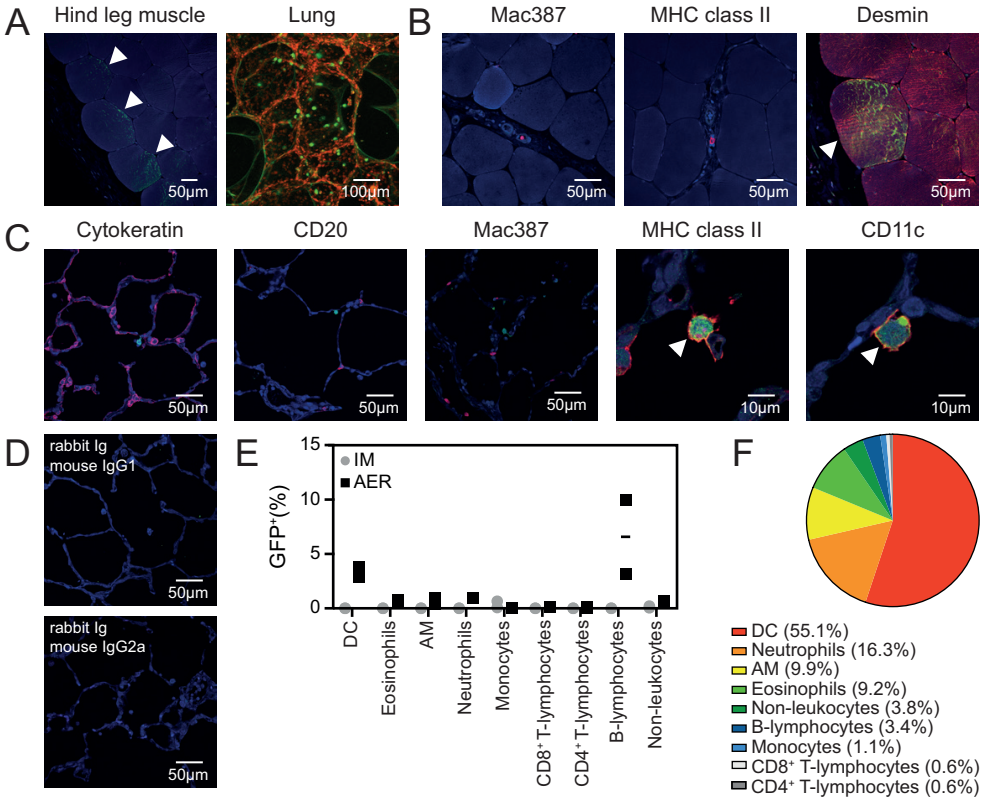

Figure 6. Identification of rMVA-GFP⁺ cells in macaque muscle or lung after IM injection or AER inhalation, respectively. *(**A**) Detection of GFP⁺ cells at site of rMVA-GFP administration. Left panel: hind leg muscle after IM injection stained with rabbit anti-GFP (green, indicated by arrows) and DAPI (blue). Right panel: direct detection of GFP fluorescence in lung slices after AER inhalation counterstained with TO-PRO3 (red). Maximum intensity projection of a Z-stack is shown. (**B**) Dual immunofluorescent staining of muscle slices after IM injection of rMVA-GFP with rabbit anti-GFP (green) in combination with DAPI (blue) and mouse anti-Mac387, anti-MHC class II or anti-desmin (red). Co-localization of GFP and desmin is indicated by an arrow. (**C**) Dual immunofluorescent staining of lung slices after AER inhalation of rMVA-GFP with rabbit anti-GFP (green) in combination with DAPI (blue) and mouse anti-cytokeratin, anti-CD20, anti-Mac387, anti-MHC class II or anti-CD11c (red). Co-localization of GFP and MHC class II or CD11c is indicated by arrows. (**D**) Lung slices stained with isotype control antibodies (rabbit Ig as control for anti-GFP, mouse IgG1 and 2a as control for cytokeratin, CD20, Mac387, MHC class II, CD11c, CD3 and desmin). (**E**) Percentage of GFP⁺ BAL cells within different cell populations after IM injection or AER inhalation of rMVA-GFP determined by flow cytometry. Mean of two macaques is indicated. (**F**) Relative contribution of the different subsets to the GFP⁺ population determined by reversed gating. The averages of the two animals that received rMVA-GFP by AER are shown. Contrast of some CLSM images has been enhanced linearly using Adobe Photoshop CC. Scale bars are indicated in images.*

Direct imaging of muscle and lung slices by CLSM did not allow identification of the phenotype of GFP⁺ cells, but guided collection of GFP⁺ tissues that could be used for subsequent dual immunofluorescent staining. Mac387⁺ interstitial macrophages (IMφ) and MHC class II⁺ antigen presenting cells were only detected infrequently in the muscles and co-localization with GFP could not be observed in non-human primates that received rMVA-GFP by IM injection. However, GFP mainly co-localized

with desmin, a specific marker for myocytes (**Fig. 6B**). Dual immunofluorescent staining of GFP$^+$ lung slices of non-human primates that were inoculated by AER inhalation revealed co-localization with MHC class II$^+$ and CD11c$^+$ APC (**Fig. 6C**). Morphologically, these cells resembled DC and AM. Co-localization of GFP with specific markers for T-lymphocytes (CD3, not shown), epithelial cells (cytokeratin), B-lymphocytes (CD20) or IMφ (Mac387) was not observed after AER inhalation (**Fig. 6C**). Isotype control stainings of lung slices were negative (**Fig. 6D**).

Subsequently, BAL samples from non-human primates inoculated by AER were analysed by multicolour flow cytometry. DC (CD45$^+$ HLA-DR$^+$ Siglec-8$^-$ CD16$^-$ CD11b$^+$ CD11c$^+$), eosinophils (CD45$^+$ HLA-DR$^+$ Siglec-8$^+$ CD16$^+$), AM (CD45$^+$ HLA-DR$^+$ Siglec-8$^-$ CD16$^-$ CD11b$^+$ CD11c$^-$), neutrophils (CD45$^+$ HLA-DR$^+$ Siglec-8$^-$ CD16$^+$), B-lymphocytes (CD45$^+$ CD3$^-$ HLA-DR$^+$), CD4$^+$/CD8$^+$ T-lymphocytes (CD45$^+$ CD3$^+$) and non-leukocytes (CD45$^-$) were analysed for GFP expression (**Fig. S6**). Respiratory samples collected after IM injection were used as negative control and indeed GFP$^+$ cells were not detected (**Fig. 6E**). The relative percentage of GFP$^+$ cells within subsets was highest in B-lymphocytes and DCs (**Fig. 6E**). In addition, GFP$^+$ eosinophils, AM, neutrophils and non-leukocytes, probably representing epithelial cells, were detected (**Fig. 6E**). Reverse gating of GFP$^+$ cells showed that DCs constituted 55.1% of the GFP$^+$ cells and were the largest GFP$^+$ cell population. Interestingly, although B-lymphocytes showed the highest rMVA-GFP infection rate, the number of B-lymphocytes recovered from non-human primate lungs was low, which explains the low contribution of B-lymphocytes to the total GFP$^+$ cell population (**Fig. 6E-F**).

<u>rMVA-GFP-infected cells migrate to the draining LN in non-human primates</u>

To determine whether rMVA-GFP$^+$ cells in non-human primates migrated to draining LN and spread systemically, WBC and single cell suspensions of the LN and spleen were analysed by flow cytometry. By performing positive/negative scorings based on flow cytometry data of the different tissues, we found that the BAL of AER inoculated macaques was consistently positive, and showed that GFP$^+$ cells had migrated to the draining ING-LN after IM injection (2/2 non-human primates, **Fig. 7A**). However, the TB-LN was not consistently GFP$^+$ after AER inhalation (1/2 non-human primates, **Fig. 7A**). GFP$^+$ cells were never detected in the spleen, and GFP$^+$ WBC were only observed after IM injection in 1/2 animals (**Fig. 7A**). Thus, apart from migration of MVA-infected cells to the draining LN, systemic spread of GFP$^+$ cells was detected to a limited extent (**Fig. 7**). Of note, some tissues that scored positive in flow cytometry (**Fig. 7A**) appear negative in **Fig. 7B**, due to the low frequency of GFP$^+$ events. **Fig. S6** illustrates when tissues were scored positive using flow cytometry.

Discussion

In this study, we systematically assessed tissue and cell tropism of the vaccine vector MVA *in vitro*, *ex vivo* and *in vivo* using an rMVA expressing a fluorescent reporter protein. Even though different animal species and administration routes were used, we demonstrated consistent predominant infection of MHC class II$^+$ APCs. In addition, in the different species local myocytes and local epithelial cells were infected after either IM injection or respiratory administration, respectively.

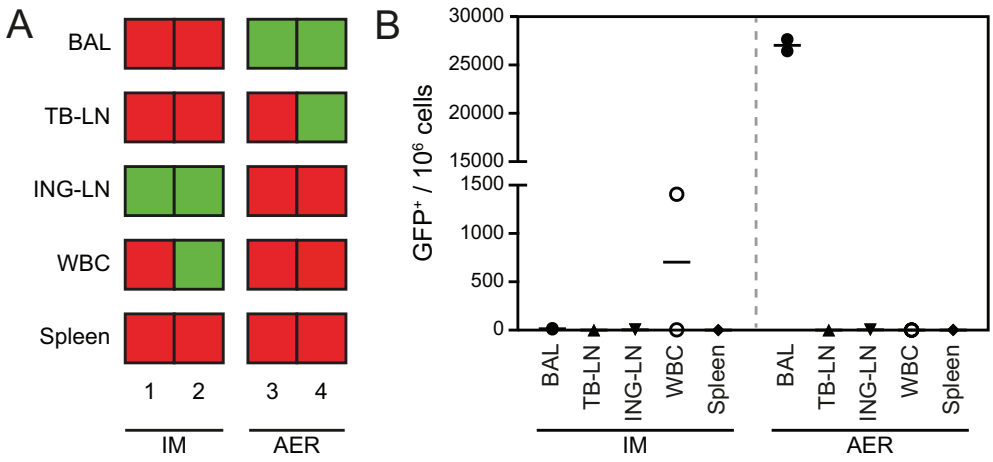

Figure 7. Dissemination of rMVA-GFP⁺ cells in macaques. *(**A**) Overview of GFP⁺ cells detected in BAL, TB-LN, ING-LN, WBC or spleen in each individual macaque (n=2 per group) after IM injection or AER inhalation of rMVA-GFP. Green = GFP⁺. Red = GFP-negative. (**B**) Frequency of GFP⁺ cells in the respective tissues after IM injection or AER inhalation of rMVA-GFP. Number of GFP⁺ cells per 10^6 total cells is shown, mean of two macaques is indicated.*

Vaccination is the cornerstone control measure to reduce morbidity and mortality caused by infectious diseases. However, vaccination against hypervariable and emerging pathogens can be challenging. For example, seasonal influenza vaccines need to be updated almost annually to antigenically match emerging drift variant viruses and to maintain vaccine efficacy. Furthermore, in case of an emerging pandemic strain of influenza virus, timely production of a pandemic influenza vaccine has proven to be challenging[132,133]. The rapid construction of recombinant viral vaccine vectors, such as MVA, which allows easy insertion of any or multiple antigens of choice and rapid production of a large number of vaccine doses, is an attractive alternative to conventional vaccine production technology[266,274]. In addition, MVA has been considered as vaccine delivery system for many other infectious diseases and cancers[298,299]. Despite the increasing number of successful clinical trials performed with rMVA-based vaccines in recent years[250], surprisingly little is known about their mode of action and the *in vivo* tissue and cell tropism of MVA, particularly in the ferret model, the golden standard for influenza virus pathogenesis studies, and animal models more closely related to humans, such as non-human primates. This gap of knowledge could potentially hamper future registration of MVA-based vaccines for use in humans.

In this study, we describe the use of rMVA-GFP, allowing detection of single rMVA-GFP infected cells with high sensitivity, to elucidate the tropism of the viral vector MVA. *In vitro* tropism was investigated by inoculating human PBMC with rMVA-GFP, *ex vivo* tropism by inoculation of mouse lung explants and *in vivo* tropism by inoculating three different animal species via two different administration routes. In general, myeloid cells (mainly DC and macrophages) were preferentially infected by rMVA-GFP, independent of the experimental set-up, animal species or route of administration. Direct targeting of APC in mice, ferrets and non-human primates

confirms the suitability of MVA as vaccine vector, since they are involved in shaping the immune response. Of note, the relation between vector tropism and vaccine immunogenicity is not always straightforward, for example optimizing DC infection by an adenovirus vector did not result in increased immunogenicity in non-human primates[300].

Upon *in vitro* inoculation of human PBMC with rMVA-GFP, DCs, monocytes and B-lymphocytes – all expressing MHC class II – were predominantly infected. NK cells were also targeted by rMVA-GFP (**Fig. 1A**) but T-lymphocytes were refractory to MVA infection, which was in accordance with previously published data obtained with both VACV and MVA[290-292]. In addition, the tropism of rMVA-GFP was assessed *ex vivo* in the respiratory tract in mouse lung slices. Due to limited use of surface markers, discrimination of distinct DC and monocyte populations was not possible. However, GFP^+ cells were mainly identified in $CD11c^{high}$ cells, most likely AM or $CD103^+$ DC[294] (**Fig. 1C**). Although these *in vitro* and *ex vivo* studies to elucidate the cellular tropism of MVA are of interest, they may not accurately reflect the *in vivo* situation and the cells infected with MVA at the site of administration.

Previous *in vivo* studies mainly focused on the tissue tropism of MVA[231,293,301], whereas this study focused on the cellular tropism. *In vivo* administration of rMVA-GFP to mice, ferrets and non-human primates – via the IM or respiratory route – consistently resulted in the detection of GFP^+ cells at the site of administration. In pre-clinical and clinical studies MVA is most commonly administered by IM injection, however, the local cell types that are initially infected by MVA have thus far not been identified. Here we showed that directly after IM injection, rMVA-GFP infected both myocytes and interdigitating cells, potentially macrophages, DC or part of the endomysium (**Fig. 3, 5, 6**). Unfortunately, we were unable to determine the exact phenotype the rMVA-GFP-infected interdigitating cells in non-human primates due to the low frequency of GFP^+ cells in the muscle tissue.

Due to sensitive detection of GFP^+ cells in single cell suspensions of lungs or BAL cells, identification of rMVA-GFP^+ cells after respiratory administration of rMVA-GFP was feasible. IN instillation of mice with a relative large volume rMVA-GFP delivered the vector both to nasal turbinates and lungs. Consequently, MVA-infected epithelial cells were detected in the nasal turbinates and lungs, however, AM in the lungs were also frequently infected (**Fig. 3**). This is in concordance with results obtained in other studies, which showed that IN instillation of mice with rMVA-GFP resulted in the infection of $CD11c^+$ MHC class II^- AM detected in BAL[244]. Targeting of myeloid cells was also observed after IT inoculation of ferrets with rMVA-GFP (**Fig. 5**), however, lack of ferret-specific antibodies required to distinguish between cell populations hampered the possibility to determine the exact phenotype of these rMVA-GFP-infected cells.

In contrast to mice, the predominant target cells for rMVA-GFP in the lungs of non-human primates were not characterized as $CD11c^+$ MHC class II^- AM, but as $CD11c^+$ MHC class II^+ DC. This was shown by both flow cytometry of BAL cells and *in situ* by CLSM after dual immunofluorescence staining of lung tissue (**Fig. 6**). In addition to

preferential targeting of DC, rMVA-GFP was also detected in AM, $CD45^-$ epithelial cells, eosinophils and neutrophils by flow cytometry of BAL cells. The highest infection rate was observed in B-lymphocytes, but the numbers of B-lymphocytes present in BAL obtained from non-human primates were low (**Fig. 6**). DC largely contributed to the total number of rMVA-GFP^+ cells, but neutrophils also formed a substantial component. Interestingly, it has been shown that after intradermal injection of MVA in mice, neutrophils become infected by MVA and subsequently migrate to the draining LN and bone marrow where they can prime phenotypically different $CD8^+$ T-lymphocyte populations[302].

In addition to detection at the site of administration, GFP^+ cells were also detected in the respective draining LN after either IM injection or administration into the airways as early as 6 HPA. As the only exception, IN instillation of mice led to detection of GFP^+ cells in the draining LN at later time-points (24-48 HPA, **Fig. 4**), possibly because the MED-LN were tested in this species instead of the TB-LN, which could not be harvested during necropsy of mice. Taken together, these data suggest that after administration, MVA locally infects APC that subsequently migrate to the draining LN. In addition, GFP^+ cells were detected systemically in both blood and spleen in mice, particularly at 24 HPA (**Fig. 4**). Ferrets and non-human primates were euthanized 6 HPA, which could explain why systemic spread of MVA-GFP^+ cells was observed only to a limited extent (**Fig. 5, 7**).

The standard route for administration of MVA-based vaccines is intramuscular (IM) injection. However, for the induction of protective mucosal immunity against respiratory pathogens, delivery of MVA to the respiratory tract has been considered (reviewed by Tonnis *et al*.[303])[206,295,304]. In this study, rMVA-GFP was administered to the respiratory tract of non-human primates as an aerosol, as best possible proxy for future studies with MVA-based respiratory vaccines. Importantly, the aerosol droplet size and nebulizer delivery system chosen in this study allowed exposure of the entire upper and lower respiratory tract to infectious virus, allowing accurate definition of target cells (**Fig. S4**). Furthermore, aerosol delivery is under extensive investigation as an alternative for vaccine delivery by injection, as it abolishes the necessity for hypodermic needles. This facilitates safety of large-scale vaccination campaigns in developing countries with high prevalence of blood-borne infections, as there is no need for a complicated infrastructure to dispose of potentially contaminated needles. Finally, direct administration of vaccines to the respiratory tract could lead to efficient induction of local immune responses leading to increased protection from respiratory pathogens. This has been evaluated extensively with a live-attenuated influenza vaccine administered IN to children (FluMist®), showing that nasal spray administration led to efficient induction of local mucosal IgA antibody responses[204-206]. Similar advantages potentially exist when rMVA is used as live vaccine against respiratory pathogens and could lead to the induction of local humoral and cellular immune responses (tissue-resident T-lymphocytes)[304,305].

In summary, we are the first to comprehensively examine the tropism of MVA *in vitro*, *ex vivo* and *in vivo* in different species. Preferential targeting of APCs by rMVA-GFP was demonstrated *in vivo* in each animal model, regardless of the route of

administration. Furthermore, delivery of rMVA-GFP to the respiratory tract of non-human primates as an aerosol also resulted in infection of local epithelial cells and IM injection resulted in infection of myocytes. In mice, AM were preferentially infected over DC which was opposite in the case of non-human primates. Of interest, preferential targeting of DC over AM would be an advantage for a vector-based vaccine, as AM are notoriously inefficient APC in comparison to DC[306-309]. As a proxy for the sequence of events after vaccination of humans with MVA, the non-human primate data show that directly after administration, MVA infects local APC, which in the case of aerosol delivery were CD11c^{+} MHC class II^{+} DC in the lung. These rMVA-GFP^{+} DC subsequently migrate to the draining LN, where they can present antigens via both MHC class I and II to responder cells, leading to an efficient shaping of the immune response (reviewed by Braciale *et al*.[310])[311]. Previously, it was shown that infection of DC with MVA induced their maturation, potentially forming the basis of direct and cross-presentation of MVA-encoded antigens by HLA class I and II[291]. Whether rMVA-GFP-infected APC present antigens to responder cells directly, or via uptake of antigen by other DC for MHC class II- and cross-presentation, was not examined in this study. Data obtained in this study show that direct targeting of professional APC could explain the excellent immunogenicity of MVA-based vaccines. Knowledge on targeting of specific cell types by MVA could guide future vaccine design and delivery strategies.

Materials and Methods

Ethics statement

The use of human PMBC for scientific research was approved by the Medical Ethics Committee (METC) of the Erasmus MC (permit number MEC-2015-095). All participants gave informed consent and permission for use of materials to study infectious diseases, no identifying information was published. All work described has been carried out in accordance with the code of ethics of the world medical association (declaration of Helsinki). Animal experiments were conducted in strict compliance with European guidelines (EU directive on animal testing 2010/63/EU) and the animal protocol was approved by an independent animal experimentation ethical review committee (Erasmus MC permit number EUR3293). Animal welfare was observed on a daily basis and to minimize animal suffering all animal handling was performed under light anaesthesia using 4% isoflurane in oxygen (mice) or a mixture of 10.mg/kg ketamine and 0.05mg/kg medetomidine (ferrets and non-human primates). To antagonize the effect of medetomidine, atipamezole was administered after handling.

Generation of rMVA-GFP

rMVA-GFP was generated by homologous recombination as described previously[247]. Briefly, MVA clonal isolate F6[223] served as the parental virus for generating rMVA-GFP. Vector plasmid pG06-P11-GFP was used to direct insertion of GFP coding sequences under the transcriptional control of the natural VACV late promotor P11 into the deletion III site in the MVA genome. Virus stocks were generated in CEF, purified by ultracentrifugation through 36% sucrose and reconstituted in a 120mM NaCl 10mM Tris-HCl buffer (pH 7.4). Titre of the rMVA-GFP stock was determined by plaque assay on CEF and the construct was validated by PCR, nucleotide sequencing and transgene expression in various cell types.

In vitro infections of human PBMC

PBMC were isolated from blood obtained from healthy humans and seeded into 96-wells low-adherent V-bottom plates at 50.000 cells/well. Subsequently, cells were inoculated with rMVA-GFP at incrementing MOI (range MOI 0.01–100, 3-fold titration), for 1h, washed and incubated for 24h in Roswell Park Memorial Institute (RPMI) 1640 medium (Lonza) supplemented with 10% heat-inactivated foetal bovine serum (HI-FBS, Greiner Bio-One), 100µg/ml penicillin, 100U/ml streptomycin (Lonza) and 2mM L-Glutamine (Lonza) (P/S/G) at 37°C. After 24h, cells were harvested and stained with CD3$^{APC/Cy7}$ (BD Pharmingen), CD11c^{APC} (BD Pharmingen), CD14$^{PerCP/Cy5.5}$ (BD Pharmingen), CD56^{PE} (BD Pharmingen), CD20$^{PE/Cy7}$ (Becton Dickinson) and HLA-DR^{PB} (Biolegend), in combination with LIVE/DEAD aqua fixable stain (Invitrogen).

Cells were analysed on a flow cytometer (FACS Canto II) and the percentage of infected cells (GFP^+) within the respective subsets was determined using FACS Diva software (BD Biosciences).

Ex vivo infection of mouse lung explants

Lungs from mice that received IM injection with rMVA-GFP (no GFP^+ events were detected in the lungs) were inflated with 4% low-melting 2-hydroxyethylagarose in PBS mixed with an equal part of Dulbeccos' Modified Eagle's Medium (DMEM, Lonza Bio-Whittaker)/Ham's F12 medium (Gibco) supplemented with 10% HI-FBS, P/S/G and amphotericin B (1µg/ml, institutional pharmacy). Lung slices of approximately 1mm thick were cut and used for *ex vivo* infections with rMVA-GFP as described previously[312]. In short, 24h post-inoculation single cell suspensions were obtained by digestion (described below), and subsequently stained with $CD3^{PerCP}$ (BD Pharmingen), $CD19^{PE\text{-}Cy7}$ (BD Pharmingen), $CD11c^{APC}$ (BD Pharmingen) and $CD11b^{APC\text{-}Cy7}$ (BD Pharmingen), in combination with LIVE/DEAD aqua fixable stain. Samples were acquired on a flow cytometer (FACS Canto II) and analysed using FACS Diva software (BD Biosciences). One mock-infected lung slice was excluded from the FACS analysis due to high aspecific background.

In vivo inoculation of mice with rMVA-GFP

Specified pathogen free, 6-8-week-old, female C57BL/6 mice (n=72) were purchased from Charles River and housed in individual ventilated cage (IVC) units with access to food and water ad libitum. Mice were inoculated with 10^7, 10^8 or 10^9 PFU rMVA-GFP in PBS administered either by IM injection in both hind legs (50µl/leg) or IN instillation (50µl). Mice were euthanized by cervical dislocation under isoflurane anaesthesia at 6, 24 and 48 HPA. After euthanasia, blood, ING-LN, spleen, head, lungs and trachea were obtained from all animals for analysis. In addition, the AX-LN and leg muscles were collected from IM injected animals and the MED-LN was collected from IN instilled mice.

In vivo inoculation of ferrets with rMVA-GFP

Four 6-12 months old female ferrets (*Mustela Putorius furo*) were housed in negatively pressurized, HEPA-filtered BSL-3 isolator cages and provided with commercial food pellets and water *ad libitum*. Ferrets were inoculated with 10^9 PFU rMVA-GFP in PBS via either IM injection, in both hind legs (200µl/leg), or IT inoculation (1ml). Ferrets were euthanized by exsanguination at 6 HPA under deep ketamine sedation (20mg/kg body weight, **Fig. 2**). Blood, ING-LN, spleen, nose, trachea, primary bronchus, lungs, BAL and TB-LN were obtained from all animals. Leg muscles were exclusively obtained from the IM injected ferrets.

Droplet size characterization of rMVA-GFP aerosol

To characterize the aerosol droplet diameter following nebulization of rMVA-GFP, 10^9 PFU rMVA-GFP diluted in 0.5ml PBS was nebulized using a vibrating mesh nebulizer (Aeroneb Lab nebulizer, Aerogen Limited) as previously described[313]. The MMAD of the resulting aerosol was determined using a Cascade Impactor at 15 litres per minute vacuum flow rate (NGI, Copley Scientific).

In vivo aerosol inoculation of non-human primates with rMVA-GFP

Four male, healthy cynomolgus macaques (6-8-years-old, *Macaca fascicularis*) were obtained and reused one year after a non-lethal measles vaccination and challenge experiment. All animals were housed in negatively pressurized, HEPA-filtered BSL-3 isolator cages and were inoculated with 10^9 PFU rMVA-GFP in PBS via either IM injection in both hind legs (200µl/leg), or by aerosol inhalation. Briefly, rMVA-GFP was administered using a nebulizer (Aeroneb Lab nebulizer, Aerogen Limited) connected to a 22mm T-piece and using a silicone pediatric resuscitation mask (ComfortSeal silicone mask assembly, small, Monaghan Medical Corp.) as the interface with the non-human primates[297]. Using this method, 10^9 PFU rMVA-GFP (0.5ml) was nebulized and administered to the non-human primates. Animals were euthanized by exsanguination at 6 HPA under deep ketamine sedation (20mg/kg body weight, **Fig. 2**). Blood, inguinal LN, spleen, nasal septum, nasal concha, trachea, primary bronchus, lungs, BAL and TB-LN were collected from all animals. Leg muscles were exclusively obtained from IM injected non-human primates.

Processing of blood, BAL and lymphoid samples

Blood samples from mice, ferrets and non-human primates were collected in Vacuette tubes containing K_3EDTA as an anticoagulant. Pure WBC were obtained by treatment of EDTA blood with red blood cell (RBC) lysis buffer (Roche diagnostics). A BAL was performed post-mortem in ferrets and non-human primates by direct infusion of 10ml PBS into the lungs, followed by immediate recovery of the fluid.

Lymphoid organs were collected from animals during necropsy in Iscove's Modified Dulbecco's Medium (IMDM, Lonza Bio-Whittaker) supplemented with 5% HI-FBS and P/S/G. Single cell suspensions were generated by using 100µm cell strainers (Falcon). Spleen single cell suspensions were subsequently treated with RBC lysis buffer in order to remove erythrocytes. Collectively, WBC, BAL cells and single cell suspensions from lymphoid organs were directly analysed for presence of GFP by flow cytometry on a FACS Canto II (BD Biosciences). GFP^+ samples were subsequently stained in order to phenotype GFP^+ events (see below). Mouse ING-LN and WBC samples after IM injection (n=1), spleen after IN instillation (n=1) were excluded from FACS analysis due to high background signal.

Preparation and processing of lungs

Mouse lungs were either fixed by inflation with 10% formalin or complete single cell suspensions were prepared by digestion. Formalin-fixed tissues were subsequently analysed by immunohistochemistry and/or dual immunofluorescent staining. Single cell suspensions were prepared by treatment with 300U/ml collagenase type I (Invitrogen) and 0.15mg/ml DNase (Roche diagnostics) diluted in Hank's Balanced Salt Solution (HBSS, Gibco) for 1h at 37°C, followed by filtration over 100µm cell strainers. Excess erythrocytes were removed by treatment with RBC lysis buffer if necessary. Single cell suspensions were used directly for detection of GFP by flow cytometry. GFP^+ samples were subsequently stained in order to phenotype GFP^+ events (see below).

Ferret and non-human primate lungs were inflated with 4% low-melting 2-hydroxyethylagarose in PBS mixed with an equal part of DMEM/Ham's F12 medium (Gibco) supplemented with 10% HI-FBS, P/S/G and amphotericin B. Lung slices of approximately 1mm thick were cut and used for direct analysis of GFP fluorescence using CLSM. After direct detection of GFP, lung slices were fixed in 10% formalin, paraffin embedded and subsequently analysed by immunohistochemistry and/or dual immunofluorescent staining.

Phenotyping by flow cytometry

Freshly isolated WBC, BAL cells and single cell suspensions prepared from lymphoid organs or the lungs were analysed directly for GFP expression using a FACS Canto II flow cytometer and FACS Diva software (BD Bioscience). Approximately 1×10^6 events were obtained per sample to allow detection of low frequent GFP^+ populations. Samples positive for GFP were subsequently stained to phenotype the GFP^+ cells. Cells obtained from mouse lungs were subdivided into DC, eosinophils, AM, neutrophils, IMφ, $CD4^+$ and $CD8^+$ T-lymphocytes, B-lymphocytes and NK cells by blocking Fc receptors with 2.4G2 and staining with Siglec-F^{PE} (BD), $CD3^{PE/CF594}$ (BD), $CD19^{PerCP/Cy5.5}$ (eBioscience), $CD8^{PE/Cy7}$ (eBioscience), $CD11c^{EF450}$ (eBioscience), $CD4^{BV605}$ (BD), $MHCII^{BV650}$ (BD), $CD45^{BV711}$ (BD), $F4/80^{Biotin}$ (eBioscience) followed by $Streptavidine^{BV786}$ (BD), $NK1.1^{APC}$ (BD), $CD11b^{AF700}$ (eBioscience) and $Gr\text{-}1^{APC/EF780}$ (eBioscience). BAL cells obtained from non-human primates were subdivided into DC, eosinophils, AM, neutrophils, monocytes, epithelial cells, $CD4^+$ and $CD8^+$ T-lymphocytes and B-lymphocytes by blocking Fc receptors with human serum and staining with $CD33^{PE}$ (eBioscience), $CD19^{PE/TXR}$ (Beckman Coulter), $CD16^{PerCP/Cy5.5}$ (BD), $CD11b^{PE/Cy7}$ (BD), $CD8a^{EF450}$ (eBioscience), $CD68^{Biotin}$ (Biolegend) followed by $Streptavidine^{BV650}$ (BD), $MHCII^{BV711}$ (BD), $CD45^{BV786}$ (BD), Siglec-8^{APC} (Biolegend), $CD11c^{AF700}$ (BD) and $CD3^{APC/Cy7}$ (BD). For both mice and non-human primates, dead cells were disregarded in the analysis by excluding cells stained with LIVE/DEAD aqua fixable stain and the percentage GFP^+ cells within each cell population was determined using a FACS LSR II (BD Biosciences).

Tissue preparation for immunohistochemistry

To determine the tropism of rMVA-GFP in the upper respiratory tract, complete mouse heads were fixed in 10% formalin. Heads were subsequently decalcified for eight days using a 10% EDTA buffer, split in two halves, and decalcification was continued for another two days, followed by embedding in paraffin. To determine cellular tropism in the upper respiratory tract from ferrets and non-human primates, nasal tissue from ferrets was harvested and formalin fixed, and the nasal septa and concha from non-human primates were harvested and fixed. Tissues were decalcified before embedding into paraffin if required. Furthermore, in addition to analysis of the nasal cavities and lungs, the trachea and primary bronchi from all animals were collected in 10% formalin. To determine the tropism of rMVA-GFP in the muscles, hind and front leg muscles were harvested in PBS. If possible, the exact site of the rMVA-GFP injection was harvested. Subsequently, slices were cut for direct examination of GFP fluorescence using CLSM. Positive slices were formalin-fixed and paraffin-embedded, followed by immunohistochemistry and/or

dual immunofluorescence staining. In all animal models, the front leg muscles formed the appropriate negative control for the inoculated hind leg muscle tissues.

Direct confocal laser scanning microscopy (CLSM)
Slices obtained from muscle tissues or agarose-inflated lungs were directly analysed for GFP fluorescence using CLSM with a LSM700 system fitted on an Axio Observer Z1 inverted microscope (Zeiss). Images and videos were generated using Zen software. GFP^+ muscle from mice and lungs slices from cynomolgus macaques were transferred to 4% (w/v) paraformaldehyde in PBS, permeabilized with 0.1% (v/v) Triton-X100 for 30min and subsequently counterstained for nuclei with TO-PRO-3 (Invitrogen).

Immunohistochemistry and dual immunofluorescence analysis of formalin-fixed tissues
Sections from formalin-fixed paraffin-embedded tissues were cut (3µm) and deparaffinised. In order to detect GFP, antigen retrieval was performed in 10mM citrate buffer. For histological evaluation, samples were subsequently incubated overnight with anti-GFP polyclonal rabbit antibody (Invitrogen) at 4°C, followed by incubation with a secondary goat-anti-rabbit-biotin antibody (DAKO) and streptavidin-HRP (DAKO). GFP was detected using 3-amino-9-ethylcarbazole (AEC) as substrate. The slides were counterstained with haematoxylin[313].

On mouse and non-human primate hind leg muscle and lung tissues dual immunofluorescence stainings were performed. After antigen retrieval in citrate buffer, tissues were incubated with 10% normal goat serum (Bio-Connect) in PBS. Mouse tissues were stained with rabbit anti-GFP (Invitrogen) or rabbit IgG isotype (R&D Systems) followed by goat-anti-rabbit Alexa Fluor (AF)488 (Life Technologies). Non-human primate tissues were stained with rabbit anti-GFP in combination with mouse-derived antibodies: anti-desmin (Abcam), anti-cytokeratin (DAKO), anti-Mac387 (AbD Serotec), anti-MHC class II (HLA-DP/DQ/DR, DAKO), anti-CD11c (Novocastra Biosystems Newcastle Ltd) or anti-CD20 (DAKO). As a negative control, lung slices were stained with rabbit IgG isotype in combination with either mouse IgG1 or IgG2a isotype (R&D Systems). Subsequently, tissues were stained with goat-anti-rabbit AF488 and goat-anti-mouse AF549 (Invitrogen). All samples were treated with ProLong Gold antifade reagent with DAPI (Life Technologies) before analysis using CLSM with a LSM700 system fitted on an Axio Observer Z1 inverted microscope (Zeiss). Images were analysed using Zen software.

Data availability
All data generated or analysed during this study are included in this published article (and its Supplementary Information files).

Acknowledgements
The authors would like to thank Mark Pronk, Nella Nieuwkoop, Stella van Trierum, Heidi De Gruyter, Alwin de Jong and Peter van Run for excellent technical assistance. This project was funded by the European Commission FP7 project FLUNIVAC (project number 602604) and the European Research Council grant FLUPLAN (250136).

Supplementary Material

[Online movie]

***Figure S1. CLSM 3D render of mouse hind leg muscle**. Z-stack of a hind leg muscle slice from a IM rMVA-GFP injected mouse was obtained by CLSM. A 3D render of the maximum intensity projection was generated using the Zen software. GPF = green. Nucleus = red.*

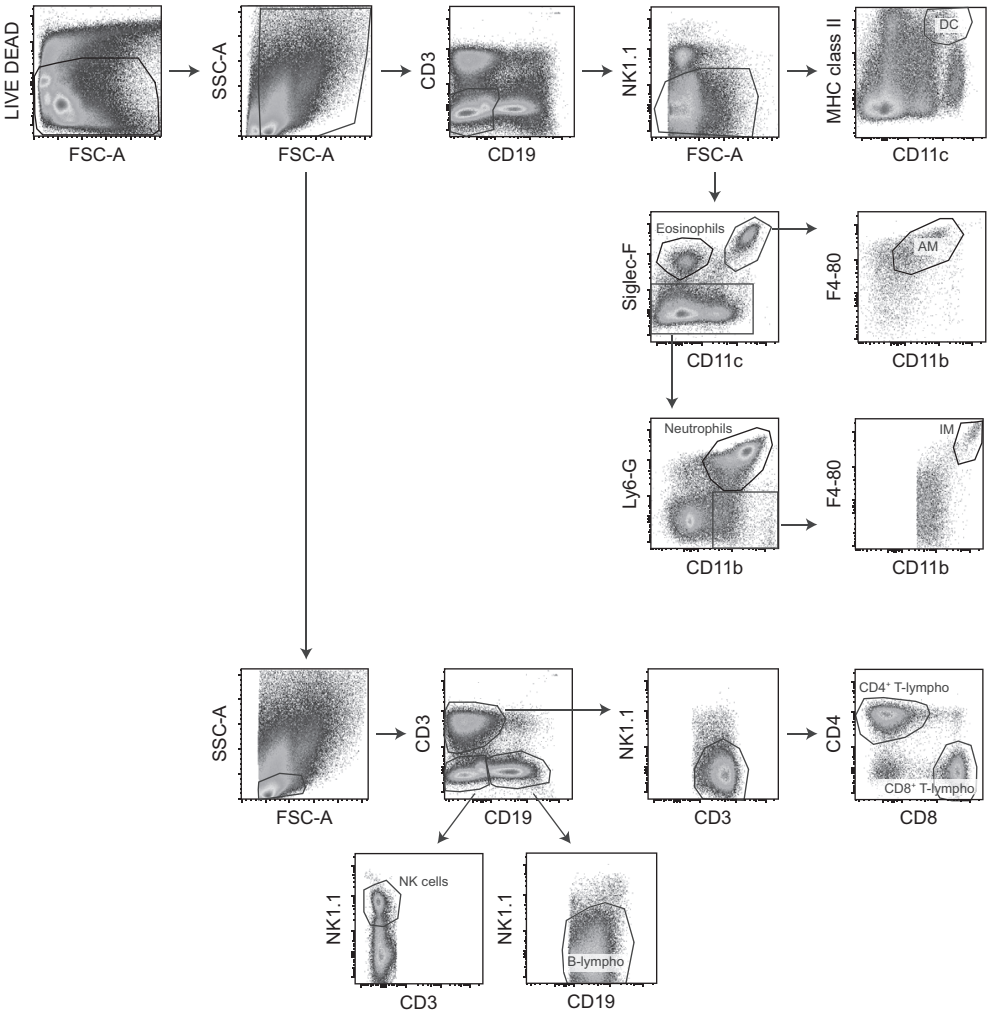

***Figure S2. Gating strategy to define populations for phenotypic analysis of GFP⁺ cells in the lungs of mice.** Live cells were gated followed by selection of non-lymphocytes and lymphocytes based on the forward / sideward scatter. Subsequently, CD3⁻ CD19⁻ NK1.1⁻ cells were selected in the non-lymphocyte population. MHC class II⁺ CD11c⁺ cells were defined as DC and Siglec-8⁺ CD11c⁻ were classified as eosinophils. Siglec-8⁺ CD11c⁺ F4-80⁺ CD11b⁺ cells were identified as alveolar macrophages (AM). Siglec-8⁻ cells were further subdivided into a Ly6-G⁺ CD11b⁺ neutrophil population and Ly6-G⁻ CD11b⁺ F4-80⁺ interstitial macrophages (IM). Following selection of lymphocytes in the forward / sideward scatterplot, CD3⁺ CD19⁻ NK1.1⁻ cells were selected and divided into CD4⁺ and CD8⁺ T-lymphocytes. Furthermore, CD3⁻ CD19⁻ NK1.1⁺ cells were defined as NK cells and CD3⁻ CD19⁺ NK1.1⁻ cells were defined as B-lymphocytes.*

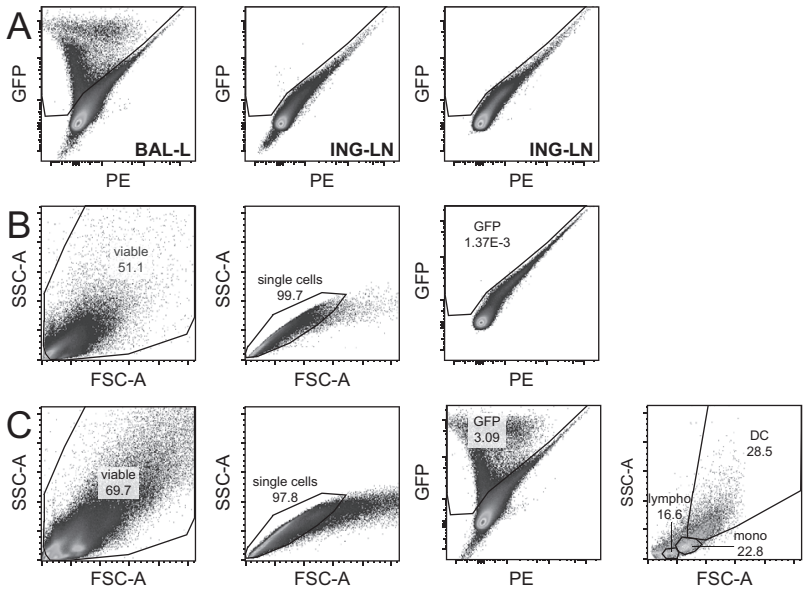

Figure S3. Gating strategy to detect GFP⁺ cells in ferret tissues. *(**A**) Example of detection of GFP⁺ cells in unstained single cell suspensions from different ferret tissues. Detection of GFP⁺ cells in a sample containing abundant GFP⁺ cells (panel 1, BAL left side after IT inoculation), background level GFP⁺ cells (panel 2, ING-LN after IM injection) or no GFP⁺ cells (panel 3, ING-LN after IT inoculation) is shown. (**B-C**) Gating strategy to define GFP⁺ DC-like, monocyte-like and lymphocyte-like cell populations in ferret tissues. As an example, the gating strategy of BAL is shown after IM injection (**B**, negative control) or IT inoculation (**C**) with rMVA-GFP. First, viable cells were gated followed by selection of single cells. Next, all GFP⁺ cells were selected after which lymphocyte-like, monocyte-like or DC-like cell populations were reversely gated in the scatter plot. Gate name and percentage of events are indicated in each gate.*

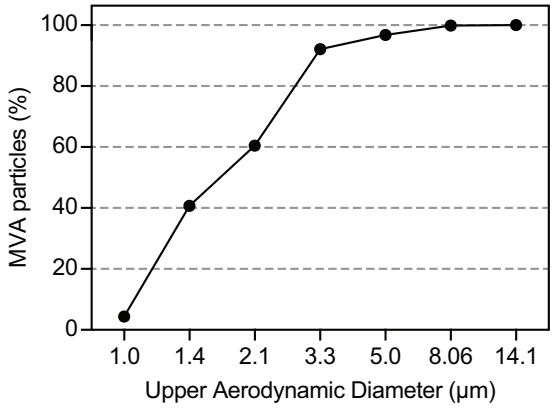

Figure S4. Droplet size characterization of rMVA-GFP aerosol. *rMVA-GFP was nebulized and several droplet fractions of increasing size between 0.98 and 14.1µm in diameter were collected using a cascade impactor. Cumulative distribution of rMVA-GFP particles across the range of droplet diameters is shown.*

[Online movie]

Figure S5. CLSM 3D render of macaque lung*. Z-stack was obtained of a lung slice from a macaque that received rMVA-GFP via AER inhalation. A 3D render of the maximum intensity projection was generated using Zen software. GPF = green. Nucleus = red.*

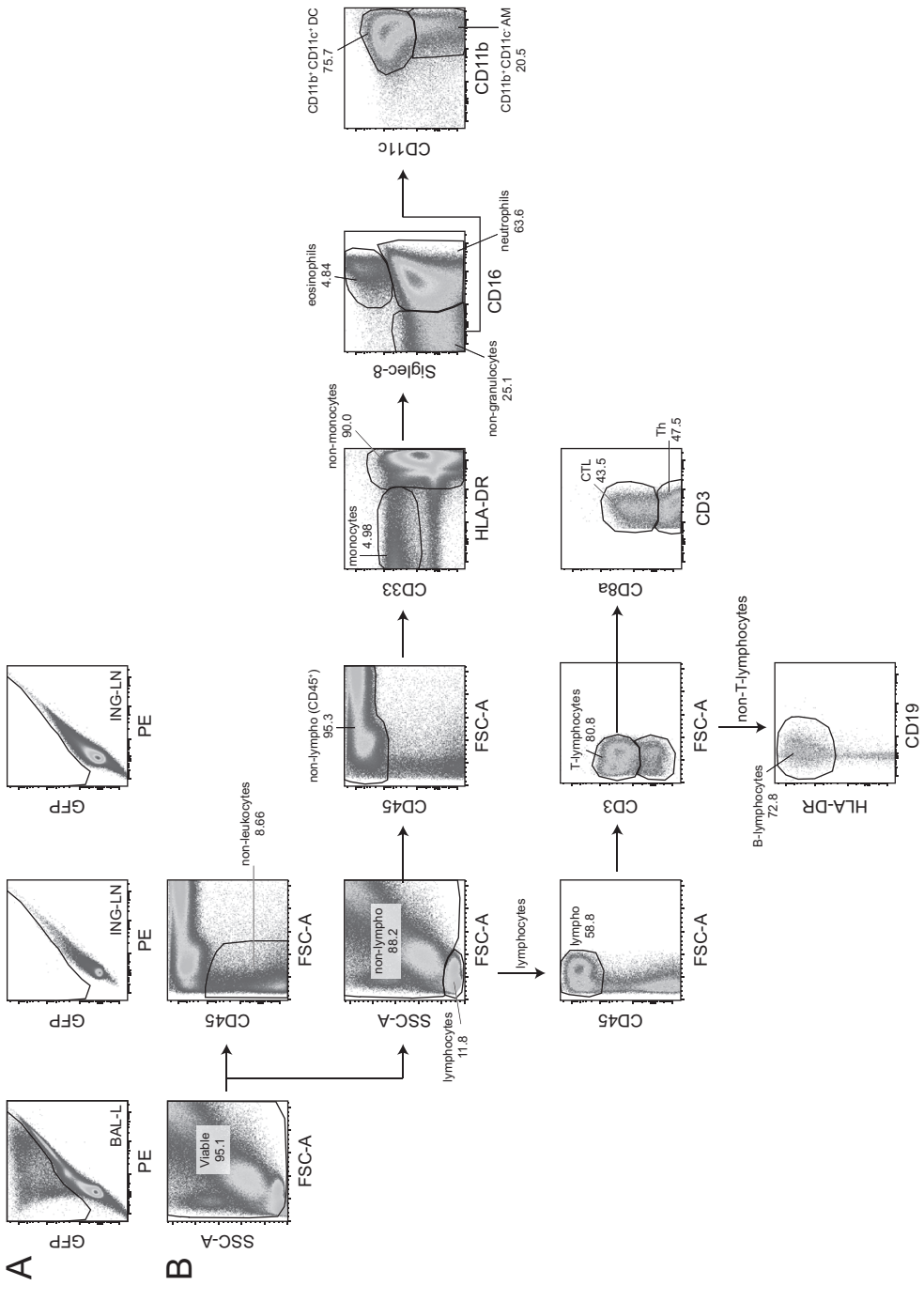
A
B
GFP
BAL-L
PE
ING-LN
PE
SSC-A
Viable
95.1
FSC-A
CD45
non-leukocytes
8.66
lymphocytes
11.8
SSC-A
non-lympho
88.2
CD45
non-lympho (CD45+)
95.3
CD33
monocytes
4.98
non-monocytes
90.0
HLA-DR
Siglec-8
eosinophils
4.84
non-granulocytes
25.1
CD16
neutrophils
63.6
CD11c
CD11b+CD11c+ DC
75.7
CD11b
CD11b+CD11c- AM
20.5
lymphocytes
CD45
lympho
58.8
CD3
T-lymphocytes
80.8
CD8a
CTL
43.5
Th
47.5
non-T-lymphocytes
HLA-DR
B-lymphocytes
72.8
CD19

▲ ***Figure S6. Gating strategy to detect GFP$^+$ cells in macaque tissues.*** *(**A**) Example of detection of GFP$^+$ cells in unstained single cell suspensions from different non-human primate tissues. Detection of GFP$^+$ cells in a sample containing abundant GFP$^+$ cells (panel 1, BAL left side after AER inhalation), background level GFP$^+$ cells (panel 2, ING-LN after IM injection) or no GFP$^+$ cells (panel 3, ING-LN after IT inoculation) is shown. (**B**) Gating strategy to define populations for phenotypic analysis of GFP$^+$ cells in BAL of macaques. Viable cells were selected after which non-leukocyte (e.g. CD45$^-$ epithelial cells) were gated. Viable cells were further discriminated into lymphocytes and non-lymphocytes based on FSC / SSC plot. CD45$^+$ cells outside the lymphogate were selected in which the CD33$^+$ monocytes were gated. The HLA-DR$^+$ population was divided into Siglec-8$^+$ CD16$^+$ eosinophils, Siglec-8$^-$ CD16$^+$ neutrophils and Siglec-8$^-$ CD16$^-$ non-granulocytes, which were further phenotyped into CD11b$^+$ CD11c$^+$ DC or CD11b$^+$ CD11c$^-$ AM. The CD45$^+$ lymphocytes were divided into CD3$^+$ T-lymphocytes, further discriminated into CD8$^+$ cytotoxic T-lymphocytes (CTL) and CD8$^-$ T helper (Th)-lymphocytes, and CD3$^-$ HLA-DR$^+$ B-lymphocytes. In this example CD19 staining did not work, thus was not included in the analysis. Gate name and percentage of events is indicated in each gate.*

CHAPTER 2.2

Effects of pre-existing orthopoxvirus-specific immunity on the performance of Modified Vaccinia virus Ankara-based influenza vaccines

AF Altenburg, SE van Trierum, E de Bruin, D de Meulder, CE van de Sandt, FRM van der Klis, RAM Fouchier, MPG Koopmans, GF Rimmelzwaan & RD de Vries

Submitted

The replication-deficient orthopoxvirus Modified Vaccinia virus Ankara (MVA) is a promising vaccine vector against various pathogens with an excellent safety record. However, pre-existing vector-specific immunity is frequently referred to as drawback for the use of MVA-based vaccines. To address if this is an issue, mice were vaccinated with MVA-based influenza vaccines in the presence or absence of orthopoxvirus-specific immunity. Importantly, protective efficacy of an MVA-based influenza vaccine against homologous challenge was not impaired in the presence of orthopoxvirus-specific pre-existing immunity. However, orthopoxvirus-specific pre-existing immunity reduced the induction of antigen-specific antibodies under suboptimal conditions and completely prevented induction of antigen-specific T cell responses by rMVA-based vaccination. Notably, antibodies induced by vaccinia virus vaccination, both in mice and humans, were not capable of neutralizing MVA. Thus, when using rMVA-based vaccines it is important to consider the main correlate of protection induced by the vaccine, the vaccine dose and the orthopoxvirus immune status of vaccine recipients.

Introduction

Recombinant viral vectors are under development as novel vaccine candidates that induce immunity to antigens of interest expressed from transgenes. Numerous vector-based vaccine candidates have been tested over the last decades, targeting a wide range of cancers or infectious diseases[209,250,280,314,315]. Modified Vaccinia virus Ankara (MVA), a member of the *Orthopoxvirus* genus, is a promising vaccine vector derived from the vaccinia virus (VACV) strain chorioallantois vaccinia virus Ankara through extensive serial passaging in chicken embryo fibroblasts (CEF). This serial passaging resulted in the loss of approximately 15% of the parental genome at so-called 'deletion sites'[223,225], allowing for easy generation of recombinant (r)MVA by insertion of one or multiple genes encoding antigens of interest into the MVA genome. Furthermore, MVA has lost the ability to replicate in most mammalian cell types, leading to an excellent safety record in humans and even safe administration to immunocompromised subjects[234,277-279]. Since MVA is a live, but replication-deficient, vector infects cells and drives endogenous expression of antigens under the control of a VACV promotor, resulting in efficient antigen presentation and subsequent induction of antigen-specific B and T cell responses[209,280,316].

There is considerable interest in the development of novel influenza vaccines that induce broadly protective or 'universal' immunity against different subtypes of influenza A viruses. Accumulation of mutations in the surface proteins of seasonal influenza viruses (antigenic drift) and the occasional zoonotic introduction of novel influenza viruses into the human population (antigenic shift) complicate the timely production of 'classical' influenza vaccines that antigenically match seasonal or pandemic viruses[132,133,317-319]. Furthermore, in case of a pandemic outbreak caused by a newly emerging influenza virus, novel technology is required to rapidly produce large batches of vaccines. rMVA vaccines expressing one or multiple influenza virus antigens could potentially fulfill both of these needs. Currently, rMVA-based vaccines expressing various wild-type and modified influenza virus antigens are evaluated in animal models and clinical trials and have shown promising results[209,250,280].

A potential drawback for the use of orthopoxvirus-based vaccines is that a proportion of the adult human population has immunity against the vaccine vector due to smallpox vaccination campaigns that were conducted until the mid 1970s and ultimately led to the eradication of smallpox[320]. In general, orthopoxvirus-specific immunity induced by smallpox vaccination is long-lived with slowly declining T cell responses (half-life of 8-15 years) and antibody responses that are maintained up to 75 years after vaccination[321]. In addition to orthopoxvirus-specific immunity induced by the historic use of smallpox vaccines, efficient induction of immunity by rMVA-based vaccines often requires repeated administration, which induces immunity not only to the antigen of interest but also against the vaccine vector[260]. There is considerable concern for interference of orthopoxvirus-specific pre-existing immunity with subsequent rMVA-based vaccinations, resulting in reduced vaccine immunogenicity and efficacy.

Previously, pre-existing vaccine vector-specific immunity was shown to interfere with VACV-[322], fowlpox virus-[323] and adenovirus-based vaccines[212,213]. In contrast to MVA, these vector-based vaccines are replication-competent in their respective hosts and therefore potentially more sensitive to pre-existing vaccine vector-specific immunity. Thus far, evidence for interference of pre-existing orthopoxvirus-specific immunity with rMVA vaccination is ambiguous. Some studies in mice and macaques showed that pre-existing immunity induced by either VACV or MVA had a negative effect on the induction of antigen-specific humoral and/or cellular immune responses by rMVA-based vaccines. However, despite the observed negative effects, pre-existing orthopoxvirus-specific immunity was not considered to interfere with rMVA-based vaccination[268,324-326]. Furthermore, results obtained in humans are also contradictory: orthopoxvirus-specific immunity was boosted by multiple rMVA vaccinations and was shown to have a negative effect on the magnitude of the antigen-specific humoral and cellular immune response. However, in all cases individuals responded to vaccination by either initial induction or boosting of antigen-specific immunity[260,327]. This indicates that rMVA-based vaccines remain immunogenic, even in the presence of vector-specific pre-existing immunity. Thus, despite the fact that claims of potential interference by pre-existing vector immunity on immunogenicity of rMVA-based vaccines are made in the literature, the topic has not been addressed sufficiently.

In this study, we addressed the effect of pre-existing immunity to MVA, VACV or influenza virus on the performance of rMVA-based influenza vaccines by evaluating induction of immune responses and the protective capacity from a lethal challenge with an influenza virus. Furthermore, (cross-)neutralizing activity of MVA- or VACV-specific antibodies against rMVA-based vaccines was assessed using mouse and human sera. Importantly, the protective capacity of an rMVA vaccine expressing a hemagglutinin (HA) gene homologous to the H5N1 challenge virus was not hampered by the presence of pre-existing immunity to MVA, VACV or influenza virus. However, pre-existing orthopoxvirus-specific immunity interfered with induction of antigen-specific antibody responses under specific suboptimal conditions and had a detrimental effect on the induction of antigen-specific T cell responses.

Results

VACV and H1N1pdm09 virus dose-finding

Sub-lethal doses of VACV and pandemic influenza virus (H1N1pdm09) were determined in dose-finding experiments in C7BL/6 mice. Inoculation of mice with 10^4-10^7 plaque-forming units (PFU) VACV-Elstree by tail scarification led to weight loss, concurrent with the appearance of blisters at the site of inoculation in all mice (**Fig. S1A-B**). Similar levels of VACV-specific antibody responses were detected in all groups two weeks after inoculation (**Fig. S1C**). In addition, VACV- and MVA-specific $CD4^+$ and $CD8^+$ T cell responses were detected with a trend for stronger T cell responses at increasing infectious doses (**Fig. S1D-E**). A dose of 10^7 PFU VACV was considered the optimal sub-lethal priming dose for subsequent experiments.

In contrast to VACV, intranasal (IN) inoculation of mice with incrementing doses of H1N1pdm09 virus resulted in more severe weight loss (**Fig. S2A**). Mortality was observed in mice inoculated with 10^5 and 10^6 50% tissue-culture infectious dose ($TCID_{50}$) of H1N1pdm09 virus (**Fig. S2B**). Optimal induction of hemagglutination inhibition (HI) antibody responses (**Fig. S2C**) and T cell responses (**Fig. S2D**) without mortality was observed after inoculation with 10^4 $TCID_{50}$, which was therefore considered the optimal dose for subsequent sub-lethal priming infections.

Induction of pre-existing orthopoxvirus-specific and influenza virus-specific immunity

According to the indicated priming regimens (**Table 1**, week 0 and/or 4) mice were inoculated with the pre-determined optimal doses of wild-type (wt)MVA (vaccine vector without transgene) or VACV in order to induce orthopoxvirus-specific immunity, or H1N1pdm09 influenza virus to induce influenza virus-specific immunity. Four weeks after the last priming inoculation (week 8), induction of orthopoxvirus- or influenza virus-specific immunity was assessed by measuring serum antibody responses by protein array (PA) and ELISA. Priming with wtMVA or H1N1pdm09 influenza virus induced homologous antibody responses measured by PA (**Fig. 1A**). Serum antibodies from VACV-primed mice did not cross-react with wtMVA in PA, thus VACV-specific antibodies could not be detected in this assay. Therefore, induction of VACV-specific antibodies by VACV priming was confirmed by ELISA (**Fig. 1B**). Conversely, serum antibodies directed to wtMVA did cross-react with VACV. Orthopoxvirus- or influenza virus-specific antibody responses were not detected in unprimed mice (**Fig. 1A-B**).

In addition to detection of serum antibodies, H1N1pdm09 virus infection was confirmed by monitoring body weight of mice for two weeks post-priming (**Table 1**, subgroup d). H1N1pdm09-virus inoculated mice lost body weight up to 7 days post-inoculation (dpi) but regained their original weight at 11 dpi (**Fig. 1C**). In summary, priming with wtMVA, VACV or H1N1pdm09 was successful and induced the desired pre-existing immunity against the respective viruses in C57BL/6 mice.

Table 1. Experimental design.

Group	Week 0 Prime 1	Week 4 Prime 2	Week 8 Vaccination 1	Week 12 Vaccination 2	Week 16 Challenge
1	a) - b) wtMVA c) - d) -	a) - b) wtMVA c) VACV d) H1N1pdm09	rMVA-NP	rMVA-NP	X
2	a) - b) wtMVA c) - d) -	a) - b) wtMVA c) VACV d) H1N1pdm09	rMVA-H5	rMVA-H5	X
3	a) - b) wtMVA c) - d) -	a) - b) wtMVA c) VACV d) H1N1pdm09	rMVA-H1	rMVA-H1	H5N1
4	a) - b) wtMVA c) - d) -	a) - b) wtMVA c) VACV d) H1N1pdm09	rMVA-H3	rMVA-H3	H5N1
5	a) - b) wtMVA c) - d) -	a) - b) wtMVA c) VACV d) H1N1pdm09	PBS	rMVA-H5	H5N1
6	a) - b) wtMVA c) - d) -	a) - b) wtMVA c) VACV d) H1N1pdm09	rMVA-H5*	rMVA-H5	H5N1
7	a) - b) wtMVA c) - d) -	a) - b) wtMVA c) VACV d) H1N1pdm09	rMVA-H1	rMVA-H5	H5N1

*C57BL/6 mice (n=6 per subgroup) were unprimed (subgroups a) or primed with 10^8 PFU wtMVA (two primings, subgroups b), 10^7 PFU VACV (one priming, subgroups c) or 10^4 $TCID_{50}$ H1N1pdm09 (one priming, subgroups d). At week 8 and 12, mice were vaccinated with 10^8 PFU of the indicated rMVA-based vaccine expressing influenza virus nucleoprotein (NP) or HA. Groups 1 and 2 were euthanized at week 13 and 14, respectively, to assess the effect of priming on induction of antigen-specific T cells by vaccination. The remainder of the mice was challenged with a lethal dose of 10^3 $TCID_{50}$ A/Vietnam/1194/04 (H5N1) influenza virus at week 16. * Mice were vaccinated with 10^7 PFU rMVA-H5.*

Pre-existing orthopoxvirus-specific immunity had limited effect on induction of antigen-specific antibody responses by rMVA

To determine the effect of pre-existing immunity on rMVA vaccine immunogenicity, unprimed and primed mice were subsequently vaccinated with rMVA expressing influenza virus nucleoprotein (NP) or HA (**Table 1**). Serum antibody responses against wtMVA and various HA1 subunits (HA from H1N1pdm09, H3N2 isolate from 2003 and 2011, and a selection of H5Nx viruses) after one rMVA vaccination were determined using PA. As expected, rMVA vaccination consistently boosted the MVA-specific antibody response in mice primed with wtMVA or VACV (**Fig. 2A**). Furthermore, boosting of H1N1pdm09-specific antibodies was observed in mice

primed with H1N1pdm09 virus and subsequently vaccinated with rMVA-H1 (**Fig. 2A**, group 3 and 7).

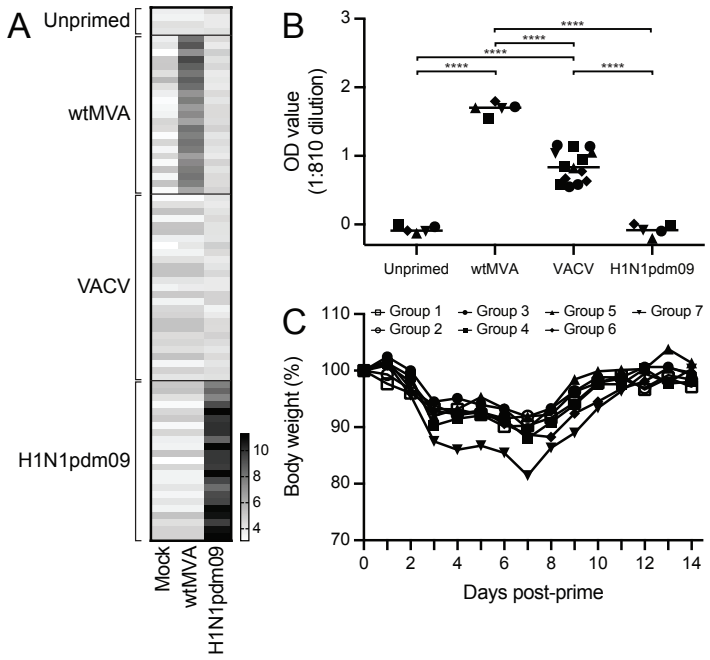

Figure 1. Induction of orthopoxvirus-specific or influenza virus-specific immunity by priming. *(**A**) Sera from individual mice obtained 4 weeks after the last priming (week 8) were assessed by PA for presence of wtMVA- or H1N1pdm09-specific antibodies. MVA-specific antibodies were detected with a wtMVA-infected cell lysate, mock-infected baby hamster kidney (BHK)-21 cell lysate was included as negative control. Each horizontal line represents an individual animal. Antigens (x-axis) and priming groups (y-axis) are indicated. Scale shows 2-log transformed titers. (**B**) VACV-specific serum antibody responses were determined by ELISA using VACV-infected HeLa cell lysate. The background signal on mock-infected cell lysate was subtracted. Individual sera from VACV-primed mice were used where possible. Serum from unprimed, wtMVA-primed or H1N1pdm09-primed mice was pooled due to limited serum availability. Mean per priming group is indicated. Statistically significant differences were determined using a one-way ANOVA with multiple comparisons. **** p<0.0001. (**C**) Mean body weight per group (n=6, group 7 n=5) after IN inoculation with 10^4 $TCID_{50}$ H1N1pdm09. No statistically significant differences between the groups were detected with a repeated measures ANOVA model.*

Serum antibody responses against the corresponding antigen – H1pdm09 and H3 (2003) – induced by one rMVA-H1 or rMVA-H3 vaccination, respectively, were not hampered by either orthopoxvirus- or influenza virus-specific pre-existing immunity (**Fig. 2A**). Antibodies against the heterologous H3 (2011) were not detected after a single vaccination with rMVA-H3. In contrast, heterologous antibody responses were detected after a single vaccination with rMVA-H5. Lower antibody titers specific for HA1 of all H5 clades tested, including the homologous A/Vietnam/1194/04 (H5N1, clade 1), were detected in wtMVA-primed mice, compared to unprimed, VACV- or H1N1pdm09-virus primed mice. This effect was especially observed when a low,

suboptimal dose of rMVA-H5 (10^7 PFU, **Table 1**, group 6 at week 12) was used for the initial vaccination and to a lesser extent with the use of a higher vaccine dose (10^8 PFU, **Table 1**, group 5 at week 16) (**Fig. 2A**-**B**). These results were confirmed with an HI assay, which is a good proxy for influenza virus neutralization. MVA-specific pre-existing immunity negatively affected the HI antibody response to influenza virus A/Vietnam/1194/04 induced after a single rMVA-H5 vaccination, particularly when a low dose was used (**Fig. 2C**).

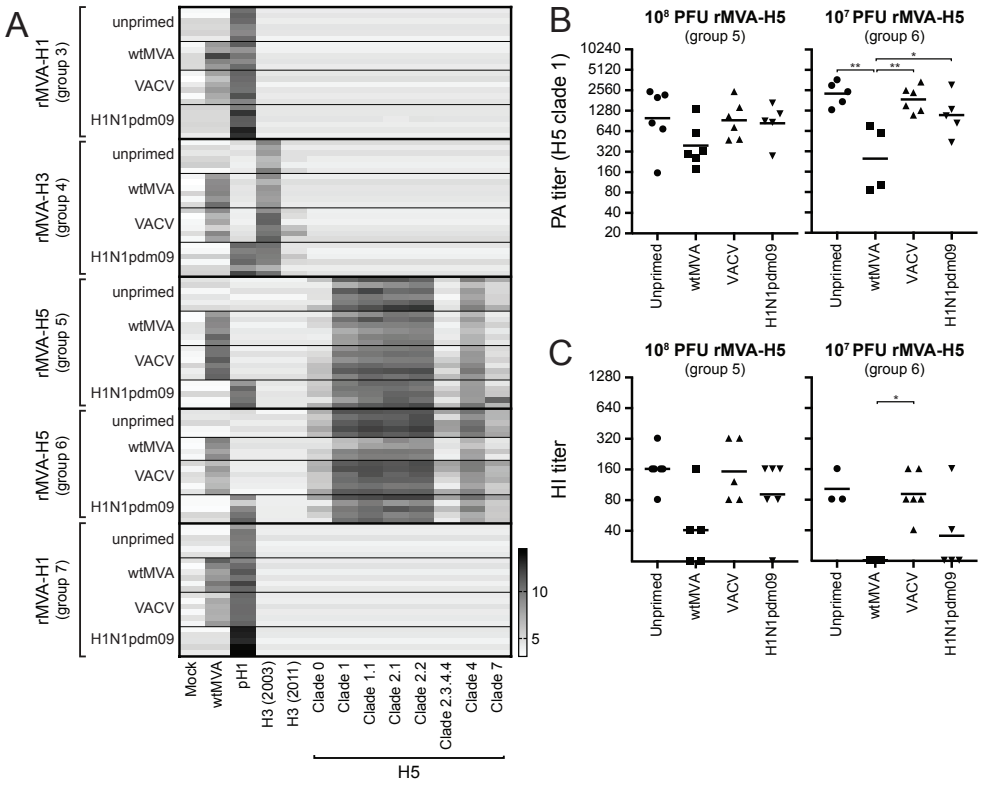

Figure 2. Effect of pre-existing immunity on induction of serum antibody responses by a single rMVA vaccination. *(**A-B**) Serum antibody responses against wtMVA and HA1 from H1N1pdm09, 2003 H3N2, 2011 H3N2 or H5 influenza viruses from the indicated clades were determined using PA 4 weeks after the first vaccination (group 3, 4, 6 & 7 week 12, group 5 week 16). Mock-infected BHK-21 cell lysates were used as negative control for the wtMVA-infected cell lysates. Each horizontal line represents an individual animal. Antigens (x-axis), vaccine groups and priming subgroups (y-axis) have been indicated. Scale represents 2-log titers as determined by PA. (**B**) PA titers against H5 from A/Vietnam/1194/04 (clade 1) four weeks after rMVA-H5 vaccination with a high dose (10^8 PFU, group 5, week 16) or a low dose (10^7 PFU, group 6, week 12). Mean per priming group is indicated. Statistically significant differences were determined using a one-way ANOVA with multiple comparisons. * p=0.0257, ** p<0.0017. (**C**) HI titers against influenza virus A/Vietnam/1194/04 were determined for each individual animal four weeks after rMVA-H5 vaccination with a high dose (10^8 PFU, group 5, week 16) or a low dose (10^7 PFU, group 6, week 12). Mean is indicated. Statistically significant differences were determined using a Kruskal-Wallis test. * p=0.0401.*

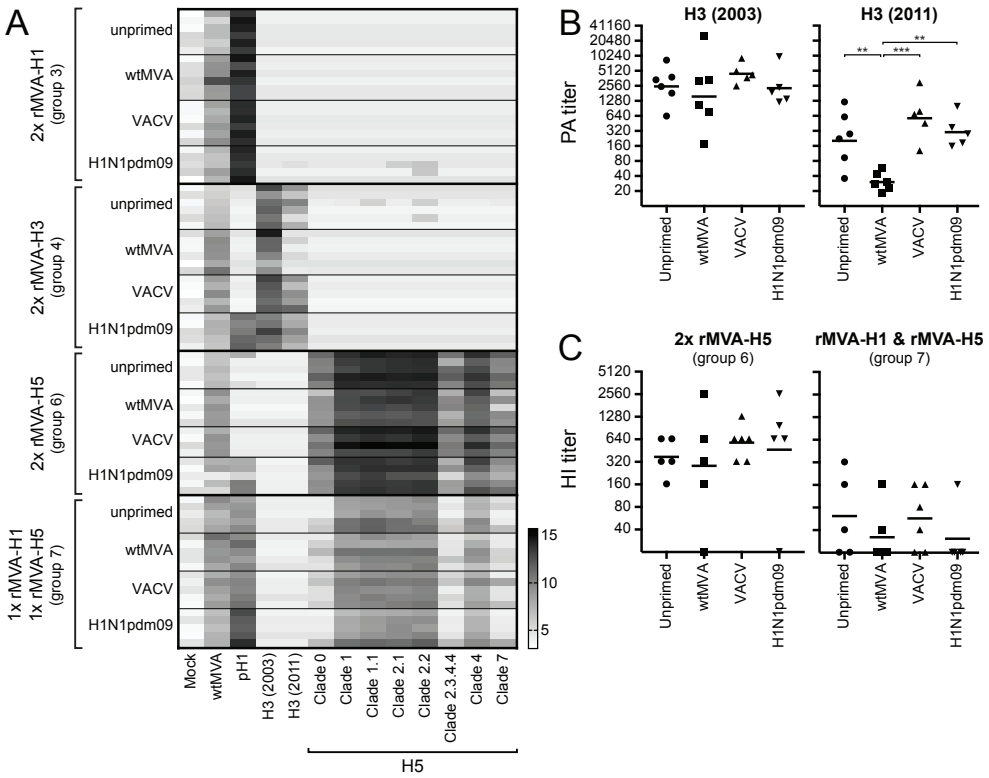

Figure 3. Effect of pre-existing immunity on induction of serum antibody responses after two rMVA vaccinations. *(**A-B**) Serum antibody responses against wtMVA and HA1 from H1N1pdm09, 2003 H3N2, 2011 H3N2 or H5 influenza viruses from the indicated clades were determined using protein array 4 weeks after the second vaccination (week 16). Each horizontal line represents an individual animal. Antigens (x-axis), vaccine groups and priming subgroups (y-axis) have been indicated. Scale represents the 2-log as determined by protein array. (**B**) Protein array titers for each individual animal against an antigenically similar H3 from 2003 or distinct H3 from 2011 four weeks after the second rMVA-H3 vaccination (group 4). Mean per priming group is indicated. Statistically significant differences were determined using a one-way ANOVA with multiple comparisons. ** p<0.0086, *** p=0.0003. (**C**) HI titers against influenza virus A/ Vietnam/1194/04 were determined for each individual animal four weeks after the second vaccination with rMVA. Mean per priming group is indicated.*

A second vaccination with rMVA (**Table 1**, week 16) boosted serum antibody responses to MVA and influenza viruses. Similar to antibody responses induced by a single vaccination, antibody responses against the corresponding antigen after two vaccinations with rMVA-H1 or rMVA-H3 were not affected by pre-existing immunity (**Fig. 3A-B**, group 3-4). The second vaccination with rMVA-H3 also induced cross-reactive antibody responses against an antigenically distinct H3 (2011), that were hardly observed after the initial vaccination. Notably, this cross-reactive response was detected in all subgroups, but was lower in mice with MVA-specific pre-existing immunity (**Fig. 3A-B**). Furthermore, in contrast to the antibody response after a single rMVA-H5 vaccination, the responses after two rMVA-H5 vaccinations (**Table 1**, group 6) or an rMVA-H1 vaccination followed by an rMVA-H5 vaccination (**Table**

1, group 7) detected by PA or HI were not affected by pre-existing immunity to the vector (**Fig. 3A, C**). In conclusion, an effect of pre-existing MVA-specific, but not VACV- or influenza virus-specific, immunity on induction of humoral responses by rMVA vaccination was observed under specific conditions.

Induction of antigen-specific T cell responses by rMVA is prevented by pre-existing orthopoxvirus-specific immunity

To determine the effect of pre-existing immunity on rMVA-induced antigen-specific T cell responses, splenocytes were obtained from unprimed and primed mice one or two weeks after the second rMVA-NP or rMVA-H5 vaccination, respectively (**Table 1**, group 1-2). Antigen-specific $CD8^+$ T cell responses were determined by measuring the number of interferon (IFN)-γ producing splenocytes after stimulation with synthetic peptide $NP_{366-374}$, an immunodominant $CD8^+$ T cell epitope. Furthermore, H5-specific $CD4^+$ T cell responses were determined after stimulation with full-length HA protein from H5N1 influenza viruses A/Vietnam/1194/04 (clade 1) or A/Indonesia/5/05 (clade 2.1).

rMVA-NP vaccination efficiently induced antigen-specific $CD8^+$ T cell responses in unprimed and H1N1pdm09-primed mice, but failed to induce NP-specific $CD8^+$ T cells in mice with orthopoxvirus-specific pre-existing immunity, induced by either wtMVA or VACV priming (**Fig. 4A**). Similar observations were made in animals efficiently vaccinated with rMVA-H5: unprimed and H1N1pdm09 primed animals developed HA-specific $CD4^+$ T cell responses against both the homologous (A/Vietnam/1194/04) and heterologous HA (A/Indonesia/5/05), but pre-existing orthopoxvirus-specific immunity had a detrimental effect on the induction of H5-specific $CD4^+$ T cell responses (**Fig. 4B**).

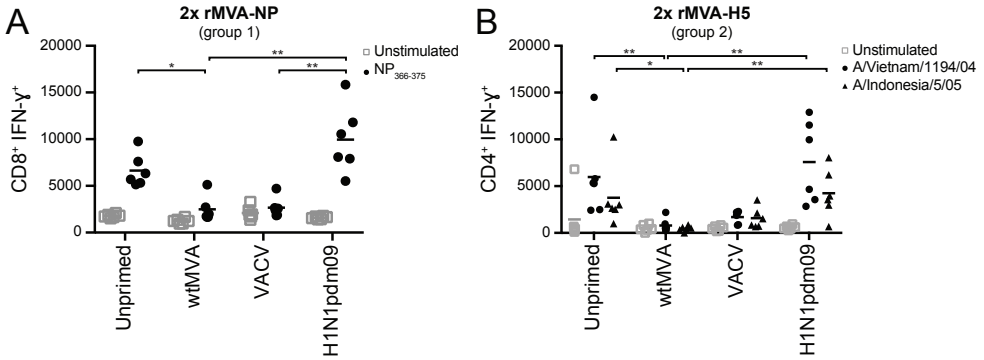

Figure 4. Pre-existing orthopoxvirus-specific immunity inhibits rMVA-induced antigen-specific T cell responses. *(**A**) Splenocytes collected one week after the second rMVA-NP vaccination were unstimulated or stimulated with $NP_{366-374}$ synthetic peptide. The number of IFN-γ producing $CD3^+$ $CD8^+$ splenocytes was measured. (**B**) Splenocytes collected two weeks after the second rMVA-H5 vaccination were unstimulated or stimulated with purified HA protein from H5N1 influenza virus A/Vietnam/1194/04 or A/Indonesia/5/05. The number of IFN-γ producing $CD3^+$ $CD4^+$ splenocytes was measured. Mean of each priming group is indicated. Statically significant differences per simulant were determined using a Kruskal-Wallis test. * p<0.0478, ** p<0.0076.*

Pre-existing orthopoxvirus-specific immunity impaired the protective efficacy of rMVA-based vaccines against a heterologous but not homologous virus challenge

Four weeks after the final vaccination, rMVA-H1, rMVA-H3 and rMVA-H5 vaccinated mice were challenged with a lethal dose of influenza virus H5N1 (A/Vietnam/1194/04) in order to determine the effect of pre-existing immunity on the protective capacity of rMVA-based influenza vaccines (**Table 1**, group 3-7). As expected, rMVA-H1 and rMVA-H3 vaccination did not fully protect against an H5N1 influenza virus challenge, which was reflected by loss of body weight, lower survival rates and high viral loads in the lungs (**Fig. 5**, **Table 2**). However, a limited level of cross-protection was observed after rMVA-H1 or rMVA-H3 vaccination in unprimed and H1N1pdm09-primed animals, which was not observed in mice primed with VACV or wtMVA (**Fig. 5**, **Table 2**). Notably, pre-existing orthopoxvirus-specific or influenza virus-specific immunity did not interfere with the protective capacity of rMVA vaccines expressing the homologous HA gene of the H5N1 challenge virus since all mice that received at least one rMVA-H5 vaccination were fully protected from lethal H5N1 challenge (**Fig. 5**, **Fig. S3**, **Table 2**).

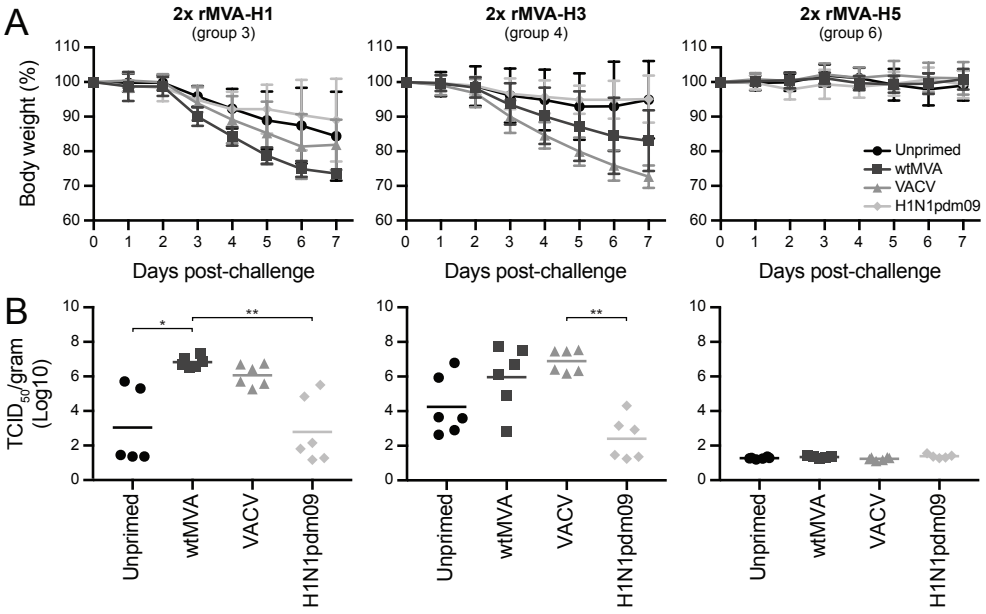

Figure 5. Pre-existing immunity does not impair protective capacity of rMVA-H5 vaccination. *Four weeks after the last rMVA vaccination (week 16), mice were challenged with a lethal dose H5N1 influenza virus. (**A**) Body weight over time for each of the priming groups for group 3 (two rMVA-H1 vaccinations), group 4 (two rMVA-H3 vaccinations) and group 6 (two rMVA-H5 vaccinations). Mean and standard deviation (SD) per priming group are shown. (**B**) Viral load in the lungs shown as $TCID_{50}$ per gram lung for each individual animal for group 3, group 4 and group 6. Mean of each priming group is shown. Statistically significant differences were determined using a Kruskal-Wallis test. * p=0.0152, ** p<0.0065.*

Table 2. Survival after lethal H5N1 influenza virus challenge.

Prime:	Unprimed		wtMVA		VACV		H1N1pdm09	
	Survival (#)	Survival (%)	Survival (#)	Survival (%)	Survival (#)	Survival (%)	Survival (#)	Survival (%)
2x rMVA-H1 (group 3)	3/6	50%	0/6	0%	2/6	33%	4/6	66,7%
2x rMVA-H3 (group 4)	5/6	83,3%	3/5	50%	1/6	16,7%	6/6	100%
1x rMVA-H5 (group 5)	6/6	100%	6/6	100%	6/6	100%	6/6	100%
2x rMVA-H5 (group 6)	6/6	100%	5/5	100%	6/6	100%	6/6	100%
1x rMVA-pH1 1x rMVA-H5 (group 7)	6/6	100%	6/6	100%	6/6	100%	5/5	100%

Four weeks after the final vaccination (week 16), mice were challenged with a lethal dose H5N1 influenza virus. The absolute number (#; live mice/total mice) and the percentage (%) of live animals at seven days post-challenge have been indicated. Mice were euthanized at >25% body weight loss.

Pre-existing MVA-specific, but not VACV-specific, antibodies have MVA-neutralizing capacities

In order to gain insight into the possible mechanism underlying the observed effects of pre-existing orthopoxvirus-specific immunity on rMVA-based vaccine immunogenicity, (cross-)reactivity of the orthopoxvirus-specific antibodies was analyzed. A single exposure to either MVA or VACV did not induce any detectable MVA-specific serum antibody responses in mice. In contrast, in mice that were exposed at least twice to MVA or once to VACV followed by at least one rMVA vaccination, MVA-specific antibodies were detected. Notably, the MVA-specific antibody response was not boosted in response to extra exposures after the third MVA exposure (**Fig. 6A**). The antibody responses induced by MVA efficiently cross-reacted with VACV (**Fig. 6B**). Furthermore, although VACV priming did not induce detectable antibody responses cross-reactive with MVA, homologous VACV-specific antibodies were detected (**Fig. 6B**). A booster effect of rMVA-based vaccination after VACV priming was observed in both MVA- and VACV-specific antibody responses (**Fig. 6A-B**). Of special interest, sera from mice exposed to MVA, but not mice exclusively exposed to VACV, orthopoxvirus-specific antibody responses showed the capacity to neutralize MVA *in vitro* (**Fig. 6C**), thereby potentially affecting subsequent rMVA vaccinations.

Human pre-existing MVA-specific, but not VACV-specific, antibodies have MVA-neutralizing capacities

Next, the presence and neutralizing capacity of serum obtained from humans vaccinated with either VACV or rMVA was assessed. Pre- and post-vaccination sera from a phase 1/2a clinical trial with rMVA-H5 were obtained[260]. MVA-specific antibody responses were detected four weeks after the third vaccination in individuals that were vaccinated with 10^8 PFU rMVA-H5 (**Fig. 7A**). Furthermore, sera from VACV-vaccinated individuals (born between 1970-1971) and unvaccinated controls (born between 1976-1978) were probed for the presence of VACV- and MVA-specific antibodies[328]. Almost four decades after vaccination, VACV-specific antibodies were still detected in VACV-vaccinated individuals, but not in the controls that were born 2-4 years after the smallpox vaccination campaign was terminated

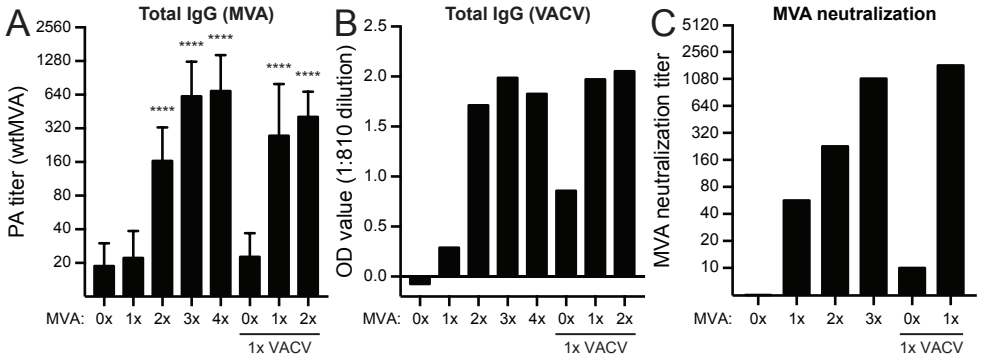

Figure 6. MVA-specific antibodies showed neutralizing capacity. *MVA and VACV-specific antibody responses were determined in sera obtained four weeks post-priming (week 8) or post-vaccination (week 12&16). (**A**) MVA-specific serum antibody responses were determined using wtMVA-infected BHK-21 cell lysates on PA. The mean and SD are indicated. Statistical differences were determined relative to the '0x MVA' sample using a Kruskal-Wallis test. **** p<0.0001. (**B**) Serum antibody responses against VACV were measured by ELISA using VACV-infected HeLa cell lysate. The background signal on mock-infected HeLa cell lysates was subtracted. Due to limited serum availability serum was pooled (n=3-6) per subgroup. The mean of n=2-17 pools is shown, except for '3x MVA' which shows data from a single pool. (**C**) Serum antibody responses in group 5 (one vaccination with rMVA-H5) and group 6 (two vaccinations with rMVA-H5) were examined for wtMVA neutralizing capacity by a plaque reduction assay on CEF. Due to limited serum availability serum was pooled (n=2-5) per subgroup. The mean of n=2 pools is shown, except for '3x MVA' and '1x VACV, 0x MVA' which show data from a single pool.*

(**Fig. 7B**). Notably, these VACV-specific antibodies displayed limited cross-reactivity with MVA (**Fig. 7A**) and were not capable of neutralizing an MVA infection *in vitro* (**Fig. 7C**). In contrast, MVA-specific antibodies did reduce plaque formation by MVA (**Fig. 7C**). Taken together, in both mice and humans, pre-existing MVA-specific antibodies induced by MVA, but not by VACV, had MVA-neutralizing capacities *in vitro*.

Discussion

Although it has been frequently suggested that pre-existing immunity to orthopoxviruses can interfere with the immunogenicity and efficacy of rMVA-based vaccines, the issue has not been addressed sufficiently. In this study, we investigated the performance of rMVA-based influenza vaccines in the presence or absence of pre-existing immunity to orthopoxviruses or influenza virus in mice and evaluated human orthopoxvirus-specific immune responses after MVA or VACV vaccination.

Induction of MVA- or VACV-specific antibodies upon priming mice with wtMVA or VACV was confirmed by PA and ELISA using wtMVA- or VACV-infected cell-lysates as antigens. Interestingly, VACV-specific antibodies did not cross-react with MVA, whereas MVA-specific antibodies clearly cross-reacted with VACV. These results are in accordance with a previous study[329] and similar results were obtained with human sera, where VACV-specific antibody responses cross-reacted with MVA only to a limited extent. In our study, the differential response can be explained by the fact that mice MVA-primed mice received a booster immunization inducing a MVA-specific recall response opposed to induction of a primary responses in VACV-primed mice. Indeed, a single vaccination with rMVA expressing H1, H3 or H5 in unprimed mice did not induce detectable levels of MVA-specific antibodies, whereas rMVA vaccination

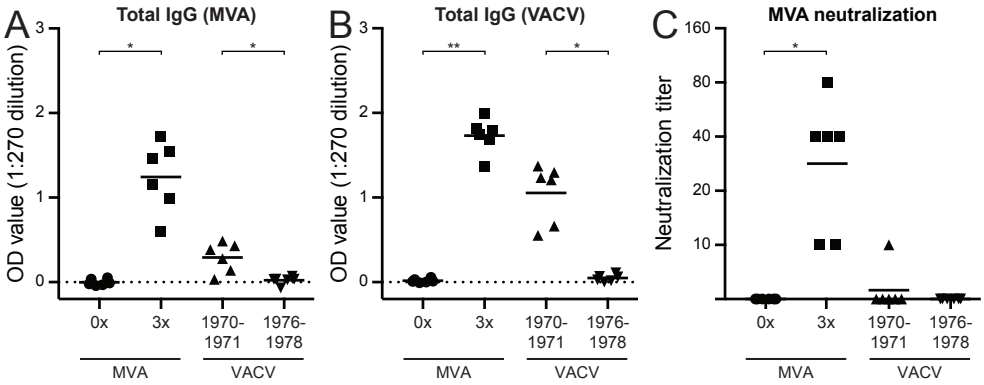

Figure 7. Human rMVA-based, but not VACV, induced MVA-specific neutralizing antibody responses. *(**A-B**) Serum antibody responses against MVA (**A**) and VACV (**B**) were measured by ELISA using infected BHK-21 or HeLa cell lysates, respectively. The background of the respective mock-infected cell lysate was subtracted. (**C**) Neutralizing capacity of orthopoxvirus-specific antibodies was determined by a plaque reduction assay on CEF using rMVA-GFP. The data shown are representative of three independent experiments. The mean per group is indicated. Statistical significant differences were determined using a Wilcoxon matched-pairs signed rank test (rMVA vaccination samples) or Mann-Whitney test (VACV vaccination samples). * p<0.0312. ** p=0.0022.*

of VACV-primed mice led to a boosting of MVA-specific antibodies. This corresponds to data obtained in humans, which show that MVA-specific antibodies were boosted upon MVA vaccination of either smallpox or rMVA vaccinated individuals[260,329].

Pre-existing orthopoxvirus-specific immunity in mice affected humoral immune responses induced by rMVA influenza vaccines to a limited extent. Effects were exclusively observed in wtMVA-primed mice and only under 'suboptimal' conditions. First, when a low rMVA-H5 vaccine dose was used, wtMVA-primed mice showed lower antibody titers to all tested H5 clades compared to the other priming groups. The reduced H5-specific antibody response observed in mice with MVA-specific pre-existing immunity was overcome by a second immunization with 10^8 PFU of rMVA-H5, as was previously reported[268]. Second, in wtMVA-primed mice the response to antigenically distinct H3N2 viruses was significantly lower after two rMVA-H3 vaccinations than that of unprimed animals. However, pre-existing immunity had no effect on the magnitude of the antibody response to a corresponding H3 antigen induced by one or two rMVA-H3 vaccinations. Importantly, VACV-specific pre-existing immunity never had a negative effect on the induction of antigen-specific antibody responses induced by rMVA.

In addition to antibody responses, the induction of antigen-specific T cell responses after rMVA vaccination in the absence or presence of pre-existing immunity was assessed. Virus-specific T cells contribute significantly to protective immunity against virus infections and can reduce duration and severity of disease[330-332]. Induction of T cells to influenza virus by vaccines is particularly attractive, since these mainly recognize epitopes in conserved internal proteins and can therefore afford cross-protection against various influenza viruses of different subtypes (heterosubtypic immunity)[82,108,194,196]. Our results indicated that induction of influenza virus-specific T

cell responses was severely hampered by presence of MVA- or VACV-specific pre-existing immunity in mice. These findings are in concordance with previous studies that examined the immunogenicity of rMVA expressing human immunodeficiency virus (HIV) antigens in both mice[333] and macaques[326,334] in the presence of pre-existing vector-specific immunity. In contrast, a recent clinical trial reported efficient induction of cytomegalovirus (CMV)-specific T cell responses with rMVA in VACV-vaccinated individuals. The authors claimed that pre-existing VACV-specific immunity did not affect immunogenicity of rMVA, however, only a limited number of study subjects with pre-existing immunity was studied and their orthopoxvirus immune status was solely defined by date of birth[335]. Furthermore, rMVA expressing NP and matrix 1 (M1) genes from influenza virus has been shown to induce T cell responses in humans[269,272], even in the elderly that potentially have orthopoxvirus-specific immunity[271]. Although this suggests that T cell responses can be induced in humans with VACV-specific immunity, the immune status of study subjects was not verified in these studies and appropriate control groups were lacking.

To assess effects of pre-existing immunity on rMVA protective efficacy, mice vaccinated with rMVA-H5 in the presence or absence of pre-existing immunity were challenged with a lethal dose of H5N1 influenza virus. As expected, pre-existing orthopoxvirus- or influenza virus-specific immunity did not affect protection and survival from the homologous challenge infection. Protection was most likely mediated by antigen-specific neutralizing antibodies, which have been shown to be the main correlate of protection induced by the rMVA-H5 vaccine[256,258-260,262], and were unaffected by the presence of pre-existing immunity at week 16. In contrast, mice that were vaccinated with either rMVA-H1 or rMVA-H3 were only partially protected from lethal H5N1 influenza virus challenge. A limited level of protection against H5N1 influenza virus infection was observed in unprimed or H1N1pdm09-primed mice, most likely mediated by cross-reactive antibody or T cell responses against influenza virus induced by priming and/or vaccination. Notably, mice with pre-existing orthopoxvirus-specific immunity had higher viral loads in the lungs and more severe weight loss compared to unprimed or H1N1pdm09 primed mice. In accordance with the described immunogenicity results, we hypothesize that orthopoxvirus-specific pre-existing immunity prevented the induction of antibody and/or T cell responses by rMVA-H1 or rMVA-H3 vaccination that are cross-reactive with H5.

It has been shown previously that VACV or MVA-based vaccination efficiently induces both orthopoxvirus-specific antibodies and T cell responses[260,321,327,336-339] (reviewed by B. Moss[340]). Hypothetically, vector-specific antibodies induced by previous immunizations could capture and neutralize rMVA virus particles upon (re-) vaccination, but non-neutralizing antibodies or orthopoxvirus-specific T cells could also play a role in interference. Interestingly, VACV-induced immunity only interfered with induction of antigen-specific T cell responses but not antibody responses whereas MVA-induced immunity could interfere with both. VACV was shown to induce cross-reactive MVA-specific T cells, but not antibody responses. Therefore, it is likely that interference of MVA-induced pre-existing immunity with induction of antigen-specific antibody responses is mediated by vector-specific antibodies. Indeed, antibodies induced by exposure of mice to MVA, but not to VACV, showed MVA-neutralizing

capacity *in vitro*. Similar results were obtained in humans, where VACV-induced antibodies hardly cross-reacted with MVA and only MVA-induced antibodies had MVA-neutralizing capacity. Follow-up adoptive transfers studies should be performed to identify the exact mechanism of interference of orthopoxvirus-specific immune responses with performance of MVA-based vaccinations.

It is important to note that our study in mice reflects a 'worst-case scenario', since a time interval of only four weeks between induction of pre-existing immunity and initial vaccination with rMVA was maintained, not allowing for waning of orthopoxvirus-specific immunity. This does not accurately reflect the human situation, where smallpox vaccination was discontinued in the mid 1970s[320]. Even though VACV-specific antibody responses were still detected in the serum of vaccinated individuals, these antibodies did not have MVA-neutralizing capacity *in vitro*. However, the timing used in this study does reflect the 'standard' interval of rMVA vaccination regimens, in which four week intervals are frequently observed between sequential vaccinations[234,260,335]. Our results show that repeated rMVA vaccination of humans does induce MVA-specific antibodies, which have neutralizing capacities *in vitro* and therefore may interfere with the immunogenicity of subsequent vaccinations.

The present study fills a gap in our understanding regarding immunogenicity of MVA-based vaccines in the presence of orthopoxvirus-specific immunity. Importantly, pre-existing immunity induced by VACV inoculation did not interfere with the induction of antigen-specific antibodies by rMVA vaccination. In sera obtained from both mice and humans, VACV-induced antibody responses could not neutralize MVA. In contrast, wtMVA-priming reduced the antigen-specific antibody response induced by vaccination with a low dose of rMVA-H5 in mice, an effect that was prevented or overcome when higher vaccine doses were used. Furthermore, the induction of antigen-specific $CD4^+$ and $CD8^+$ T cell responses was severely hampered by the presence of either MVA- or VACV-specific pre-existing immunity. Importantly, the presence of orthopoxvirus-specific immunity induced by VACV or MVA did not affect the protective efficacy of an rMVA-H5 vaccine against a lethal homologous challenge infection with H5N1 influenza virus. Although the responses to homologous influenza virus HA were not affected by pre-existing orthopoxvirus specific immunity, cross-reactivity with antigenic variants was reduced as shown by vaccination with rMVA-H1 and rMVA-H3. In conclusion, the present study shows that rMVA is still immunogenic in the presence of orthopoxvirus-specific immunity, however, it is essential to consider the orthopoxvirus immune status of vaccine recipients, the interval between vaccinations in case of repeated rMVA-based vaccination, the vaccine dose used and the main correlate of protection induced by rMVA-based vaccines.

Materials & Methods

Experimental design

To assess the effect of pre-existing orthopoxvirus-specific or influenza virus-specific immunity on rMVA vaccine immunogenicity, C57BL/6 mice were primed with either wtMVA, VACV or H1N1pdm09, and then vaccinated with rMVA expressing the influenza virus NP or HA gene. The effect of pre-existing immunity induced by priming on vaccine induced antigen-specific antibody and T cell responses was assessed, as well as the effect on the protective efficacy against a lethal H5N1 influenza virus challenge (**Table 1**). Furthermore, antibody responses against MVA and VACV were analyzed in sera from MVA- and VACV-exposed mice and humans, in order to establish the presence of MVA-specific neutralizing antibodies.

Ethics statement

Animal experiments were conducted in strict compliance with European guidelines (EU directive on animal testing 2010/63/EU). The animal protocol was approved by an independent animal experimentation ethical review committee (Erasmus MC permit number EUR3277-02). Animal welfare was observed on a daily basis, and all invasive animal handling was performed under anesthesia using 4% isoflurane in oxygen to minimize animal suffering. Human sera pre- and post-rMVA vaccination (three vaccinations at week 0 and 56 with 10^8 PFU rMVA-H5, n=6) were obtained during a randomized, double-blind phase 1/2a study at the Erasmus MC, Rotterdam, the Netherlands. The study involved adult volunteers (male/female, between ages 18-28) who provided informed consent. The study design was reviewed and approved by the Central Committee on Research involving Human Subjects in the Netherlands[260]. Furthermore, serum samples from VACV vaccinated (n=6) and unvaccinated (n=6) healthy individuals (male/female) were collected during a cross-sectional population-based study performed in the Netherlands from February 2006 until June 2007 (PIENTER2 study)[328]. Smallpox vaccination campaigns lasted until September 1974 in the Netherlands. To limit the inevitable age bias, sera from individuals born between 1970-1971 and 1976-1978 were selected for the VACV vaccinated and unvaccinated group, respectively. The work described here has been carried out in accordance with the code of ethics of the world medical association (declaration of Helsinki).

Cell lines

Madin-Darby Canine Kidney (MDCK) cells were cultured in Eagle's Minimum Essential Medium (EMEM, Sartorius Stedim BioWhittaker) supplemented with 10% fetal bovine serum (FBS, Greiner Bio-One), 20mM HEPES (Lonza BioWhittaker), 0.1% $CHNaO_3$ (Lonza BioWhittaker), and 100µg/ml penicillin, 100U/ml streptomycin and 2mM L-Glutamine (P/S/G, Lonza). CEF were isolated from 11-day-old chicken embryos (Drost Loosdrecht BV) and passaged once before use as described previously[256]. CEF were cultured in Virus Production-Serum Free Medium (VP-SFM, Gibco) containing P/S. HeLa cells were cultured in Dulbecco's Modified Eagle Medium (DMEM, Lonza) supplemented with 10% FBS, 20mM HEPES, 0.1% $CHNaO_3$ and P/S/G. Baby Hamster Kidney (BHK)-21 cells were cultured in DMEM supplemented with 10% FBS, 20mM HEPES, 0.1% $CHNaO_3$, 0.1mM non-essential amino acids (NEAA, Lonza) and P/S/G. HeLa cells were cultured in DMEM supplemented with 10% FBS, 20mM HEPES and 0.1% $CHNaO_3$ and P/S/G. All cells were cultured at 37°C in a humidified atmosphere with 5% CO_2.

Viruses

rMVA expressing the NP gene of influenza virus A/Puerto Rico/8/34 (PR8, rMVA-NP), the HA gene of A/Vietnam/1194/04 (rMVA-H5) or A/Netherlands/213/03 (rMVA-H3) under the control of the psynII promotor, rMVA expressing the HA gene of influenza virus A/California/4/09 (rMVA-H1) under control of the PH5 promotor and rMVA expressing GFP under control of the P11 promotor were prepared as described previously[253,256,341,342]. To generate final vaccine preparations of MVA-F6 (empty vector, wtMVA) or rMVA, the viruses were propagated in CEF, purified by ultracentrifugation through 36% sucrose and resuspended in 120mM NaCl 10mM Tris-HCl pH 7.4. rMVA constructs were validated by PCR analysis, sequencing and/or plaque titration. Furthermore, expression of antigens was validated by western blot and/or flow cytometry. The VACV strain Elstree was grown in HeLa cells as described above for the rMVA constructs on CEF cells. Influenza A viruses A/Netherlands/602/09 (H1N1pdm09) and A/Vietnam/1194/04 (H5N1) were propagated and titrated ($TCID_{50}$) in MDCK cells as described previously[343].

Mice

Specified pathogen free (SPF) female C57BL/6 mice 6-8 weeks of age were purchased from Charles River. The animals were housed at biosafety level (BSL-)2 in individual ventilated cage (IVC) units during priming and vaccination (week 0-15). During the H5N1 influenza virus challenge, mice were housed in filter-top cages in negatively pressured BSL-3 isolators (week 16-17). At all times, mice had access to food and water *ad libitum*.

H1N1pdm09 virus and VACV-Elstree dose-finding

Four groups of mice (10-12 weeks old, n=6) were inoculated with 10^4, 10^5, 10^6 or 10^7 PFU VACV-Elstree in 10µl PBS by intradermal (ID) tail scarification with a 25-29G needle[344] or with 10^3, 10^4, 10^5 or 10^6 $TCID_{50}$ H1N1pdm09 in 50µl PBS by the IN route. Clinical signs, weight loss and survival were recorded for 14 days, mice were euthanized 14 dpi or earlier when pre-defined humane endpoint criteria were met (>25% body weight loss).

Priming, rMVA vaccination and challenge

Mice (6-8 weeks old) were divided into seven groups (n=24) with four subgroups (n=6) each (**Table 1**). Animals were either unprimed (subgroup a) or were primed with 10^8 PFU wtMVA in 100µl PBS intramuscularly (IM, two shots, four-week interval [week 0 and 4], subgroup b), 10^7 PFU VACV-Elstree (single exposure, week 4, subgroup c) or 10^4 $TCID_{50}$ H1N1pdm09 (single exposure, week 4, subgroup d). VACV-Elstree and H1N1pdm09 were administered as described above at the optimal priming dose determined in the dose-finding experiments. After priming, mice received one or two IM vaccinations at week 8 and/or 12 with 10^8 PFU of rMVA-NP, rMVA-H1, rMVA-H3 and/or rMVA-H5 in 100µl PBS. Of note, 10^7 PFU rMVA-H5 was administered at week 8 to the mice of group 6 (**Table 1**) to establish if pre-existing immunity affects low dose rMVA-HA vaccination and if a boost with a high dose could overcome potential negative effects. After vaccination, a proportion of the mice vaccinated with rMVA-NP or rMVA-H5 were not challenged and were euthanized one (week 13) or two weeks (week 14) after the second vaccination, respectively (**Table 1**, group 1-2). The remainder of the animals (**Table 1**, group 3-7) was challenged IN with 10^3 $TCID_{50}$ A/Vietnam/1194/04 (H5N1) influenza virus four weeks after the second vaccination (week 16) and monitored twice daily. Mice were euthanized when pre-defined humane endpoint criteria (>25% body weight loss) were reached or at seven days post-challenge (week 17). Blood, spleen and/or lung samples were harvested during necropsy. A single mouse in the wtMVA-primed subgroup of the 2x rMVA-H5 challenge group (group 6, subgroup b) had to be euthanized due to a wound unrelated to the experiment at week 4. One mouse in the H1N1pmd09-prime group of the 1x rMVA-H1 and 1x rMVA-H5 group (group 7, subgroup d) had to be euthanized 10 days after priming because humane endpoint criteria were met. These mice were excluded from further analysis.

Virus isolation from lungs

Directly after necropsy, all lungs were snap frozen and stored at -80°C for processing at a later time point. To perform virus isolations, lungs were thawed, lung weight was recorded and lungs were homogenized with a Polytron homogenizer (Kinematica AG) in MDCK infection medium (EMEM supplemented with 20mM HEPES, 0.1% $CHNaO_3$ and P/S/G). Quadruplicate ten-fold serial dilutions of these samples in MDCK infection medium supplemented with 0.002% TPCK-Trypsin (Lonza) were used to determine the virus titers on MDCK cells as described previously[343].

Stimulation and intracellular cytokine staining of splenocytes

During necropsy spleens were collected in Iscove's Dulbecco's Medium (IMDM, Lonza) supplemented with 5% FBS and P/S/G for direct preparation of single cell suspensions using 100µm strainers (Falcon). Erythrocytes were removed from single cell suspensions by treatment with red blood cell lysis buffer (Roche diagnostics). For intracellular cytokine staining, splenocytes were stimulated with 5µM synthetic peptide (epitope $NP_{366-374}$: ASNENVEIM [**Fig. S2**] or ASNEMMETM [**Fig. 4**]) or 1µg / 250.000 cells recombinant HA protein from H5N1 influenza virus A/Vietnam/1203/04 or A/Indonesia/5/05 (Protein Sciences) in IMDM supplemented with GolgiStop and incubated for 6h at 37°C. Mock-treated splenocytes and splenocytes stimulated with 50ng/ml PMA (Sigma-Aldrich) and 0.5µg/ml ionomycin (Sigma-Aldrich) served as appropriate negative and positive controls. After stimulation, splenocytes were incubated with fluorochrome-labeled antibodies to $CD3e^{APC\text{-}Cy7}$ (BD Pharmingen), $CD8b^{FITC}$ (BD Pharmingen), $CD4^{PerCP}$ (BD Pharmingen) and viable cells were identified with Aqua LIVE/DEAD (Invitrogen). Subsequently, cells were fixed and permeabilized using BD Cytofix/Cytoperm™ Plus (BD Biosciences), and incubated with anti-IFN-$\gamma^{PacificBlue}$ (Biolegend). Samples were acquired on a FACS Canto II and data was analyzed as described previously[341,345] using FACS Diva software (BD Biosciences).

Protein Array (PA) assay

Mouse sera collected at week 8 and 16 (**Table 1**) were used to determine the presence of antibodies to selected antigens by PA as described previously[346,347]. In short, recombinant HA1 derived from influenza viruses A/California/6/09 (pH1), A/Wyoming/3/03 (H3 2003), A/Victoria/361/11 (H3 2011), A/Hong Kong/156/97 (H5 clade 0), A/Vietnam/1194/04 (H5 clade 1), A/Cambodia/R045050/07 (H5 clade 1.1), A/Indonesia/5/05 (H5 clade 2.1), A/Turkey/15/06 (H5 clade 2.2), A/Turkey/Germany-MV/R2472/14 (H5 clade 2.3.4.4), A/goose/Guiyang/337/06 (H5 clade 4) and A/chicken/Vietnam/NCVD-016/08 (H5 clade 7), as well as uninfected and wtMVA infected BHK-21 cells lysed in 1% Triton-X100 (Sigma) in PBS supplemented with mini cOmplete™ EDTA free protease inhibitor tablet (Roche) were printed onto nitrocellulose slides by asciFlexarraver (Scienion). Sera were incubated on the slides in Blotto Blocking Buffer (Thermo Fisher Scientific Inc.) supplemented with 0.1% Surfactant-Amps (Thermo Fisher Scientific

Inc.). Subsequently, goat-anti-human IgG labelled with AlexaFluor647 (Jackson ImmunoResearch Laboratories Inc.) was used as conjugate and fluorescent signals were measured using a Powerscanner (Tecan Group Ltd). The titer of each serum sample was defined as the interpolated serum concentration generating the 50% point using a four-parameter logistic nonlinear regression model using R (R Statistical Computing, version 3.1.0. Measured titers were corrected for the positive control included on each slide.

Detection of MVA- or VACV-specific antibodies by ELISA

For detection of VACV-specific antibodies, HeLa cells were mock-treated or infected with VACV-Elstree at MOI 1 and harvested in 1% Triton-X100 in PBS supplemented with mini cOmplete EDTA free protease inhibitor tablet. Similar procedures were used to obtain BHK-21 cell lysates mock-treated or infected with wtMVA. Sera used for detection of MVA- or VACV-specific antibodies were pre-cleared O/N at 4°C in a 96-well plate with confluent BHK-21 or HeLa cells, respectively. For ELISA, 96-well plates (Corning Costar) were coated overnight at 4°C with 10-25µl cell lysate per well in 0.05M Carbonate/Bicarbonate pH 9.6. Plates coated with cell lysate were washed and all plates were blocked for 1h at room temperature (RT) with blocking buffer consisting of PBS supplemented with 0.05% Tween-20 (PBST, Merck-solutions) and 2% milk powder (w/v, Campina). Subsequently, a 3-log dilution series of serum in blocking buffer was prepared, starting dilution 1:10 or 1:30, and 50µl was transferred to wells of the antigen-coated plates and incubated for 1-1.5h at RT. Blocking buffer and VACV-positive serum served as appropriate negative or positive control, respectively. Plates were washed with PBST and incubated for 1h at RT with HRP-conjugated goat-anti-mouse IgG (DAKO) or goat-anti-human IgG (Southern Biotech). Plates were washed with PBST and incubated for 10min with 50µl TMB peroxidase substrate (KPL) after which the reaction was stopped with 0.5M H_2SO_4 (Merck). Absorbance was measured at 450nm using a Tecan infinite F200. The OD_{450} values at a single dilution in the linear area of the curve were determined and analyzed. Due to limited amounts of serum, sera were pooled per subgroup (**Table 1**, n=3-6). Sera of VACV-primed animals were tested individually in VACV ELISA as much as possible, although in some groups a few samples had to be pooled (indicated in figure legends). The OD_{450} value obtained with mock-infected BHK-21 or HeLa cell lysate was subtracted from the OD_{450} value obtained with the respective infected cell lysate to determine a net OD_{450} response.

Hemagglutination inhibition (HI) assay

Sera were treated with a receptor-destroying enzyme (cholera filtrate) overnight at 37°C, followed by heat-inactivation for 1h at 56°C. HI assay was performed in a 2-fold serial dilution in duplicate following a standard protocol using 1% turkey erythrocytes and four HA units of an H5N1 reverse genetics influenza virus with HA (without multibasic cleavage site) and NA gene segments of A/Vietnam/1194/04 and the remaining gene segments of influenza virus A/Puerto Rico/8/34 (6+2)[348].

Plaque reduction assay

Mouse sera were pooled per subgroup (**Table 1**, n=2-5) due to limited serum availability. Sera were heat-inactivated for 30min at 56°C. A 2-log dilution series – starting dilution 1:10 – was prepared in CEF culture medium and incubated for 2h with 200 PFU/well wtMVA (mouse sera) or rMVA-GFP (human sera) in a 1:1 ratio at 37°C. Human serum with antibodies against MVA was used as a positive control. Subsequently, the serum-virus mixture was incubated for 2h at 37°C on a confluent monolayer of CEF cells in 96-wells culture plates. Cells were washed with PBS and incubated for 44-48h 37°C. CEF used for serology of mouse samples were fixed with acetone:methanol in a 1:1 ratio (Sigma-Aldrich). Plates were blocked with 3% FBS in PBS for 1h. Subsequently, plaques were stained with rabbit anti-VACV (Lister strain, Acris) followed by goat-anti-rabbit HRP-conjugate (Jackson ImmunoResearch Laboratories Inc.). Samples were developed using True Blue (KPL). The percentage of area covered by stained plaques was measured using a CTL immunospot reader with CTL biospot software. CEF used for serology of human samples were fixed with 2% paraformaldehyde (PFA) for 10min after which fluorescent plaques were detected using a Typhoon™ FLA9500 (GE Healthcare). Plaques were counted using ImageQuant TL Colony v8.1 software (GE Healthcare). The MVA-neutralization titer was determined as the reciprocal of the highest dilution at which the area covered by plaques was below 50% of the average percentage of the area covered (mouse sera, **Fig. S4A**) or counted spots (human sera, **Fig. S4B**) in n=12 wells without any added serum.

Statistical analysis

Longitudinal body weight data after H1N1pdm09 priming from different groups were analyzed using a repeated measures ANOVA model, with time as within factor. One way ANOVA with multiple comparisons was used to compare the normally distributed (according to the Shapiro-Wilk test) VACV-specific antibody responses after priming (week 8), H5-specific PA antibody responses after one vaccination and the 2003/2011 H3-specific PA antibody responses in mice. A Kruskal-Wallis test was used to compare the not normally distributed HI titers against A/Vietnam/1194/04 after a single vaccination, NP- or H5-specific T cell responses and viral lung titers. HI titers below the detection limit (titer 40) were set to a titer of 20 (the highest possible titer below 40). Statistical differences in the MVA-specific PA response were determined relative to the '0x MVA' control sample using a Kruskal-Wallis test. Furthermore, the ELISA and neutralization titers in human serum samples were compared using a Wilcoxon matched-pairs signed rank test (MVA sera) or a Mann-Whitney test (VACV sera). Neutralization titers in the plaque reduction assay below the detection limit (10) were set to a titer of 5 (the highest possible titer below 10).

Acknowledgements

Thanks to Theo Besteboer, Rogier Bodewes, Joost Kreijtz, Heidi de Gruyter for contributing to preparation of the virus stocks. Asisa Volz and Gerd Sutter kindly provided the rMVA-H1 and rMVA-GFP stocks. The authors acknowledge Felicity Chandler and Mark Pronk for excellent technical assistance. In addition, thanks to Manon Cox from Protein Sciences who generously provided purified recombinant HA protein.

Supplementary Material

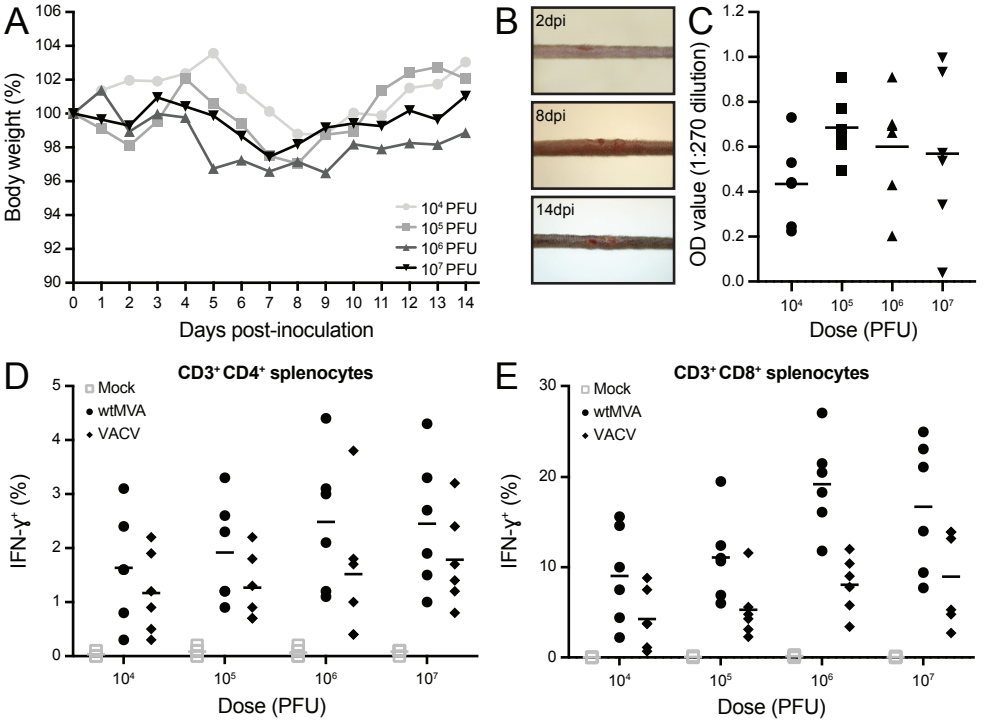

Figure S1. VACV-Elstree dose-finding. *C57BL/6 mice (n=6 per group) were inoculated with 10^4, 10^5, 10^6 or 10^7 PFU via tail scarification. (**A**) Mean body weight post-inoculation per group. (**B**) Representative images of blister formation at 2, 8 and 14 days post-inoculation (dpi). (**C**) VACV-Elstree specific antibody responses at 14 dpi were measured by ELISA using VACV-infected HeLa cell lysate. The background signal on mock-infected cell lysate was subtracted. The mean is indicated. (**D-E**) Percentage of interferon (IFN)-γ producing $CD3^+$ $CD4^+$ (**D**) and $CD3^+$ $CD8^+$ (**E**) splenocytes after stimulation with wild-type (wt)MVA or VACV at 14 dpi. Unstimulated samples were included as negative control and are shown in grey. The mean is indicated.*

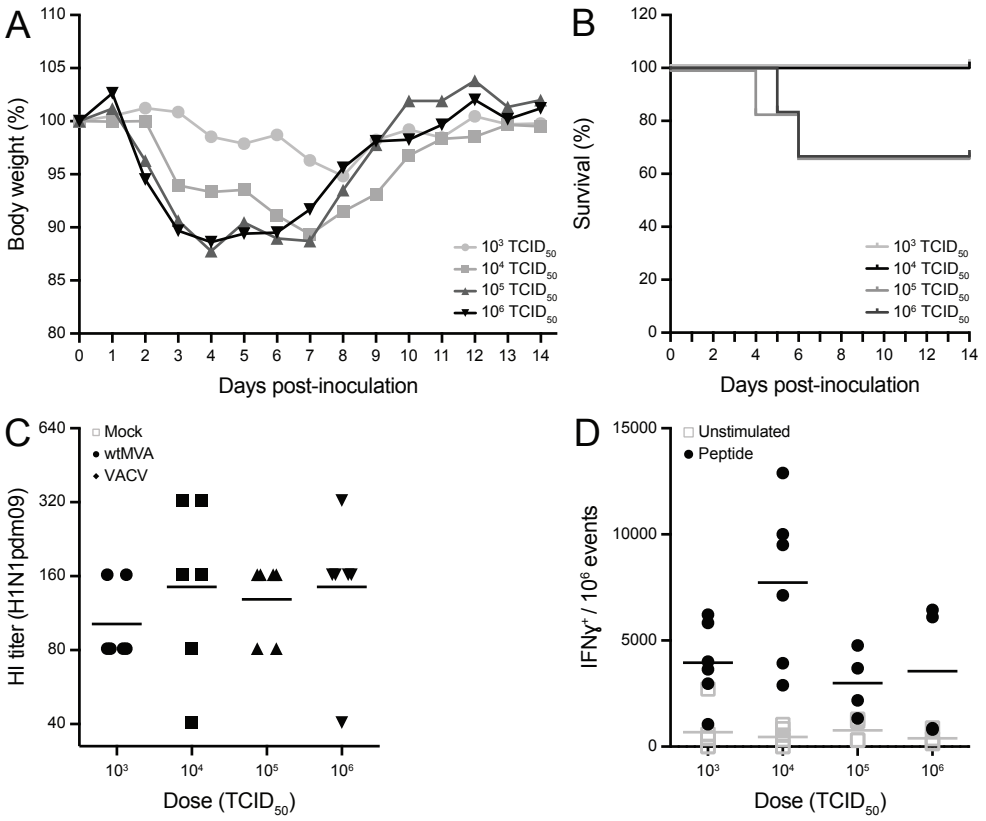

Figure S2. H1N1pdm09 dose-finding. *C57BL/6 mice (n=6 per group) were inoculated with 10^3, 10^4, 10^5 or 10^6 TCID$_{50}$ influenza virus H1N1pdm09. (**A**) Mean body weight post-inoculation per group. (**B**) Survival curves per group. (**C**) HI antibody titers against H1N1pdm09 of individual mice at 14 dpi. The mean is indicated. (**D**) Number of IFN-γ producing CD3$^+$ CD8$^+$ splenocytes of individual mice after stimulation with NP$_{366-374}$ peptide. Unstimulated samples were included as negative control and are shown in grey. The mean is indicated.*

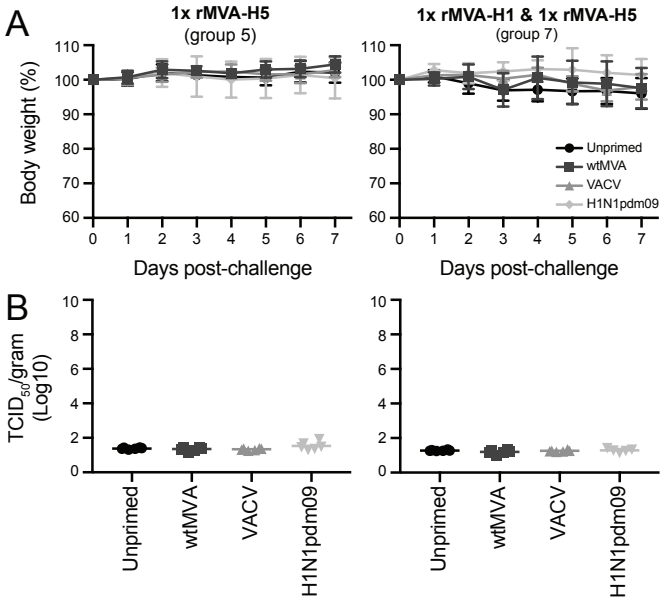

Figure S3. Pre-existing immunity does not impair protective capacity of a single rMVA-H5 vaccination. *(**A**) Body weight for each of the priming groups after challenge with a lethal dose H5N1 influenza virus, shown for group 5 (one rMVA-H5 vaccination) and group 7 (one rMVA-H1 and one rMVA-H5 vaccination). Mean and standard deviation (SD) are indicated per priming group. (**B**) Viral load in the lungs shown as $TCID_{50}$ per gram lung for each individual animal. Mean is indicated per priming group.*

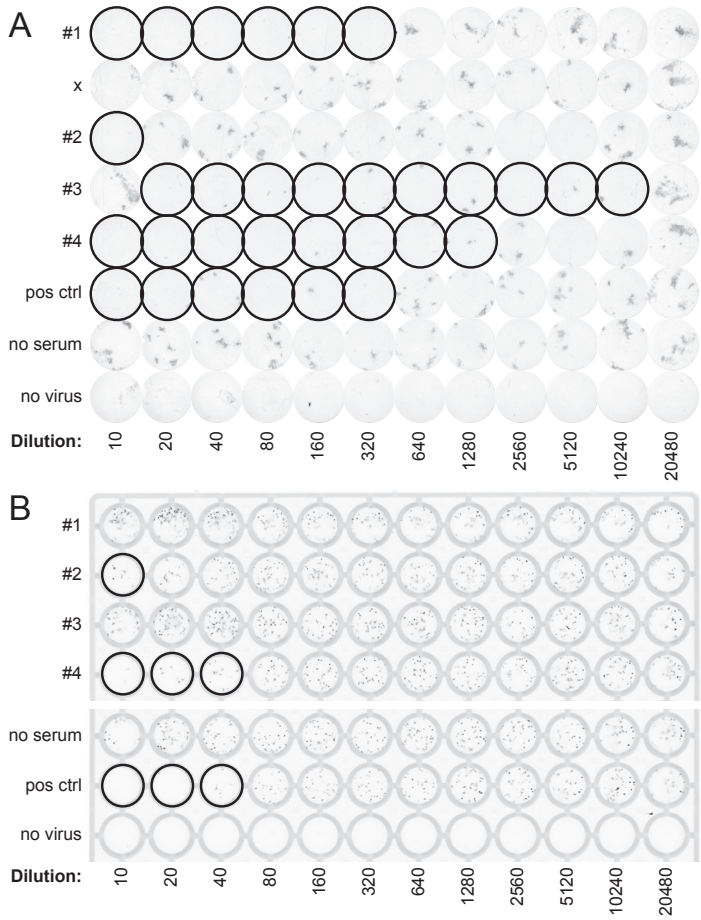

Figure S4. Quantification of MVA neutralization in plaque reduction assay*. Two-fold serial dilutions of mouse sera (**A**) or human sera (**B**) were incubated with 200 PFU/well wtMVA or rMVA-GFP, respectively. After 2h, the serum-virus mixtures were transferred to CEF cells and incubated for 44-48h. (**A**) For the plaque reduction assay using mouse sera, cells were fixated with acetone and methanol in a 1:1 ratio, followed by staining with rabbit anti-VACV and a goat-anti-rabbit HRP conjugate. Substrate was revealed using True Blue. Shown is a representative image of an CTL immunospot scan. (**B**) For the plaque reduction assay using human sera, cells were fixated with 2% PFA and directly scanned for GFP fluorescence. Shown are representative images of a Typhoon scan. Neutralization titer was determined as the reciprocal of the highest dilution at which the area covered by plaques was below background (defined as 50% of the average percentage of the area covered in n=12 wells without any added serum). Wells with values below the cutoff are indicated with a bold outline. #1-4 = number of mouse or human samples, x = no serum added.*

Chapter 3

Pre-clinical assessment of MVA-based influenza vaccines

CHAPTER 3.1

Increased protein degradation improves influenza virus nucleoprotein-specific CD8$^+$ T cell activation *in vitro* but not in C57BL/6 mice

AF Altenburg, CE van de Sandt, SE van Trierum, HLM De Gruyter, PRWA van Run, RAM Fouchier, K Roose, X Saelens, A Volz, G Sutter, RD de Vries & GF Rimmelzwaan

Journal of Virology, 2016; 90(22): 10209–10219

Due to antigenic drift of influenza viruses, seasonal influenza vaccines need to be updated annually. These vaccines are based on predictions of strains likely to circulate in the next season. However, vaccine efficacy is greatly reduced in the case of a mismatch between circulating and vaccine strains. Furthermore, novel antigenically distinct influenza viruses are introduced into the human population from animal reservoirs occasionally and may cause pandemic outbreaks. To dampen the impact of seasonal and pandemic influenza, vaccines that induce broadly protective and long-lasting immunity are preferred. Because influenza virus-specific CD8$^+$ T cells are directed mainly against relatively conserved internal proteins, like nucleoprotein (NP), they are highly cross-reactive and afford protection against infection with antigenically distinct influenza virus strains, so-called heterosubtypic immunity. Here, we used Modified Vaccinia virus Ankara (MVA) as a vaccine vector for the induction of influenza virus NP-specific CD8$^+$ T cells. To optimize the induction of CD8$^+$ T cell responses, we made several modifications to NP, aiming at retaining the protein in the cytosol or targeting it to the proteasome. We hypothesized that these strategies would increase antigen processing and presentation and thus improve the induction of CD8$^+$ T cell responses. We showed that NP with increased degradation rates improved CD8$^+$ T cell activation *in vitro* if the amount of antigen was limited or if CD8$^+$ T cells were of low functional avidity. However, after immunization of C57BL/6 mice, no differences were detected between modified NP and wild-type NP (NPwt), since NPwt already induced optimal CD8$^+$ T cell responses.

IMPORTANCE – Due to the continuous antigenic drift of seasonal influenza viruses and the threat of a novel pandemic, there is a great need for the development of novel influenza vaccines that offer broadly protective immunity against multiple subtypes. CD8$^+$ T cells can provide immunity against multiple subtypes of influenza viruses by the recognition of relatively conserved internal antigens. In this study, we aimed at optimizing the CD8$^+$ T cell response to influenza A virus by making modifications to influenza A virus nucleoprotein (NP) expressed from the Modified Vaccinia virus Ankara (MVA) vaccine vector. These modifications resulted in increased antigen degradation, thereby producing elevated levels of peptides that can be presented on major histocompatibility complex (MHC) class I molecules to CD8$^+$ T cells. Although we were unable to increase the NP-specific immune response in the mouse

strain used, this approach may have benefits for vaccine development using less-immunogenic proteins.

Introduction

Influenza virus infections have a major impact on public health worldwide. Influenza A (subtypes H1N1 and H3N2) and influenza B viruses cause epidemics annually, which can be attributed to their capacity to accumulate mutations in the two major influenza virus surface proteins, hemagglutinin (HA) and neuraminidase (NA), a process known as antigenic drift[4,17,18]. This allows these viruses to escape recognition by virus-neutralizing antibodies induced after previous infections or vaccination. In addition, zoonotic transmission of influenza A viruses of alternative subtypes, such as avian influenza viruses of the H5N1 and H7N9 subtypes, occurs sporadically. Occasionally, the introduction of an influenza A virus of a novel subtype, which usually emerges after a genetic reassortment event, causes a pandemic outbreak because virus-neutralizing antibodies to these novel viruses are virtually absent in the human population.

Upon infection with influenza viruses, neutralizing antibody responses are induced, which are directed mainly against the variable globular head domain of HA[1]. In addition, antibodies that are directed to the more conserved stem region of the HA molecule and that are more broadly neutralizing than those directed to the head region have been identified[146,152,159-161]. However, the contribution of stem region-specific antibodies to the overall antibody response is limited[349] and fails to reach protective levels after natural infection.

In addition, infection with influenza viruses results in the induction of virus-specific $CD4^+$ and $CD8^+$ T cell responses (reviewed by Altenburg *et al*.[316]). Upon recognition of viral epitopes presented by major histocompatibility complex (MHC) class I molecules on virus-infected cells, $CD8^+$ T cells eliminate these cells and thus contribute to the clearance of infection[316]. Viral peptides are generated in infected cells through the processing of viral proteins by the proteasome in the cytosol. After transport into the endoplasmic reticulum (ER) by transporter associated with antigen processing (TAP), the peptides are loaded onto MHC class I molecules and transported to the cell surface for recognition by cytotoxic $CD8^+$ T lymphocytes (CTLs) (reviewed by Hewitt *et al*.[58]). Because the majority of influenza virus-specific $CD8^+$ T cells recognize epitopes located in more-conserved viral proteins, such as nucleoprotein (NP) and the matrix 1 (M1) protein[73,107,350,351], they display a high degree of cross-reactivity. Indeed, it has been shown that CTLs raised after infection with human seasonal influenza A viruses cross-react with avian influenza A viruses of other subtypes and contribute to so-called heterosubtypic immunity[53,54,57,72,82,193,352,353].

Currently used seasonal and pandemic influenza vaccines aim at the induction of mainly HA-specific antibodies and do not efficiently induce $CD8^+$ T cell responses[136,137]. However, if there is an antigenic mismatch between vaccine strains and circulating influenza virus strains, the vaccines offer little or no protection, as was the case for the H3N2 vaccine component during the 2014-2015 influenza season[317-319]. Furthermore, the production of sufficient vaccine doses is a time-

consuming process, as was demonstrated during the influenza pandemic of 2009 caused by H1N1pdm09 virus, when in most countries, vaccines became available after the peak of the pandemic[132,133]. Therefore, the availability of influenza vaccines that induce more broadly protective immune responses and/or novel technologies that allow more rapid production of sufficient vaccine doses are highly desirable.

In order to induce protection against multiple subtypes of influenza viruses, vaccines ideally induce cross-reactive T cell responses. For the efficient induction of $CD8^+$ T cell responses, proteins need to be processed endogenously for MHC class I-restricted antigen presentation, which requires the delivery of vaccine antigens to the cytosol of antigen-presenting cells (APCs). Modified Vaccinia virus Ankara (MVA) is a vaccine vector that has been shown to efficiently induce T cell responses in various animal models and in humans[235,266-269,271-275]. Other advantages include the rapid production of an MVA-based vaccine, the easy and stable insertion of a transgene of interest, intrinsic adjuvant capacities, and an excellent safety record, even in immunosuppressed macaques and elderly people[260,271,279,280]. Thus, MVA is considered an ideal vector system for the delivery of conserved influenza virus proteins.

We hypothesized that the immunogenicity of NP expressed from an MVA vector could be increased by enhancing the cytosolic degradation of this protein. In influenza virus-infected cells, NP is imported into the nucleus via interactions of host cell proteins with nuclear localization signals (NLSs) in NP. In the nucleus, NP binds to newly replicated viral RNA (reviewed by Eisfeld *et al*.[354]). In order to achieve increased antigen degradation[355], we modified the NLS of influenza virus NP to prevent import into the nucleus and to retain the protein in the cytosol[356,357] or fused NP to ubiquitin (Ubq) to target the protein for degradation by the proteasome[358-364]. Although we observed differential recognition by human virus-specific $CD8^+$ T cells *in vitro*, the modifications did not alter the virus-specific $CD8^+$ T cell response or the protective efficacy of recombinant MVA (rMVA) expressing NP in C57BL/6 mice.

Materials and Methods

Ethics statement

Animals were housed and experiments were conducted in strict compliance with European guidelines (European Union directive on animal testing 2010/63/EU). The protocol was approved by an independent animal experimentation ethical review committee in Driebergen, the Netherlands (Erasmus MC permit number EUR3277). Animal welfare was observed daily, and to minimize animal suffering, all animal handling was performed under anesthesia using 4% isoflurane in oxygen.

Cell culture

Madin-Darby Canine Kidney (MDCK) cells were cultured in Eagle's Minimum Essential Medium (EMEM; Lonza) supplemented with 10% fetal bovine serum (FBS, Greiner Bio-One); 20mM HEPES (Lonza); 0.1% $CHNaO_3$ (Lonza); and 100µg/ml penicillin, 100U/ml streptomycin, and 2mM L-glutamine (P/S/G; Lonza). Chicken Embryo Fibroblasts (CEFs) were isolated from 11-day-old chicken embryos (Drost Loosdrecht BV) and passaged once before use. CEFs were cultured in virus production serum-free medium (VP-SFM, Gibco) containing penicillin and streptomycin (P/S). Baby Hamster Kidney 21 (BHK-21) cells were cultured in Dulbecco's Modified Eagle Medium (DMEM, Lonza) supplemented with 10% FBS, 20mM HEPES, 0.1% $CHNaO_3$, 0.1mM non-essential amino acids (NEAA, Lonza), and P/S/G. HeLa cells were cultured in DMEM supplemented with 10% FBS, 20mM HEPES, 0.1% $CHNaO_3$, and P/S/G. B lymphoblastoid cell lines (BLCLs) were prepared as described previously[365]. BLCLs were cultured in RPMI 1640 (Lonza) containing 10% FBS and P/S/G. All cell lines were cultured at 37°C with 5% CO_2.

Influenza virus
Influenza virus A/Puerto Rico/8/34 (PR8) was propagated in MDCK cells for *in vitro* experiments and in embryonated chicken eggs for *in vivo* experiments, as described previously[54,353]. Infectious virus titers were determined in MDCK cells as described previously[343].

Generation of recombinant MVA
The respective (modified) NP nucleotide sequences (PR8 [GenBank accession number NC_002019]) were purchased from Baseclear BV. rMVA constructs expressing various NP molecules (rMVA-NP constructs) under the control of the PsynII promoter were prepared by mCherry-dependent plaque selection on CEFs after infection with MVA clonal isolate F6 and transfection with 1µg pMKIII-Red carrying the respective NP gene, as described previously[256]. rMVA-NP genomes were analyzed by PCR to verify the NP gene insertion and genetic stability. To generate a final vaccine preparation, the virus was amplified in CEFs, purified by ultracentrifugation through 36% sucrose, and reconstituted in a solution containing 10mM Tris-HCl (pH 9) or 120mM NaCl + 10 mM Tris-HCl (pH 7.4).

NP protein expression from recombinant MVA
BHK-21 cells were uninfected (mock-treated) or infected with the indicated rMVA-NP constructs at a multiplicity of infection (MOI) of 10. After 24h, cells were harvested in 1% NP-40 (Sigma-Aldrich) 0.1% sodium dodecyl sulfate (SDS, Invitrogen) lysis buffer supplemented with a cOmplete Protease Inhibitor Cocktail tablet (Roche) and resolved by SDS-PAGE. Blots were probed with a monoclonal anti-NP antibody (clone HB65 IgG2a, American Type Culture Collection) and subsequently probed with goat anti-mouse (GaM)-IRDye (Li-Cor Biosciences). The blot was scanned by using an Odyssey Li-Cor instrument (Westburg BV) and Odyssey 2.1 software. Image colors were inverted, and the contrast was linearly enhanced by using Adobe Photoshop CC.

Intracellular localization of NP determined by confocal microscopy
HeLa cells were seeded onto glass coverslips and left uninfected (mock) or infected with influenza virus PR8 or with the respective rMVA-NP constructs at an MOI of 1. At the indicated time points, cells were fixed by using 4% paraformaldehyde (PFA, Sigma-Aldrich), permeabilized with 0.1% Triton X-100 (Sigma-Aldrich), and stained with an anti-NP antibody or IgG2a isotype-matched control antibody (R&D Systems), followed by GaM-fluorescein isothiocyanate (FITC, BD Bioscience) under pre-determined optimal conditions. Subsequently, coverslips were mounted onto slides by using ProLong Gold with 4',6-diamidino-2-phenylindole (DAPI, Invitrogen). Samples were analyzed with a confocal laser scanning microscope with an LSM700 system fitted onto an Axio Observer Z1 inverted microscope (Zeiss). Images were generated by using Zen software. The contrast was linearly enhanced by using Adobe Photoshop CC.

Radiolabeling and immunoprecipitation experiments
HeLa cells were left uninfected (mock) or were infected with the respective MVA constructs at an MOI of 3. After 6h, the cells were harvested by using 0.05% trypsin–EDTA (Gibco) and resuspended in DMEM without methionine-cysteine (Gibco) supplemented with 10% dialyzed FBS (Invitrogen), 20mM HEPES, and P/S. The cells were pulsed with 30µCi/10^6 cells [^{35}S] cysteine-methionine (PerkinElmer Life Sciences) for 10min. Subsequently, the cells were washed and incubated in HeLa culture medium. Zero hours or 11h after pulse-labeling, the cells were washed with phosphate-buffered saline (PBS) and resuspended in lysis buffer containing 0.75% Triton X-100 and 0.25% NP-40. The lysate was precleared for 1h at 4°C with 0.5µg IgG2a isotype antibody and protein G-Sepharose (GE Healthcare). Subsequently, the samples were incubated with 1µg anti-NP (Hb65) plus protein G-Sepharose. The beads were washed three times and resuspended in lysis buffer plus Laemmli buffer. Samples were resolved by SDS-PAGE and visualized by autoradiography.

Activation of $CD8^{\pm}$ T cell clones *in vitro*
Infected target cells were prepared by inoculating HLA-A*01:01^{+} B*27:05^{+} BLCLs with the respective MVA constructs at an MOI of 0.3 or 3. As a positive control, cells were pulsed with 10µM either the HLA-A*01:01-restricted synthetic peptide spanning NP residues 44 to 52 ($NP_{44–52}$, CTELKLSDY) or the HLA-B*27:05-restricted $NP_{383–391}$ synthetic peptide (SRYWAIRTR). The inoculum was removed after 1h, and the cells were cocultured with either the $NP_{44–52}$- or the $NP_{383–391}$-specific $CD8^{+}$ T cell clone (TCC) at an effector-to-target cell (E:T) ratio of 1:5 in the presence of GolgiStop (4µl/6ml, BD Biosciences) and a

fluorochrome-labeled antibody to CD107a. The cells were cultured at 37°C for 10h, a time carefully chosen based on previous work[366], allowing us to investigate early events of T cell activation. Subsequently, cells were stained with fluorochrome-labeled $CD8^{FITC}$ (Dako), $CD3^{PerCP}$ (BD Biosciences), $CD107a^{V450}$ (BD Biosciences), and IFN-γ^{APC} (BD Biosciences) antibodies and a marker for excluding dead cells (Aqua Live/Dead; Invitrogen). Samples were analyzed by flow cytometry using FACSCanto II and FACSDiva software.

Vaccination-challenge experiments

Specific-pathogen-free female C57BL/6 mice were purchased from Charles River and were 6 to 8 weeks of age at the start of the experiment. Animals were housed in individual ventilated cage (IVC) units and had access to food and water *ad libitum*. Groups of 20 mice each (n=10 for the PBS and wild-type MVA [wtMVA] control groups, which were combined for statistical purposes) were vaccinated intramuscularly (i.m.) twice at a time interval of 4 weeks with 10^8 PFU MVA in the two hind legs (50µl/leg). Four weeks after the second vaccination, mice were challenged intranasally (i.n.) with 5 x 10^2 50% tissue culture infective doses ($TCID_{50}$) of influenza virus PR8 in 50µl. Four mice (week 5) or eight mice (4 or 7 days post-challenge) were euthanized, and spleen and lung samples were harvested for analysis.

Intracellular cytokine staining of splenocytes after peptide stimulation

Spleens were collected during necropsy in Iscove's modified Dulbecco's medium (IMDM, Lonza) supplemented with 5% FBS and P/S/G for direct preparation of single-cell suspensions using 100µm strainers (Falcon). Spleen single-cell suspensions were treated with red blood cell lysis buffer (Roche Diagnostics). Splenocytes were mock treated, stimulated with 5µM synthetic peptide ($NP_{366–374}$ epitope [ASNEMMETM]) or with 50pg phorbol myristate acetate (PMA, Sigma-Aldrich) and 500pg ionomycin (Sigma-Aldrich) as positive controls in IMDM supplemented with GolgiStop, and incubated for 6h at 37°C. Cells were stained with fluorochrome-labeled $CD3e^{APC\text{-}Cy7}$ (BD Pharmingen), $CD8b^{FITC}$ (BD Pharmingen), $CD4^{PerCP}$ (BD Pharmingen), and IFN-$\gamma^{Pacific\ Blue}$ (PB; BioLegend) antibodies and Aqua Live/Dead stain. Subsequently, cells were fixed and permeabilized by using BD Cytofix/Cytoperm Plus (BD Biosciences) and stained for IFN-ɣ. Samples were analyzed by flow cytometry using a FACSCanto II instrument.

Virus isolation form lungs

Directly after harvest, lungs (n=6 per group at 4 and 7 days post-infection [dpi]) were snap-frozen by using dry ice with ethanol and stored at -80°C for processing at a later time point. Lungs were homogenized with a Polytron homogenizer (Kinematica AG) in MDCK culture medium supplemented with 0.002% tosylsulfonyl phenylalanyl chloromethyl ketone (TPCK)-trypsin (Lonza). Quadruplicate 10-fold serial dilutions of these samples were used to determine virus titers in MDCK cells as described previously[343].

Histopathological examination of lungs

Lungs (n=2 for each group at week 5 and at 4 and 7 dpi) were inflated *in situ* with 10% neutral buffered formalin. After fixation in formalin and embedding in paraffin, lungs were sectioned at 3µm and stained with hematoxylin and eosin (HE) for histological evaluation. Furthermore, influenza A virus-infected cells were detected by staining tissues with a primary antibody against NP as described previously, followed by GaM-IgG2a-HRP (Southern Biotech)[367]. An IgG2a isotype control was included as a negative control. Samples were analyzed by using an Olympus BX51 light microscope. Images were taken by using a 20x ocular and Olympus cell^A software.

Statistical analysis

Differences in $CD8^+$ T cell clone activation (**Fig. 4C-F**) were analyzed by one-way analysis of variance (ANOVA) with a Tukey test, which compares the mean for each column to the mean for every other column. Parametric tests did not apply for mouse lung titrations (**Fig. 5C-D**) or peptide-stimulated $CD3^+$ $CD8^+$ mouse splenocyte samples (**Fig. 5F-H**) according to the D'Agostino-Pearson omnibus normality test, either due to a small number of samples or because data were not normally distributed. Therefore, the Kruskal-Wallis test with Dunn's correction was used. From multiple previous experiments, it was observed that the PBS and wtMVA control groups gave similar results. These two control groups were combined for statistical purposes to reduce the number of animals used in this study, as required by the animal experimentation ethical review committee.

Results

Construction of rMVA-based vaccines driving expression of NP with or without modifications

In order to increase antigen processing and presentation and improve subsequent $CD8^+$ T cell activation, modifications were made to NP from influenza virus A/Puerto Rico/8/34 (PR8). First, NP genes in which the NLS was mutated (NPmut) or deleted (NPΔNLS) were designed[356,357] (**Fig. 1A**). Second, Ubq was fused to the N-terminus of NP (UbqNP). The C-terminus of ubiquitin was mutated to prevent hydrolysis[362-364] (**Fig. 1A**). rMVA constructs driving the expression of wild-type NP (NPwt) or modified NP genes were generated. The identity of the rMVA-NP constructs was confirmed by PCR analysis (data not shown), nucleotide sequencing (data not shown), and assessment of protein expression (**Fig. 1B**). NP has a caspase cleavage site at amino acid position 16, resulting in full-length (56 kDa) and truncated (53 kDa) versions of the protein[368-370]. Due to the deletion of the NLS, NPΔNLS is the same size as the truncated NPwt protein. The full-length UbqNP fusion protein has an increased molecular mass of 64.5 kDa (**Fig. 1B**).

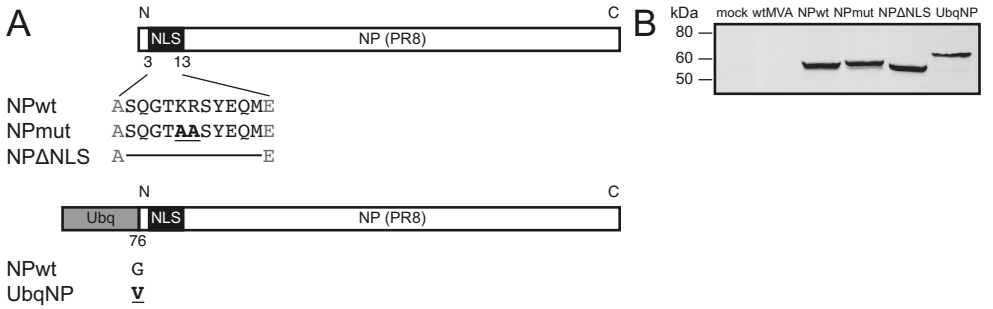

***Figure 1. Modifications of NP and confirmation of expression by rMVA**. (**A**) In order to promote cytosolic localization, the NLS of NP was mutated (NPmut) or deleted (NPΔNLS). Additionally, a ubiquitin-NP (UbqNP) fusion construct was made, in which the C-terminal glycine of ubiquitin was mutated to valine in order to prevent hydrolysis. (**B**) rMVAs expressing the different (modified) NP molecules were generated. Expression of NP in infected BHK-21 cells was demonstrated by western blot probed with an NP-specific antibody. Full-length NPwt and NPmut are 56 kDa. Full-length NPΔNLS and truncated NPwt, NPmut, and UbqNP are 53 kDa. Full-length UbqNP is 64.5 kDa. The image is representative of results from at least 3 independent experiments.*

Modifications of NP have the anticipated effect on cellular localization

Mutation and deletion of the NLS were done with the aim of retaining the protein in the cytosol. Therefore, the cellular localization of NP expressed by the respective rMVA constructs was analyzed by using confocal microscopy. During influenza virus PR8 infection, NP localizes to the nucleus at 4 and 6h post-infection (hpi), and after 24h, NP has translocated to the cytosol (**Fig. 2A**). NPwt expressed by rMVA shows a cellular localization similar to that of NP expressed during infection with influenza virus PR8 (**Fig. 2B**). Mutation or deletion of the NLS of NP prevented the translocation of the protein to the nucleus almost completely (**Fig. 2C-D**). Similarly, the UbqNP fusion protein was present predominantly in the cytosol at 4 and 6 hpi. However, low levels of UbqNP were also detected in the nucleus. Hardly any UbqNP protein was detected at 24 hpi. (**Fig. 2E**). These results confirm that the modifications had the intended effect on the cellular localization of NP.

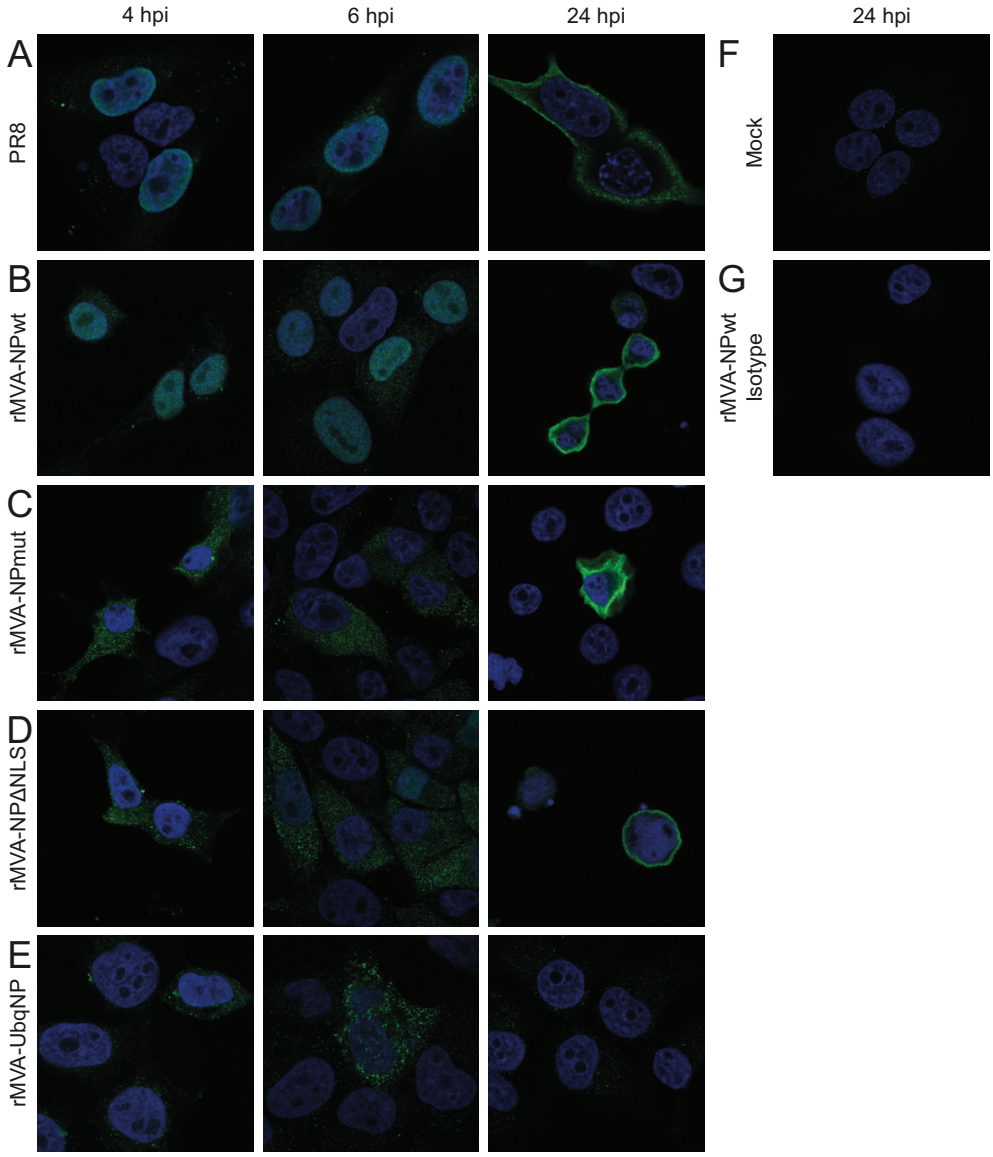

Figure 2. Cellular localization of (modified) NP expressed from rMVA*. HeLa cells were infected with influenza virus PR8 or one of the indicated rMVA constructs. (**A**) During PR8 infection, NP localizes to the nucleus at 4 and 6 hpi. After 24h, NP localizes mainly to the cytosol. (**B**) NPwt expressed from MVA behaves similarly to NP expressed during PR8 infection. (**C-D**) Mutation or deletion of the NLS retains NP in the cytosol. (**E**) NP fused to ubiquitin is dispersed throughout the cell and hardly detectable after 24h. (**F**) Uninfected control. (**G**) Control infected with rMVA-NPwt and stained with an isotype antibody. Images were taken by using a 100x ocular. Images are representative of results from at least 3 independent experiments.*

Deletion of the NLS or fusion of ubiquitin to NP results in increased protein degradation
In order to assess whether the degradation of the modified NPs was faster than that of NPwt, a metabolic radiolabeling experiment was performed. Over a time span of 11h, NPwt levels were relatively stable (**Fig. 3**). Mutation of the NLS (NPmut) did not affect protein stability. In contrast, deletion of the NLS (NPΔNLS) strongly accelerated the degradation of NP. Furthermore, fusion of NP to ubiquitin resulted in an even more rapid degradation of NP than for the NP molecule without NLS (**Fig. 3**). This indicates that the deletion of the NLS and fusion of ubiquitin to NP increased degradation and thus potentially enhanced the liberation of peptides from the protein for improved antigen presentation.

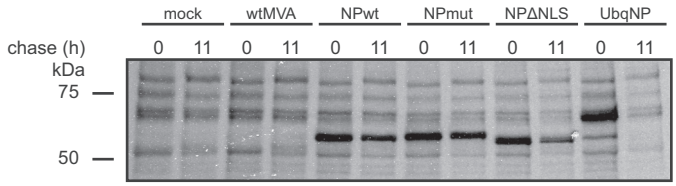

***Figure 3. NPΔNLS and UbqNP display enhanced degradation**. At 6 hpi, HeLa cells were pulsed with [^{35}S]cysteine-methionine for 10min, chased for 0 and 11h, and immunoprecipitated with an NP-specific antibody. Mock- or wtMVA-infected cells indicate the background.*

Removal of the NLS or fusion to ubiquitin has differential effects on T cell activation *in vitro*
To address whether increased NP protein turnover indeed improves the CD8$^+$ T cell response against NP *in vitro*, the activation of NP-specific CD8$^+$ TCCs was measured after 10h of co-culture with human leukocyte antigen (HLA)-matched rMVA-NP-infected BLCLs. CD107a, a degranulation marker[371], and IFN-ɣ cytokine levels were used as a marker for CD8$^+$ T cell activation (**Fig. 4A**). Two TCCs of different functional avidities, specific for the $NP_{44–52}$ and $NP_{383–391}$ epitopes, were tested[372]. After infection at a low MOI, NPmut, but especially NPΔNLS and UbqNP, activated TCCs of low ($NP_{44–52}$) and high ($NP_{383–391}$) functional avidities more efficiently than did NPwt (**Fig. 4B-E**). In contrast, after infection with the respective rMVAs at a high MOI, the differences in the activation of TCCs specific for the $NP_{383–391}$ epitope were no longer detectable (**Fig. 4C, E**). The differential activation of low-avidity CD8$^+$ T cells specific for the $NP_{44–52}$ epitope was still apparent (**Fig. 4B, D**). The results were consistent for both the CD107a and IFN-ɣ activation markers. Thus, under suboptimal conditions, when antigen amounts are limited (low MOI) or when CD8$^+$ T cells are of low functional avidity ($NP_{44–52}$), modifying NP by deleting the NLS or by fusion to ubiquitin improved the CD8$^+$ T cell response *in vitro*.

Immunization of C57BL/6 mice with rMVA-NP constructs affords protection against lethal challenge infection but does not reveal differences between the NP constructs
After *in vitro* validation, the various rMVA-NP vaccine candidates were tested *in vivo*. C57BL/6 mice were vaccinated twice, 4 weeks apart (**Fig. 5A**). One week after the second vaccination, mice were euthanized to assess the vaccine-induced CD8$^+$ T cell response (**Fig. 5G**). Although not statistically significant, the results indicate that vaccination with rMVA-NPΔNLS, rMVA-NPmut, and, to a lesser extent, rMVA expressing NPwt or UbqNP induces an NP-specific CD8$^+$ T cell response (**Fig. 5G**).

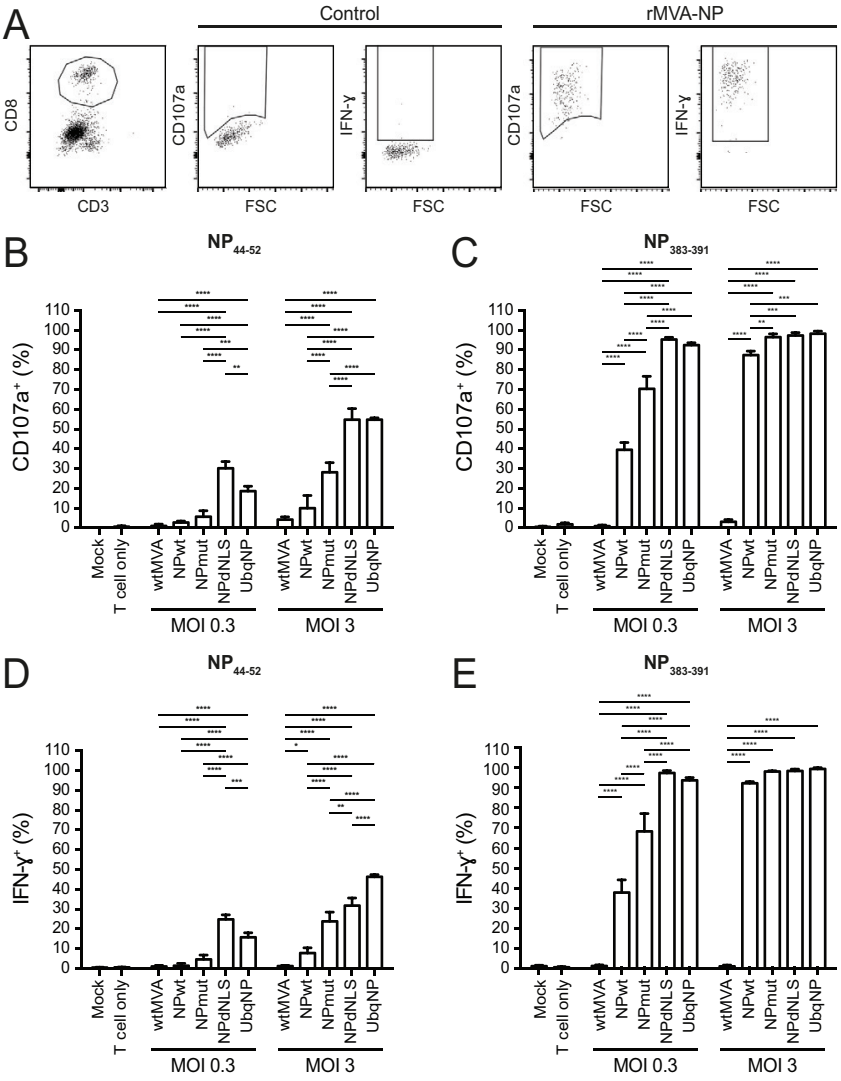

Figure 4. Increased NP degradation leads to stronger activation of TCCs* in vitro *at a low MOI or TCCs of low functional avidity. *BLCLs were infected with the indicated rMVA constructs and subsequently cocultured with HLA-matched NP-specific TCCs. Mock-infected cells, TCCs alone, or cells expressing an empty vector (wtMVA) were used as negative controls. (**A**) Gating strategy. Live, single CD3⁺ CD8⁺ T cells were gated, from which the percentage of CD107a- or IFN-γ-positive cells was determined. Representative dot plots for mock- or MVA-infected cells are shown. FSC, forward scatter. (**B-C**) Percentage of CD107a-positive cells of $NP_{44–52}$-specific (**B**) or $NP_{383–391}$-specific (**C**) TCCs within the CD3⁺ CD8⁺ T cell population. (**D-E**) Percentage of IFN-γ-positive cells of $NP_{44–52}$-specific (**D**) or $NP_{383–391}$-specific (**E**) TCCs within the CD3⁺ CD8⁺ T cell population (n=4). The graph shows means and standard deviations. * p=0.0251; ** p<0.0010; *** p<0.0032; **** p<0.0001.*

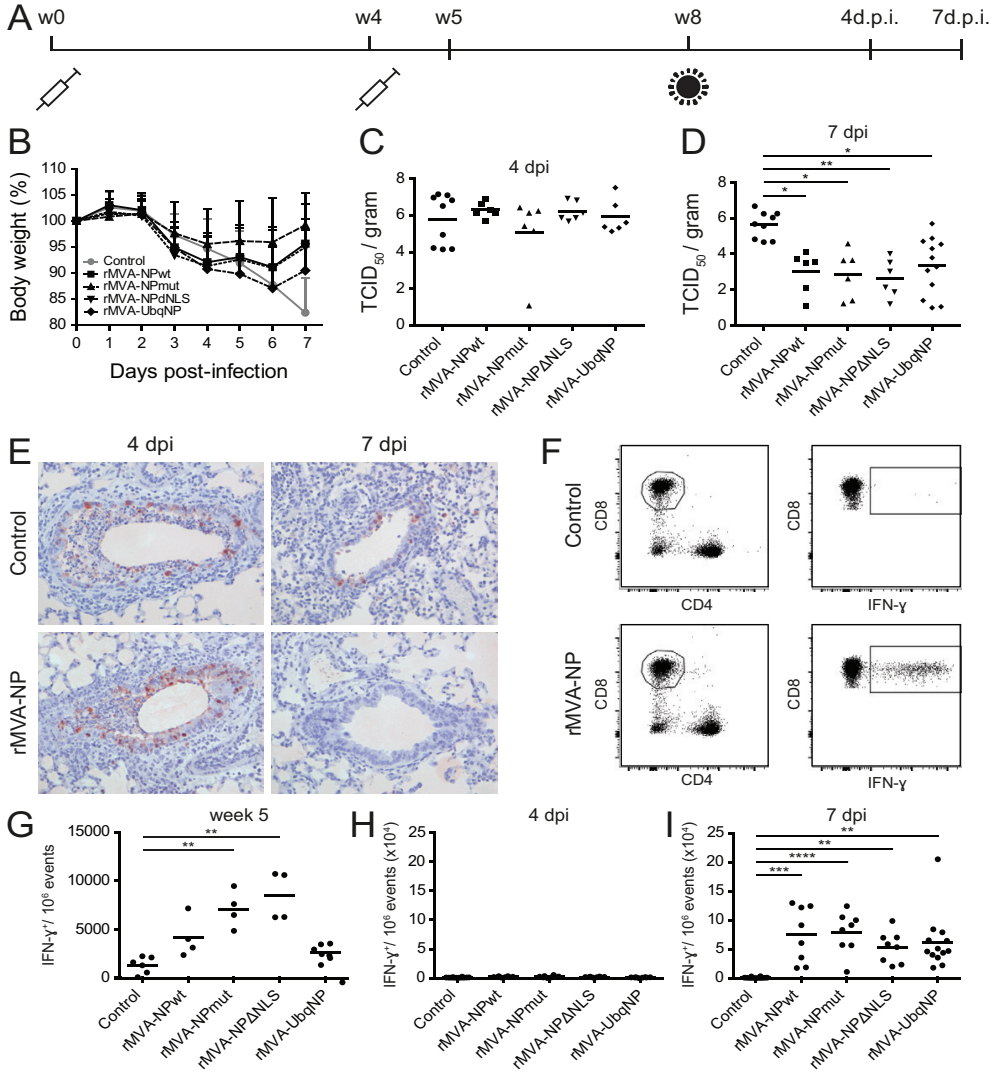

***Figure 5. rMVA-NP vaccination reduces disease severity and lethality* in vivo.** *(**A**) Mice were vaccinated twice, 4 weeks apart, with PBS or wtMVA (combined as controls) or with one of the four rMVA-NP constructs. Four weeks later, mice were challenged with a lethal dose of influenza virus PR8. One week after the second vaccination (week 5) and at 4 and 7 dpi, mice were euthanized. (**B**) Weight loss after challenge with a lethal dose of PR8. Body weight on the day of challenge was set at 100%. The graph shows means and standard deviations. (**C-D**) Viral load in $TCID_{50}$ per gram lung at 4 dpi (**C**) and 7 dpi (**D**). Bars indicate means. * p<0.0187; ** p=0.037. (**E**) Representative immunohistochemistry images of lungs from control or vaccinated mice at 4 and 7 dpi. Lungs were stained for influenza virus NP (red) and counterstained with hematoxylin. (**F-I**) Splenocytes were pulsed with the $NP_{366–374}$ peptide. IFN-γ production by $CD3^+$ $CD8^+$ splenocytes was used as a readout for $CD8^+$ T cell activation. (**F**) Gating strategy. The $CD3^+$ $CD8^+$ population was first selected from the live, single-cell lymphocyte population, after which the numbers of IFN-γ-producing cells were determined. Representative images for control groups and vaccine groups are shown. (**G-I**) $CD8^+$ T cell activation at week 5 (**G**), 4 dpi (**H**), and 7 dpi (**I**). Of note, y axis scales vary between graphs in panels G to I. Bars indicate means. ** p<0.0074; *** p=0.0005; ****, p<0.0001. Each symbol represents data for an individual mouse.*

Four weeks after the second vaccination, mice were inoculated with a lethal dose of influenza virus PR8 and euthanized at 4 or 7 dpi (**Fig. 5A**). Although both the control and vaccinated groups initially lost weight after inoculation, the body weight of mice vaccinated with rMVA-NP constructs stabilized and even increased again after 4 days and onward, whereas the control groups continued to lose weight (**Fig. 5B**). The viral loads in the lungs were similar between control groups and vaccinated groups at 4 dpi; however, rMVA-NP-vaccinated mice had reduced lung viral titers at 7 dpi (**Fig. 5C-D**). This correlated with the detection of virus-infected cells in the lungs, which were detected in both the control and rMVA-NP-vaccinated groups at 4 dpi but were detected only in the control groups at 7 dpi (**Fig. 5E**). Consistent with these data, an NP-specific $CD3^+$ $CD8^+$ T cell response was detected in vaccinated mice at 7 dpi but not yet at 4 dpi (**Fig. 5H-I**). Thus, vaccination with the rMVA-NP constructs reduced disease severity and protected mice from lethal challenge with an influenza A virus. However, no differences between the various rMVA-NP constructs were detected.

Discussion

In the present study, MVA-based vaccine candidates expressing influenza virus NP with or without modifications aiming at increasing antigen processing and presentation were designed, constructed, and tested *in vitro* and *in vivo*. We hypothesized that retention of NP in the cytosol of APCs or targeting of the protein to the proteasome would result in accelerated processing and improved activation of NP-specific $CD8^+$ T cells. The modifications that we made to influenza virus NP had the anticipated effects regarding cellular localization, as demonstrated by confocal microscopy (**Fig. 2**). Despite retention in the cytosol, the rate of degradation of NPmut was not enhanced compared to that of NPwt. In contrast, we observed that increased protein degradation can be achieved by the removal of the NLS or, in agreement with data from previous studies, by N-terminal fusion to ubiquitin[358-360,362-364,373]. The increased degradation of NPΔNLS might be caused by defective folding of the protein due to the removal of a stretch of amino acids. An N-terminal fusion of ubiquitin to the substrate may lead to a rapid hydrolysis of ubiquitin from the substrate, thereby exposing an N-terminal amino acid that is not a methionine. By the so-called “N-end rule”, the protein is marked as faulty and degraded[359,360,374]. However, in our rMVA-UbqNP construct, hydrolysis was prevented by the introduction of a C-terminal mutation into the ubiquitin molecule. Therefore, the ubiquitin moiety most likely serves as the first molecule in the polyubiquitin chain, flagging the fusion protein as a proteasomal degradable product[358,362-364,373].

Both mutation and deletion of the NLS prevented the transport of NP into the nucleus. However, the most substantial effect on the degree of $CD8^+$ T cell activation *in vitro* was observed with NP variants that were degraded more rapidly due to a deletion of the NLS or fusion to ubiquitin. These findings are in agreement with previously reported observations that indicate that enhanced antigen processing leads to stronger $CD8^+$ T cell activation *in vitro*[359,360,363,364]. Thus, enhanced degradation of NP, as observed for NPΔNLS and UbqNP, resulted in stronger $CD8^+$ T cell activation, which was not observed for NPwt or NPmut, which is retained in the cytosol but does not display enhanced degradation (**Fig. 4**).

Of interest, as described in previous studies with ubiquitin fusion proteins, we observed a differential effect on $CD8^+$ T cell activation, depending on the specificity of the $CD8^+$ T cells that were used[359,360,364,375]. A larger increase in $CD8^+$ T cell activation was measured for the $NP_{44–52}$ epitope than for the $NP_{383–391}$ epitope. This difference may be explained by differences in the functional avidities of $CD8^+$ T cells specific for these two epitopes: $NP_{44–52}$-specific $CD8^+$ T cells are of relatively low functional avidity compared to $CD8^+$ T cells specific for the $NP_{383–391}$ epitope[372]. Thus, especially for $CD8^+$ T cells of low functional avidity, modifications that lead to more-rapid protein degradation improve their activation. For $CD8^+$ T cells of high functional avidity, which thus require lower concentrations of the peptide for their activation, there may not be a window of opportunity because the minimal threshold for their activation is reached more readily.

After immunization of C57BL/6 mice with the respective rMVA-NP constructs, increased $CD8^+$ T cell responses to the H2-Db-restricted $NP_{366–374}$ epitope were observed for NP with a modified NLS. Mice vaccinated with rMVA-UbqNP showed hardly any $CD8^+$ T cell reactivity 7 days after the second vaccination, although, due to the enhanced degradation rates and potentially increased antigen presentation kinetics, we could have missed the peak of the $CD8^+$ T cell response to this protein (**Fig. 5G**). Following subsequent challenge infection with influenza virus PR8, no differences in anamnestic $NP_{366–374}$-specific $CD8^+$ T cell responses were observed, which correlated with the lack of differences in clinical protection from weight loss or reduction of virus replication: all NP-immunized mice were equally protected compared to control mice (**Fig. 5**). The lack of differences in NP-specific $CD8^+$ T cell responses may be explained by the same reasoning as that outlined above for the *in vitro* activation of different human NP-specific $CD8^+$ T cells. The $CD8^+$ T cell response to influenza viruses in C57BL/6 mice is dominated by $NP_{366–374}$-specific $CD8^+$ T cells[376-378]. Therefore, it is likely that in this mouse strain, with the rMVA dosage used, NPwt already reached minimal thresholds for an optimal $CD8^+$ T cell response to the $NP_{366–374}$ epitope. It would be of interest to study $CD8^+$ T cell responses after vaccination with the respective rMVA-NP constructs in other mouse strains, e.g. BALB/c mice, which mount NP-specific $CD8^+$ T cell responses to epitopes that are less dominant than those observed in C57BL/6 mice, or to study the effect of the modification of less-immunogenic proteins.

Previously, it was suggested that cross-priming by professional APCs is important for the efficient induction of virus-specific $CD8^+$ T cells. This would require a prolonged presence of the viral protein and antigen presentation for optimal $CD8^+$ T cell responses, as opposed to increased protein degradation (reviewed by J.W. Yewdell[379])[363,380,381]. Our *in vitro* data obtained with human TCCs suggested that infection of APCs and rapid proteasomal degradation favor the rapid activation of $CD8^+$ T cells. However, the results obtained with the mouse model do not support this; thus, both cross-priming and direct antigen presentation by MVA-infected APCs may contribute to the induction of NP-specific $CD8^+$ T cell responses. Of interest, upon immunization with rMVA, especially dendritic cells and macrophages are targeted, which subsequently express transgenes of interest[342]. Thus, direct infection of these

professional APCs most likely contributes to the induction of specific $CD8^+$ T cell responses substantially, but cross-priming cannot be excluded.

Collectively, using rMVA expressing wild-type and modified influenza virus NPs, we have shown that retention of NP in the cytosol by mutation of the NLS (NPmut) does not significantly affect antigen processing and presentation and subsequent $CD8^+$ T cell activation. However, deletion of the NLS or N-terminal fusion to ubiquitin increases NP degradation compared to that of NPwt. These modifications result in the improved activation of NP-specific $CD8^+$ T cells, especially those with low functional avidity for their epitope. Furthermore, vaccination with rMVA expressing NPwt, NPmut, NPΔNLS, or UbqNP protected C57BL/6 mice from lethal challenge with influenza A virus, and no differences in $CD8^+$ T cell responses between experimental groups were observed. In C57BL/6 mice, the immunodominant $CD8^+$ T cell response to the $NP_{366–374}$ epitope may have obscured the differential $CD8^+$ T cell activation observed *in vitro* with human NP-specific $CD8^+$ T cells. Thus, the strategy of modifying proteins may have limited use for proteins that already mount immunodominant $CD8^+$ T cell responses of high avidity but may be useful for poorly immunogenic proteins or when suboptimal vaccine doses are used.

CHAPTER 3.2

Protein- and Modified Vaccinia virus Ankara-based influenza virus nucleoprotein vaccines are differentially immunogenic in BALB/c mice

AF Altenburg*, SE Magnusson*, F Bosman, L Stertman, RD de Vries & GF Rimmelzwaan
*Authors contributed equally

Clinical & Experimental Immunology, 2017; 190(1): 19–28

Because of the high variability of seasonal influenza viruses and the eminent threat of influenza viruses with pandemic potential, there is great interest in the development of vaccines that induce broadly protective immunity. Most probably, broadly protective influenza vaccines are based on conserved proteins, such as nucleoprotein (NP). NP is a vaccine target of interest as it has been shown to induce cross-reactive antibody and T cell responses. Here, we tested and compared various NP-based vaccine preparations for their capacity to induce humoral and cellular immune responses to influenza virus NP. The immunogenicity of protein-based vaccine preparations with Matrix-M™ adjuvant as well as recombinant viral vaccine vector Modified Vaccinia virus Ankara (MVA) expressing the influenza virus NP gene, with or without modifications that aim at optimization of $CD8^+$ T cell responses, was addressed in BALB/c mice. Addition of Matrix-M™ adjuvant to NP wild-type protein-based vaccines significantly improved T cell responses. Furthermore, recombinant MVA expressing the influenza virus NP induced strong antibody and $CD8^+$ T cell responses, which could not be improved further by modifications of NP to increase antigen processing and presentation.

Introduction

Influenza A (H1N1 and H3N2) and B viruses are responsible for seasonal epidemics in the human population and cause substantial morbidity and mortality in high-risk groups such as elderly people. The antigenic properties of these viruses change regularly due to accumulation of mutations in the two major surface proteins, haemagglutinin (HA) and neuraminidase (NA), resulting in escape from pre-existing virus-neutralizing antibodies induced by previous infections or vaccinations (antigenic drift)[4,17,18]. In addition to seasonal influenza viruses, avian and swine influenza A viruses – for example, viruses of the A(H5N1)[382], A(H5N6)[383] and A(H7N9)[384] subtype – cause occasional human infections. These zoonotic influenza viruses have the potential to cause pandemic outbreaks, as the human population is immunologically virtually naïve.

Currently used inactivated vaccines against seasonal influenza viruses predominantly induce neutralizing antibodies against the globular head-domain of HA that neutralize homologous influenza viruses efficiently[4]. However, the breadth of reactivity of these antibodies is limited due to the high degree of variability in the head-domain of the HA glycoprotein between different influenza viruses, resulting in

reduced vaccine efficacy in case of a vaccine mismatch with epidemic strains[4,317-319]. Due to the antigenic drift of seasonal influenza viruses, vaccines need to be updated almost annually[120]. Furthermore, in case of a pandemic outbreak it is essential that a tailor-made vaccine can be produced rapidly, which proved to be difficult during the pandemic of 2009. Thus, alternative cross-reactive correlates of protection induced by a 'universal' influenza vaccine with the capacity to provide intra- or intersubtypic immunity, such as virus-specific T cells, have gained renewed interest.

Virus-specific $CD8^+$ cytotoxic T cells predominantly recognize internal viral antigens, such as matrix (M1) and nucleoprotein (NP), that are relatively conserved and contain epitopes shared by various subtypes of influenza virus. These cells are induced by natural infection but are induced inefficiently by inactivated influenza vaccines[316,82,136,137]. It has been shown that cross-reactive virus-specific $CD8^+$ cytotoxic T cells contribute to reduction of disease duration and severity after infection with a heterologous influenza virus[76,82]. In addition, antibodies directed against the conserved stalk-domain of HA have been identified, which display cross-protective potential against infection with heterologous influenza viruses[146,152,160,169,349]. Thus, the development of vaccines that induce broadly protective HA stalk-specific antibodies and/or cellular immune responses against conserved proteins such as NP or M1 is highly desirable and is listed high on the research agenda[385,386,387].

Viral vaccine vectors, such as Modified Vaccinia virus Ankara (MVA), have been shown to efficiently induce antigen-specific humoral and cellular responses[209,280]. Recombinant (r)MVA vaccines have been tested extensively in various animal models and multiple clinical trials against different pathogens, including influenza virus, and has proved that the use of rMVA-based vaccines is safe[209,250,278,388]. As it is relatively easy to insert genes encoding antigens of interest into the genome of MVA, recombinant (r)MVA-based vaccines can be rapidly produced.[209,280]. rMVA drives *de novo* synthesis of one or multiple antigens of interest, leading to endogenous antigen processing and major histocompatibility complex (MHC) class I antigen presentation, which is important for the efficient induction of $CD8^+$ T cells[58].

Humoral and cellular immunity could also be improved by the use of adjuvants in combination with for example virosomal, trivalent, split virion and inactivated influenza vaccines[389-396]. Addition of Matrix-M™ adjuvant, made of saponins extracted from the tree *Quillaja saponaria* Molina[397], to influenza vaccines enhances significantly humoral responses and the induction of virus-specific T cells in mice, ferrets and humans[391-394,398-400]. Furthermore, Matrix-M™ adjuvant has been evaluated in three clinical Phase I studies using seasonal and pandemic (H5N1 and H7N9) influenza vaccines[391,399,401,402]. All studies showed promising results with increased humoral and cellular responses along with good safety data.

Most adjuvanted influenza vaccine studies have focused upon the immune response towards HA[403]. Additionally, a couple of studies have shown that adjuvanted recombinant influenza virus NP protein vaccines are able to induce T helper type 1 (Th1)-skewed $CD4^+$ T cell response and protect C57BL/6 mice from influenza A virus challenge[404,405]. Here, we explore the effect of Matrix-M™ adjuvant on a recombinant

influenza virus NP protein-based vaccine and compare it to rMVA-NP vaccines in BALB/c mice. Accordingly, the immunogenicity of unadjuvanted or Matrix-M™ adjuvanted wild-type NP (NPwt) protein-based vaccines and rMVA-based vaccines expressing NPwt or modified NP, optimized for proteasomal processing[341], were investigated. With rMVA expressing modified NP, enhanced activation of a human $CD8^+$ T cells *in vitro* was observed previously, but the use of these constructs did not improve NP-specific $CD8^+$ T cell responses compared to NPwt in the C57BL/6 mouse model[341]. As we speculated that the immune response in C57BL/6 mice was directed mainly against the immunodominant $NP_{366–374}$ epitope[341,376], we next addressed the immunogenicity of rMVA vaccines expressing either NPwt or modified NP in BALB/c mice, which do not mount a response to this immunodominant NP epitope.

In this study, we show that Matrix-M™ adjuvant can improve the immunogenicity of protein-based NPwt vaccines substantially. Comparison of the two types of recombinant NP vaccines showed that while Matrix-M™ adjuvant improved the immunogenicity of NPwt vaccine by enhancing the antibody titer and T cell responses compared to unadjuvanted NPwt vaccine, rMVA-NPwt vaccines also induced antigen-specific interferon (IFN)-ɣ-positive $CD8^+$ T cells and higher IgG2a NP-specific antibody titers. However, rMVA-driven expression of NP modified to increase antigen processing did not improve the NP-specific $CD8^+$ T cell response in BALB/c mice.

Materials and methods

NPwt protein preparation

The NP was expressed in *Escherichia coli* BL21 as a His-tagged maltose binding protein (MBP) fusion protein containing a DEVD sequence as cleavage site for murine (m)caspase3. Expression of the tagged MBP-NP fusion protein was induced by addition of 1mM isopropyl β-D-1-thiogalactopyranoside (IPTG). After 4h induction at 28ºC the cells were harvested, lysed by sonication at 4ºC followed by centrifugation. The supernatant was loaded on Ni-Sepharose 6 FF (GE Healthcare) and proteins were eluted by applying an imidazole gradient. The 50mM imidazole fractions containing the MBP-NP fusion protein were pooled and after incubation for 1h at 37ºC in the presence of 0.06mg mcaspase3/mg fusion protein reloaded on Ni-IMAC resin. Analysis by sodium dodecyl sulphate-polyacrylamide gel electrophoresis/Coomassie Brilliant Blue (SDS-PAGE/CBB) staining and western blot showed that more than 90% pure NP was recovered in the flow-through. NP was concentrated to 1mg/ml and dialyzed against 25mM HEPES, 300mM NaCl pH 7.5. The lipopolysaccharide (LPS) content (<0.25EU/µg NP) was determined with EndoSafe-PTS test (Charles River).

Matrix-M™ adjuvant

Novavax proprietary Matrix-M™ adjuvant is a saponin-based adjuvant consisting of two individually formed 40nm-sized particles, each with a different and well-characterized saponin fraction (fraction-A and fraction-C, respectively). The Matrix-A and C particles are formed by formulating purified saponin from the tree *Quillaja saponaria* Molina with cholesterol and phospholipid[406].

Generation of recombinant MVA

The rMVA constructs expressing NP under control of the early/late PsynII promotor were prepared as described recently[341]. In short, the respective (modified) NP nucleotide sequences (PR8-based, Accession number NC002019) were synthesized by Baseclear BV and clonal rMVA viruses were prepared through transient mCherry-dependent plaque selection in chicken embryo fibroblasts (CEF)[256,341]. To generate a final vaccine preparation, virus was propagated in CEF, purified by ultracentrifugation through 36% sucrose and reconstituted in 120mM NaCl 10mM Tris-HCl pH 7.4. rMVA-NP constructs were previously extensively characterized *in vitro* by sequencing, western blot, confocal microscopy and radiolabelling experiments[341].

Vaccination of BALB/c mice

Specified pathogen-free female BALB/c mice were purchased from Charles River Laboratories and were 8-10 weeks of age at the start of the experiment. Animals were housed in Makrolon type 3 cages, had access to food and water *ad libitum* and animal welfare was observed on a daily basis. All experiments were conducted in strict compliance with European guidelines (EU directive on animal testing 2010/63/EU) and the protocol was approved by an independent animal experimentation ethical review committee (Uppsala djurförsöksetiska nämnd). Experiments were performed in two sets, the first set focused on the comparison of protein vaccines with MVA-based vaccines (**Table 1**) and the second set focused on the comparison of NPwt with modified NP expressed by MVA (**Table 2**). BALB/c mice received two vaccinations (time interval of 4 weeks) with 10^8 plaque-forming units (PFU) rMVA, 10µg NPwt protein or 1 or 10µg NPwt protein adjuvanted with 5 or 10µg Matrix-M™ adjuvant. All vaccines were administered subcutaneously in 100µl at the base of the tail. Blood was sampled 21 days after the first vaccination and before mice were euthanized; 14 or 10 days after the second vaccination for the first and second set, respectively. Spleens were collected in phosphate-buffered saline (PBS) during necropsy and subsequently single-cells suspensions were prepared as described previously[393].

Detection of NP-specific antibodies

Maxisorp microplates (Nunc) were coated O/N at 4ºC with 50ng/well NPwt protein (AmatsiQ-Biologicals) in 0.05M carbonate/ bicarbonate (Sigma Aldrich) buffer pH 9.6. Plates were blocked for 1h at room temperature using PBS with 0 05% Tween-20 (PBST; Thermo Fisher Scientific) pH 7.2-7.6 supplemented with 2% (W/V) milk powder (Semper). A three- or fivefold dilution series of the sera was prepared in blocking buffer starting at 1:30 and incubated on the coated plates for 1h. Blocking buffer and anti-NP positive serum were used as a negative or positive control, respectively. Plates were washed with PBST and incubated with anti-IgG1 (Star 132P; AbD Serotec) or anti-IgG2a (Star 133P; AbD Serotec) horseradish peroxidase (HRP)-conjugated antibodies – indicative for a Th2 or Th1 response, respectively[407] – for 1h. Subsequently, plates were washed with PBST and 100µl 3,3',5,5'-tetramethylbenzidine (TMB) peroxidase substrate (Svanova Biotech) was added. Reactions were stopped by adding 1.8M H_2SO_4 and absorbance was measured subsequently at 450nm using a SpectraMax Plus 384 Microplate Reader (Molecular Devices Corporation). Immunoglobulin (Ig)G1 and IgG2a anti-NP titers were calculated using a four-parameter logistic equation (Softmax software; Molecular Devices). The inflection point of the titration curve, *i.e.* half maximal effective concentration (EC_{50}) titer, was used for analysis.

FluoroSpot analysis of protein- or peptide-stimulated splenocytes

The number of interleukin (IL-)2 and IFN-ɣ-producing cells in single-cell suspensions of the spleen was analysed using FluoroSpot assay (Mabtech), according to the manufacturer's instructions. In brief, single-cell suspensions were seeded in triplicate on filter plates at 0.25 x 10^6 cells/well in Roswell Park Memorial Institute (RPMI) medium (Sigma Aldrich) supplemented with 10% heat-inactivated fetal bovine serum (FBS; Sigma Aldrich), 100U/ml penicillin / 100µg/ml streptomycin / 2mM L-glutamine (P/S/G; Sigma Aldrich) and stimulated with 1µg NP (AmatsiQ-Biologicals) or 5µM synthetic peptide (epitope $NP_{147–155}$, TYQRTRALV[273]) per well. Concanavalin A (Sigma Aldrich) and RPMI supplemented with 10% FBS were used as positive and negative controls, respectively. Samples were incubated for 20h at 37ºC after which spots were developed and analysed using an AID ELR02 reader (Autoimmune Diagnostika GmbH).

Intracellular cytokine staining (ICS) of peptide-stimulated splenocytes

Single-cell suspensions of splenocytes were mock-treated, stimulated with 5µM synthetic peptide (epitope $NP_{147–155}$) or stimulated 20ng/ml phorbol myristate acetate (PMA) and 1µg/ml ionomycin as positive control in Iscove's modified Dulbecco's medium (IMDM; GIBCO) supplemented with 5% FBS (Sigma Aldrich), P/S/G and GolgiStop. Stimulation lasted 12h at 37ºC, which is longer than the optimal 6h incubation with GolgiStop. However, enough viable events were measured for reliable analysis. Cells were stained with fluorochrome-labelled antibodies $CD3e^{APC–Cy7}$ (BD Pharmingen), $CD8b^{FITC}$ (BD Pharmingen, San Diego, CA, USA), $CD4^{PerCP}$ (BD Pharmingen) and Aqua LIVE/DEAD (Invitrogen). Subsequently, cells were fixed and permeabilized using BD Cytofix/Cytoperm™ Plus (BD Biosciences) and stained with IFN-$ɣ^{Pacific\ Blue}$ (Biolegend). Samples were analysed by flow cytometry using a FACS Celesta flow cytometer and FACS DIVA software (BD Biosciences).

Statistical analysis

NP-specific antibody responses were analysed by a one-way analysis of variance (ANOVA) to establish statistically significant differences. FluoroSpot and ICS data were first assessed with a D'Agostino & Pearson omnibus normality test. Non-normally distributed data (FluoroSpot set 1 and ICS set 2) were analysed using a Kruskal–Wallis rank test. If a normal distribution was assumed, a one-way ANOVA was performed to determine statistical significance (FluoroSpot set 2).

Results

Matrix-M™ adjuvant enhanced immunogenicity of NPwt protein-based vaccine

As Matrix-M™ adjuvant has been shown to induce high levels of biologically active antibodies, balanced type Th1 and Th2 immune responses, multi-functional T cells and cytotoxic $CD8^+$ T lymphocytes in combination with various subunit vaccines[400,408-410], we addressed the effect of addition of Matrix-M™ adjuvant to NPwt protein-based vaccines and compared this to unadjuvanted NPwt protein and rMVA-NPwt vaccination. To this end, mice were vaccinated twice with one of three different NPwt protein 1 Matrix-M™ adjuvant combinations, NPwt protein alone or rMVA-NPwt (**Table 1**).

Table 1. Vaccines used to assess the effect of Matrix-M™ adjuvant on protein-based wild-type nucleoprotein (NPwt) vaccine immunogenicity.

Vaccine	*n*	Formulation	Adjuvant
Protein	5	10µg NPwt	-
	8	1µg NPwt	5µg Matrix-M™ adjuvant
	8	10µg NPwt	5µg Matrix-M™ adjuvant
	8	1µg NPwt	10µg Matrix-M™ adjuvant
rMVA	8	10^8 PFU rMVA-NPwt	-

BALB/c mice were vaccinated twice at a 4-week interval with the respective vaccines. Mice were euthanized 14 days after the second vaccination; n indicates the number of animals per group. PFU = plaque-forming units; rMVA = recombinant Modified Vaccinia virus Ankara.

Vaccine immunogenicity was assessed by determining NP-specific antibody titers after one or two vaccinations (**Fig. 1**). NP-specific antibody responses induced by the protein-based vaccines, with or without Matrix-M™ adjuvant, could not be detected after a single vaccination (**Fig. 1A-B**). In contrast, 21 days after the primary vaccination an NP-specific IgG2a response was detected after vaccination with rMVA-NPwt (**Fig. 1B**). At 14 days after either protein or rMVA-NPwt booster vaccination NP-specific antibody responses were detected. Protein-based NPwt vaccines predominantly induced an IgG1 antibody response, whereas rMVA-NPwt induced both IgG1 and IgG2a NP-specific antibodies with a bias towards IgG2a (**Fig. 1C-D**). The NP-specific IgG1 responses induced by protein-based vaccines and rMVA-NPwt were comparable (**Fig. 1C**). Although not statistically significant, the immunogenicity of the protein-based NPwt vaccines was enhanced by the addition of Matrix-M™ adjuvant to the vaccine formulation, particularly for 10µg NPwt + 5µg Matrix-M™ adjuvant (**Fig. 1C-D**).

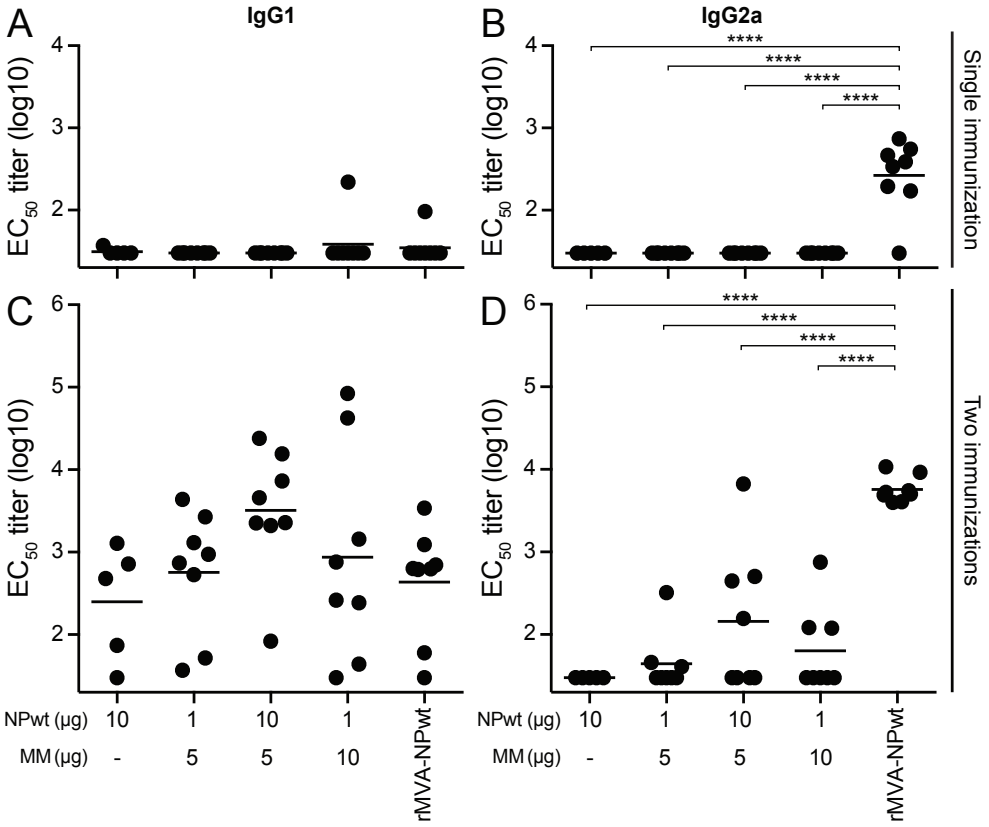

Figure 1. Nucleoprotein (NP)-specific antibody responses after NP wild-type (NPwt) protein (with or without Matrix-M™ adjuvant) or recombinant Modified Vaccinia virus Ankara (rMVA)-NPwt vaccination. *The immunoglobulin (Ig)G1 and IgG2a NP-specific antibody responses 21 days after the primary vaccination (**A-B**) or 14 days after the booster vaccination (**C-D**). IgG1 (**A & C**) or IgG2a (**B & D**) serum antibodies were detected using purified NPwt protein and anti-IgG1 or anti-IgG2a horseradish peroxidase (HRP)-conjugated antibodies. Mean of each group is indicated. MM = Matrix-M™ adjuvant. **** p<0.0001.*

Next, the vaccine-induced NP-specific T cell responses were evaluated. T cell activation was measured by stimulation of splenocytes obtained 14 days after the booster vaccination and subsequent detection of IL-2-, IFN-ɣ- or IL-2/IFN-ɣ-producing NP-specific splenocytes. NP-specific T cell responses induced by protein-based vaccine formulations were enhanced significantly by Matrix-M™ adjuvant (**Fig. 2**). Furthermore, Matrix-M™ adjuvanted NPwt protein vaccines induced more IL-2-producing T cells compared to rMVA-NPwt vaccination (**Fig. 2A**). In contrast, no differences in IFN-ɣ- or IL-2/IFN-ɣ-producing cells between the Matrix-M™ adjuvanted NPwt protein vaccines and the rMVA-NPwt vaccine were observed (**Fig. 2B-C**). Collectively, NPwt protein vaccines, especially with the Matrix-M™ adjuvant, and rMVA-NPwt were immunogenic in BALB/c mice. In general, rMVA-NPwt induced stronger IgG2a and similar IgG1 NP-specific antibody responses compared to protein-based vaccines. Addition of Matrix-M™ adjuvant to protein-based NP vaccine improved T cell responses significantly, but not antibody responses.

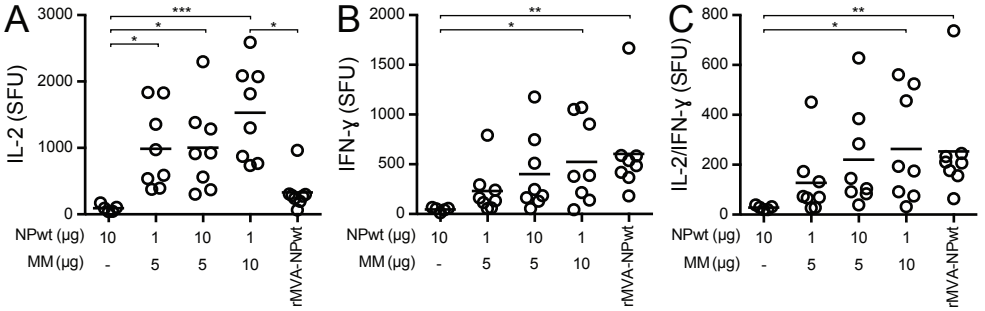

Figure 2. Vaccination with wild-type nucleoprotein (NPwt) protein with Matrix-M™ adjuvant or recombinant Modified Vaccinia virus Ankara (rMVA)-NPwt induced NP-specific splenocyte responses*. Spleens obtained 14 days after the booster vaccination were stimulated with purified NPwt protein. The number of interleukin (IL-)2 (**A**), interferon (IFN-)γ (**B**) and IL-2/IFN-γ (**C**)-producing T cells was used to determine NP-specific splenocyte activation in spot-forming units (SFU)/10^6 cells. Samples were tested in triplicate. Mean of each group is indicated. MM = Matrix-M™ adjuvant. * p<0.0306; ** p<0.0082; *** p=0.0005.*

Modification of NP does not enhance NP-specific cytotoxic T cells in BALB/c mice

In order to optimize the NP-specific CD8$^+$ cytotoxic T cell response, modifications were made to the NP protein that aimed at increasing protein processing and subsequent antigen presentation. Various NP mutant constructs were generated. First, the nuclear localization signal (NLS) of NP was mutated (NPmut) or deleted (NPΔNLS) to retain the protein in the cytosol and increase the amount of protein available for proteasomal processing[341,356,357]. Secondly, NP was fused to ubiquitin (UbqNP), a small molecule marking proteins for proteasomal degradation[341,362]. Previously, we have shown that these modified proteins could be expressed by rMVA and were immunogenic in C57BL/6 mice[341]. To determine whether the modified NP constructs are capable of inducing stronger NP-specific T cell responses than NPwt in BALB/c mice, animals were vaccinated twice with rMVA-NPwt, rMVA-NPmut, rMVA-NPΔNLS or rMVA-UbqNP. Wild-type (wt)MVA was used as a negative empty-vector control. The rMVA-based vaccines were compared to vaccination with 10µg NPwt protein formulated with 5µg Matrix-M™ adjuvant (**Table 2**).

NP-specific antibody responses were determined using serum collected 21 and 10 days after the first and booster vaccination, respectively. Similar to the results obtained in the initial experiment, vaccination with NPwt protein + Matrix-M™ adjuvant did not induce an NP-specific antibody response after a single vaccination. However, after two vaccinations both IgG1 and IgG2a NP-specific antibodies were detected with a bias towards IgG1 (**Fig. 3A, C**). The IgG1 response of the adjuvanted protein vaccine was significantly higher than the response induced by the rMVA-NP constructs (**Fig. 3C**). rMVA-NPwt induced NP-specific IgG2a antibodies after a single vaccination. Similar results were obtained for vaccination with rMVA-NPmut. In contrast, rMVA expressing NPΔNLS (not statistically significant) or UbqNP seemed less immunogenic (**Fig. 3B**). The differences in the induction of NP-specific IgG2a antibodies by the various rMVA-NP constructs was not detected after two vaccinations (**Fig. 3D**). NP-specific antibody responses induced by the empty vector (wt)MVA were never observed (**Fig. 3**).

Table 2. Recombinant Modified Vaccinia virus Ankara (rMVA)-based vaccines expressing (modified) nucleoprotein (NP) used to address optimization of the NP-specific CD8⁺ T cell response.

Vaccine	*n*	Formulation
Protein	10	10µg NPwt + 5µg Matrix-M™ adjuvant
rMVA	5	10^8 PFU wtMVA
	10	10^8 PFU rMVA-NPwt
	10	10^8 PFU rMVA-NPmut
	10	10^8 PFU rMVA-NPΔNLS
	10	10^8 PFU rMVA-UbqNP

BALB/c mice were vaccinated twice at a 4-week interval with the respective vaccines. Mice were euthanized 10 days after the booster vaccination; n indicates the number of animals per group. PFU = plaque-forming units.

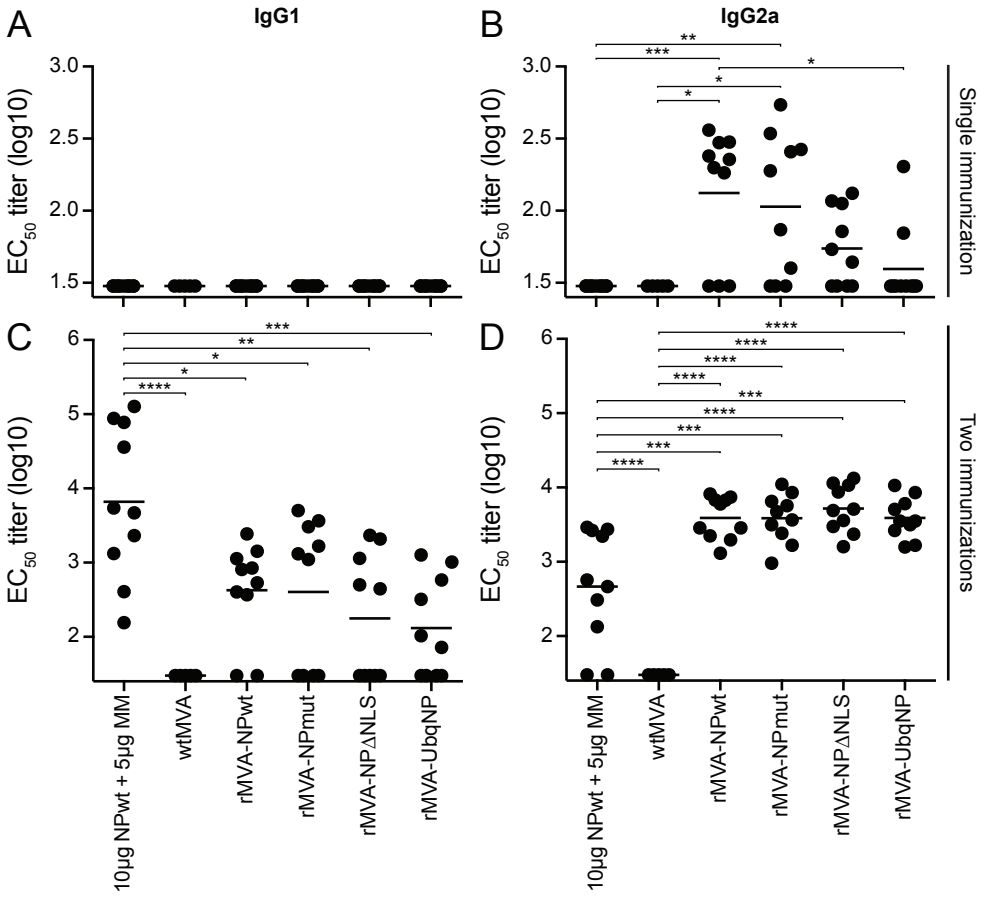

Figure 3. Nucleoprotein (NP)-specific antibody responses induced by vaccination with NP wild-type (NPwt) protein + Matrix-M™ adjuvant or the respective recombinant Modified Vaccinia virus Ankara (rMVA)-NP constructs. *Immunoglobulin (Ig)G1 and IgG2a NP-specific antibody responses in mice 21 days after the primary vaccination (**A-B**) or 14 days after booster vaccination (**C-D**). IgG1 (**A & C**) or IgG2a (**B & D**) serum antibodies were detected using purified NPwt protein and anti-IgG1 or anti-IgG2a horseradish peroxidase (HRP)-conjugated antibodies. Mean for each group is indicated. MM = Matrix-M™ adjuvant. * p<0.0432; ** p<0.0068; *** p<0.0009; **** p<0.0001.*

Subsequently, NP-specific T cell responses induced by vaccination with 10µg NPwt protein with 5µg Matrix-M™ adjuvant or the respective rMVA-NP vaccines were addressed using two different assays. Using the FluoroSpot assay, the induction of specific T cells was demonstrated by detection of IL-2-, IFN-ɣ- or IL-2/IFN-ɣ-producing cells after splenocyte stimulation with an $NP_{147–155}$ peptide, representing a $CD8^+$ T cell epitope. wtMVA vaccination was used as a negative control and did not induce any $NP_{147–155}$-specific T cell responses (**Fig. 4**). $NP_{147–155}$-specific IL-2-, IFN-ɣ- or IL-2/IFN-ɣ-producing T cells were detected for all rMVA-NP vaccine groups (**Fig. 4A-C**). In general, the number of IL-2-, IFN-ɣ- or IL-2/IFN-ɣ-producing cells induced by the respective rMVA-NP vaccines were similar, although the number of virus-specific T cells induced by rMVA-NPΔNLS seemed slightly elevated and by rMVA-UbqNP seemed slightly reduced compared to rMVA-NPwt (**Fig. 4A-C**). Similar to the first experiment, NPwt protein + Matrix-M™ adjuvant vaccination induced similar numbers of IL-2- or IL-2/IFN-ɣ-producing cells compared to rMVA-NPwt. In contrast, the numbers of IFN-ɣ-producing cells after protein-based vaccination was significantly lower than after rMVA-NP vaccination (**Fig. 4B**).

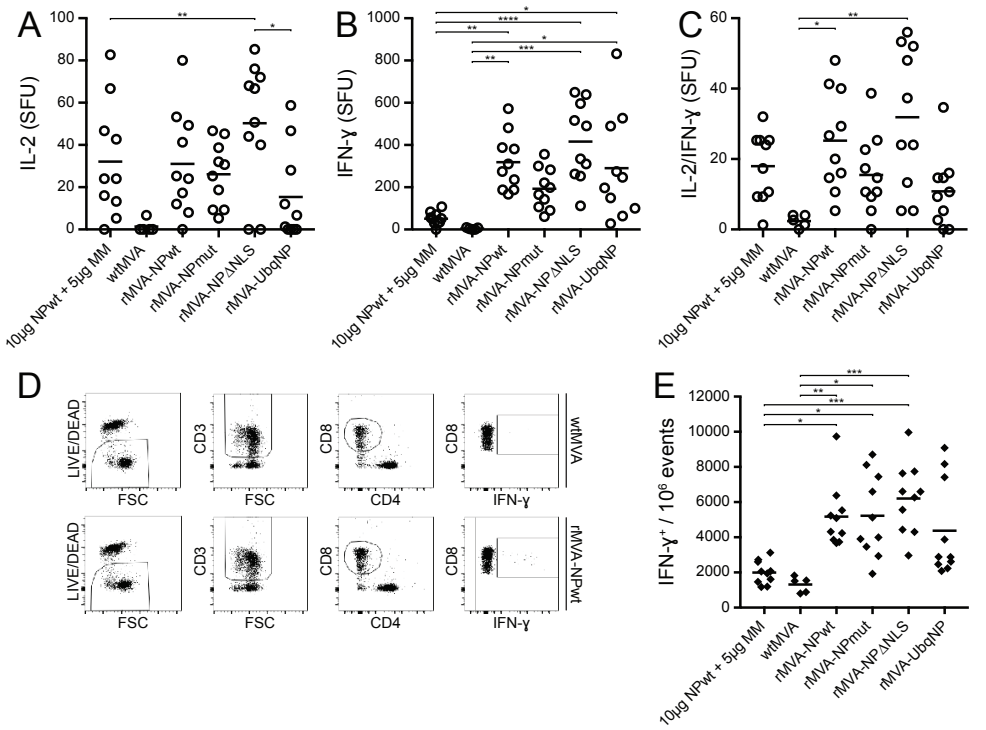

Figure 4. Vaccine-induced nucleoprotein (NP)-specific T cell responses. *(**A-C**) Splenocytes were stimulated with the $N_{P147–155}$ peptide after which the number of interleukin (IL-)2 (**A**), interferon (IFN-)ɣ (**B**) or IL-2/IFN-ɣ (**C**) spot-forming units (SFU)/10^6 splenocytes were determined. Samples were measured in triplicate. The mean for each group is indicated. (**D**) Splenocytes were stimulated with the $NP_{147–155}$ peptide for 12h. Using flow cytometry, live splenocytes were selected and subsequently $CD3^+$, $CD8^+$ and $IFN\text{-}ɣ^+$ cells were gated. Representative graphs of mice vaccinated with wild-type Modified Vaccinia virus Ankara (wtMVA) as a control or recombinant MVA (rMVA)-NPwt are shown. (**E**) IFN-ɣ production of $CD3^+$ $CD8^+$ splenocytes per 10^6 events measured using flow cytometry. Mean for each group is indicated. MM = Matrix-M™ adjuvant. * p<0.0227; ** p=0.0073; *** p=0.0005; **** p<0.0001.*

The vaccine-induced NP-specific T cell responses were also assessed using flow cytometry. IFN-ɣ production after stimulation of splenocytes with $NP_{147–155}$ peptide was used to measure induction of NP-specific $CD3^+$ $CD8^+$ T cells (**Fig. 4D**). A similar pattern to the FluoroSpot data was observed; all rMVA-NP vaccine groups induced NP-specific $CD3^+$ $CD8^+$ IFN-ɣ-producing cells and, although not statistically significant, rMVA-NPΔNLS induced slightly elevated and rMVA-UbqNP slightly reduced numbers of IFN-ɣ-producing T cells compared to rMVA-NPwt (**Fig. 4E**). The use of NPwt protein, in combination with Matrix-M™ adjuvant, induced an $NP_{147–155}$-specific $CD8^+$ T cell response inefficiently (**Fig. 4E**). Thus, vaccination with rMVA-NP induced stronger NP-specific cytotoxic $CD8^+$ T cells than with adjuvanted recombinant NP preparation. However, MVA-driven expression of NP modified in order to increase its processing and presentation did not result in increased T cell responses in BALB/c mice.

Discussion

In this study, we investigated the immunogenicity of various influenza virus NP-based vaccines. Influenza virus NP is relatively conserved and an interesting target for the induction of (cross-)protective immune responses to influenza virus. Both NP-specific antibodies[188,189,411] and T cells[412] have been shown to contribute to protective immunity to influenza virus infections. Here, we compared the immunogenicity of unadjuvanted and Matrix-M™ adjuvanted protein and rMVA expressing NPwt or modified NP for their capacity to induce influenza virus NP-specific antibody and T cell responses in BALB/c mice.

Differential induction of NP-specific antibodies was observed after protein or MVA-based NP vaccination (**Fig. 1**). As rMVA expresses full-length NP similar to the way it is expressed in influenza virus infection, it is likely that NP is exposed on the surface of rMVA-NP infected cells, leading potentially to more efficient induction of antibody responses after a single vaccination compared to vaccination with NPwt protein. The effect of this differential induction of antibody responses on a challenge infection was not addressed in this study.

As MVA is a replication-deficient virus capable of infecting cells it has intrinsic adjuvant capacities, such as activation of the innate immune system[413,414] – including activation of Toll-like receptors (TLRs)[243]. Matrix-M™ adjuvant also recruits and activates innate immune cells, but does not activate TLRs. The Matrix-M™ adjuvant increases antigen uptake and processing[406,415,416], resulting in a significant increase in the cellular immune response to NP, as demonstrated by the detection of IL-2- and/or IFN-ɣ-producing splenocytes that were stimulated with NP *in vitro*. Also, after vaccination with rMVA-NPwt, potent cellular immune responses were observed dominated by IFN-ɣ- or IL-2/IFN-ɣ-producing cells, although the number of cells that produced IL-2 only seemed lower compared to vaccination with Matrix-M™ adjuvanted NP (**Fig. 2**). Of note, the concentration of protein or adjuvant used for vaccination did not make a significant difference in vaccine immunogenicity.

In an attempt to optimize the NP-specific $CD8^+$ T cell response induced by vaccination, we previously generated rMVA constructs expressing modified NP. We have shown

that deletion of the NLS or fusion of NP to ubiquitin increased degradation of NP and enhanced activation of NP-specific T cells *in vitro*. However, these modifications did not improve $CD8^+$ T cell responses *in vivo* or protection from a lethal challenge with influenza A virus in C57BL/6 mice[341]. We hypothesized that MVA-NPwt already induced an optimal T cell response in C57BL/6 (H-2Kb/Db) mice, because these mice mount a highly dominant $CD8^+$ T cells response to a single epitope located in NP ($NP_{366–374}$), which might mask any potential positive effects of the modifications. As this epitope is not recognized in in BALB/c mice (H-2Kd/Db), we addressed if differences in immunogenicity of the various rMVA-NP constructs could be detected in this mouse model and compared it to NPwt + Matrix-M™ protein-based vaccination.

The NP-specific IgG1 response induced by NPwt protein with Matrix-M™ adjuvant was significantly higher than the response induced by the rMVA-NP constructs (**Fig. 3C**), similar to the trend in the first experiment (**Fig. 1C**). Furthermore, NPΔNLS and particularly UbqNP modifications resulted in lower IgG2a responses after a single vaccination, and lower IgG1 responses after two vaccinations compared to NPwt (**Fig. 3B-C**). As these vaccines were designed to enhance NP degradation, the amount of antigen and the time window that these antigens are available for antibody recognition and induction of B cell responses is limited. Therefore, induction of lower antibody responses by these constructs is not surprising. However, after two immunizations comparable IgG2a responses were observed.

The induction of NP-specific $CD8^+$ T cells was detected after stimulation of splenocytes with the H-2Kd restricted $CD8^+$ T cell epitope $NP_{147–155}$ using the FluoroSpot assay and flow cytometry after intracellular IFN-ɣ staining. IFN-ɣ responses measured by the FluoroSpot assay were significantly higher after vaccination with rMVA-NP constructs compared to NPwt + Matrix-M™ vaccination, whereas comparable low numbers of IL-2- and IFN-ɣ/IL-2-producing cells were detected. Using flow cytometry, no $NP_{147–155}$-specific $CD8^+$ T cells were detected after vaccination with NPwt + Matrix-M™ adjuvant, indicating that the protein vaccine generates a mainly antigen-specific $CD4^+$ T cell response. This can be concluded from the experiment shown in **Fig. 2**, in which splenocytes were stimulated with NP protein which predominantly activates $CD4^+$ T cells.

Both in the FluoroSpot assay and using flow cytometry, rMVA-NPwt induced a NP-specific $CD8^+$ T cell response that could not be improved by modifying the NP protein (**Fig. 4**). Notably, rMVA-UbqNP even induced slightly lower levels of NP-specific T cells compared to rMVA expressing NPwt, NPmut or NPΔNLS (**Fig. 4**), possibly in contrast to our hypothesis, the result of reduced availability of NP for direct antigen processing and presentation or cross-presentation[363,379,417]. We have shown previously in pulse-chase experiments that the degradation kinetics vary for the different NP constructs; NPΔNLS and particularly UbqNP had a higher degradation rate than NPwt and NPmut[341]. Therefore, the kinetics of the induction of the T cell response could differ between the different rMVA-NP constructs. In general, experiments in C57BL/6 and BALB/c mice show that NPwt is already optimally processed and presented, and that this cannot be improved by increasing the number of peptides available for presentation to T cells.

In conclusion, addition of the Matrix-M™ adjuvant to NPwt protein-based vaccines enhanced immunogenicity significantly, resulting in the induction of IgG2a as well as IgG1 antibody responses and increased T cell responses. Furthermore, rMVA-based NP vaccines seem to be capable of inducing a more diverse antibody (IgG1 and IgG2a) and cellular (IL-2, IFN-ɣ, IL-2/IFN-ɣ) response compared to protein-based NP vaccines, and only a single vaccination is enough to induce IgG2a antibody responses. The humoral and cellular immune response induced by rMVA expressing NPwt in BALB/c mice could not be enhanced further by increasing NP protein degradation. These results show that NP does not need any modifications to induce an optimal immune response.

Acknowledgements
The authors would like to thank Heidi De Gruyter and Stella van Trierum for their help in generating the rMVA constructs. Jurgen Haustraete is acknowledged for providing the BL21codon + pICA2 *E. coli* strain and the mCaspase enzyme and Dr Cecilia Carnrot, Eva Spennare and Dr. Carolina Lunderius Andersson for excellent technical assistance. This work was supported financially by the European Research Council FP7 project FLUNIVAC (project number 602604).

CHAPTER 3.3

Matrix-M™ adjuvant enhances immunogenicity of both protein- and Modified Vaccinia virus Ankara-based influenza vaccines in mice

SE Magnusson*, AF Altenburg*, K Lövgren Bengtsson, F Bosman,
RD de Vries, GF Rimmelzwaan & L Stertman
*Authors contributed equally

Submitted

Influenza viruses continuously circulate in the human population and escape from recognition by virus neutralizing antibodies induced by prior infection or vaccination through the accumulation of mutations in the surface proteins hemagglutinin (HA) and neuraminidase (NA). Various strategies to develop an influenza vaccine that provides broad protection against different influenza A viruses are currently under investigation, including the use of recombinant viral vectors and adjuvants. The replication-deficient Modified Vaccinia virus Ankara (MVA) is a promising vaccine vector with an excellent safety record that can efficiently induce B- and T-lymphocyte responses specific for an antigen of interest. It is generally assumed that live vaccine vectors do not require an adjuvant to be immunogenic because the vector already mediates recruitment and activation of immune cells. In order to address this topic, BALB/c mice were vaccinated with either protein- or recombinant (r)MVA-based hemagglutinin (HA) influenza vaccines, formulated with or without the saponin-based Matrix-M™ adjuvant. Co-formulation with Matrix-M™ adjuvant significantly increased HA vaccine immunogenicity, resulting in antigen-specific humoral and cellular immune responses comparable to those induced after vaccination with unadjuvanted rMVA-HA. Of special interest, the immunogenicity of rMVA-HA was also enhanced by the addition of Matrix-M™ adjuvant, as was demonstrated by enhanced hemagglutinin inhibition antibody titers and cellular immune responses. Matrix-M™ adjuvant added to either protein- or rMVA-based HA vaccines mediated recruitment and activation of antigen-presenting cells and lymphocytes to the draining lymph node at 24 and 48 hours post-vaccination. Taken together, these results suggest that adjuvants can not only be used with protein-based vaccines, but also in combination with rMVA to increase vaccine immunogenicity, which may be a step forward to generate new and more effective influenza vaccines.

Introduction

Influenza A (H1N1 and H3N2) and B viruses cause respiratory tract infections and are responsible for substantial morbidity and mortality during seasonal epidemics, particularly in patients at high risk, such as the elderly. Due to accumulation of mutations in the surface proteins hemagglutinin (HA) and neuraminidase (NA), the antigenic properties of the virus change continuously, resulting in escape from recognition by neutralizing antibodies induced by prior infection or vaccination[4,17,18].

Furthermore, avian influenza viruses of various subtypes have been shown to infect humans sporadically[382-384]. Since virus neutralizing antibodies to these viruses are virtually absent in the human population, they are considered to have pandemic potential.

Currently used inactivated influenza vaccines contain components from seasonal influenza viruses and aim at the induction of HA-specific neutralizing antibodies[1,418]. Despite annual assessment of virus strains to be included in the seasonal influenza vaccine, a mismatch between circulating influenza viruses and the vaccine strains occasionally occurs, resulting in reduced vaccine effectiveness[317-319]. Furthermore, novel tailor-made influenza vaccines need to be developed momentarily in case of an influenza virus pandemic. Clearly, there is a need for improved influenza vaccines that can be produced rapidly and are highly immunogenic, inducing broadly protective immunity to various influenza viruses.

Novel vaccine targets, adjuvants and delivery systems are under currently investigation to develop 'next-generation' influenza vaccines. Recombinant viral vaccine vectors, including Modified Vaccinia virus Ankara (MVA) and adenoviruses, can be used to drive expression of any antigen of interest, resulting in efficient induction of antigen-specific B- and T-lymphocyte responses[209,280]. Particularly MVA is considered to be of interest since it has an excellent safety record in humans, including immunocompromised individuals[209,234,280,419]. Design and rescue of recombinant (r)MVA expressing one or more antigens is relatively easy and can be performed rapidly, and large numbers of vaccine doses can be produced[280]. Previously, several rMVA vaccines expressing HA from various influenza viruses have been evaluated *in vitro* and *in vivo*, and have shown to be immunogenic and capable of inducing protective immunity against homologous and heterologous influenza virus infections[209].

Another approach to enhance influenza vaccine immunogenicity is the use of adjuvants[420]. Adjuvants such as MF59, AS03, Alum, ISCOMATRIX® and Matrix-M™ adjuvant have successfully been evaluated in clinical trials in combination with seasonal and pandemic influenza vaccines, including inactivated whole virus, split-virion, virosomal and virus-like particle vaccines[391,401,402,421-424]. Furthermore, MF59 and AS03 have been approved for use in a seasonal and pre-pandemic A(H5N1) influenza vaccine, respectively[425]. Matrix-M™ adjuvant, made of *Quillaja saponins* formulated with cholesterol and phospholipids into nanoparticles, is known to augment Th1 and Th2 responses, induce antibodies of multiple subclasses, enhance immune cell trafficking and allow antigen dose-sparing[390,392,393,398,426-428]. Importantly, Matrix-M™-adjuvanted vaccines have been shown to have an acceptable safety profile in clinical trials[391,401,402]. Compared to other adjuvants, Matrix-M™ performed as well or better in combination with influenza vaccines in mice[393,429].

In contrast to protein-based vaccines, which are poorly immunogenic without adjuvant, vector-based vaccines are generally thought not to require adjuvants due to the intrinsic adjuvant activity of the vector backbone[245]. However, recently it was shown that immunogenicity of malaria and Rift Valley Fever virus antigens expressed

from adenovirus or MVA was improved by addition of Matrix-M™ adjuvant [430,431]. In the present study, we show that the immunogenicity of both HA protein- and MVA-based influenza vaccines was enhanced by Matrix-M™ adjuvant. Co-formulation of either vaccine with Matrix-M™ adjuvant increased absolute immune cell numbers and activation in the lymph node (LN) draining the site of vaccination.

Material and Methods

Matrix-M™ adjuvant

Novavax proprietary Matrix-M™ adjuvant consists of two individually formed 40nm sized particles, each with a different and well-characterized saponin fraction (Fraction-A and Fraction-C). The Matrix-A and -C particles are formed by formulating purified saponin from the tree *Quillaja saponaria* Molina with cholesterol and phospholipid[397].

Preparation of HA protein

Recombinant HA (H1N1, A/Puerto Rico/8/34 [PR8]) was produced in HEK293F cells as an amino-terminal His-tagged fusion protein containing a linker sequence (PGGPGS) and mcaspase3 cleavage site (DELD) but lacking the HA transmembrane sequence. The secreted (His6-PGGPGSDELD)-HA protein was purified by metal affinity chromatography. After mcaspase treatment (E/S mass ratio: 1/30), the protein solution was loaded on a Superdex G200 gel filtration column and the HA were fractions pooled. Analysis by SDS-PAGE/CBB staining and western blot showed that mature (cleaved) HA protein was obtained with a purity of at least 90%.

Generation of rMVA-HA

rMVA expressing HA under control of the early/late vaccinia virus promotor PsynII using the MVA clonal isolate F6, was produced as previously described[256]. In short, the codon-optimized HA nucleotide sequence (PR8, accession number CY033577) was purchased from Baseclear B.V. and rMVA was prepared through mCherry-dependent plaque selection in chicken embryo fibroblasts (CEF). To generate a final vaccine preparation, the virus was amplified in CEF, purified by ultracentrifugation through 36% sucrose and reconstituted in 120mM NaCl, 10mM Tris-HCl pH 7.4. rMVA-HA constructs were characterized by PCR, sequencing, plaque titration, western blot and *in vitro* infection of various cell types.

Vaccination of BALB/c mice

Specified pathogen free female BALB/c mice (8-10-week-old) were purchased from Charles River Laboratories (Germany). Animals were housed in Makrolon type 3 cages, had access to food and water *ad libitum* and animal welfare was observed daily. All experiments were conducted in compliance with European guidelines and the protocol approved by an independent animal experimentation ethical review committee (Uppsala djurförsöksetiska nämnd). Two separate experiments were performed. In the first experiment, mice (n=5 or 8/group) received two vaccinations with 10^8 plaque-forming units (PFU) of rMVA-HA or 1 or 10µg of HA, formulated with or without 5µg Matrix-M™, at a four-week interval. All vaccines were administered subcutaneously (s.c.) in 100µL at the base of the tail. Blood samples were obtained at day 21 and day 42. Spleens were collected in PBS during necropsy. In the second experiment mice (n=30/group) were immunized intramuscularly (i.m.) in the hind leg with a volume of 50µL containing 10^8 PFU rMVA-HA or 10µg HA with or without 5µg Matrix-M™. The inguinal LN draining the hind leg muscle was collected in PBS at 4h, 24h or 48h post-vaccination(n=10/group/time-point).

Detection of IgG1 and IgG2a HA-specific serum antibodies

Quantification of HA-specific IgG1 and IgG2a antibodies was performed by ELISA as described previously[393]. Briefly, 96-well Maxisorp microplates (Nunc) coated overnight (O/N) at 4°C with 50ng/well HA protein in 0.05M Carbonate/Bicarbonate buffer (Sigma Aldrich). Serum from untreated mice and HA-positive mouse serum was used as negative or positive control, respectively. IgG1 and IgG2a anti-HA titers were calculated using a four-parameter logistic equation (Softmax software, Molecular Devices). The inflection point of the titration curve (EC_{50} value) was taken as titer value.

Hemagglutination Inhibition (HI) assay
Sera were treated with a receptor-destroying enzyme (filtrate of *V. Cholera*) O/N at 37°C followed by heat-inactivation at 56°C. Sera were titrated in a 2-fold-serial dilution. The HI assay was performed in duplicate following a standard protocol with 1% turkey erythrocytes and four HA-units of influenza virus PR8, as described previously[348].

Fluorospot analysis of antigen-stimulated splenocytes
Single cell suspensions from spleens of individual mice, prepared as previously described[393], were seeded on filter plates coated with anti-interleukin 2 (IL-2) and/or anti-interferon gamma (IFN-ɣ) antibodies (Mabtech), at 0.25 x 10^6 cells/well in culture medium (Roswell Park Memorial Institute, Sigma Aldrich) supplemented with 10% heat-inactivated fetal bovine serum (Sigma Aldrich) and 100U/ml penicillin, 100µg/ml streptomycin, 2mM L-glutamin (Sigma Aldrich), followed by stimulation with 0.5µg/well HA protein. Concanavalin A (Sigma Aldrich) and culture medium were used as positive and negative controls, respectively. Triplicate samples were incubated for 18h at 37°C and IL-2 and/or IFN-ɣ spots were developed according to the manufacturer's instructions (Mabtech). Spots were detected using an AID ELR02 ELISpot reader (Autoimmune Diagnostika GmbH).

Flow cytometry analysis of immune cells in the dLN
Single cell suspensions from the draining (d)LN, prepared as described previously[393], were stained with FVS780 (BD Biosciences) for 15min at room temperature to exclude dead cells during analysis. Cells were washed and resuspended in FACS buffer (PBS with 0.5% bovine serum albumin, 2mM EDTA and 0.1% NaN3,) and incubated for 20min at 4°C with anti-mouse CD16/CD32 (2.4G2, BD Biosciences). 5x10^5 cells/well were transferred to a 96-well microtiter plate (Nunc) and incubated with anti-mouse CD86^{FITC} (GL1), I-A/I-E^{BV605} (M5/114), CD8a^{BV650} (53-6.7), CD19$^{PerCP\text{-}Cy5.5}$ (1D3), CD3e$^{PerCP\text{-}Cy5.5}$ (145-2C11), Ly-6G^{BV786} (1A8) (all BD Biosciences) and CD169^{AlexaFluor647} (3D6.112), CD11c^{BV650} (N418), Ly-6C^{APC} (HK1.4), CD69^{BV421} (H1.2F3), CD3e^{PE} (145-2C11), F4/80^{BV421} (BM8), CD11b^{PE} (M1/70), CD49b^{APC} (DX5) and CD4^{BV785} (RM4-5) (all Nordic Biosite) for 30min at 4°C. Fluorescence minus one controls were prepared for each antibody in all antibody panels at acquisition time points. Samples were analyzed on FACSCelesta with FACSDiva software (BD Biosciences).

Statistical analysis
Serological and cellular data were analyzed using one-way ANOVA with Tukey's post test for multiple comparisons or Kruskal-Wallis with Dunn's multiple comparisons test when applicable.

Results

Addition of Matrix-M™ adjuvant enhanced HA-specific humoral responses

To assess HA-specific antibody responses after vaccination with either protein- or rMVA-based vaccines with or without Matrix-M™ adjuvant, mice were immunized at day 0 and 28. At 21 days after the primary vaccination, HA-specific serum antibody responses were detected in all groups. Strongest antibody responses of both IgG1 and IgG2a were detected after vaccination with 10µg HA adjuvanted with Matrix-M™. Without Matrix-M™, protein-based HA vaccines induced IgG1 and IgG2a responses inefficiently. After one immunization with rMVA-HA, HA-specific IgG1 and IgG2a antibody responses were induced, which were not further enhanced by Matrix-M™ addition (**Fig. 1A-B**). Fourteen days after the second vaccination, HA-specific IgG1 and IgG2a levels were boosted in all groups (**Fig. 1C-D**). Addition of Matrix-M™ to both HA doses significantly increased IgG1 responses compared to unadjuvanted HA or rMVA-HA vaccination with or without Matrix-M™ (**Fig. 1C**). The IgG2a responses after the second vaccination were comparable between Matrix-M™-adjuvanted HA groups and both rMVA-HA vaccine groups, and were elevated compared to the unadjuvanted HA group (**Fig. 1D**). Use of Matrix-M™ did not increase IgG1 or IgG2a responses after the second vaccination with rMVA-HA.

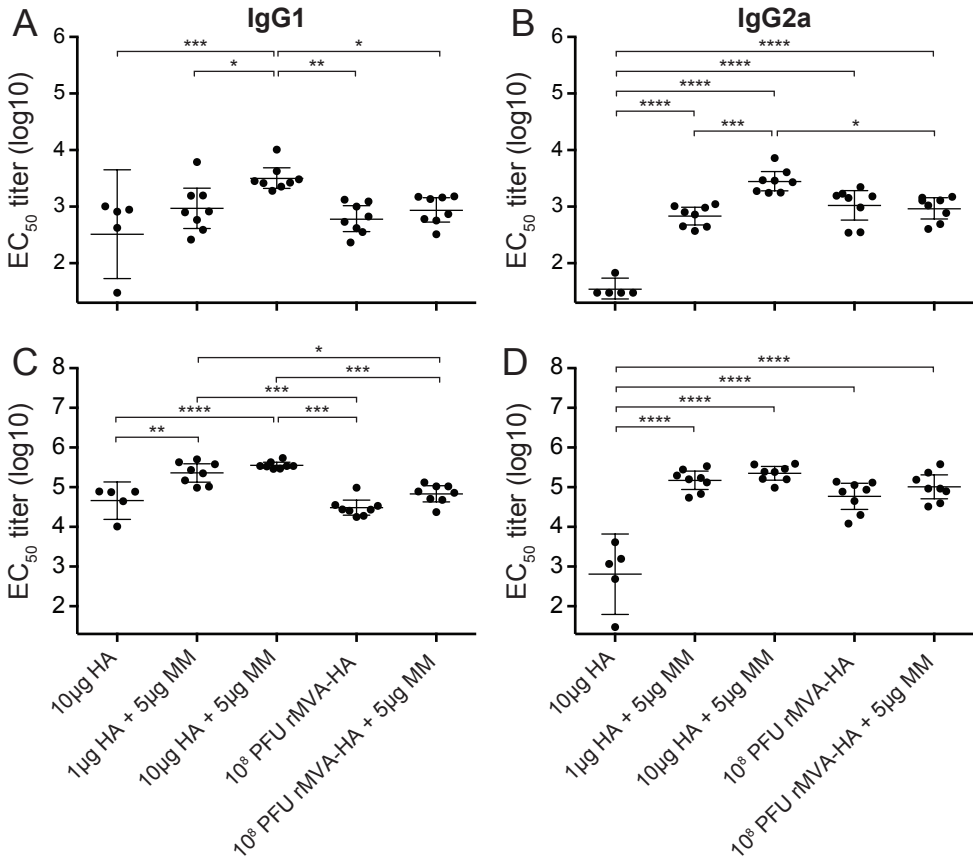

Figure 1. HA-specific antibody responses induced after vaccination with HA protein or rMVA-HA with or without Matrix-M™ adjuvant. *(**A-B**) IgG1 and IgG2a HA-specific antibody responses 21 days after the primary vaccination. (**C-D**) IgG1 and IgG2a HA-specific antibody responses 14 days after the booster vaccination. IgG1 (**A, C**) or IgG2a (**B, D**) serum antibodies were detected by ELISA using purified HA protein and anti-IgG1 or anti-IgG2a HRP-conjugated antibodies. Data is shown as mean ±95% confidence interval (CI). * p<0.05, ** p<0.01, *** p<0.001, **** p<0.0001. MM = Matrix-M™ adjuvant.*

Next, HI antibody titers were determined, which is considered a good proxy for the virus-neutralizing antibody response. In contrast to the IgG1 and IgG2a responses detected after primary vaccination, mice vaccinated with rMVA-HA displayed significantly elevated HI titers compared to those vaccinated with HA, regardless of antigen dose and use of adjuvant (**Fig. 2A**). After booster vaccination, HI titers were detected in mice receiving Matrix-M™-adjuvanted HA, whereas lower HI titers were detected in only two out of five mice receiving unadjuvanted HA. After two immunizations, Matrix-M™-adjuvanted HA induced similar HI titers as rMVA-HA vaccination (**Fig. 2B**). Of special interest, higher HI titers were observed in mice vaccinated with Matrix-M™-adjuvanted rMVA-HA compared to mice that received unadjuvanted rMVA-HA.

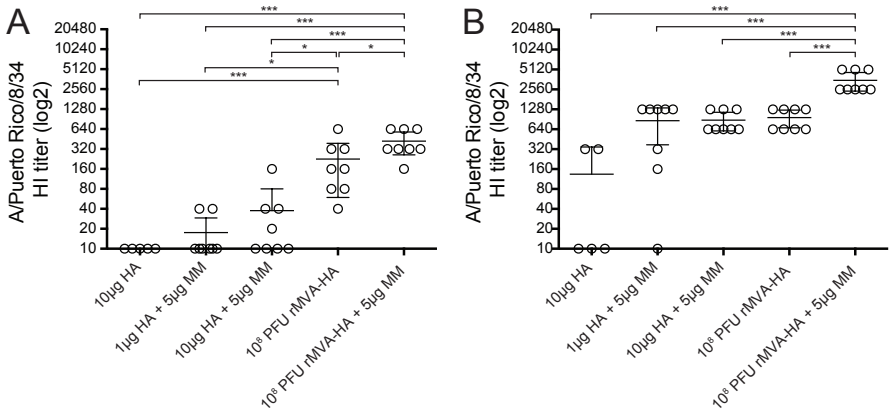

Figure 2. Induction of HA-specific HI antibody responses after vaccination with rMVA-HA adjuvanted with Matrix-M™. *HI serum antibody responses against influenza virus A/Puerto Rico/8/34 (H1N1) were measured 21 days after the primary (**A**) or 14 days after the booster (**B**) vaccination. Data is shown as mean ±95% CI. * p<0.05, ** p<0.01, *** p<0.001. MM = Matrix-M™ adjuvant.*

Addition of Matrix-M™ adjuvant enhanced HA-specific cellular responses

To investigate HA-specific T-lymphocyte responses after booster vaccination, splenocytes were stimulated with HA protein and the number of IL-2 and/or IFN-ɣ producing cells was measured. Matrix-M™-adjuvanted HA and rMVA-HA, with or without Matrix-M™, induced significantly more IL-2 and/or IFN-ɣ producing splenocytes than HA alone. Unadjuvanted HA hardly induced any IL-2 and/or IFN-ɣ splenocyte responses (**Fig. 3A-C**). In contrast, co-formulation of HA with Matrix-M™ resulted in higher IL-2 responses compared to rMVA-HA, adjuvanted or not, whereas rMVA-HA induced higher IFN-ɣ responses compared to adjuvanted HA (**Fig. 3A-C**). Mice vaccinated with Matrix-M™-adjuvanted rMVA-HA displayed stronger IL-2, IFN-ɣ and IL-2/IFN-ɣ double-positive responses compared those receiving unadjuvanted rMVA-HA, although the differences were exclusively statistically significant for the IL-2 response (**Fig. 3A-C**).

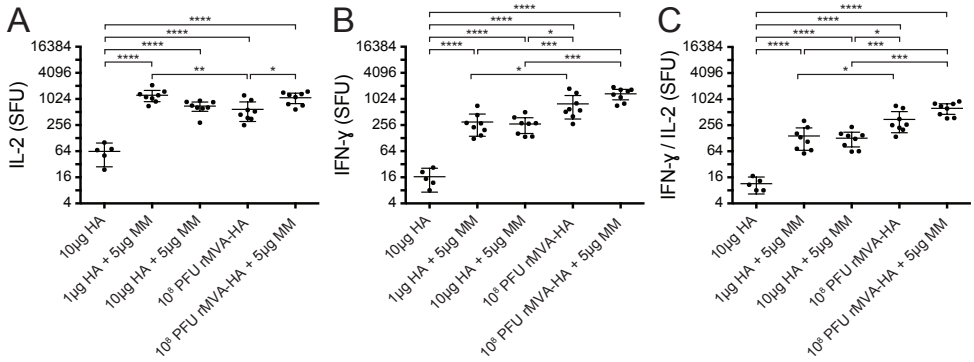

Figure 3. Enhanced HA-specific splenocyte responses by Matrix-M™ adjuvanted vaccines. *Spleens obtained 14 days after the booster vaccination were stimulated with purified HA protein and the number of IL-2 (**A**), IFN-γ (**B**) and IL-2/IFN-γ (**C**) producing splenocytes was determined in spot-forming units (SFU)/10⁶ cells by Fluorospot assay. Samples were tested in triplicate. The mean ±95% CI of each group is indicated. * p<0.05, ** p<0.01, *** p<0.001, **** p<0.0001. MM = Matrix-M™ adjuvant.*

Matrix-M™ adjuvanted vaccines increased cell numbers in the dLN

Since addition of Matrix-M™ adjuvant to either protein- or MVA-based vaccines increased both HA-specific humoral and cellular immune responses, the early cellular immune response in the dLN was evaluated after vaccination with the respective vaccines in presence or absence of Matrix-M™. Mice were vaccinated i.m. with HA or rMVA-HA, with or without Matrix-M™, and dLNs were collected 4h, 24h and 48h post-vaccination. At 4h post-vaccination the mean number of total cells in the dLN of all vaccine groups was similar (**Fig. 4A**). In contrast, after 24h and 48h the total cell count per dLN of mice vaccinated with adjuvanted HA or rMVA-HA showed more than a two-fold increase compared to the unadjuvanted groups (**Fig. 4A**). Of note, although not as strong as the Matrix-M™ adjuvanted vaccines, vaccination with unadjuvanted rMVA-HA also resulted an increase in cell count per dLN.

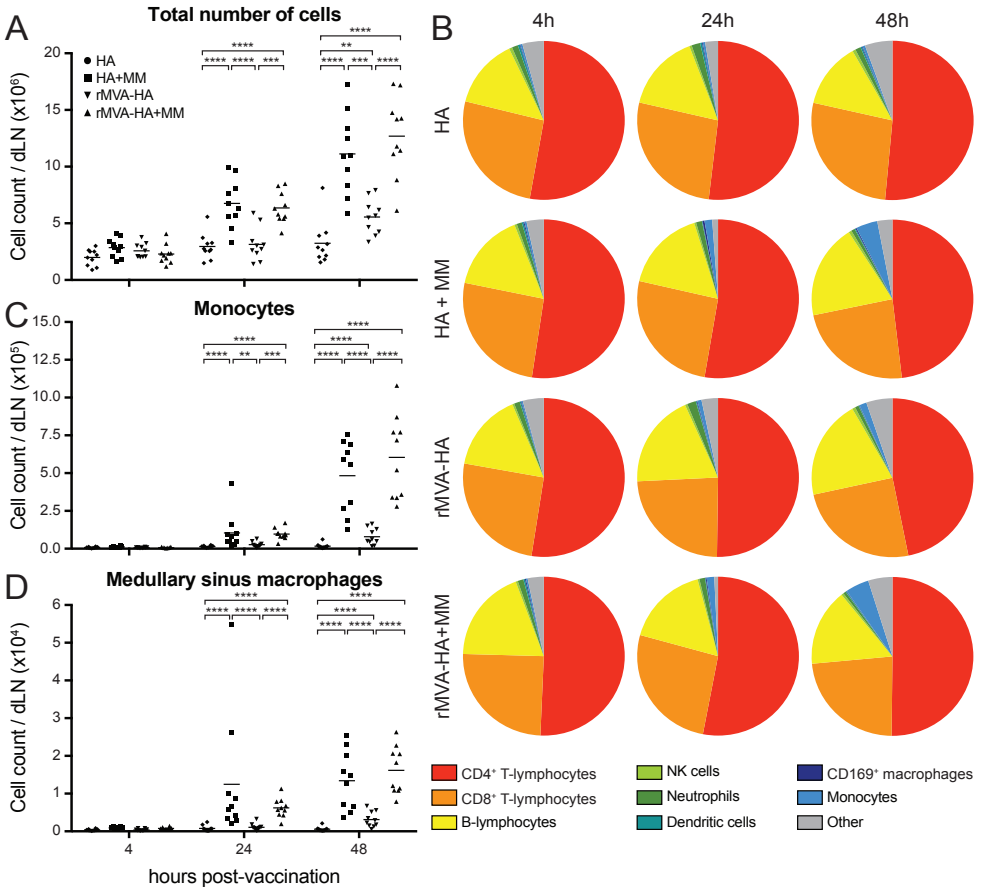

Figure 4. Matrix-M™ adjuvanted influenza vaccines induce influx of immune cells in the dLN with maintained composition of cellular subsets except for an increased monocyte population. *(**A**) The total number of cells per dLN. (**B**) Contribution (%) of the indicated cellular subsets in the dLN was measured by flow cytometry at 4, 24 or 48 h after i.m. vaccination. (**C-D**) Total cell count of CD11b⁺ Ly6C⁺ monocytes (**C**) and CD169⁺ F4/80⁺ medullary sinus macrophages (**D**) was determined by flow cytometry. Data are shown as mean of 10 mice per group. * p<0.05, ** p<0.01, *** p<0.001, **** p<0.0001. MM = Matrix-M™ adjuvant.*

The relative contribution of different cell populations (**Fig. S1**) to the total cell number in each dLN (n=10/group) was determined. At all time-points, regardless of vaccine type or use of adjuvant, $CD4^+$ T-lymphocytes comprised the largest proportion of the total cell population, followed by $CD8^+$ T- and B-lymphocytes (**Fig. 4B**). No significant difference in the percentage of neutrophils, macrophages, NK cells or DCs was observed (**Fig. 4B**). In contrast, mice vaccinated with Matrix-M™-adjuvanted HA or rMVA-HA, and to a lesser extent unadjuvanted rMVA-HA, showed a strong increase in proportion and total number of monocytes in the dLN over time, indicating recruitment and/or proliferation (**Fig. 4B-C**). Notably, the number of medullary sinus macrophages ($CD169^+$ $F4/80^+$) was increased by Matrix-M™-adjuvanted HA and rMVA-HA at 24h and 48h after vaccination compared to unadjuvanted vaccine preparations (**Fig. 4D**). At 48h the unadjuvanted rMVA-HA group showed an increase in medullary sinus macrophages compared to the unadjuvanted HA group, but to a lesser extent compared to adjuvanted vaccines.

Cell activation in the dLN after vaccination with Matrix-M™ adjuvanted vaccines

Activation of different cellular subsets was investigated by measuring expression of CD69 (early activation marker[432]), CD86 (T-lymphocyte co-stimulatory signal[433]) and/or MHC class II (often upregulated on antigen-presenting cells (APC) after activation). Expression of both CD69 and CD86 was upregulated on DCs, monocytes and B-lymphocytes 24h and 48h after vaccination with either Matrix-M™-adjuvanted HA or rMVA-HA compared to the respective unadjuvanted vaccine preparation (**Fig. 5A-B**). Unadjuvanted rMVA-HA also induced an increase in $CD69^+$ and $CD86^+$ DCs, monocytes and B-lymphocytes compared to unadjuvanted HA at 24h and 48h post-vaccination, however, only to a limited extent compared to the adjuvanted vaccines (**Fig. 5A-B**). In addition to the increase in $CD69^+$ and $CD86^+$ APCs, MHC class II expression in DCs was elevated at 24h and 48h post-vaccination with Matrix-M™-adjuvanted vaccine preparations (**Fig. 5C**). CD69 expression was also assessed for T-lymphocytes and NK cells. The number of $CD69^+$ NK cells and T-lymphocytes was significantly increased after vaccination with Matrix-M™-adjuvanted HA, or rMVA-HA, compared to their unadjuvanted counterparts (**Fig. 6A-C**).

Altogether, rMVA-HA induced relatively more activation, recruitment and/or proliferation of APC and lymphocytes than unadjuvanted HA. However, addition of Matrix-M™ adjuvant to either protein- or MVA-based HA vaccines significantly increased activation and recruitment and/or proliferation for both vaccine preparations.

Discussion

Adjuvants increase vaccine immunogenicity via different mechanisms, including antigen delivery and general activation of innate immune responses[434]. Although use of adjuvants for protein-based vaccines is well established and essential for efficient immune responses, addition of adjuvants to vector-based influenza vaccines has not been previously studied. Here, the immunogenicity of influenza virus HA and rMVA-HA vaccines was tested in the presence and absence of Matrix-M™ adjuvant. Although unadjuvanted rMVA-HA was more immunogenic than unadjuvanted HA, co-formulation of either vaccine preparation with Matrix-M™ enhanced HA-specific immune responses and increased the cell number and activation in the dLN.

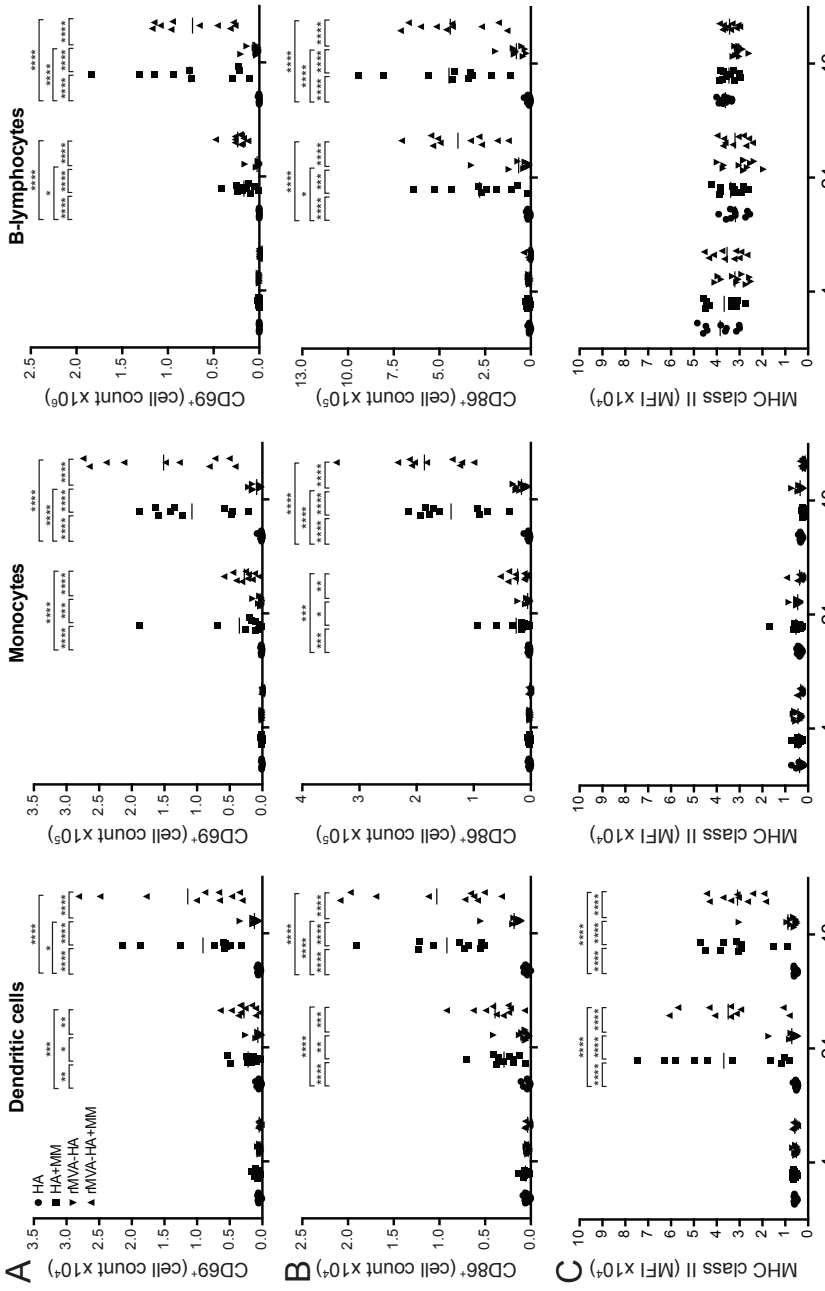

Figure 5. Increased activation of APCs in the dLN 24 and 48h after vaccination with Matrix-M™ adjuvanted influenza HA vaccines. *(**A-B**) The number of CD69⁺ or CD86⁺ DCs, monocytes and B-lymphocytes recruited to the dLN was measured by flow cytometry 4, 24 and 48h after i.m. injection of the respective vaccine. (**C**) The mean fluorescence intensity (MFI) of MHC class II of on DCs, monocytes and B lymphocytes in the dLN was measured by flow cytometry 4, 24 and 48h post injection. Data are shown as mean of 10 mice per group. * p<0.05, ** p<0.01, *** p<0.001, **** p<0.0001. MM = Matrix-M™ adjuvant.*

For induction of proper HA-specific antibody responses of IgG1 (indicative of Th2 responses) or IgG2a (indicative of Th1 responses) subclasses, addition of Matrix-M™ adjuvant to HA was required, but not to rMVA-HA. After two immunizations, adjuvanted HA induced significantly higher IgG1 antibody responses than rMVA-HA, whereas IgG2a antibody responses were similar. This is in line with previously published data showing that MVA-based vaccines preferentially induce Th1 responses[209,280]. The observed potentiating effect of Matrix-M™ on the IgG2a antibody responses has been shown previously with various vaccine preparations in mice[392,393,398]. Induction of potent IgG2a responses bares relevance, as murine IgG2 has key immunological effector functions, such as enhanced FcγR binding important for protection against viral infection[435]. Accordingly, passive immunization with HA stalk-specific IgG2a antibodies has shown to protect mice against influenza virus infection, while HA stalk-specific IgG1 antibodies did not[45]. To induce functional antibodies a single vaccination with rMVA-HA was sufficient for generating acceptable HI antibody titers, whereas for HA, regardless of co-formulation with Matrix-M™ adjuvant, two vaccinations were required. This may reflect a better conformational integrity of HA expressed *in vivo* by rMVA-HA. Strikingly, addition of Matrix-M™ adjuvant to the rMVA-HA vaccine significantly increased the HI antibody response.

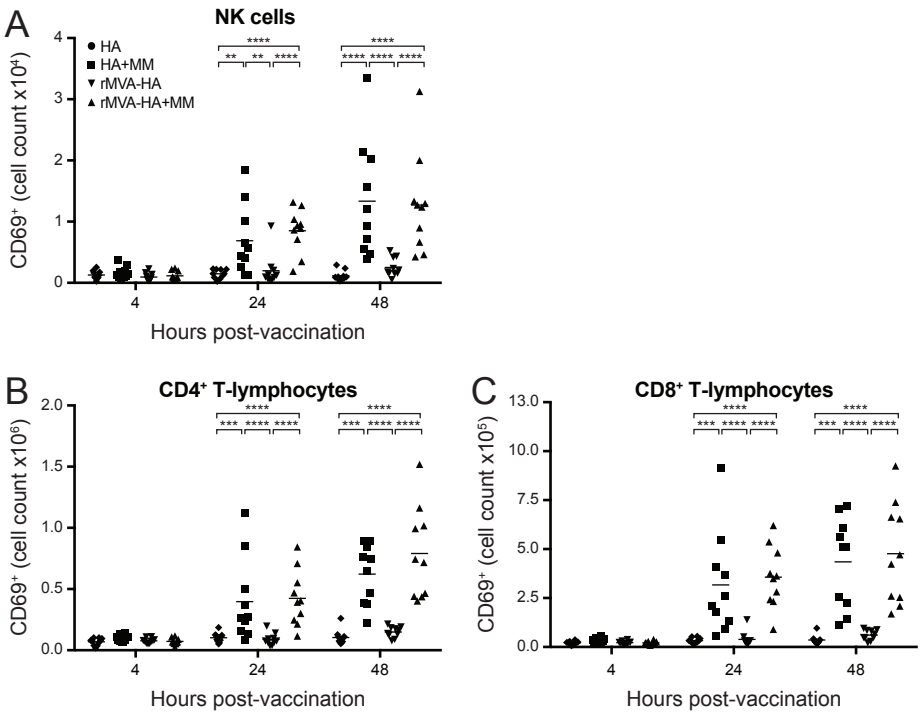

Figure 6. Increased number of activated NK- and T lymphocytes in the dLN at 24 and 48h post vaccination with Matrix-M™ adjuvanted influenza HA vaccines. *The number of CD69⁺ NK cells (**A**), CD4⁺ (**B**) and CD8⁺ (**C**) T-lymphocytes in the dLN was measured by flow cytometry 4, 24 and 48h after i.m. injection of the respective vaccines. Data are shown as mean of 10 mice per group. * p<0.05, ** p<0.01, *** p<0.001, **** p<0.0001. MM = Matrix-M™ adjuvant.*

Addition of Matrix-M™ adjuvant to HA potentiated HA-specific IFN-ɣ and IL-2/IFN-ɣ cellular responses significantly compared to HA alone, in concordance with previous studies[390,392,398,410]. Interestingly, mice vaccinated with rMVA-HA showed stronger IFN-ɣ responses than those vaccinated with adjuvanted HA. The rMVA-HA induced cellular responses could be even further increased by addition of Matrix-M™. Although the phenotype of the responding cells was not determined, these are most likely $CD4^+$ T-lymphocytes as exogenous HA protein was used for stimulation.

It was previously shown in mice that injection with Matrix-M™ adjuvant alone led to increased numbers of activated immune cells in the dLN compared to PBS or other adjuvants[393,428]. Here, the absolute number of cells in the dLN of mice vaccinated with Matrix-M™-adjuvanted HA or rMVA-HA vaccines was significantly higher compared to mice vaccinated with unadjuvanted vaccines 24h and 48h post-vaccination, indicative of proliferation and/or recruitment. The dLN cell composition was stable, except for an increase in monocytes after vaccination with adjuvanted vaccine preparations. Recruited monocytes could mature into DCs and/or macrophages *in situ* and subsequently act as professional APC[436], potentially improving vaccine efficacy. This could also be the effect of the increase in $CD169^+$ medullary sinus macrophages also detected in the dLN after injection with Matrix-M™-adjuvanted vaccines. Recently, $CD169^+$ macrophages were shown to be important for the adjuvant properties of the saponin-based adjuvant QS21[437]. $CD169^+$ macrophages haven been shown to transport antigens trapped inside the LN follicle to B-lymphocytes, and can cross-present antigen directly to $CD8^+$ T-lymphocytes[438-440]. Thus, the increase in $CD169^+$ macrophages may play a role in the improved adaptive immune responses induced by Matrix-M™-adjuvanted vaccines.

Vaccination with unadjuvanted rMVA-HA induced a relative increase in monocytes accompanied by increased activation of $CD86^+$ DC, $CD86^+$ B-lymphocytes and $CD169^+$ macrophages, confirming that MVA has intrinsic adjuvant properties. Of interest, it was recently shown that APCs can be infected by MVA and detected in the dLN of various species including non-human primates[342]. Thus, the observed adjuvant capacities of MVA may be explained by direct infection of APCs, which travel to the dLN, shaping the immune response.

In conclusion, our results show that influenza vaccines based on HA or rMVA-HA can be potentiated by Matrix-M™ adjuvant, resulting in improved humoral and cellular responses. This is potentially mediated by recruitment and activation of immune cells in the dLN. Combination of a vector-based vaccine with Matrix-M™ adjuvant might prove a promising step towards next-generation influenza vaccines.

Acknowledgements
The authors would like to thank Mark Pronk, Jennifer Petersson, Dr. Cecilia Carnrot, Dr. Carolina Lunderius Andersson and Eva Spennare for excellent technical assistance.

Supplementary Material

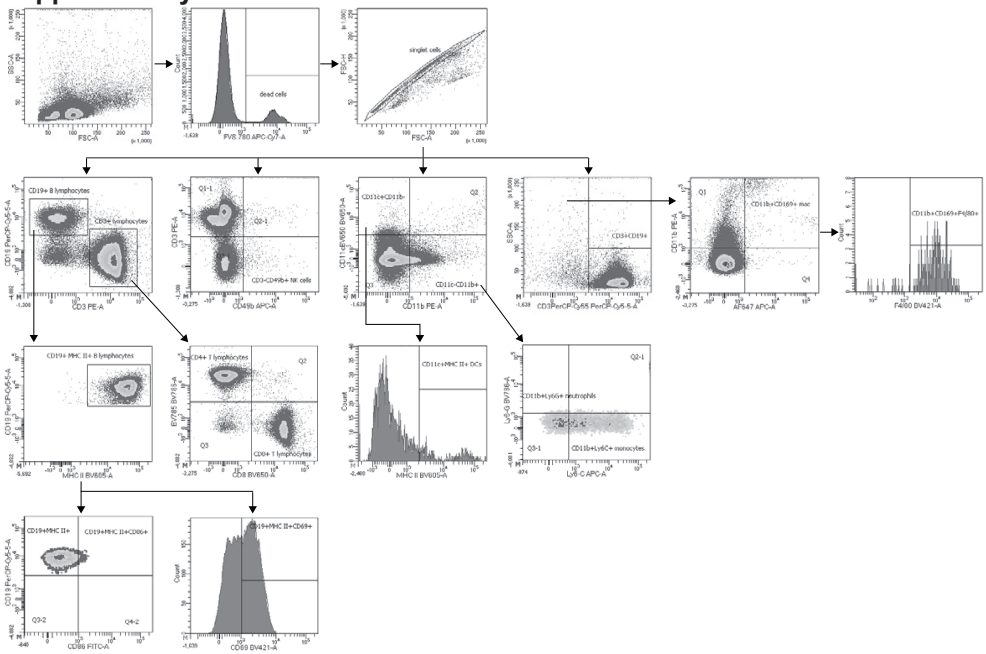

Figure S1. Gating strategy to define different immune cell populations in the draining lymph node. *Live cells were defined as FVS780$^-$, from which singlet cells were selected. Subsequently, CD3$^+$ and CD19$^+$ cells were selected and B-lymphocytes were further defined as CD19$^+$ MHC class II$^+$. The B-lymphocytes activation was assessed by CD86 and/or CD69 expression. All defined cell populations were gated in the same way for CD86 and/or CD69 expression. The CD3$^+$ cells were further defined as CD4$^+$ or CD8$^+$ T-lymphocytes. NK cells were defined as CD3$^-$ CD49b$^+$. Furthermore, from the singlet gate, cells were selected for CD11c or CD11b expression and the CD11c$^+$ cells further selected for MHC class II expression and defined as dendritic cells. The CD11b$^+$ cells were further defined into either Ly6G$^+$ cells,* i.e. *neutrophils, or Ly6C$^+$ cells,* i.e. *monocytes. Furthermore, from the singlet cells, cells were selected as non-CD3$^+$ CD19$^+$ cells and these cells were further selected for CD11b and CD169 expression and defined as subcapsular sinus macrophages and further defined as medullary sinus macrophages based on F4/80 expression. Data is shown from a mouse vaccinated with Matrix-M™ adjuvanted HA protein that is representative of the other mice and groups from the experiment.*

Chapter 4

Clinical assessment of an MVA-based H5N1 influenza vaccine

CHAPTER 4.1

Induction of cross-clade antibody and T cell responses by an MVA-based influenza H5N1 vaccine in a randomized phase I/IIa clinical trial

RD de Vries*, AF Altenburg*, NJ Nieuwkoop, E de Bruin, SE van Trierum, MR Pronk, MM Lamers, M Richard, DF Nieuwenhuijse, MPG Koopmans, JHCM Kreijtz, RAM Fouchier, ADME Osterhaus, G Sutter & GF Rimmelzwaan

*Authors contributed equally

Manuscript in preparation

Highly pathogenic avian influenza viruses of the H5 subtype continue to circulate in poultry and wild birds and occasionally infect humans, sometimes with fatal outcome. To prepare for potential future pandemics caused by these viruses, the development of effective H5 vaccines is considered a high priority. However, influenza vaccine development is complicated by antigenic variation of the surface glycoprotein hemagglutinin (HA), the most important target for virus-neutralizing antibodies. Here, we report the analysis of (cross-reactive) immune responses induced by immunization of humans with recombinant Modified Vaccinia virus Ankara expressing the HA gene of the H5N1 influenza virus A/Vietnam/1194/04 (rMVA-H5). In a double-blind phase 1/2a clinical trial, 79 young healthy adults were randomly assigned to one of eight groups, receiving one or two intramuscular injections with 10^7 or 10^8 plaque-forming units of rMVA-H5 or MVA-F6 (vector control). Twenty-seven study subjects received a booster immunization after one year. The breadth, magnitude and properties of vaccine-induced antibody and T cell responses were characterised. rMVA-H5 induced broadly-reactive antibody responses as demonstrated by protein microarray, hemagglutination inhibition, virus neutralization and antibody-dependent cellular cytotoxicity assays. The results confirmed induction of antibodies with neutralizing and non-neutralizing modes of action, directed to antigenically distinct H5 influenza viruses, including the recently emerged H5N6 and H5N8 viruses and vaccine strains representing circulating H5N1 viruses. In addition, the induction of T cells specific for H5 viruses of two different clades was demonstrated. The rMVA-H5 vaccine induced antibody and T cell responses that cross-reacted with H5 viruses of various clades. These findings validate rMVA-H5 as vaccine candidate with efficacy against antigenically distinct H5 influenza viruses.

Introduction

Highly pathogenic avian influenza (HPAI) viruses of the H5 subtype continue to cause outbreaks in poultry in various countries. Sporadically, these viruses – in particular influenza A viruses (IAV) of the H5N1 and H5N6 subtypes – infect humans, resulting in disease with variable severity. Since the first case of human infection with an H5N1 influenza virus in 1997[441-443], 859 human cases have been reported as of July 2017 of which 453 had a fatal outcome[382]. In addition to circulating H5N1 viruses, several novel H5 influenza virus subtypes have emerged, including H5N2[444],

H5N5[445,446], H5N6[447] and H5N8[446]. Recently, H5N8 and related viruses have caused large outbreaks in wild birds and poultry in Asia, Europe and North America. To date, no human infections with H5N8 virus have been reported, however, there is evidence for H5N2 virus infections in humans[448]. Furthermore, since the first report in 2015, severe infections of humans with H5N6 virus continue to be reported sporadically[23].

Although influenza viruses of the H5N1 and H5N6 subtype can infect humans, they do not have the ability to be transmitted from human-to-human efficiently. Studies in ferrets, the 'gold standard' model used to study IAV replication, pathogenesis and transmission, have shown that only a limited number of mutations in viral proteins hemagglutinin (HA) and the polymerase subunit PB2 are required to facilitate airborne transmission of an H5N1 virus[19,21]. If these H5N1 viruses acquire the capacity to be transmitted from human-to-human, they have the potential to cause severe a pandemic since the human population at large has not been exposed to these viruses and therefore virus neutralizing (VN) antibodies to these viruses are virtually absent.

Vaccination is the most important measure against IAV infections and the availability of an effective H5 vaccine would be pivotal in preventing severe disease, mortality and interrupting potential human-to-human transmission of H5 influenza viruses. Although a mock-up dossier allowing for fast track licensing of inactivated influenza vaccines produced through conventional methods has been drafted in Europe[449], vaccines became available too late in most countries during the 2009 pandemic caused by an H1N1 influenza virus[132,133]. In addition to problems with production and distribution of sufficient vaccine doses during the earliest stages of a pandemic, conventional H5N1 vaccine formulations suffer from other problems, including intrinsically low immunogenicity compared to seasonal influenza vaccines. To overcome this problem, repeated vaccinations, increased antigen doses or use of adjuvants are required[450]. Furthermore, H5 vaccine development is complicated by the genetic diversification of H5 viruses into various clades and subclades leading to large antigenic diversity of HA[451]. Collectively, this illustrates the need for novel (pre-) pandemic H5 vaccines that can be produced rapidly at a large-scale and ideally confer broad protection against antigenically distinct H5 viruses.

Vector-based H5 influenza vaccines, such as those based on Modified Vaccinia virus Ankara (MVA), potentially fulfill the needs described above. Since generation of recombinant (r)MVA by insertion of genes encoding antigens of interest into the viral genome is relatively easy, rMVA vaccine candidates have been developed for numerous infectious diseases, including influenza (reviewed by Altenburg *et al*.[280] & de Vries *et al*.[209]). rMVA drives endogenous antigen production in cells infected by the vector, leading to efficient and processing and presentation, and subsequent induction of antigen-specific B- and T cell responses. Furthermore, many viral vectors, including MVA, allow for rapid and large-scale production of vaccine doses. MVA has an excellent safety record as was demonstrated in various animal models, including immune-suppressed non-human primates, and clinical trials[277,279,280].

Previously, rMVA expressing the HA-gene of the clade 1 influenza virus A/Vietnam/1194/04 (VN/04, rMVA-H5) was generated and assessed in pre-clinical studies. This vaccine proved to be safe and immunogenic in both C57BL/6 mice and non-human primates[256,258,262], and offered protection from a lethal challenge with either the homologous or the antigenically distinct clade 2.1 H5N1 virus A/Indonesia/5/05 (IND/05)[256,262]. Subsequently, rMVA-H5 was assessed in a double-blind phase 1/2a clinical trial and proved to be safe in humans[260]. The immunogenicity of rMVA-H5 was solely assessed by detection of hemagglutination inhibition (HI) and VN antibodies against the homologous and two heterologous viruses; IND/05 and clade 2.3.4.4 H5N8 A/chicken/Netherlands/EMC-3/2014 (ch/H5N8/14)[260,261]. Here, we report a detailed analysis of the antibody and T cell responses induced by immunization of humans with rMVA-H5, with emphasis on cross-reactivity with H5 viruses of antigenically distinct clades. Such cross-reactivity was identified as a key step on the pathway to a universal influenza vaccine[452]

Materials & Methods

Ethics statement

The study design was reviewed and approved by the Central Committee on Research involving Human Subjects in the Netherlands. All volunteers provided written informed consent, the trial was registered in the Netherlands' trial register under NTR3401.

Study design

A randomised, double-blind phase 1/2a study was previously conducted at the Erasmus MC, Rotterdam, the Netherlands[260]. Briefly, N=79 healthy adult volunteers (aged 18-28 years) were included in the study and randomly assigned to one of eight groups (N=10) on basis of the number of immunizations (one or two), the immunization dose (10^7 or 10^8 plaque-forming units [PFU]) and the vaccine administered (rMVA-H5 or MVA-F6). The group receiving a single dose 10^8 PFU rMVA-H5 consisted of N=9 individuals. The rMVA-H5 vaccine expressed the HA gene of influenza virus VN/04 under control of the PsynII promotor. Immunization with MVA-F6 (empty vector) was used as a control. Immunizations were administered as intramuscular (IM) injections on the first (week 0) and second (week 4) visit. Blood samples were obtained at week 0, 4, 8 and 20. To assess whether the H5-specific immune response could be boosted by an additional immunization, N=27 individuals who received the rMVA-H5 vaccine during the main study received an additional immunization one year after the first immunization. Blood was drawn before (week 52), and 4 and 20 weeks after the booster immunization (week 56 and 72, respectively). Serum and peripheral blood mononuclear cells (PBMC) were obtained from all blood samples, as described previously[260], and stored at -20ºC and -135ºC, respectively.

Protein array (PA) assay

Sera collected at the respective time-points were used to determine the presence of antibodies directed to a large panel of antigens by protein array (PA) as described previously[346,347]. In short, recombinant HA1 derived from a selection of IAV were printed onto nitrocellulose slides by a sciFlexarrayer SX (Scienion). Sera were incubated on the slides in Blotto Blocking Buffer (Thermo Fisher Scientific Inc.) supplemented with 0.1% Surfact-Amps (Thermo Fisher Scientific Inc.). Subsequently, AlexaFluor647-labelled goat-anti-human IgG (Jackson ImmunoResearch Laboratories Inc.) was used as conjugate and fluorescent signals were measured using a Powerscanner (Tecan Group Ltd). The titer of each serum sample was defined as the interpolated serum concentration generating the 50% point using a four-parameter logistic nonlinear regression model. Measured titers were corrected for the positive control included on each slide. PA titers against 18 different H5 antigens were determined, in addition to a single seasonal H1 (A/NewCaledonia/20/99 [sH1N1]) and H3 (A/Wyoming/3/03 [sH3N2]) antigen, using recombinant HA1 from influenza virus VN/04, A/chicken/Jilin/9/04 (H5N1, not assigned to a clade, JI/04), A/Cambodia/R0405050/07 (H5N1, clade 1.1, CAM/07), A/duck/Hunan/795/02 (H5N1, clade 2.1.3.2, HUN/02), A/chicken/Yamaguchi/7/04 (H5N1, clade 2.5, YAM/04), IND/05, A/Anhui/1/05 (H5N1, clade 2.3.4, Anhui/05), A/Egypt/N03072/10 (H5N1, clade 2.2.1, Egypt/10), A/HongKong/156/97 (H5N1, clade 0, HK/97), A/Vietnam/HN31432M/08 (H5N1, clade 2.3.4.2, VN/08), A/Hubei/1/10 (H5N1, clade 2.3.2.1,

Hubei/10), A/chicken/Egypt/0879-NLQP/08 (H5N1, clade 2.2.1.1, Egypt/08), A/goose/Guiyang/337/06 (H5N1, clade 4, GUI/06), A/duck/Hokkaido/167/07 (H5N3, lowly pathogenic avian influenza [LPAI], H5N3/07), A/Turkey/15/06 (H5N1, clade 2.2, TUR/06), A/chicken/Vietnam/NCVD-016/08 (H5N1, clade 7, ch/VN/08), A/turkey/Germany-MV/R2472/14 (H5N8, clade 2.3.4.4, tu/H5N8/14), A/duck/NY/191255-59/02 (H5N8, LPAI, H5N8/02) (**Table 1**, **Fig. 1B**).

Phylogenetic analysis

Phylogenetic trees of influenza viruses were based on the nucleotide sequences of the HA1 domain of the influenza virus HA gene. A phylogenetic tree based on the HA1 amino acid sequence was also drawn and showed similar results (data not shown). Multiple sequence alignment was performed using the MUSCLE algorithm integrated into MEGA 6.06[457]. The phylogenetic tree was drawn according to the Maximum likelihood method using the best-fit model in MEGA 6.06. Bootstrap analyses with 1,000 re-samplings were performed to determine confidence values for groupings within the phylogenetic tree. The tree was visualized in FigTree version 1.3.1 (http://tree.bio.ed.ac.uk/software/figtree). The clade 2.3.4.4 H5N8 virus tu/H5N8/14 was not included in the analysis due to sequence unavailability.

Hemagglutination inhibition (HI) assay

Sera were thawed, treated with a receptor-destroying enzyme (cholera filtrate) overnight at 37°C followed by heat-inactivation at 56°C. Sera were initially tested for aspecific agglutination and were pre-treated with horse erythrocytes if required. Subsequently, sera were tested in a 2-fold-serial dilution in duplicate (starting dilution 1:10) following a standard protocol with 2% horse erythrocytes in PBS supplemented with 0.5% BSA and four HA units of influenza virus. Presence of HI antibodies was determined using six different IAV: VN/04, IND/05, A/Duck/Bangladesh/19097/13 (H5N1 clade 2.3.2.1, BANG/13), A/Egypt/N01753/14 (H5N1 clade 2.2.1.2, Egypt/14), A/Guangzhou/39715/14 (H5N6 clade 2.3.4.4, H5N6/14) and A/Chicken/Netherlands/EMC-3/14 (H5N8 clade 2.3.4.4, ch/H5N8/14) (**Table 1**, **Fig. 1B**). Reverse genetics viruses of the selected H5 viruses were used[348]. Egypt/14 and BANG/13 contained only the HA gene segment (without multibasic cleavage site, 7+1 viruses), other viruses also contained the NA gene segment (6+2 viruses). The remaining gene segments were obtained from influenza virus A/Puerto Rico/8/34. Sera from ferrets and New Zealand white rabbits inoculated with the homologous H5 viruses were used as positive controls.

Virus neutralization (VN) assay

Sera were tested in a VN assay, performed with the same reverse-genetic viruses used in the HI assay as described above (**Table 1**, **Fig. 1B**). VN assay was performed as described previously[453], with small adaptations. Briefly, a 2-log dilution series (starting dilution 1:5) was prepared in infection medium (Eagle's Minimum Essential Medium [EMEM, Sartorius Stedim BioWhittaker] supplemented with 20mM HEPES [Lonza BioWhittaker], 0.1% $CHNaO_3$ [Lonza BioWhittaker], and 100ug/ml penicillin, 100U/ml streptomycin and 2mM L-Glutamine [P/S/G, Lonza]) and incubated for 18h with 100 or 1000 PFU/well of the selected influenza viruses in a 1:1 ratio at 37°C. Sera from ferrets and New Zealand white rabbits inoculated with the homologous H5 viruses were used as positive controls. Subsequently, the serum-virus mixture was incubated for 1h at 37°C on a confluent monolayer of Madin-Darby canine kidney (MDCK) cells in 96-wells culture plates. Cells were washed with PBS and incubated for 2-5 days at 37°C. Influenza virus neutralization was determined by performing an HA assay on the culture supernatant to detect residual virus replication. The neutralization titer was determined as the reciprocal of the highest dilution at which the culture supernatant did not contain detectable influenza virus.

Antibody-dependent cellular cytotoxicity (ADCC) assay

A solid-phase ADCC assay was performed as described previously to measure presence of ADCC mediating antibodies[454,455]. Briefly, sera were thawed, heat-inactivated, diluted 1:160 and incubated for 2h at 37ºC on high-binding 96-well flat-bottom plates (Immunolon) coated overnight at 4ºC with 200ng/well recombinant HA protein from influenza virus VN/04 or IND/05 (made available by Protein Sciences, **Table 1, Fig. 1B**). Subsequently, plates were washed and incubated with 1 x 10^5 NK92.05-CD16 cells[456] per well in the presence of mouse-anti-human CD107a-V450 (BD Biosciences), golgistop and golgiplug (BD Biosciences) for 5h at 37°C. To identify live NK cells, staining with fixable LIVE/DEAD (Molecular Probes) and CD56-PE (BD Biosciences) was performed. After staining, cells were fixed and acquired on FACS Canto II and analyzed using DIVA software (BD Biosciences). The percentages of $CD107a^+$ (marker of degranulation) cells were determined within the respective LIVE $CD56^+$ NK cell populations[454].

IFN-ɣ ELISpot assay

HA-specific interferon (IFN)-ɣ responses were assessed in PBMC collected at week 0, 4, 8, 52 and 56 by performing an enzyme-linked immunosorbent spot (ELISpot) assay, which was performed according to the manufacturer's instructions (Mabtech). Briefly, PBMC were thawed, seeded into 96-wells U-bottom plates at 125.000 cells/well (less cells were used if not enough cells were available), and stimulated overnight with 500ng/well recombinant HA protein from influenza virus VN/04 or IND/05 (made available by Protein Sciences, **Table 1**, **Fig. 1B**). These antigen presenting cells (APC) were subsequently co-cultured with 125.000 (or an equal amount of less cells if not enough cells were available) autologous, unstimulated PBMC for 22-24h in triplicate on plates pre-coated with a monoclonal anti-IFN-ɣ antibody (Mabtech). IFN-ɣ spots were developed using a monoclonal anti-IFN-ɣ antibody, followed by 7-B6-1-biotin and streptavidin-ALP, and subsequent BCIP/NBT substrate revelation. The average number of spots per 125.000 cells cultured in triplicate was determined using a CTL immunospot reader with CTL biospot software.

Statistical analysis

HI and VN titers against different viruses (not normally distributed as tested by D'Agostino Pearson normality test) were compared by a Friedman test on paired samples. All individuals vaccinated with rMVA-H5 were analyzed as a single group, despite different dosing regimens. Different treatment groups (not normally distributed) were compared by a Kruskal-Wallis test. ADCC percentages at different time-points (not normally distributed) were compared by a Friedman test on paired samples. A comparison between rMVA-H5- and MVA-F6-vaccinated individuals was made by performing a Mann-Whitney test on samples obtained at week 0, 4 and 8. All individuals vaccinated with rMVA-H5 were regarded a single group, despite different dosing regimens. Different treatment groups (normally distributed at week 0, 4 and 8, not normally distributed at week 52, 56 and 72) were compared by a one-way ANOVA or a Kruskal-Wallis test, respectively. Numbers of IFN-ɣ producing spot-forming cells (SFC) between mock-stimulated and VN/04- or IND/05-stimulated PBMC (not normally distributed) were compared by a Friedman test on paired samples. Numbers of IFN-ɣ producing SFC at different time-points (not normally distributed) were compared by a Friedman test on paired samples. All individuals vaccinated with rMVA-H5 were regarded a single group, despite different dosing regimens. Different treatment groups (not normally distributed) were compared by a Kruskal-Wallis test.

Results

H5-specific antibodies induced by rMVA-H5 immunization showed broad reactivity

In order to assess the breadth of the antibody response induced by rMVA-H5 immunization, the profile of antibody binding to HA1 derived from 18 different H5 influenza viruses belonging to various clades (**Fig. 1A-B**) was determined by PA using sera collected at week 0, 4, 8, 52 and 56 post-immunization (p.i.). HA1 derived from sH1N1 and sH3N2 influenza viruses were included on the array as controls.

H5-specific antibodies were readily detected at week 8, especially in subjects that received two immunizations with a high dose of rMVA-H5. H5-specific antibodies were still detectable at week 52, albeit at lower titers in the recipients of the high dose rMVA-H5. Of special interest, four weeks after the booster immunization given at week 52 (week 56), H5-binding antibodies were detected in all subjects that received rMVA-H5 (**Fig. 1A**). These results correspond well to data from the original study[260], which showed that low levels of HI and VN antibodies were induced after the first and second immunization and that the booster immunization at week 52 resulted in a major increase in antibody titers. Antibody levels waned four months after the booster (week 72) in subjects that received the low vaccine dose (10^7 PFU). In contrast, high levels of H5-specific antibodies remained detectable in subjects immunized with the high dose (10^8 PFU) of rMVA-H5 (**Fig. 1A**).

Table 1. Antigens used in various assays.

Strain name	Abbreviation	Subtype	Clade	Pathogenicity	Assays
A/NewCaledonia/20/99	sH1N1	H1N1	-	seasonal	PA
A/Wyoming/3/03	sH3N2	H3N2	-	seasonal	PA
A/duck/Hokkaido/167/07	H5N3/07	H5N3	-	LPAI	PA
A/duck/NY/191255-59/02	H5N8/02	H5N8	-	LPAI	PA
A/HongKong/156/97	HK/97	H5N1	0	HPAI	PA
A/Vietnam/1194/04	VN/04	H5N1	1	HPAI	PA / HI / VN / ADCC / T cell
A/Cambodia/R0405050/07	CAM/07	H5N1	1.1	HPAI	PA
A/Indonesia/5/05	IND/05	H5N1	2.1	HPAI	PA / HI / VN / ADCC / T cell
A/duck/Hunan/795/02	HUN/02	H5N1	2.1.3.2	HPAI	PA
A/Turkey/15/06	TUR/06	H5N1	2.2	HPAI	PA
A/Egypt/N03072/10	Egypt/10	H5N1	2.2.1	HPAI	PA
A/chicken/Egypt/0879-NLQP/08	Egypt/08	H5N1	2.2.1.1	HPAI	PA
A/Egypt/N01753/14	Egypt/14	H5N1	2.2.1.2	HPAI	HI / VN
A/Hubei/1/10	Hubei/10	H5N1	2.3.2.1	HPAI	PA
A/duck/Bangladesh/19097/13	BANG/13	H5N1	2.3.2.1	HPAI	HI / VN
A/Anhui/1/05	Anhui/05	H5N1	2.3.4	HPAI	PA
A/Vietnam/HN31432M/08	VN/08	H5N1	2.3.4.2	HPAI	PA
A/turkey/Germany-MV/R2472/14	tu/H5N8/14	H5N8	2.3.4.4	HPAI	PA
A/Guangzhou/39715/14	H5N6/14	H5N6	2.3.4.4	HPAI	HI / VN
A/chicken/Netherlands/EMC-3/14	ch/H5N8/14	H5N8	2.3.4.4	HPAI	HI / VN
A/chicken/Yamaguchi/7/04	YAM/04	H5N1	2.5	HPAI	PA
A/goose/Guiyang/337/06	GUI/06	H5N1	4	HPAI	PA
A/chicken/Vietnam/NCVD-016/08	ch/VN/08	H5N1	7	HPAI	PA
A/chicken/Jilin/9/04	JI/04	H5N1	-	HPAI	PA

LPAI: low-pathogenic avian influenza virus; HPAI: highly-pathogenic avian influenza virus; PA: protein array; HI: hemagglutination inhibition; VN: virus neutralization; ADCC: antibody-dependent cellular cytotoxicity.

Interestingly, antibodies induced by rMVA-H5 did not only bind to HA1 of the homologous influenza virus strain VN/04, but also to virtually all other H5 antigens tested (**Fig. 1A**). In general, the H5 antibody binding profiles could be subdivided into two clusters. First, antibody responses against 13 H5 antigens from various clades showed a similar binding profile as the homologous VN/04 antigen. Second, weaker antibody binding to the HA1 from VN/08, tu/H5N8/14, H5N3/07 and Egypt/08 was observed (**Fig. 1A**). Of note, antibody binding to the control antigens of sH1N1 and sH3N2 viruses was similar between all groups and time-points.

Genetic relationships between the antigens used in various assays were determined by performing a phylogenetic analysis based on the HA1 domain of the influenza virus HA gene (**Fig. 1B**). Among the H5 viruses, the two LPAI clustered separately, whereas all HPAI H5 clustered together as expected to their respective clades. Interestingly, the two antigenic clusters determined by PA (**Fig. 1A**) were not necessarily defined by differences in genetic clades (**Fig. 1B**). Collectively, antibody responses induced by rMVA-H5 immunization showed strong cross-reactivity with the HA of H5 influenza viruses from antigenically and genetically diverse clades.

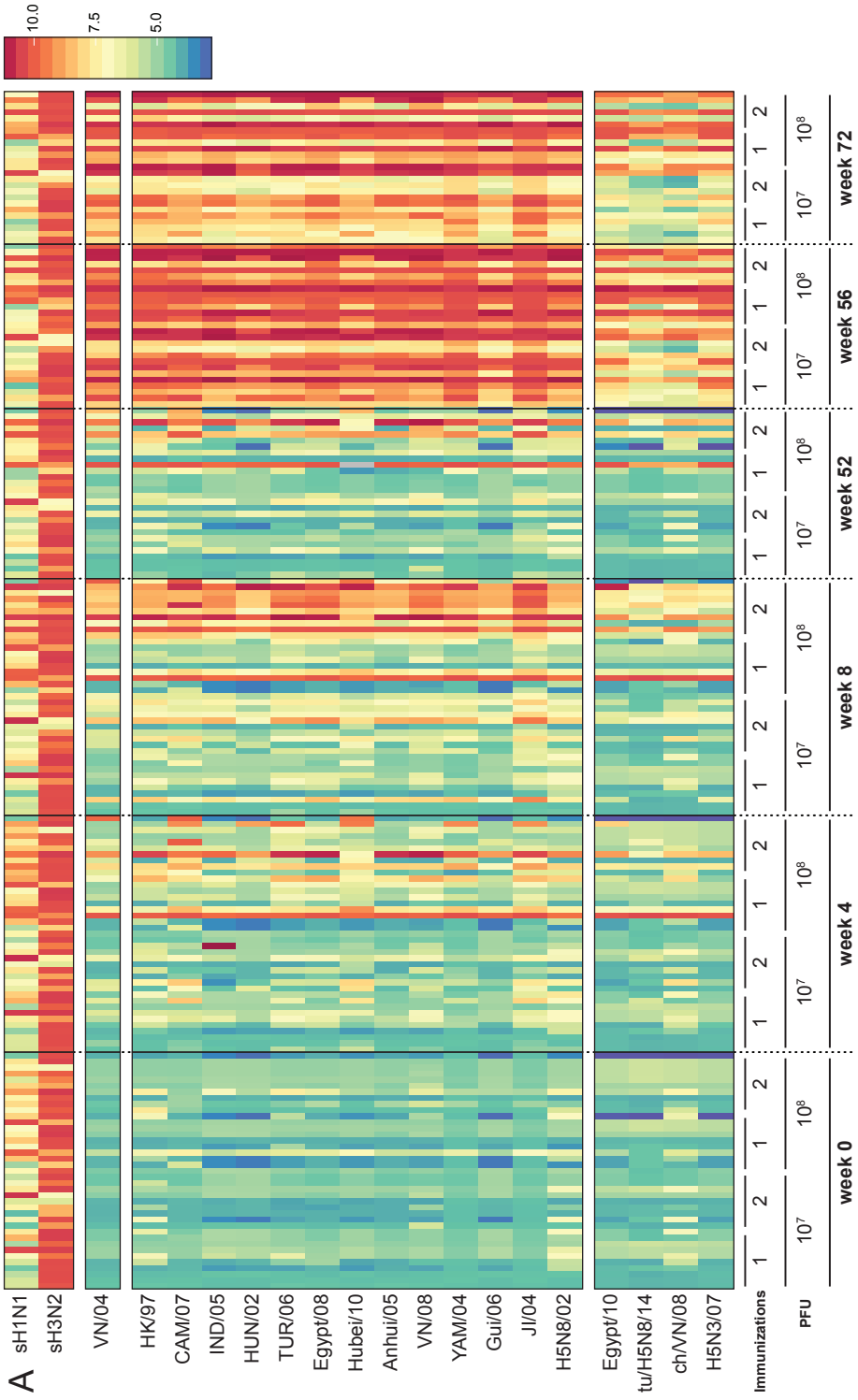
A
sH1N1
sH3N2
VN/04
HK/97
CAM/07
IND/05
HUN/02
TUR/06
Egypt/08
Hubei/10
Anhui/05
VN/08
YAM/04
Gui/06
JI/04
H5N8/02
Egypt/10
tu/H5N8/14
ch/VN/08
H5N3/07
10.0
7.5
5.0
Immunizations
PFU
week 0
week 4
week 8
week 52
week 56
week 72

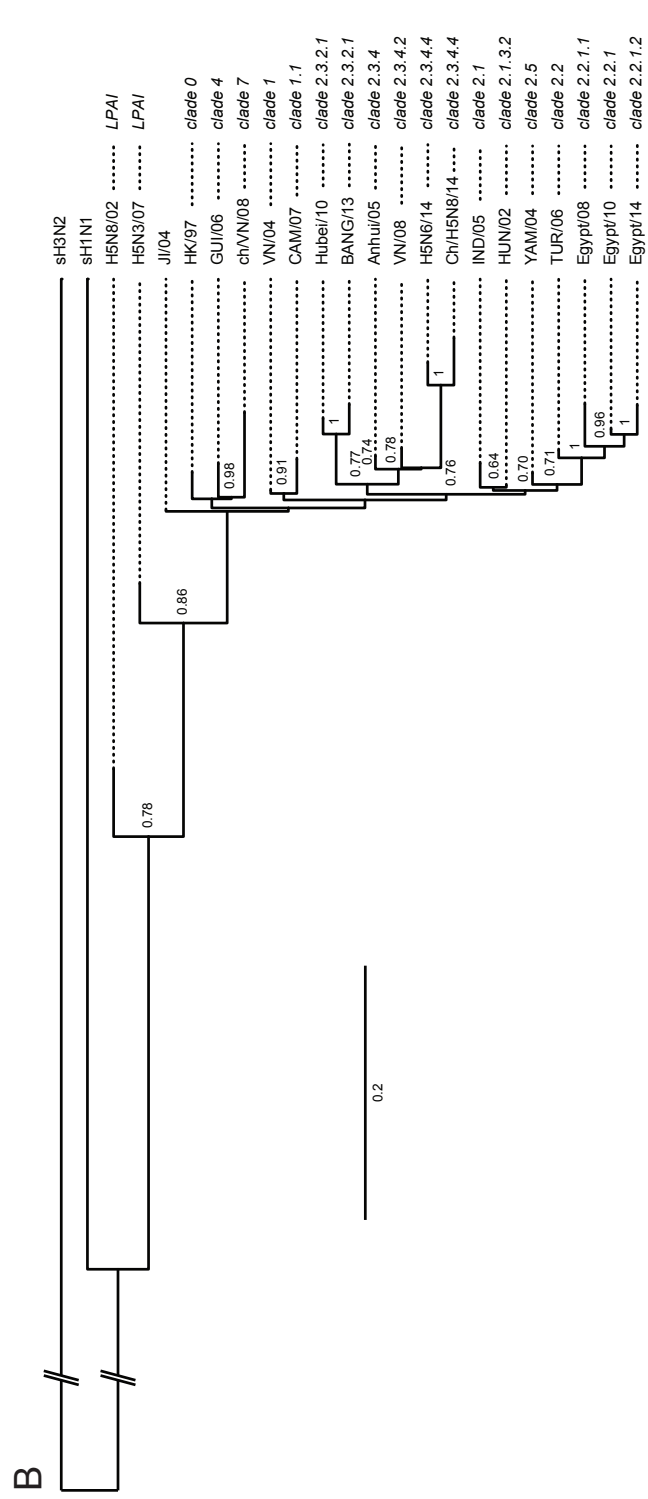

Figure 1. rMVA-H5 induced a broadly-reactive antibody response profile. *(**A**) PA titers in sera obtained at week 0, 4, 8, 52, 56 and 72 were determined against HA1 from 18 antigenically distinct H5 influenza viruses. The seasonal influenza viruses sH1N1 and sH3N2 were included as a control. Each vertical line represents an individual serum sample. The scale indicates 2-log transformed PA titers. (**B**) Phylogenetic tree of influenza virus antigens used in this study based on the HA1 domain of the HA gene. The maximum-likelihood tree was constructed using the best-fit model (HKY+G) in MEGA 6.06 and visualized in FigTree version 1.3.1 (http://tree.bio.ed.ac.uk/software/figtree). Bootstrap values were calculated from 1,000 replicates; only values >0.6 are shown. Scale bars indicate nucleotide substitutions per site.*

rMVA-H5 induced cross-reactive VN antibodies against H5N1, H5N6 and H5N8 influenza viruses

To test rMVA-H5-induced cross-reactive antibodies, sera collected at week 56 post-primary immunization (containing the highest level of H5-specific antibodies to the homologous virus) were used in HI (**Fig. 2A**) and VN (**Fig. 2B**) assays. Antibody reactivity with the homologous strain VN/04 and the heterologous strains IND/05 and ch/H5N8/14 was tested previously[260,261] and was confirmed in the present study. In addition, the activity against Egypt/14 and BANG/13, which are among the H5N1 vaccine strains selected by the WHO, and H5N6/14 (recently causing human infections) was tested.

HI antibodies specific for the homologous VN/04 virus were detected, which displayed considerable cross-reactivity with two other H5N1 viruses: IND/05 (clade 2.1) and Egypt/14 (clade 2.2.1.2). Cross-reactivity with the viruses BANG/13 (clade 2.3.2.1), ch/H5N8/14 and H5N6/14 (both clade 2.3.4.4) was also observed, but only to a limited extent (**Fig. 2A**, significantly lower titers than VN/04: $p<0.0001$). Although statistical significant differences between treatment groups were not observed, study subjects that received a high dose immunization prior to the booster immunization at week 52, displayed the highest HI antibody titers.

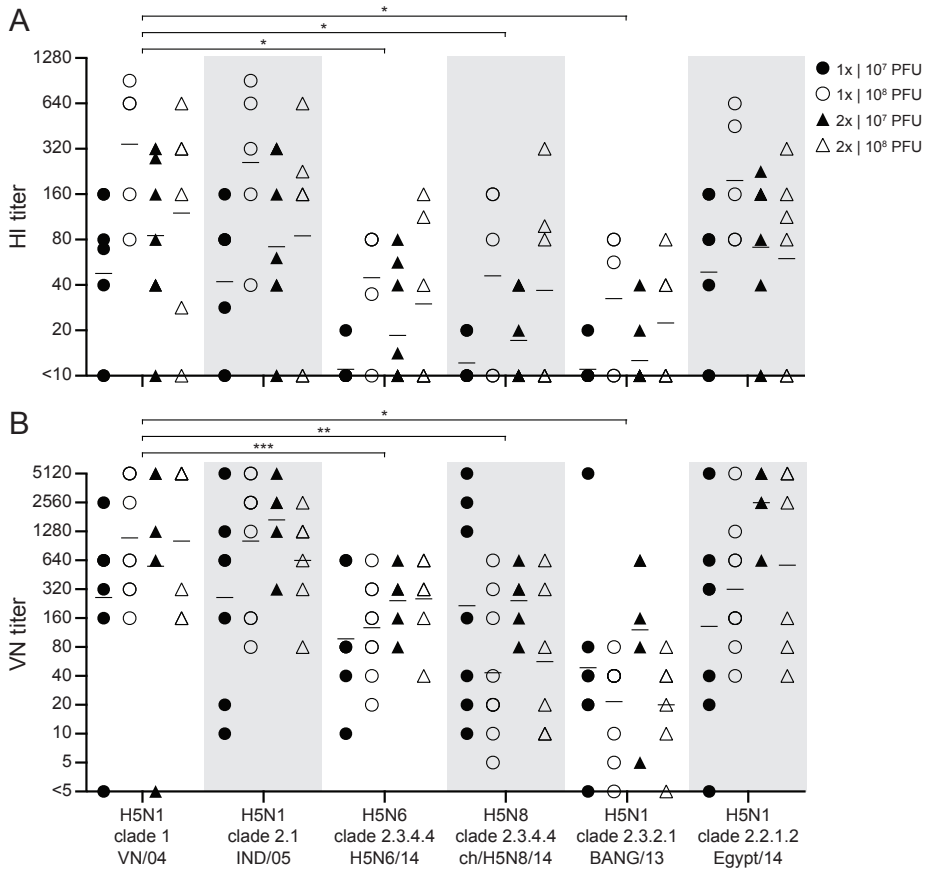

◄ ***Figure 2. rMVA-H5 induced HI and VN antibodies reactive with homologous and antigenically distinct H5 viruses.*** *Sera obtained four weeks after the booster immunization (week 56) were tested for the presence of HI (**A**) and VN (**B**) antibodies reactive with the homologous VN/04 and five antigenically distinct H5 viruses. (**A**) Reciprocal HI titers obtained by a 2-fold serum dilution series. Sera without HI activity or HI titer of 10 were set at a titer of <10. * p<0.0001 compared to reference virus VN/04. (**B**) Reciprocal VN titers obtained by a 2-fold serum dilution series, incubated with 100 or 1000 PFU of influenza virus. Sera without VN activity were set at a titer of <5. * p<0.0001, ** p=0.0002 and *** p=0.0031 when different viruses were compared with reference VN/04. The symbols indicate the different treatment groups (1 or 2 immunizations, 10^7 or 10^8 PFU); geometric mean titers are displayed as bars.*

Next, the week 56 sera were tested for VN activity against the same six influenza viruses (**Fig. 2B**). Although the titers observed in VN were higher than HI titers in general, similar findings were obtained. Serum antibodies efficiently neutralized the homologous VN/04 virus and cross-neutralized the clade 2.1, 2.2.1.2, 2.3.2.1 and 2.3.4.4 viruses. As observed in HI, higher cross-neutralizing antibody titers were observed against IND/05 and Egypt/14 compared to BANG/13, ch/H5N8/14 and H5N6/14 (**Fig. 2B**, significantly lower titers than VN/04: p=0.031, p=0.0002 and p<0.0001 respectively). Again, statistical significant differences between treatment groups were not observed. Taken together, serum antibodies induced by immunization with rMVA-H5 are broadly-reactive and display cross-neutralizing capacity.

rMVA-H5 immunization induced ADCC-mediating antibodies

Sera obtained at the respective time-points p.i. were tested for the presence of antibodies that mediate ADCC. ADCC activity was never observed using negative control sera obtained from MVA-F6 immunized individuals at week 0, 4 and 8 (p<0.0001, **Fig. 3A-B**). A single immunization with rMVA-H5 induced a significant raise in ADCC activity against HA of the homologous strain VN/04 (**Fig. 3A**). The level of ADCC-mediating antibodies was maintained until week 8, but was not further boosted by a second immunization. Subsequently, the level of ADCC-mediating antibodies waned at week 52, although the level of ADCC-mediating antibodies at this time-point was still significantly higher compared to week 0. Four weeks after the booster immunization (week 56), the ADCC activity substantially increased and showed limited waning over the following 4 months (week 72, **Fig. 3A**).

The ADCC-mediating antibody responses were comparable between the vaccine groups, regardless of the dose and number of rMVA-H5 immunizations the subjects received. Notably, cross-reactive ADCC-mediating antibodies were observed with the HA of the clade 2.1 influenza virus IND/05 in a similar pattern, although the percentages of activated $CD107a^+$ NK cells were somewhat lower (**Fig. 3B**). The ADCC activity to HAs of VN/04 and IND/05 correlated significantly, which confirmed the cross-reactivity of the ADCC antibody response (**Fig. 3C**, linear regression r^2=0.7584).

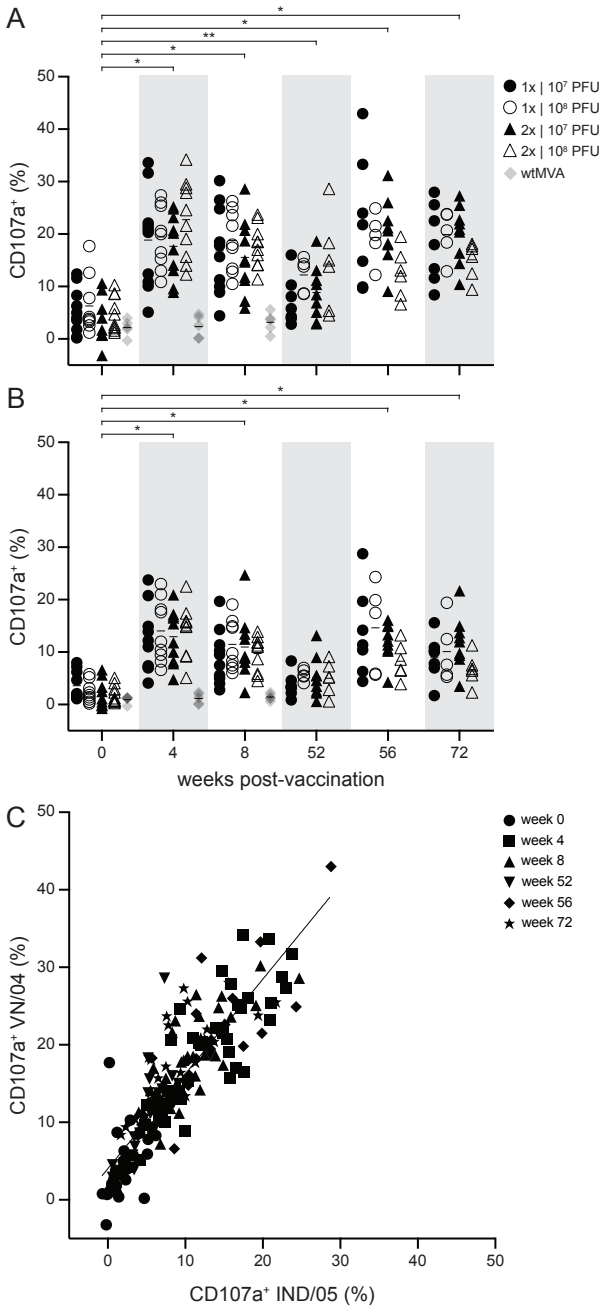

Figure 3. Presence of ADCC-mediating antibodies reactive with homologous and an antigenically distinct H5N1 virus. *(**A-B**) Presence of ADCC-mediating antibodies expressed as percentage of degranulating NK cells at a set serum dilution. Sera obtained at the indicated time-points were tested against VN/04 (**A**) and IND/05 (**B**). * p<0.0001 and ** p=0.0342 (compared with reference week 0). Symbols indicate the different treatment groups; geometric mean titer is displayed as bars. (**C**) Correlation between ADCC-mediating antibodies specific for VN/04 and IND/05. Symbols indicate the different time-points. Linear regression r^2=0.7584.*

rMVA-H5 immunization induced HA-specific T cell responses

In order to assess induction of HA-specific T cell responses at the respective time-points p.i., PBMC were stimulated with full-length HA derived from influenza viruses VN/04 or IND/05. HA-specific T cells were detected in an IFN-ɣ ELISpot assay. As expected, H5-specific T cells were not detected in any of the samples after mock stimulation (**Fig. 4A**) or prior to immunization with rMVA-H5, with the exception of one subject (**Fig. 4B-C**). Four weeks after the first immunization, T cells specific for HA derived from the strain used in the vaccine (VN/04) were detected, particularly in the study subjects that received a high dose of rMVA-H5, although this increase was not statistically significant (**Fig. 4B**). The number of HA-specific T cells did not increase after a second immunization (week 8), and only limited cross-reactivity with the HA of the heterologous strain IND/05 was observed at week 4 and 8 (**Fig. 4B-C**). Interestingly, significantly higher numbers of T cells specific for HA of strain VN/04 or IND/05 were detected prior to the booster immunization at week 52, when compared to week 0 or mock stimulation. Subsequently, after the booster immunization, the number of H5-specific T cells further increased and substantial cross-reactivity was observed with the HA of the strain IND/05 (**Fig. 4B-C**). At all time-points, with the exception of week 0, T cells stimulated with VN/04 or IND/05 had significantly higher numbers of IFN-ɣ SFC compared to mock-stimulated cells. Similar to the rMVA-H5-induced antibody responses, at week 52 and 56 a trend towards stronger T cell responses in study subjects that received the high dose of rMVA-H5 was detected (**Fig. 4B-C**).

Discussion

In this study, we performed a comprehensive immunological analysis on blood samples obtained during a phase 1/2a clinical trial[260] with a (pre-)pandemic H5 vaccine candidate based on the replication-deficient viral vector MVA. Immunization of healthy young adults with rMVA-H5 induced cross-reactive antibodies that not only bound to HA corresponding to the vaccine strain, but also to virtually any other antigenically distinct HA. The vaccine-induced antibodies cross-neutralized recently circulating H5N1 viruses, as well as the recently emerged clade 2.3.4.4 HPAI viruses of the H5N8 (as described previously by de Vries *et al*.[261]) and H5N6 subtypes. Furthermore, ADCC-mediating antibodies reactive with the homologous virus and an H5N1 virus from an antigenically distinct clade were induced by rMVA-H5 immunization. In addition to humoral responses, rMVA-H5 efficiently induced (cross-reactive) cellular responses, as both clade 1 and 2.1 H5-specific T cells were detected in PBMC of vaccine recipients.

Although avian H5 viruses do not spread efficiently from human-to-human, viruses of the H5N1 and the H5N6 subtype regularly infect humans and cause severe morbidity and mortality[382,383]. A limited number of mutations have been identified that potentially allow these viruses to become transmissible by air from human-to-human[19,21]. These mutations can accumulate upon passage in mammalian species and some have already been identified in viruses circulating in birds[21]. The threat of a potential pandemic caused by influenza viruses of the H5 subtype emphasizes the need for the development of effective (pre-)pandemic vaccines. Conventional inactivated H5N1 vaccines are poorly immunogenic and repeated vaccinations,

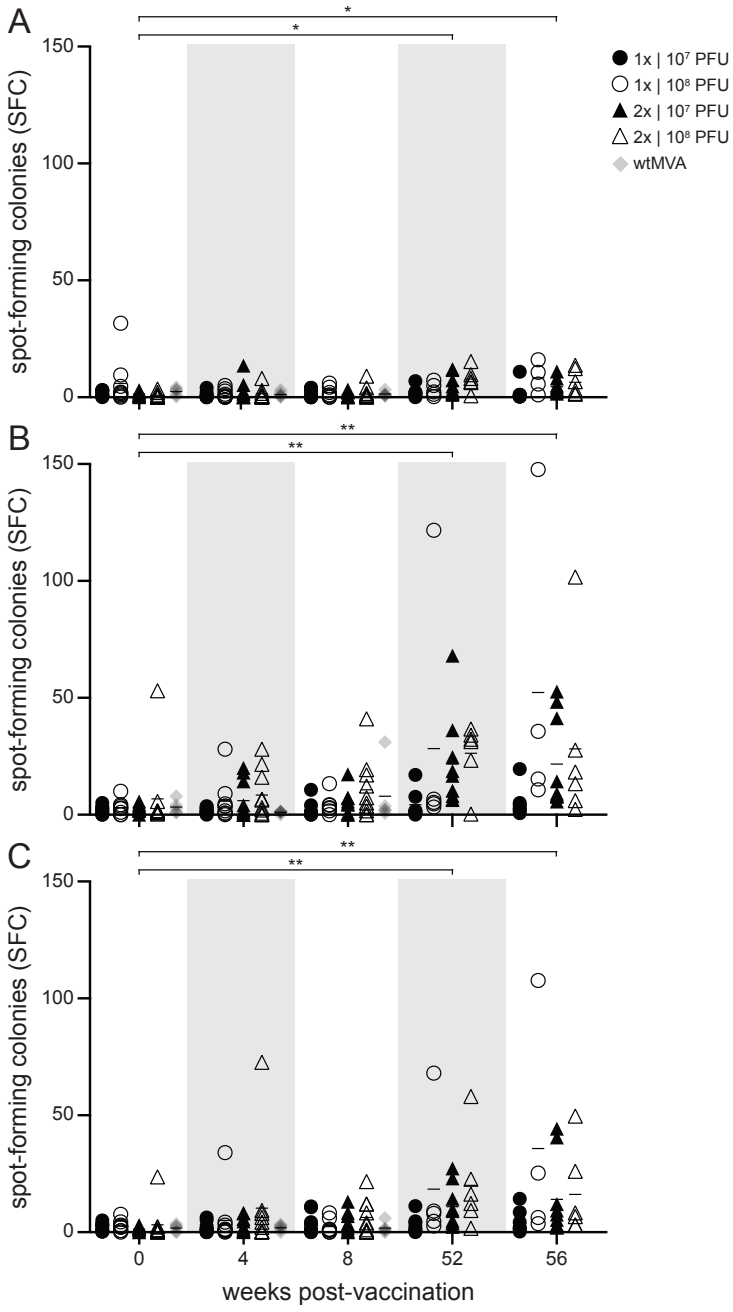

Figure 4. rMVA-H5 induced HA-specific T-cell responses specific for homologous and an antigenically distinct H5 virus*. Presence of HA-specific T-cells in PBMC obtained at the indicated time-points was tested by IFN-γ ELISpot assay. PBMC mock-treated (**A**), or stimulated with purified HA protein from VN/04 (**B**) or IND/05 (**C**). Results are shown as number of spot-forming cells (SFC) per 125.000 PBMC. * p<0.05 and ** p<0.0005. The symbols indicate the different treatment groups; mean SFC count is displayed as bars.*

relatively high doses or the use of adjuvants are required to induce protective antibody levels[450,458]. Furthermore, antibody responses induced by conventional vaccines often display limited cross-clade reactivity. Since H5 viruses have evolved into various (sub)clades, which are antigenically diverse[451], novel vaccines that induce broadly-reactive immunity are highly desirable. Although a direct comparison between conventional H5 vaccines and rMVA-H5 was not performed, we show that the (pre-)pandemic vector-based vaccine candidate rMVA-H5 fulfills these needs through efficient induction of cross-reactive immune responses against two or more strains of influenza virus.

Broad reactivity of antibody responses induced by rMVA-H5 was initially demonstrated by PA. This technique is valuable, since it allows the detection of antibody responses against a large panel of antigens in a high-throughput fashion with minute amounts of serum, however there are some limitations. First, predominantly HA-head-specific antibodies were detected, since only the HA1 subunit was used for coating the slides. Because the HA-stalk is relatively conserved, and antigenic diversification of H5 is mainly based on mutations in proximity of the receptor binding site (RBS) of the HA-head domain, stalk-specific antibodies could significantly contribute to broadly-reactive immune responses. Nevertheless, the induction of cross-(sub)clade antibodies recognizing the HA-head of the homologous vaccine strain (clade 1) and of viruses belonging to clade 0, 1.1, 2.1, 2.1.3.2, 2.2, 2.2.1, 2.2.1.1, 2.3.2.1, 2.3.4, 2.3.4.2, 2.3.4.4, 2.5, 4 and 7 was detected by PA assay. The reactivity detected in PA did not necessarily reflect specific genetic H5 clades, indicating that there is a clear distinction between antigenic and genetic differences.

The second limitation of the PA assay is that it exclusively measures binding of antibodies to HA1 and does not measure functional activity. Therefore, functional activity of rMVA-H5-induced antibodies was confirmed by HI and VN assays performed with a selection of viruses. For conventional inactivated influenza vaccines, a HI titer of 40 or higher is considered to provide protection *in vivo*[459]. In this study, induction of neutralizing antibodies against the homologous VN/04 and the heterologous IND/05 and ch/H5N8/14 viruses by rMVA-H5 immunization was observed, as was described previously[260,261]. In addition, cross-neutralization against the recently emerged H5N6 virus and two H5N1 vaccine strains selected by the WHO was observed in this study. Collectively, these data demonstrate that rMVA-H5 immunization induces antibodies that are capable of neutralizing recently emerged HPAI viruses of the H5N1, H5N6 and H5N8 subtypes.

Antibodies directed to antigenic sites in proximity of the RBS have the capacity to neutralize influenza viruses. In addition to neutralization, virus-specific antibodies of particularly the IgG1 and IgG3 subclass can have other modes of action[460]. After binding to antigens displayed on virus-infected cells with the Fragment Antigen Binding (Fab)-domain, the Fragment crystallisable (Fc)-domain of antibodies can engage Fc-receptors on host effector cells, leading to killing of virus-infected cells through a mechanism known as ADCC[44,45]. The ADCC response against influenza virus is mainly mediated by the interaction between the Fc region of virus-specific antibodies and Fcγ-receptor IIIα (FcγRIIIα, CD16), present on NK cells. It was

recently shown that particularly antibodies specific for the HA-stalk are capable of mediating ADCC[455,461-463]. Since the HA-stalk is conserved among different subtypes of influenza viruses, ADCC-mediating antibodies may contribute to broadly protective immunity[168,386,464]. A single immunization with rMVA-H5 already induced ADCC-mediating antibodies reactive with the homologous and a heterologous H5N1 influenza virus. Antibodies waned over a year after the primary immunization, but were readily boosted upon re-immunization. Thus, in addition to induction of broadly-reactive neutralizing antibodies recognizing the HA-head, rMVA-H5 induced broadly-reactive ADCC-mediating antibodies, most likely directed to the stalk region of HA.

In addition to antibody responses, rMVA-H5 immunization induced T cell responses specific for the homologous VN/04 and a heterologous IND/05 influenza virus. H5-specific T cell responses were predominantly detected directly prior to and after the booster immunization one year after the initial immunization and particularly in subjects that received two prior immunizations (week 0 & 4) and/or a vaccine dose of 10^8 PFU.

A potential limitation of the use of influenza vaccines based on MVA (or other vectors) in humans is interference by pre-existing vector-specific immunity. In this study, subjects were young adults that had not been previously exposed to MVA or any other orthopoxvirus. However, a proportion of the adult human population does have immunity against the vector due to smallpox vaccination campaigns that were carried out until the mid 1970s[320]. Furthermore, pre-existing vector immunity can be induced by repeated MVA-based vaccinations[260]. Whether pre-existing immunity interferes with the immunogenicity and effectivity of MVA vaccination is not yet fully understood, however, antibodies induced by vaccination against smallpox did not have the capacity to neutralize MVA *in vitro* (Altenburg *et al*., submitted). In the present study, we showed that rMVA-H5 immunization elicits strong anamnestic HA-specific antibody and T cell responses upon a second or third immunization, despite the induction of anti-vector immunity by the first (and second) immunization[260].

In summary, we showed that rMVA-H5 efficiently induced humoral and cellular immune responses in humans that display remarkable cross-reactivity with H5 viruses of various clades. One or two immunizations with rMVA-H5 at a four-week interval induced moderate immune responses, but primed individuals showed potent cross-reactive H5-specific antibody and T cell responses upon booster immunization administered after one year. Therefore, priming of immunologically naive individuals by pre-pandemic immunization with rMVA-H5 and subsequent boosting after the emergence of a pandemic H5 virus seems an attractive approach in the face of a pandemic outbreak with these viruses.

Chapter 5
Summarizing discussion

Partially based on:
AF Altenburg *et al*. Modified Vaccinia virus Ankara (MVA) as production platform for vaccines against influenza and other viral respiratory diseases. *Viruses, 2014; 6(7): 2735-2761.*

Influenza viruses continuously circulate in the human population and are estimated to cause 3-5 million cases of severe respiratory illness annually worldwide of which 250.000-500.000 have a fatal outcome[7]. Vaccination is the most efficient measure to control infectious diseases, however, vaccination against influenza viruses is complicated by their antigenic variability. Current seasonal influenza vaccines are comprised of components from influenza A(H1N1), A(H3N2) and B viruses that are expected to circulate in the next influenza season. These seasonal vaccines aim at the induction of virus neutralizing antibodies against HA and are efficient in providing protective immunity against antigenically similar influenza viruses. However, they afford little or no protection from infection with antigenically distinct seasonal or pandemic influenza viruses. In order to induce broadly protective immunity against multiple and antigenically distinct influenza viruses, novel vaccine targets and antigen delivery systems are investigated. Furthermore, novel techniques are under development to facilitate production of large quantities of vaccine doses in a short period of time. The vaccine vector MVA expressing one or multiple influenza virus antigens could potentially provide in these needs.

In this thesis, the development and use of rMVA-based influenza vaccines was addressed. Even though MVA has been tested extensively in various animal models and has been administered to >100.000 human volunteers, a few key questions regarding the MVA vaccine vector remained to be answered. To that end, the studies described in chapter 2 elucidated the *in vivo* cell tropism of MVA-based vaccines and assessed the potential risk of interference with rMVA-based vaccination by orthopoxvirus-specific pre-existing immunity. Furthermore, novel rMVA-based influenza vaccine candidates were developed and evaluated by pre-clinical and clinical testing in chapters 3 and 4.

***In vivo* tropism of MVA**

Previously, several studies have been performed to assess MVA tropism *in vitro* and in mice, however, these studies mainly focussed on elucidating the tissue tropism[231,291-293]. In chapter 2.1 these results were confirmed in the mouse model. In addition, the cellular tropism of MVA in ferrets – the animal model most commonly used for influenza virus replication, pathogenesis and transmission studies – and in macaques, representative for humans, was described. The most common route of administration of rMVA in pre-clinical studies and clinical trials is IM injection, however, respiratory vaccination is under consideration for the optimal induction of local tissue resident immune responses against respiratory pathogens. Therefore, tropism of MVA *in vivo* after IM injection was compared to that after administration to the respiratory tract. Using rMVA expressing a fluorescent reporter protein (rMVA-GFP), low-frequency MVA-infected cells could be sensitively detected.

In mice, ferrets and macaques, local myocytes or epithelial cells at the site of inoculation (the hind leg muscle or respiratory tract, respectively) were infected by MVA. However, the contribution of these cell types to the total MVA-infected population was limited. In mice and macaques, MVA was predominantly detected in macrophages and DCs, regardless of the administration route used. Myeloid cells were also infected by MVA in ferrets, however, further phenotyping of the MVA-

infected cells was difficult due to the lack of ferret-specific antibodies. In all tested animal models, MVA-positive cells were detected in the LN draining the inoculation site as soon as 6 hours after administration, which suggests direct infection of APC rather than uptake of remains of MVA-infected apoptotic cells. This indicates that MVA-infected cells are directly involved in the shaping of the immune response, which can be regarded as a beneficial feature for a vaccine vector.

Only slight differences in MVA tropism were detected between the different animal models. After respiratory tract administration of rMVA-GFP in mice, alveolar macrophages were the dominant MVA-positive cell type opposed to DCs in macaques. Of note, alveolar macrophages are considered to be inefficient antigen presenting cells compared to DCs[306,307]. Nonetheless, rMVA-based vaccines have been shown to efficiently induce antigen-specific immune responses in all tested animal models[209].

Since similar cell types were infected by MVA in the various animal models, it can reasonably be assumed that myeloid cells are also targeted by MVA in humans. Indeed, using human PBMC *in vitro,* MVA was shown to predominantly infect DCs, monocytes and B cells[291] (chapter 2.1). Even though it seems beneficial to infect DCs, since these cells are directly involved in the shaping of the immune response, direct infection does not necessarily lead to improved vaccine immunogenicity, which was previously shown for an adenovirus vector in mice and non-human primates[300]. Nevertheless, the data obtained in this study potentially explain the excellent immunogenicity of MVA-based vaccines.

The effect of pre-existing vaccine vector-specific immunity on rMVA-based vaccination

Another key question that remained unanswered in current MVA literature was the effect of pre-existing orthopoxvirus-specific immunity on immunogenicity and efficacy of rMVA-based vaccines. There is concern that immunity against MVA, induced either during historic smallpox vaccination campaigns or by multiple rMVA-based vaccinations, may have negative effects on the performance of rMVA-based vaccines. In order to address this issue, the effect of presence of pre-existing immunity to MVA, VACV or influenza virus on immunogenicity and efficacy of rMVA-based influenza vaccines was assessed (chapter 2.2). In mice, pre-existing MVA-specific immune responses negatively affected the antigen-specific antibody response induced by rMVA-based vaccination, but only under suboptimal conditions, e.g. when a lower vaccine dose was used. Furthermore, induction of an antigen-specific T cell response was severely hampered by the presence of orthopoxvirus-specific immunity induced by either MVA or VACV. Importantly, mice vaccinated with an rMVA-based vaccine expressing HA homologous to the A(H5N1) influenza virus used for challenge infection were completely protected from disease, regardless of the presence of pre-existing vector-specific immunity. In contrast, mice previously exposed to MVA or VACV and subsequently vaccinated with rMVA-based vaccines expressing the heterologous HA gene from A(H1N1) or A(H3N2) lost more body weight and showed higher viral loads in the lungs after the challenge infection compared to mice without pre-existing vector-specific immunity. This corresponds

to the prevention of induction of HA-specific cross-reactive immune responses by the respective MVA-based vaccines in the presence of pre-existing vector-specific immunity. Collectively, the results showed that under specific conditions pre-existing orthopoxvirus-specific immunity could negatively influence rMVA-based vaccine immunogenicity in mice, but the protective efficacy of an rMVA-HA-based vaccine against a homologous influenza virus remained unaffected.

Strikingly, negative effects on rMVA-induced antigen-specific cellular and humoral immune responses were detected in the presence of pre-existing immunity induced by MVA, whereas pre-exposure to VACV only influenced subsequent induction of antigen-specific T cell responses. At least two exposures to MVA and/or VACV were required to induce MVA-specific neutralizing antibodies, which could indicate why interference with induction of antigen-specific antibody responses was only observed in mice previously exposed to MVA (primed twice) but not VACV (primed only once). The detrimental effect of pre-existing orthopoxvirus-specific immunity on the induction of antigen-specific T cell responses is therefore likely caused by non-neutralizing immune responses, since this was also observed in mice primed with a single VACV exposure. Further studies, e.g. adoptive transfer studies, are required to obtain a thorough understanding of the mechanisms underlying the interference of pre-existing orthopoxvirus-specific immunity on rMVA-based vaccine immunogenicity.

It is important to note that in this mouse study a 'worst-case scenario' was investigated as the interval between induction of pre-existing immunity and vaccination was only four weeks. Obviously, this deviates from the human situation were the last VACV vaccinations were administered over 40 years ago and antibody responses are likely to have waned over time. However, VACV-specific antibody responses could still be detected in serum of VACV vaccinated individuals born in 1970 and 1971, shortly before the smallpox vaccination campaigns were discontinued. Importantly, these antibody responses cross-reacted with MVA only to a limited extent and were not able to neutralize MVA *in vitro* in a plaque reduction assay. Indeed, an rMVA-based vaccine inducing antigen-specific T cell responses was still immunogenic in people born before 1962, which is before smallpox vaccination campaigns were discontinued[271]. Of note, in this study the number of study subjects was limited, the immune status against MVA or VACV was not validated and no proper control group was included. Nonetheless, these results indicate that pre-existing orthopoxvirus-specific immunity induced by historic smallpox vaccination campaigns does not substantially interfere with rMVA-based vaccination in humans.

The interference of pre-existing orthopoxvirus-specific immunity is likely to be more relevant in the context of repeated rMVA-based vaccination, in which a four-week interval between vaccinations is frequently used[234,260,335]. Human study subjects that were exposed to rMVA repeatedly (up to 3x) in clinical trials showed a boost of MVA-specific immunity induced by every vaccination[234,260,327] (chapter 2.2). However, the rMVA-based vaccine still remained immunogenic, even after a third vaccination administered one year after the initial rMVA-based vaccination[260].

Taken together, the results from the study described in chapter 2.2 suggest that the concern of pre-existing immunity affecting rMVA-based vaccine immunogenicity is valid, but only under specific circumstances. Further studies are warranted to address if the specific conditions described in this study in which pre-existing orthopoxvirus-specific immunity can interfere with subsequent rMVA-based vaccination are similar between mice and humans. To circumvent or overcome potential negative effects of pre-existing vaccine vector-specific immunity, several strategies could be adopted. First, a booster vaccination with a high dose of an rMVA-based vaccine was shown to overcome observed negative effects on the antibody response after a single vaccination[268] (chapter 2.2). Second, administration of the rMVA-based vaccine to different sites, e.g. IM injection followed by respiratory tract administration, could circumvent local vector-specific immunity[333]. It was shown in non-human primates that rMVA can be nebulized and administered to the respiratory tract (chapter 2.1) to induce local immunity against respiratory pathogens, thereby preventing the use of needles[305]. Third, rMVA-based vaccines could be used in heterologous prime-boost regimens, for example in combination with DNA or recombinant adenovirus-based vaccines[325], thereby preventing a boost of the vector-specific immune responses. Finally, in order to assure optimal induction of antigen-specific immune responses using rMVA-based vaccines, it seems important to take into account the immune status of a vaccine recipient, the vaccine dose used and the main correlate of protection to be induced by rMVA-based vaccination.

Immunogenicity of protein- and rMVA-based influenza vaccines

For decades, inactivated protein-based influenza vaccines have been used to reduce influenza virus-related morbidity and mortality through the induction of HA-specific neutralizing antibodies[131]. In chapter 3, the immunogenicity of protein- and rMVA-based influenza vaccines was compared in mice using NP (target of virus-specific T cells, chapter 3.2) or HA (major target of virus neutralizing antibodies, chapter 3.3) as vaccine antigens. In both studies, unadjuvanted protein-based vaccines were poorly immunogenic, but the addition of Matrix-M™ adjuvant potentiated the immune response substantially and allowed significant antigen dose sparing. Compared to the protein-based vaccines, rMVA-based influenza vaccines were more immunogenic as they induced stronger functional immune responses (NP-specific $CD8^+$ T cells or HA-specific HI antibodies) than either unadjuvanted or adjuvanted protein-based vaccines. The enhanced immunogenicity of rMVA-based vaccines can be explained by *de novo* antigen synthesis. Subsequently, NP is endogenously processed and presented on MHC class I to induce $CD8^+$ T cell responses. Furthermore, expression of large quantities of HA in its native conformation on the surface of rMVA-infected cells contributes to the induction of potent HA-specific antibody responses. In addition to the antigen delivery route, the lack of many immune evasion and suppression proteins in MVA compared to the parental VACV allows for recruitment and activation of (innate) immune cells by the vector backbone, which contributes to vaccine immunogenicity. These results underline the advantages of using MVA-based vaccines compared to protein-based vaccines for the induction of potent antigen-specific humoral and cellular immune responses.

It is generally assumed that addition of an adjuvant to rMVA-based vaccines (or any vector-based vaccine) is not required because the vector backbone itself potently induces innate immune responses and directly infects APC involved in the shaping of the immune response. Indeed, the recruitment, proliferation and/or activation of immune cells in the LN draining the site of vaccine injection was enhanced after vaccination with an rMVA-based influenza vaccine expressing HA (rMVA-HA) compared to a protein-based HA vaccine (chapter 3.3). Of special interest, the immunogenicity of the rMVA-HA vaccine could be improved by adding Matrix-M™ adjuvant to the vaccine preparation. Co-formulation with Matrix-M™ adjuvant resulted in enhanced total cell counts in the draining LN and monocytes, including the $CD169^{+}$ medullary sinus macrophages, in particular. The medullary sinus macrophages are known to phagocytose antigens and viruses in the lymphatic system, and have been shown to be an important effector mechanism of saponin-based adjuvants[437,439,465]. Along with the total cell count, also the number of activated DC, B cells, T cells, monocytes and NK cells was enhanced after injection of Matrix-M™ adjuvanted vaccines. Interestingly, no differences between Matrix-M™ adjuvanted protein- and rMVA-based vaccines were observed in the recruitment, proliferation and/or activation of immune cells in the draining LN. However, rMVA-HA co-formulated with Matrix-M™ adjuvant induced stronger functional immune responses than HA protein with Matrix-M™. This indicates that Matrix-M™ adjuvant potentiated the immune response, but the quality of the response is still dependent on the antigen delivery system.

The results in chapter 3.3 describe the effects of adding Matrix-M™ adjuvant to a high dose of rMVA-HA vaccine. It was not addressed in this study if Matrix-M™ adjuvant allows rMVA-HA dose sparing, as was described for protein-based vaccines. This would be of particular interest in the context of an influenza virus pandemic where a large number of vaccine doses need to be available in a short period of time. Furthermore, in chapter 2.2 it was demonstrated in mice that a high dose of the rMVA-H5 vaccine is required to overcome negative effects induced by MVA-specific pre-existing immunity observed after the first vaccination with a low dose of rMVA-H5. Hypothetically, a lower dose of rMVA-HA vaccine can be used to overcome this pre-existing vector immunity barrier if Matrix-M™ adjuvant is added to the vaccine formulation. In addition to antigen dose sparing, it would be interesting to address if the observed increase in immunogenicity of rMVA-HA, expressing HA from an A(H1N1) influenza virus, co-formulated with Matrix-M™ adjuvant broadens the immune response induced by vaccination to protect from a lethal challenge with, for example, a heterologous A(H5N1) influenza virus.

Pre-clinical and clinical assessment of novel rMVA-based influenza vaccines

Different approaches are under investigation to improve currently used influenza vaccines. These include the use of novel vaccine platforms allowing faster production, novel antigen delivery systems, more conserved vaccine antigens, activation of non-neutralizing antibodies or T cell responses to confer protective immunity or various combinations of these approaches.

Currently used inactivated influenza vaccines inefficiently induce $CD8^+$ T cell responses[136]. However, the main targets of $CD8^+$ T cell responses during an influenza virus infection, including NP and M1, are relatively conserved. Therefore, these T cell responses have the capacity to provide protection against different influenza virus subtypes. Indeed, $CD8^+$ and $CD4^+$ T cells have been shown to contribute to heterologous protection in humans during the 2009 A(H1N1) influenza virus pandemic[82,108]. It is important to note that for efficient induction of T cell responses, an infection needs to be established because endogenous protein synthesis is required. Thus, vaccines that exclusively induce cellular immunity do not afford sterile immunity, but their use can reduce the extent of viral shedding, severity and/or duration of the disease. Therefore, when aiming for broadly protective immune responses, it is important to include a vaccine component designed for efficient induction of cross-reactive $CD8^+$ T cell responses.

rMVA vector-based vaccines allow for efficient induction of antigen-specific T cells by driving *de novo* synthesis of the antigen of interest, followed by processing via the endogenous route of antigen presentation. One of the crucial steps in antigen presentation to $CD8^+$ T cells is processing of antigens by the proteasome in order to release peptides from proteins, which subsequently are transported from the cytosol to the endoplasmic reticulum to be loaded onto MHC class I molecules. By increasing protein degradation, potentially more peptides are available for presentation to $CD8^+$ T cells, which could lead to better T cell activation. In order to test this hypothesis, three different modifications were made to NP that was expressed from rMVA (chapter 3.1 & 3.2). Two modifications (deletion of the nuclear localization signal [NLS] and fusion of NP to the proteasome signalling molecule ubiquitin) resulted in increased protein degradation and showed enhanced activation of a $CD8^+$ T cell clone *in vitro*. Beneficial effects of enhanced protein degradation were only observed *in vitro* under suboptimal conditions*, i.e.* when a low avidity T cell clone was used or APC were infected at a low multiplicity of infection (MOI). However, vaccination with rMVA expressing one of the modified NP proteins did not improve the NP-specific $CD8^+$ T cell response *in vivo* and did not result in enhanced protection from a homologous influenza virus challenge infection in either C57BL/6 or BALB/c mice. This suggests that wild-type NP is already optimally processed and presented *in vivo*, therefore, the modifications did not have any added effect. However, NP is known as a highly immunogenic protein. Potentially, less immunogenic proteins, such as M1 and the polymerase subunits, could benefit from increased protein degradation.

Contrary to the hypothesis tested in chapter 3.1 and 3.2, it has been hypothesized in literature that for activation of antigen-specific $CD8^+$ T cell responses the delivery of stable proteins might be more advantageous compared to antigens that were designed for rapid intracellular degradation[363,364,466]. Stable antigens would allow for more cross-presentation because the protein is still present by the time the infected and apoptotic cell is engulfed by a professional APC[467]. It is debatable if this would apply to rMVA-based vaccines because APC are directly infected (chapter 2.1), therefore, the contribution of cross-priming might be limited.

In addition to evaluation of rMVA-NP vaccines in mice, the human immune response induced by vaccination with an rMVA-based vaccine expressing HA from influenza virus A/Vietnam/1194/04 (H5N1, rMVA-H5) was assessed (chapter 4). Previously, it was shown that HA-specific antibody responses induced by rMVA-H5 displayed HI and VN activity, and cross-reacted with antigenically different A(H5N1) and A(H5N8) influenza viruses[260,261]. The results in chapter 4 describe vaccine-induced antibodies that cross-react with all tested A(H5N1), A(H5N3), A(H5N6) and A(H5N8) influenza viruses in protein microarray. Functional antibodies reactive with multiple A(H5N1), A(H5N6) and A(H5N8) viruses were detected by HI and/or VN assay. In addition, efficient induction of ADCC-mediating antibodies and T cells was observed after rMVA-H5 vaccination. Different vaccination regimens, including a high (10^8 PFU) and low (10^7 PFU) dose rMVA-H5, and a single and two vaccinations at a four-week interval were evaluated. Two vaccinations with a high dose rMVA-H5 seemed to most efficiently induce (broadly reactive) immune responses, although no clear differences between the various vaccination regimens could be detected after a booster vaccination after one year. Taken together, the results showed that rMVA-H5 efficiently induces broadly reactive immune responses against antigenically distinct A(H5Nx) influenza viruses.

The human immune responses induced by rMVA-H5 vaccination will most likely protect from disease after infection with the homologous and even a heterologous A(H5Nx) virus, as was demonstrated in a non-human primate model[258,259]. However, considering the large and ever-increasing diversity in HA within the H5 influenza virus subtype, the full extent of cross-protection against A(H5N1) influenza viruses is unclear. Heterologous prime-boost regimens may be required to improve the breadth of the virus-specific antibody response. For example, vaccination with rMVA expressing the HA gene from A/Vietnam/1194/04 could be followed by vaccination against an influenza virus from an antigenically distinct clade, which would boost antibody responses against conserved epitopes. Nevertheless, the results obtained in this study confirm that the rMVA-H5 vaccine candidate holds promise in the face of a potential pandemic outbreak with an H5 influenza virus or even as a pre-pandemic vaccine in pandemic preparedness plans.

Practical and regulatory issues regarding the use of rMVA-based influenza vaccines

The continuing advances in genetic engineering, process development and large-scale manufacturing have brought rMVA-based vaccines into clinical trials at an increasing scale[249,250,468,469]. However, there are some hurdles to overcome in the development of novel rMVA-based influenza vaccines, particularly in the context of a pandemic. First, there are practical issues regarding the timely development of suitable animal models for newly emerging respiratory infections. Second, for each new vaccine antigen potency and purity assays need to be developed for the appropriate quality assessment of rMVA vaccine preparations. Although all the hands-on development work can be performed rapidly, non-clinical safety testing, e.g. toxicity studies and ethics approval for animal experiments and clinical trials, always depends on external parties, which could substantially slow down vaccine development.

In addition to practical issues, there are regulatory issues that need to be addressed regarding the registration of an rMVA-based vaccine. Thus far, only one guideline for the quality and (non-)clinical aspects of live recombinant viral vectors exists[470]. However, to date no rMVA-based has been approved for human use. For novel influenza vaccines, special procedures are in place in the European Union to speed up the authorization process. First, using the 'mock-up procedure' a proof-of-principle vaccine is registered using a prototype influenza virus. Once the viral strain that is causing a pandemic is identified, this can be included in the mock-up dossier and approved rapidly to develop a tailor-made vaccine. Second, the 'emergency procedure' allows for fast-track approval (within 70 days) of a vaccine during a pandemic. Currently, rMVA and other vector-based vaccines are not covered by these pandemic influenza vaccine registration procedures. This complicates approval of rMVA-based vaccines as each rMVA virus is regarded as a new biological entity. Furthermore, combination vaccination strategies, e.g. priming with an adenovirus vector and boosting with an rMVA-based vaccine, will lead to complicated regulatory procedures because two distinct biological entities need to be approved. Thus, there is a need for the development of 'mock-up procedures' for vector-based vaccines that allow for fast-track development and approval. Defining MVA tropism *in vivo* in non-human primates, with high relevance for the use of MVA in humans (as described in chapter 2.1), provides essential knowledge for the eventual approval of rMVA-based vaccines.

Universal influenza vaccines

Considering the extensive antigenic variation of influenza viruses there clearly is the need for the development of a 'universal influenza vaccine': a single vaccine that protects against all influenza A virus subtypes. However, development of an influenza vaccine that protects against all HA group 1 or group 2 influenza viruses would already be a major advancement. For that matter, even broad protection within a single subtype, e.g. A(H1N1), induced by a single vaccine would be an improvement over the currently used influenza vaccines. A few promising new vaccine antigens and delivery systems that allow for broadly reactive immune responses are currently under development and have advanced to clinical trials. Thus, on a relatively short term, possibly within the next decade, substantial advances towards the development of 'next-generation' influenza vaccines can be made.

Induction of broadly protective immunity against antigenically distinct influenza viruses, whether within a subtype or across subtypes, most likely requires a multifaceted approach. First, a novel influenza vaccine should still contain an HA component that induces neutralizing antibodies, even if they only afford protection against a narrow antigenic range of influenza viruses. The HA component can be combined with an antigen that induces cross-reactive non-neutralizing antibodies and/or T cells, which confer protective immunity in the event of an HA antigenic mismatch. In this case, sterile immunity and full protection might not be conferred, however, disease duration and severity can be substantially reduced. At the population level this results in reduced spread of the virus due to reduced viral loads and duration of shedding.

For the evaluation of novel influenza vaccines that induce correlates of protection other than virus neutralizing antibodies there are some hurdles to overcome. The currently used vaccines are designed to induce strain-specific antibodies against the head-domain of HA for which correlates of protection have been defined: an HI (a good proxy for VN) antibody titre of 40 or higher is considered to provide protection *in vivo*[459]. Even though this value may not always correlate with protection[471], it is the best available guide to predict and compare vaccine efficacy. In contrast, standardized immunological assays for detection and quantification of virus-specific non-neutralizing antibodies and/or T cells are lacking. It is important to invest in the development of these assays and defining cut-off values for protection to predict the efficacy of novel vaccine candidates.

Concluding remarks

The variable nature of influenza A virus complicates development of effective influenza vaccines. MVA holds promise as a vaccine platform in the context of an emerging influenza virus pandemic because rMVA can be rapidly constructed and produced. Furthermore, the vector is of considerable interest for the development of broadly protective influenza vaccines since foreign antigens can be expressed in their native conformation and will be properly processed and presented to the immune system. This allows for induction of humoral and cellular responses that induce solid pathogen-specific immunity. The excellent immunogenicity of rMVA-based vaccines can partially be explained by direct infection of APC and can further be improved by the use of an adjuvant. However, there are some hurdles to overcome regarding the use of rMVA-based vaccines. First, in mice, pre-existing immunity to the vector induced by previous exposure to MVA, and to a lesser extent VACV, can hamper the induction of antigen-specific immunity by rMVA vaccination under specific conditions. However, the impact of pre-existing immunity on the outcome of rMVA-based vaccination is limited compared to other vaccine vectors such as replication competent VACV or adenovirus[212,213,322]. The relevance of the in chapter 2.2 defined conditions where pre-existing orthopoxvirus-specific immunity interferes with rMVA-based vaccination needs to be addressed in humans to be able to predict the effectiveness of rMVA-based vaccines. Second, there are some practical and regulatory issues that need to be addressed to allow rapid approval for the use of rMVA-based vaccines, particularly if the MVA vector vaccine platform is to be used in the face of an emerging influenza virus pandemic outbreak. Finally, there are currently no standardized assays and defined cut-off values to predict if heterosubtypic immunity, conferred by for example cross-reactive ADCC-mediating antibodies or $CD8^+$ T cells, actually protect from infection. Taken together, although there are issues that need to be addressed before rMVA-based vaccines can be used in humans, the vector platform holds considerable promise as a (pre-)pandemic or 'universal' influenza vaccine.

Chapter 6

References

1 Shaw, M. L. *et al. Orthomyxoviridae*. *Fields Virology* **1**, 6th edn, 1151-1185 (Lippincott Williams & Wilkins, 2013).
2 International Committee on Taxonomy of Viruses. Virus Taxonomy: The Classification and Nomenclature of Viruses. The Online (10th) Report of the ICTV. https://talk.ictvonline.org/ictv-reports/ictv_online_report/ Accessed: 19-8-2017. (2017).
3 Webster, R. G. *et al. Textbook of Influenza*. 2nd edn, (John Wiley & Sons, Ltd, 2013).
4 Wright, P. *et al.* Orthomyxoviruses. *Fields Virology* **1**, 6th edn, 1186-1243 (Lippincott Williams & Wilkins, 2013).
5 Tong, S. *et al.* A distinct lineage of influenza A virus from bats. *Proc. Natl. Acad. Sci. U. S. A.* **109**, 4269-4274, doi:10.1073/pnas.1116200109 (2012).
6 Tong, S. *et al.* New world bats harbor diverse influenza A viruses. *PLoS Pathog.* **9**, e1003657, doi:10.1371/journal.ppat.1003657 (2013).
7 World Health Organization. Fact sheet - Influenza (seasonal). http://www.who.int/mediacentre/factsheets/fs211/en/ Accessed: 16-06-2017. (2016).
8 Moeller, A. *et al.* Organization of the influenza virus replication machinery. *Science* **338**, 1631-1634, doi:10.1126/science.1227270 (2012).
9 Chen, W. *et al.* A novel influenza A virus mitochondrial protein that induces cell death. *Nat. Med.* **7**, 1306-1312, doi:10.1038/nm1201-1306 (2001).
10 Wise, H. M. *et al.* A complicated message: Identification of a novel PB1-related protein translated from influenza A virus segment 2 mRNA. *J. Virol.* **83**, 8021-8031, doi:10.1128/JVI.00826-09 (2009).
11 Shinya, K. *et al.* Avian flu: influenza virus receptors in the human airway. *Nature* **440**, 435-436, doi:10.1038/440435a (2006).
12 Yamada, S. *et al.* Haemagglutinin mutations responsible for the binding of H5N1 influenza A viruses to human-type receptors. *Nature* **444**, 378-382, doi:10.1038/nature05264 (2006).
13 Helenius, A. Unpacking the incoming influenza virus. *Cell* **69**, 577-578 (1992).
14 Ulmanen, I. *et al.* Role of two of the influenza virus core P proteins in recognizing cap 1 structures (m7GpppNm) on RNAs and in initiating viral RNA transcription. *Proc. Natl. Acad. Sci. U. S. A.* **78**, 7355-7359 (1981).
15 Te Velthuis, A. J. *et al.* Influenza virus RNA polymerase: insights into the mechanisms of viral RNA synthesis. *Nat. Rev. Microbiol.* **14**, 479-493, doi:10.1038/nrmicro.2016.87 (2016).
16 Pritlove, D. C. *et al.* Polyadenylation of influenza virus mRNA transcribed in vitro from model virion RNA templates: requirement for 5' conserved sequences. *J. Virol.* **72**, 1280-1286 (1998).
17 Koel, B. F. *et al.* Substitutions near the receptor binding site determine major antigenic change during influenza virus evolution. *Science* **342**, 976-979, doi:10.1126/science.1244730 (2013).
18 Westgeest, K. B. *et al.* Genetic evolution of the neuraminidase of influenza A (H3N2) viruses from 1968 to 2009 and its correspondence to haemagglutinin evolution. *J. Gen. Virol.* **93**, 1996-2007, doi:10.1099/vir.0.043059-0 (2012).
19 Herfst, S. *et al.* Airborne transmission of influenza A/H5N1 virus between ferrets. *Science* **336**, 1534-1541, doi:10.1126/science.1213362 (2012).
20 Imai, M. *et al.* Transmission of influenza A/H5N1 viruses in mammals. *Virus Res.* **178**, 15-20, doi:10.1016/j.virusres.2013.07.017 (2013).
21 Linster, M. *et al.* Identification, characterization, and natural selection of mutations driving airborne transmission of A/H5N1 virus. *Cell* **157**, 329-339, doi:10.1016/j.cell.2014.02.040 (2014).
22 Russell, C. A. *et al.* The potential for respiratory droplet-transmissible A/H5N1 influenza virus to evolve in a mammalian host. *Science* **336**, 1541-1547, doi:10.1126/science.1222526 (2012).
23 Yang, Z. F. *et al.* Human Infection with a Novel Avian Influenza A(H5N6) Virus. *N. Engl. J. Med.* **373**, 487-489, doi:10.1056/NEJMc1502983 (2015).
24 Yuan, J. *et al.* Origin and molecular characteristics of a novel 2013 avian influenza A(H6N1) virus causing human infection in Taiwan. *Clin. Infect. Dis.* **57**, 1367-1368, doi:10.1093/cid/cit479 (2013).
25 Tweed, S. A. *et al.* Human illness from avian influenza H7N3, British Columbia. *Emerg. Infect. Dis.* **10**, 2196-2199, doi:10.3201/eid1012.040961 (2004).
26 Fouchier, R. A. *et al.* Avian influenza A virus (H7N7) associated with human conjunctivitis and a fatal case of acute respiratory distress syndrome. *Proc. Natl. Acad. Sci. U. S. A.* **101**, 1356-1361, doi:10.1073/pnas.0308352100 (2004).
27 World Health Organization. Influenza at the human-animal interface. (2017).
28 Butt, K. M. *et al.* Human infection with an avian H9N2 influenza A virus in Hong Kong in 2003. *J. Clin. Microbiol.* **43**, 5760-5767, doi:10.1128/JCM.43.11.5760-5767.2005 (2005).

29 Chen, H. *et al.* Clinical and epidemiological characteristics of a fatal case of avian influenza A H10N8 virus infection: a descriptive study. *Lancet* **383**, 714-721, doi:10.1016/S0140-6736(14)60111-2 (2014).
30 Bouvier, N. M. *et al.* Animal Models for Influenza Virus Pathogenesis and Transmission. *Viruses* **2**, 1530-1563, doi:10.3390/v20801530 (2010).
31 Kindt, T. J. *et al.* in *Kuby Immunology* Ch. 3, 52-75 (W.H. Freeman and company, 2007).
32 Iwasaki, A. *et al.* Innate Responses to Viral Infections. *Fields Virology* **1**, 6th edn, 190-213 (Lippincott Williams & Wilkins, 2013).
33 Iwasaki, A. *et al.* Innate immunity to influenza virus infection. *Nat. Rev. Immunol.* **14**, 315-328, doi:10.1038/nri3665 (2014).
34 Jayasekera, J. P. *et al.* Natural antibody and complement mediate neutralization of influenza virus in the absence of prior immunity. *J. Virol.* **81**, 3487-3494, doi:10.1128/JVI.02128-06 (2007).
35 O'Brien, K. B. *et al.* A protective role for complement C3 protein during pandemic 2009 H1N1 and H5N1 influenza A virus infection. *PLoS One* **6**, e17377, doi:10.1371/journal.pone.0017377 (2011).
36 Kindt, T. J. *et al.* in *Kuby Immunology* Ch. 7, 168-188 (W.H. Freeman and company, 2007).
37 Kindt, T. J. *et al.* in *Kuby Immunology* Ch. 14, 351-370 (W.H. Freeman and company, 2007).
38 Braciale, T. J. *et al.* Adaptive Immune Response to Viral Infections. *Fields Virology* **1**, 6th edn, 213-250 (Lippincott Williams & Wilkins, 2013).
39 Zhang, J. *et al.* Influenza A virus M1 blocks the classical complement pathway through interacting with C1qA. *J. Gen. Virol.* **90**, 2751-2758, doi:10.1099/vir.0.014316-0 (2009).
40 Kindt, T. J. *et al.* in *Kuby Immunology* Ch. 11, 271-301 (W.H. Freeman and company, 2007).
41 Ana-Sosa-Batiz, F. *et al.* Influenza-Specific Antibody-Dependent Phagocytosis. *PLoS One* **11**, e0154461, doi:10.1371/journal.pone.0154461 (2016).
42 Terajima, M. *et al.* Complement-dependent lysis of influenza a virus-infected cells by broadly cross-reactive human monoclonal antibodies. *J. Virol.* **85**, 13463-13467, doi:10.1128/JVI.05193-11 (2011).
43 El Bakkouri, K. *et al.* Universal vaccine based on ectodomain of matrix protein 2 of influenza A: Fc receptors and alveolar macrophages mediate protection. *J. Immunol.* **186**, 1022-1031, doi:10.4049/jimmunol.0902147 (2011).
44 Jegaskanda, S. *et al.* Age-associated cross-reactive antibody-dependent cellular cytotoxicity toward 2009 pandemic influenza A virus subtype H1N1. *J. Infect. Dis.* **208**, 1051-1061, doi:10.1093/infdis/jit294 (2013).
45 DiLillo, D. J. *et al.* Broadly neutralizing hemagglutinin stalk-specific antibodies require FcgammaR interactions for protection against influenza virus in vivo. *Nat. Med.* **20**, 143-151, doi:10.1038/nm.3443 (2014).
46 Marcelin, G. *et al.* Contribution of antibody production against neuraminidase to the protection afforded by influenza vaccines. *Rev. Med. Virol.* **22**, 267-279, doi:10.1002/rmv.1713 (2012).
47 Couch, R. B. Challenge studies. *Dev. Biol. (Basel)* **115**, 119-121 (2003).
48 Smith, D. J. *et al.* Mapping the antigenic and genetic evolution of influenza virus. *Science* **305**, 371-376, doi:10.1126/science.1097211 (2004).
49 Skehel, J. J. *et al.* A carbohydrate side chain on hemagglutinins of Hong Kong influenza viruses inhibits recognition by a monoclonal antibody. *Proc. Natl. Acad. Sci. U. S. A.* **81**, 1779-1783 (1984).
50 Wei, C. J. *et al.* Cross-neutralization of 1918 and 2009 influenza viruses: role of glycans in viral evolution and vaccine design. *Sci. Transl. Med.* **2**, 24ra21, doi:10.1126/scitranslmed.3000799 (2010).
51 Medina, R. A. *et al.* Glycosylations in the globular head of the hemagglutinin protein modulate the virulence and antigenic properties of the H1N1 influenza viruses. *Sci. Transl. Med.* **5**, 187ra170, doi:10.1126/scitranslmed.3005996 (2013).
52 He, B. *et al.* Putative suppressing effect of IgG Fc-conjugated haemagglutinin (HA) stalk of influenza virus H7N9 on the neutralizing immunogenicity of Fc-conjugated HA head: implication for rational design of HA-based influenza vaccines. *J. Gen. Virol.* **97**, 327-333, doi:10.1099/jgv.0.000365 (2016).
53 Jameson, J. *et al.* Human CD8+ and CD4+ T lymphocyte memory to influenza A viruses of swine and avian species. *J. Immunol.* **162**, 7578-7583 (1999).
54 Kreijtz, J. H. *et al.* Primary influenza A virus infection induces cross-protective immunity against a lethal infection with a heterosubtypic virus strain in mice. *Vaccine* **25**, 612-620, doi:10.1016/j.vaccine.2006.08.036 (2007).

55 Kreijtz, J. H. *et al.* Cross-recognition of avian H5N1 influenza virus by human cytotoxic T-lymphocyte populations directed to human influenza A virus. *J. Virol.* **82**, 5161-5166, doi:10.1128/JVI.02694-07 (2008).

56 Hillaire, M. L. *et al.* Human T-cells directed to seasonal influenza A virus cross-react with 2009 pandemic influenza A (H1N1) and swine-origin triple-reassortant H3N2 influenza viruses. *J. Gen. Virol.* **94**, 583-592, doi:10.1099/vir.0.048652-0 (2013).

57 van de Sandt, C. E. *et al.* Human cytotoxic T lymphocytes directed to seasonal influenza A viruses cross-react with the newly emerging H7N9 virus. *J. Virol.* **88**, 1684-1693, doi:10.1128/jvi.02843-13 (2014).

58 Hewitt, E. W. The MHC class I antigen presentation pathway: strategies for viral immune evasion. *Immunology* **110**, 163-169 (2003).

59 Roche, P. A. *et al.* The ins and outs of MHC class II-mediated antigen processing and presentation. *Nat. Rev. Immunol.* **15**, 203-216, doi:10.1038/nri3818 (2015).

60 Jung, S. *et al.* In vivo depletion of CD11c+ dendritic cells abrogates priming of CD8+ T cells by exogenous cell-associated antigens. *Immunity* **17**, 211-220 (2002).

61 Joffre, O. P. *et al.* Cross-presentation by dendritic cells. *Nat. Rev. Immunol.* **12**, 557-569, doi:10.1038/nri3254 (2012).

62 GeurtsvanKessel, C. H. *et al.* Clearance of influenza virus from the lung depends on migratory langerin+CD11b- but not plasmacytoid dendritic cells. *J. Exp. Med.* **205**, 1621-1634, doi:10.1084/jem.20071365 (2008).

63 Kim, T. S. *et al.* Respiratory dendritic cell subsets differ in their capacity to support the induction of virus-specific cytotoxic CD8+ T cell responses. *PLoS One* **4**, e4204, doi:10.1371/journal.pone.0004204 (2009).

64 Kim, T. S. *et al.* Distinct Dendritic Cell Subsets Dictate the Fate Decision between Effector and Memory CD8(+) T Cell Differentiation by a CD24-Dependent Mechanism. *Immunity* **40**, 400-413, doi:10.1016/j.immuni.2014.02.004 (2014).

65 Lanzavecchia, A. *et al.* Dynamics of T lymphocyte responses: intermediates, effectors, and memory cells. *Science* **290**, 92-97 (2000).

66 Hillaire, M. L. *et al.* Clearance of influenza virus infections by T cells: risk of collateral damage? *Curr. Opin. Virol.* **3**, 430-437, doi:10.1016/j.coviro.2013.05.002 (2013).

67 Voeten, J. T. *et al.* Antigenic drift in the influenza A virus (H3N2) nucleoprotein and escape from recognition by cytotoxic T lymphocytes. *J. Virol.* **74**, 6800-6807 (2000).

68 Boon, A. C. *et al.* Sequence variation in a newly identified HLA-B35-restricted epitope in the influenza A virus nucleoprotein associated with escape from cytotoxic T lymphocytes. *J. Virol.* **76**, 2567-2572 (2002).

69 Berkhoff, E. G. *et al.* A mutation in the HLA-B*2705-restricted NP383-391 epitope affects the human influenza A virus-specific cytotoxic T-lymphocyte response in vitro. *J. Virol.* **78**, 5216-5222 (2004).

70 Berkhoff, E. G. *et al.* The loss of immunodominant epitopes affects interferon-gamma production and lytic activity of the human influenza virus-specific cytotoxic T lymphocyte response in vitro. *Clin. Exp. Immunol.* **148**, 296-306, doi:10.1111/j.1365-2249.2007.03340.x (2007).

71 Berkhoff, E. G. *et al.* Functional constraints of influenza A virus epitopes limit escape from cytotoxic T lymphocytes. *J. Virol.* **79**, 11239-11246, doi:10.1128/JVI.79.17.11239-11246.2005 (2005).

72 McMichael, A. J. *et al.* Cytotoxic T-cell immunity to influenza. *N. Engl. J. Med.* **309**, 13-17, doi:10.1056/nejm198307073090103 (1983).

73 Yewdell, J. W. *et al.* Influenza A virus nucleoprotein is a major target antigen for cross-reactive anti-influenza A virus cytotoxic T lymphocytes. *Proc. Natl. Acad. Sci. U. S. A.* **82**, 1785-1789 (1985).

74 McMichael, A. J. *et al.* Recognition of influenza A virus nucleoprotein by human cytotoxic T lymphocytes. *J. Gen. Virol.* **67 (Pt 4)**, 719-726 (1986).

75 Gotch, F. *et al.* Identification of viral molecules recognized by influenza-specific human cytotoxic T lymphocytes. *J. Exp. Med.* **165**, 408-416 (1987).

76 Bender, B. S. *et al.* Transgenic mice lacking class I major histocompatibility complex-restricted T cells have delayed viral clearance and increased mortality after influenza virus challenge. *J. Exp. Med.* **175**, 1143-1145 (1992).

77 Eichelberger, M. *et al.* Clearance of influenza virus respiratory infection in mice lacking class I major histocompatibility complex-restricted CD8+ T cells. *J. Exp. Med.* **174**, 875-880 (1991).

78 Scherle, P. A. *et al.* Mice can recover from pulmonary influenza virus infection in the absence of class I-restricted cytotoxic T cells. *J. Immunol.* **148**, 212-217 (1992).

79 Epstein, S. L. *et al.* (beta)-Microglobulin-deficient mice can be protected against influenza A infection by vaccination with vaccinia-influenza recombinants expressing hemagglutinin and neuraminidase. *J. Immunol.* **150**, 5484-5493 (1993).

80 Graham, M. B. *et al.* Resistance to and recovery from lethal influenza virus infection in B lymphocyte-deficient mice. *J. Exp. Med.* **186**, 2063-2068, doi:10.1084/jem.186.12.2063 (1997).

81 Hamada, H. *et al.* Multiple redundant effector mechanisms of CD8+ T cells protect against influenza infection. *J. Immunol.* **190**, 296-306, doi:10.4049/jimmunol.1200571 (2013).

82 Sridhar, S. *et al.* Cellular immune correlates of protection against symptomatic pandemic influenza. *Nat. Med.* **19**, 1305-1312, doi:10.1038/nm.3350 (2013).

83 Yewdell, J. W. *et al.* Immunodominance in major histocompatibility complex class I-restricted T lymphocyte responses. *Annu. Rev. Immunol.* **17**, 51-88, doi:10.1146/annurev.immunol.17.1.51 (1999).

84 Cukalac, T. *et al.* The Influenza Virus-Specific CTL Immunodominance Hierarchy in Mice Is Determined by the Relative Frequency of High-Avidity T Cells. *J. Immunol.*, doi:10.4049/jimmunol.1301403 (2014).

85 Topham, D. J. *et al.* CD8+ T cells clear influenza virus by perforin or Fas-dependent processes. *J. Immunol.* **159**, 5197-5200 (1997).

86 Klein, J. R. *et al.* Cytotoxic T lymphocytes produce immune interferon in response to antigen or mitogen. *J. Exp. Med.* **155**, 1198-1203 (1982).

87 Catalfamo, M. *et al.* Human CD8+ T cells store RANTES in a unique secretory compartment and release it rapidly after TcR stimulation. *Immunity* **20**, 219-230 (2004).

88 Xu, L. *et al.* Cutting edge: pulmonary immunopathology mediated by antigen-specific expression of TNF-alpha by antiviral CD8+ T cells. *J. Immunol.* **173**, 721-725 (2004).

89 Zhao, M. Q. *et al.* Alveolar epithelial cell chemokine expression triggered by antigen-specific cytolytic CD8(+) T cell recognition. *J. Clin. Invest.* **106**, R49-58, doi:10.1172/JCI9786 (2000).

90 Cerwenka, A. *et al.* Migration kinetics and final destination of type 1 and type 2 CD8 effector cells predict protection against pulmonary virus infection. *J. Exp. Med.* **189**, 423-434 (1999).

91 Hamada, H. *et al.* Tc17, a unique subset of CD8 T cells that can protect against lethal influenza challenge. *J. Immunol.* **182**, 3469-3481, doi:10.4049/jimmunol.0801814 (2009).

92 Price, G. E. *et al.* Perforin and Fas cytolytic pathways coordinately shape the selection and diversity of CD8+-T-cell escape variants of influenza virus. *J. Virol.* **79**, 8545-8559, doi:10.1128/jvi.79.13.8545-8559.2005 (2005).

93 Marois, I. *et al.* Initial infectious dose dictates the innate, adaptive, and memory responses to influenza in the respiratory tract. *J. Leukocyte Biol.* **92**, 107-121, doi:10.1189/jlb.1011490 (2012).

94 Hogan, R. J. *et al.* Activated antigen-specific CD8+ T cells persist in the lungs following recovery from respiratory virus infections. *J. Immunol.* **166**, 1813-1822 (2001).

95 De Bree, G. J. *et al.* Selective accumulation of differentiated CD8+ T cells specific for respiratory viruses in the human lung. *J. Exp. Med.* **202**, 1433-1442, doi:10.1084/jem.20051365 (2005).

96 Zammit, D. J. *et al.* Residual antigen presentation after influenza virus infection affects CD8 T cell activation and migration. *Immunity* **24**, 439-449, doi:10.1016/j.immuni.2006.01.015 (2006).

97 Piet, B. *et al.* CD8+ T cells with an intraepithelial phenotype upregulate cytotoxic function upon influenza infection in human lung. *J. Clin. Invest.* **121**, 2254-2263, doi:10.1172/jci44675 (2011).

98 Wu, T. *et al.* Lung-resident memory CD8 T cells (TRM) are indispensable for optimal cross-protection against pulmonary virus infection. *J. Leukoc. Biol.* **95**, 215-224, doi:10.1189/jlb.0313180 (2014).

99 Ray, S. J. *et al.* The collagen binding alpha1beta1 integrin VLA-1 regulates CD8 T cell-mediated immune protection against heterologous influenza infection. *Immunity* **20**, 167-179 (2004).

100 Slutter, B. *et al.* Lung airway-surveilling CXCR3(hi) memory CD8(+) T cells are critical for protection against influenza A virus. *Immunity* **39**, 939-948, doi:10.1016/j.immuni.2013.09.013 (2013).

101 Homann, D. *et al.* Differential regulation of antiviral T-cell immunity results in stable CD8+ but declining CD4+ T-cell memory. *Nat. Med.* **7**, 913-919, doi:10.1038/90950 (2001).

102 Liang, S. *et al.* Heterosubtypic immunity to influenza type A virus in mice. Effector mechanisms and their longevity. *J. Immunol.* **152**, 1653-1661 (1994).

103 Humphreys, I. R. *et al.* Avidity of influenza-specific memory CD8+ T-cell populations decays over time compromising antiviral immunity. *Eur. J. Immunol.* **42**, 3235-3242, doi:10.1002/eji.201242575 (2012).

104 Topham, D. J. *et al.* Clearance of an influenza A virus by CD4+ T cells is inefficient in the absence of B cells. *J. Virol.* **72**, 882-885 (1998).

105 Alam, S. *et al.* Infection with seasonal influenza virus elicits CD4 T cells specific for genetically conserved epitopes that can be rapidly mobilized for protective immunity to pandemic H1N1 influenza virus. *J. Virol.* **85**, 13310-13321, doi:10.1128/jvi.05728-11 (2011).

106 McKinstry, K. K. *et al.* Memory CD4+ T cells protect against influenza through multiple synergizing mechanisms. *J. Clin. Invest.* **122**, 2847-2856, doi:10.1172/jci63689 (2012).

107 Lee, L. Y. H. *et al.* Memory T cells established by seasonal human influenza A infection cross-react with avian influenza A (H5N1) in healthy individuals. *J. Clin. Invest.* **118**, 3478-3490, doi:10.1172/jci32460 (2008).

108 Wilkinson, T. M. *et al.* Preexisting influenza-specific CD4+ T cells correlate with disease protection against influenza challenge in humans. *Nat. Med.* **18**, 274-280, doi:10.1038/nm.2612 (2012).

109 Purwar, R. *et al.* Resident memory T cells (T(RM)) are abundant in human lung: diversity, function, and antigen specificity. *PLoS One* **6**, e16245, doi:10.1371/journal.pone.0016245 (2011).

110 Swain, S. L. *et al.* Expanding roles for CD4(+) T cells in immunity to viruses. *Nat. Rev. Immunol.* **12**, 136-148, doi:10.1038/nri3152 (2012).

111 Strutt, T. M. *et al.* Memory CD4+ T cells induce innate responses independently of pathogen. *Nat. Med.* **16**, 558-564, 551p following 564, doi:10.1038/nm.2142 (2010).

112 Boyden, A. W. *et al.* Pulmonary infection with influenza A virus induces site-specific germinal center and T follicular helper cell responses. *PLoS ONE* **7**, doi:10.1371/journal.pone.0040733 (2012).

113 Brown, D. M. *et al.* Multifunctional CD4 cells expressing gamma interferon and perforin mediate protection against lethal influenza virus infection. *J. Virol.* **86**, 6792-6803, doi:10.1128/jvi.07172-11 (2012).

114 Sette, A. *et al.* Selective CD4+ T cell help for antibody responses to a large viral pathogen: deterministic linkage of specificities. *Immunity* **28**, 847-858, doi:10.1016/j.immuni.2008.04.018 (2008).

115 Alam, S. *et al.* CD4 T cell help is limiting and selective during the primary B cell response to influenza virus infection. *J. Virol.* **88**, 314-324, doi:10.1128/jvi.02077-13 (2014).

116 Brown, D. M. *et al.* CD4 T cell-mediated protection from lethal influenza: perforin and antibody-mediated mechanisms give a one-two punch. *J. Immunol.* **177**, 2888-2898 (2006).

117 Strutt, T. M. *et al.* Memory CD4+ T-cell-mediated protection depends on secondary effectors that are distinct from and superior to primary effectors. *Proc. Natl. Acad. Sci. U. S. A.* **109**, E2551-2560, doi:10.1073/pnas.1205894109 (2012).

118 Teijaro, J. R. *et al.* Memory CD4 T cells direct protective responses to influenza virus in the lungs through helper-independent mechanisms. *J. Virol.* **84**, 9217-9226, doi:10.1128/jvi.01069-10 (2010).

119 Jelley-Gibbs, D. M. *et al.* Repeated stimulation of CD4 effector T cells can limit their protective function. *J. Exp. Med.* **201**, 1101-1112, doi:10.1084/jem.20041852 (2005).

120 World Health Organization. Recommended composition of influenza virus vaccines for the use in the 2017-2018 northern hemisphere influenza season. (2017).

121 World Health Organization. Weekly epidemiological record. **47**, 461-476 (2012).

122 SAGE Working Group on Influenza Vaccines and Immunizations. Influenza A (H5N1) Vaccine Stockpile and Inter-Pandemic Vaccine Use. (2013).

123 Pandey, A. *et al.* Egg-independent vaccine strategies for highly pathogenic H5N1 influenza viruses. *Hum. Vaccin.* **6**, 178-188 (2010).

124 U.S. Food & Drug Administration. November 20, 2012 Approval Letter - Flucelvax. http://wayback.archive-it.org/7993/20170723030346/https://www.fda.gov/BiologicsBloodVaccines/Vaccines/ApprovedProducts/ucm328684.htm Accessed: 26-09-2017. (2012).

125 European Medicines Agency. Guideline on Influenza vaccines - Quality module. (2017).

126 Cox, M. M. *et al.* A fast track influenza virus vaccine produced in insect cells. *J. Invertebr. Pathol.* **107 Suppl**, S31-41, doi:10.1016/j.jip.2011.05.003 (2011).

127 Calabro, S. *et al.* Vaccine adjuvants alum and MF59 induce rapid recruitment of neutrophils and monocytes that participate in antigen transport to draining lymph nodes. *Vaccine* **29**, 1812-1823, doi:10.1016/j.vaccine.2010.12.090 (2011).

128 Morel, S. *et al.* Adjuvant System AS03 containing alpha-tocopherol modulates innate immune response and leads to improved adaptive immunity. *Vaccine* **29**, 2461-2473, doi:10.1016/j.vaccine.2011.01.011 (2011).

129 Garcon, N. *et al.* Development and evaluation of AS03, an Adjuvant System containing alpha-tocopherol and squalene in an oil-in-water emulsion. *Expert Rev. Vaccines* **11**, 349-366, doi:10.1586/erv.11.192 (2012).

130 Awate, S. *et al.* Mechanisms of action of adjuvants. *Front. Immunol.* **4**, 114, doi:10.3389/fimmu.2013.00114 (2013).
131 Osterholm, M. T. *et al.* Efficacy and effectiveness of influenza vaccines: a systematic review and meta-analysis. *Lancet Infect. Dis.* **12**, 36-44, doi:10.1016/s1473-3099(11)70295-x (2012).
132 Skowronski, D. M. *et al.* Effectiveness of AS03 adjuvanted pandemic H1N1 vaccine: case-control evaluation based on sentinel surveillance system in Canada, autumn 2009. *BMJ* **342**, c7297, doi:10.1136/bmj.c7297 (2011).
133 Kotsimbos, T. *et al.* Influenza A/H1N1_09: Australia and New Zealand's winter of discontent. *Am. J. Respir. Crit. Care Med.* **181**, 300-306, doi:10.1164/rccm.200912-1878CP (2010).
134 Broadbent, A. J. *et al.* Influenza virus vaccines: lessons from the 2009 H1N1 pandemic. *Curr. Opin. Virol.* **1**, 254-262, doi:10.1016/j.coviro.2011.08.002 (2011).
135 Partridge, J. *et al.* Global production capacity of seasonal influenza vaccine in 2011. *Vaccine* **31**, 728-731, doi:10.1016/j.vaccine.2012.10.111 (2013).
136 He, X. S. *et al.* Cellular immune responses in children and adults receiving inactivated or live attenuated influenza vaccines. *J. Virol.* **80**, 11756-11766, doi:10.1128/jvi.01460-06 (2006).
137 Forrest, B. D. *et al.* Correlation of cellular immune responses with protection against culture-confirmed influenza virus in young children. *Clin. Vaccine. Immunol.* **15**, 1042-1053, doi:10.1128/cvi.00397-07 (2008).
138 Bodewes, R. *et al.* Vaccination against human influenza A/H3N2 virus prevents the induction of heterosubtypic immunity against lethal infection with avian influenza A/H5N1 virus. *PLoS ONE* **4**, doi:10.1371/journal.pone.0005538 (2009).
139 Bodewes, R. *et al.* Vaccination with whole inactivated virus vaccine affects the induction of heterosubtypic immunity against influenza virus A/H5N1 and immunodominance of virus-specific CD8+ T-cell responses in mice. *J. Gen. Virol.* **91**, 1743-1753, doi:10.1099/vir.0.020784-0 (2010).
140 Bodewes, R. *et al.* Annual vaccination against influenza virus hampers development of virus-specific CD8+ T cell immunity in children. *J. Virol.* **85**, 11995-12000, doi:10.1128/jvi.05213-11 (2011).
141 Bodewes, R. *et al.* Vaccination against seasonal influenza A/H3N2 virus reduces the induction of heterosubtypic immunity against influenza A/H5N1 virus infection in ferrets. *J. Virol.* **85**, 2695-2702, doi:10.1128/jvi.02371-10 (2011).
142 Murphy, B. R. Use of Live Attentuated Cold-Adapted Influenza A Reassortant Virus Vaccines in Infants, Children, Young Adults and Elderly Adults. *Infectious Diseases in Clinical Practice* **2**, 174-181 (1993).
143 World Health Organization. Recommendations to assure the quality, safety and efficacy of influenza vaccines (human, live attenuated) for intranasal administration. (2009).
144 World Health Organization. WHO Meeting on Live Attenuated Influenza Vaccine Effectiveness - Executive Summary. (2016).
145 Penttinen, P. M. *et al.* Decreased effectiveness of the influenza A(H1N1)pdm09 strain in live attenuated influenza vaccines: an observational bias or a technical challenge? *Euro. Surveill.* **21**, doi:10.2807/1560-7917.ES.2016.21.38.30350 (2016).
146 Corti, D. *et al.* Heterosubtypic neutralizing antibodies are produced by individuals immunized with a seasonal influenza vaccine. *J. Clin. Invest.* **120**, 1663-1673, doi:10.1172/jci41902 (2010).
147 Krause, J. C. *et al.* A broadly neutralizing human monoclonal antibody that recognizes a conserved, novel epitope on the globular head of the influenza H1N1 virus hemagglutinin. *J. Virol.* **85**, 10905-10908, doi:10.1128/jvi.00700-11 (2011).
148 Krause, J. C. *et al.* Human monoclonal antibodies to pandemic 1957 H2N2 and pandemic 1968 H3N2 influenza viruses. *J. Virol.* **86**, 6334-6340, doi:10.1128/jvi.07158-11 (2012).
149 Ekiert, D. C. *et al.* Cross-neutralization of influenza A viruses mediated by a single antibody loop. *Nature* **489**, 526-532, doi:10.1038/nature11414 (2012).
150 Dreyfus, C. *et al.* Highly conserved protective epitopes on influenza B viruses. *Science* **337**, 1343-1348, doi:10.1126/science.1222908 (2012).
151 Lee, P. S. *et al.* Heterosubtypic antibody recognition of the influenza virus hemagglutinin receptor binding site enhanced by avidity. *Proc. Natl. Acad. Sci. U. S. A.* **109**, 17040-17045, doi:10.1073/pnas.1212371109 (2012).
152 Throsby, M. *et al.* Heterosubtypic neutralizing monoclonal antibodies cross-protective against H5N1 and H1N1 recovered from human IgM+ memory B cells. *PLoS One* **3**, e3942, doi:10.1371/journal.pone.0003942 (2008).

153 Kashyap, A. K. *et al.* Combinatorial antibody libraries from survivors of the Turkish H5N1 avian influenza outbreak reveal virus neutralization strategies. *Proc. Natl. Acad. Sci. U. S. A.* **105**, 5986-5991, doi:10.1073/pnas.0801367105 (2008).
154 Sui, J. *et al.* Structural and functional bases for broad-spectrum neutralization of avian and human influenza A viruses. *Nat. Struct. Mol. Biol.* **16**, 265-273, doi:10.1038/nsmb.1566 (2009).
155 Friesen, R. H. *et al.* New class of monoclonal antibodies against severe influenza: prophylactic and therapeutic efficacy in ferrets. *PLoS One* **5**, e9106, doi:10.1371/journal.pone.0009106 (2010).
156 Kashyap, A. K. *et al.* Protection from the 2009 H1N1 pandemic influenza by an antibody from combinatorial survivor-based libraries. *PLoS Pathog.* **6**, e1000990, doi:10.1371/journal.ppat.1000990 (2010).
157 Friesen, R. H. *et al.* A common solution to group 2 influenza virus neutralization. *Proc. Natl. Acad. Sci. U. S. A.* **111**, 445-450, doi:10.1073/pnas.1319058110 (2014).
158 Krammer, F. *et al.* Assessment of influenza virus hemagglutinin stalk-based immunity in ferrets. *J. Virol.* **88**, 3432-3442, doi:10.1128/jvi.03004-13 (2014).
159 Okuno, Y. *et al.* A common neutralizing epitope conserved between the hemagglutinins of influenza A virus H1 and H2 strains. *J. Virol.* **67**, 2552-2558 (1993).
160 Ekiert, D. C. *et al.* Antibody recognition of a highly conserved influenza virus epitope. *Science* **324**, 246-251, doi:10.1126/science.1171491 (2009).
161 Margine, I. *et al.* H3N2 influenza virus infection induces broadly reactive hemagglutinin stalk antibodies in humans and mice. *J. Virol.* **87**, 4728-4737, doi:10.1128/jvi.03509-12 (2013).
162 Steel, J. *et al.* Influenza virus vaccine based on the conserved hemagglutinin stalk domain. *MBio* **1**, doi:10.1128/mBio.00018-10 (2010).
163 Lu, Y. *et al.* Production and stabilization of the trimeric influenza hemagglutinin stem domain for potentially broadly protective influenza vaccines. *Proc. Natl. Acad. Sci. U. S. A.* **111**, 125-130, doi:10.1073/pnas.1308701110 (2014).
164 Yassine, H. M. *et al.* Hemagglutinin-stem nanoparticles generate heterosubtypic influenza protection. *Nat. Med.* **21**, 1065-1070, doi:10.1038/nm.3927 (2015).
165 Impagliazzo, A. *et al.* A stable trimeric influenza hemagglutinin stem as a broadly protective immunogen. *Science* **349**, 1301-1306, doi:10.1126/science.aac7263 (2015).
166 Eggink, D. *et al.* Guiding the immune response against influenza virus hemagglutinin toward the conserved stalk domain by hyperglycosylation of the globular head domain. *J. Virol.* **88**, 699-704, doi:10.1128/jvi.02608-13 (2014).
167 Hai, R. *et al.* Influenza viruses expressing chimeric hemagglutinins: globular head and stalk domains derived from different subtypes. *J. Virol.* **86**, 5774-5781, doi:10.1128/jvi.00137-12 (2012).
168 Krammer, F. *et al.* Influenza virus hemagglutinin stalk-based antibodies and vaccines. *Curr. Opin. Virol.* **3**, 521-530, doi:10.1016/j.coviro.2013.07.007 (2013).
169 Margine, I. *et al.* Hemagglutinin stalk-based universal vaccine constructs protect against group 2 influenza A viruses. *J. Virol.* **87**, 10435-10446, doi:10.1128/jvi.01715-13 (2013).
170 Goff, P. H. *et al.* Adjuvants and immunization strategies to induce influenza virus hemagglutinin stalk antibodies. *PLoS One* **8**, e79194, doi:10.1371/journal.pone.0079194 (2013).
171 Krammer, F. *et al.* H3 stalk-based chimeric hemagglutinin influenza virus constructs protect mice from H7N9 challenge. *J. Virol.* **88**, 2340-2343, doi:10.1128/jvi.03183-13 (2014).
172 Marcelin, G. *et al.* Inactivated seasonal influenza vaccines increase serum antibodies to the neuraminidase of pandemic influenza A(H1N1) 2009 virus in an age-dependent manner. *J. Infect. Dis.* **202**, 1634-1638, doi:10.1086/657084 (2010).
173 Sandbulte, M. R. *et al.* Cross-reactive neuraminidase antibodies afford partial protection against H5N1 in mice and are present in unexposed humans. *PLoS Med.* **4**, e59, doi:10.1371/journal.pmed.0040059 (2007).
174 Marcelin, G. *et al.* A contributing role for anti-neuraminidase antibodies on immunity to pandemic H1N1 2009 influenza A virus. *PLoS One* **6**, e26335, doi:10.1371/journal.pone.0026335 (2011).
175 Wohlbold, T. J. *et al.* Vaccination with adjuvanted recombinant neuraminidase induces broad heterologous, but not heterosubtypic, cross-protection against influenza virus infection in mice. *MBio* **6**, e02556, doi:10.1128/mBio.02556-14 (2015).
176 Chen, Z. *et al.* Cross-protection against a lethal influenza virus infection by DNA vaccine to neuraminidase. *Vaccine* **18**, 3214-3222 (2000).

177 Bosch, B. J. *et al.* Recombinant soluble, multimeric HA and NA exhibit distinctive types of protection against pandemic swine-origin 2009 A(H1N1) influenza virus infection in ferrets. *J. Virol.* **84**, 10366-10374, doi:10.1128/jvi.01035-10 (2010).

178 Zebedee, S. L. *et al.* Influenza A virus M2 protein: monoclonal antibody restriction of virus growth and detection of M2 in virions. *J. Virol.* **62**, 2762-2772 (1988).

179 Schotsaert, M. *et al.* Universal M2 ectodomain-based influenza A vaccines: preclinical and clinical developments. *Expert Rev. Vaccines* **8**, 499-508, doi:10.1586/erv.09.6 (2009).

180 Jegerlehner, A. *et al.* Influenza A vaccine based on the extracellular domain of M2: weak protection mediated via antibody-dependent NK cell activity. *J. Immunol.* **172**, 5598-5605 (2004).

181 Song, J. M. *et al.* Influenza virus-like particles containing M2 induce broadly cross protective immunity. *PLoS One* **6**, e14538, doi:10.1371/journal.pone.0014538 (2011).

182 Wu, F. *et al.* Characterization of immunity induced by M2e of influenza virus. *Vaccine* **25**, 8868-8873, doi:10.1016/j.vaccine.2007.09.056 (2007).

183 Heinen, P. P. *et al.* Vaccination of pigs with a DNA construct expressing an influenza virus M2-nucleoprotein fusion protein exacerbates disease after challenge with influenza A virus. *J. Gen. Virol.* **83**, 1851-1859 (2002).

184 Kim, M. C. *et al.* Multiple heterologous M2 extracellular domains presented on virus-like particles confer broader and stronger M2 immunity than live influenza A virus infection. *Antiviral Res.* **99**, 328-335, doi:10.1016/j.antiviral.2013.06.010 (2013).

185 Tompkins, S. M. *et al.* Matrix protein 2 vaccination and protection against influenza viruses, including subtype H5N1. *Emerg. Infect. Dis.* **13**, 426-435, doi:10.3201/eid1303.061125 (2007).

186 Neirynck, S. *et al.* A universal influenza A vaccine based on the extracellular domain of the M2 protein. *Nat. Med.* **5**, 1157-1163, doi:10.1038/13484 (1999).

187 Turley, C. B. *et al.* Safety and immunogenicity of a recombinant M2e-flagellin influenza vaccine (STF2.4xM2e) in healthy adults. *Vaccine* **29**, 5145-5152, doi:10.1016/j.vaccine.2011.05.041 (2011).

188 Carragher, D. M. *et al.* A novel role for non-neutralizing antibodies against nucleoprotein in facilitating resistance to influenza virus. *J. Immunol.* **181**, 4168-4176 (2008).

189 LaMere, M. W. *et al.* Contributions of antinucleoprotein IgG to heterosubtypic immunity against influenza virus. *J. Immunol.* **186**, 4331-4339, doi:10.4049/jimmunol.1003057 (2011).

190 Bodewes, R. *et al.* In vitro assessment of the immunological significance of a human monoclonal antibody directed to the influenza a virus nucleoprotein. *Clin. Vaccine Immunol.* **20**, 1333-1337, doi:10.1128/CVI.00339-13 (2013).

191 Jegaskanda, S. *et al.* Human seasonal influenza A viruses induce H7N9-cross-reactive antibody-dependent cellular cytotoxicity (ADCC) antibodies that are directed towards the nucleoprotein. *J. Infect. Dis.*, doi:10.1093/infdis/jiw629 (2016).

192 Sridhar, S. *et al.* Predominance of heterosubtypic IFN-gamma-only-secreting effector memory T cells in pandemic H1N1 naive adults. *Eur. J. Immunol.* **42**, 2913-2924, doi:10.1002/eji.201242504 (2012).

193 Tu, W. *et al.* Cytotoxic T lymphocytes established by seasonal human influenza cross-react against 2009 pandemic H1N1 influenza virus. *J. Virol.* **84**, 6527-6535, doi:10.1128/JVI.00519-10 (2010).

194 Hayward, A. C. *et al.* Natural T Cell-mediated Protection against Seasonal and Pandemic Influenza. Results of the Flu Watch Cohort Study. *Am. J. Respir. Crit. Care Med.* **191**, 1422-1431, doi:10.1164/rccm.201411-1988OC (2015).

195 Hillaire, M. L. *et al.* Characterization of the human CD8(+) T cell response following infection with 2009 pandemic influenza H1N1 virus. *J. Virol.* **85**, 12057-12061, doi:10.1128/jvi.05204-11 (2011).

196 Wang, Z. *et al.* Recovery from severe H7N9 disease is associated with diverse response mechanisms dominated by CD8(+) T cells. *Nat. Commun.* **6**, 6833, doi:10.1038/ncomms7833 (2015).

197 Hillaire, M. L. *et al.* Induction of virus-specific cytotoxic T lymphocytes as a basis for the development of broadly protective influenza vaccines. *J. Biomed. Biotechnol.* **2011**, 939860, doi:10.1155/2011/939860 (2011).

198 Laidlaw, B. J. *et al.* Cooperativity between CD8+ T cells, non-neutralizing antibodies, and alveolar macrophages is important for heterosubtypic influenza virus immunity. *PLoS Pathog.* **9**, e1003207, doi:10.1371/journal.ppat.1003207 (2013).

199 Epstein, S. L. *et al.* Mechanism of protective immunity against influenza virus infection in mice without antibodies. *J. Immunol.* **160**, 322-327 (1998).

200 Richards, K. A. *et al.* Infection of HLA-DR1 transgenic mice with a human isolate of influenza a virus (H1N1) primes a diverse CD4 T-cell repertoire that includes CD4 T cells with heterosubtypic cross-reactivity to avian (H5N1) influenza virus. *J. Virol.* **83**, 6566-6577, doi:10.1128/jvi.00302-09 (2009).
201 Nguyen, H. H. *et al.* Heterosubtypic immunity to influenza A virus infection requires B cells but not CD8+ cytotoxic T lymphocytes. *J. Infect. Dis.* **183**, 368-376, doi:10.1086/318084 (2001).
202 Droebner, K. *et al.* Antibodies and CD4+ T-cells mediate cross-protection against H5N1 influenza virus infection in mice after vaccination with a low pathogenic H5N2 strain. *Vaccine* **26**, 6965-6974, doi:10.1016/j.vaccine.2008.09.051 (2008).
203 Benton, K. A. *et al.* Heterosubtypic immunity to influenza a virus in mice lacking IgA, all Ig, NKT cells, or (gamma)(delta) T cells. *J. Immunol.* **166**, 7437-7445 (2001).
204 Belshe, R. B. *et al.* Correlates of immune protection induced by live, attenuated, cold-adapted, trivalent, intranasal influenza virus vaccine. *J. Infect. Dis.* **181**, 1133-1137, doi:10.1086/315323 (2000).
205 Ambrose, C. S. *et al.* The role of nasal IgA in children vaccinated with live attenuated influenza vaccine. *Vaccine* **30**, 6794-6801, doi:10.1016/j.vaccine.2012.09.018 (2012).
206 Barria, M. I. *et al.* Localized mucosal response to intranasal live attenuated influenza vaccine in adults. *J. Infect. Dis.* **207**, 115-124, doi:10.1093/infdis/jis641 (2013).
207 Schwartzman, L. M. *et al.* An Intranasal Virus-Like Particle Vaccine Broadly Protects Mice from Multiple Subtypes of Influenza A Virus. *MBio* **6**, e01044, doi:10.1128/mBio.01044-15 (2015).
208 Tripp, R. A. *et al.* Virus-vectored influenza virus vaccines. *Viruses* **6**, 3055-3079, doi:10.3390/v6083055 (2014).
209 de Vries, R. D. *et al.* Viral vector-based influenza vaccines. *Hum. Vaccin. Immunother.* **12**, 2881-2901, doi:10.1080/21645515.2016.1210729 (2016).
210 Marshall, E. Gene therapy death prompts review of adenovirus vector. *Science* **286**, 2244-2245 (1999).
211 Duerr, A. *et al.* Extended follow-up confirms early vaccine-enhanced risk of HIV acquisition and demonstrates waning effect over time among participants in a randomized trial of recombinant adenovirus HIV vaccine (Step Study). *J. Infect. Dis.* **206**, 258-266, doi:10.1093/infdis/jis342 (2012).
212 McCoy, K. *et al.* Effect of preexisting immunity to adenovirus human serotype 5 antigens on the immune responses of nonhuman primates to vaccine regimens based on human- or chimpanzee-derived adenovirus vectors. *J. Virol.* **81**, 6594-6604, doi:10.1128/JVI.02497-06 (2007).
213 Pine, S. O. *et al.* Pre-existing adenovirus immunity modifies a complex mixed Th1 and Th2 cytokine response to an Ad5/HIV-1 vaccine candidate in humans. *PLoS One* **6**, e18526, doi:10.1371/journal.pone.0018526 (2011).
214 Roy, S. *et al.* Partial protection against H5N1 influenza in mice with a single dose of a chimpanzee adenovirus vector expressing nucleoprotein. *Vaccine* **25**, 6845-6851, doi:10.1016/j.vaccine.2007.07.035 (2007).
215 Singh, N. *et al.* Bovine adenoviral vector-based H5N1 influenza vaccine overcomes exceptionally high levels of pre-existing immunity against human adenovirus. *Mol. Ther.* **16**, 965-971, doi:10.1038/mt.2008.12 (2008).
216 Pichla-Gollon, S. L. *et al.* Effect of preexisting immunity on an adenovirus vaccine vector: in vitro neutralization assays fail to predict inhibition by antiviral antibody in vivo. *J. Virol.* **83**, 5567-5573, doi:10.1128/JVI.00405-09 (2009).
217 Patel, A. *et al.* A porcine adenovirus with low human seroprevalence is a promising alternative vaccine vector to human adenovirus 5 in an H5N1 virus disease model. *PLoS One* **5**, e15301, doi:10.1371/journal.pone.0015301 (2010).
218 Weaver, E. A. *et al.* Low seroprevalent species D adenovirus vectors as influenza vaccines. *PLoS One* **8**, e73313, doi:10.1371/journal.pone.0073313 (2013).
219 Mayr, A. M., E.;. Veränderung von Vaccinevirus durch Dauerpassagen in Hühnerembryofibroblastenkulturen. *Zentralbl. Bakteriol. B.* **I**, 24–35 (1964).
220 Mayr, A. *et al.* [The smallpox vaccination strain MVA: marker, genetic structure, experience gained with the parenteral vaccination and behavior in organisms with a debilitated defence mechanism (author's transl)]. *Zentralbl. Bakteriol. B.* **167**, 375-390 (1978).
221 Antoine, G. *et al.* The complete genomic sequence of the modified vaccinia Ankara strain: comparison with other orthopoxviruses. *Virology* **244**, 365-396, doi:10.1006/viro.1998.9123 (1998).

222 Meisinger-Henschel, C. *et al.* Introduction of the six major genomic deletions of modified vaccinia virus Ankara (MVA) into the parental vaccinia virus is not sufficient to reproduce an MVA-like phenotype in cell culture and in mice. *J. Virol.* **84**, 9907-9919, doi:10.1128/JVI.00756-10 (2010).

223 Meyer, H. *et al.* Mapping of deletions in the genome of the highly attenuated vaccinia virus MVA and their influence on virulence. *J. Gen. Virol.* **72 (Pt 5)**, 1031-1038, doi:10.1099/0022-1317-72-5-1031 (1991).

224 Carroll, M. W. *et al.* Host range and cytopathogenicity of the highly attenuated MVA strain of vaccinia virus: propagation and generation of recombinant viruses in a nonhuman mammalian cell line. *Virology* **238**, 198-211, doi:10.1006/viro.1997.8845 (1997).

225 Drexler, I. *et al.* Highly attenuated modified vaccinia virus Ankara replicates in baby hamster kidney cells, a potential host for virus propagation, but not in various human transformed and primary cells. *J. Gen. Virol.* **79 (Pt 2)**, 347-352 (1998).

226 Sutter, G. *et al.* Nonreplicating vaccinia vector efficiently expresses recombinant genes. *Proc. Natl. Acad. Sci. U. S. A.* **89**, 10847-10851 (1992).

227 Kibler, K. V. *et al.* Double-stranded RNA is a trigger for apoptosis in vaccinia virus-infected cells. *J. Virol.* **71**, 1992-2003 (1997).

228 Somogyi, P. *et al.* Fowlpox virus host range restriction: gene expression, DNA replication, and morphogenesis in nonpermissive mammalian cells. *Virology* **197**, 439-444, doi:10.1006/viro.1993.1608 (1993).

229 Tartaglia, J. *et al.* Highly attenuated poxvirus vectors. *AIDS Res. Hum. Retroviruses* **8**, 1445-1447, doi:10.1089/aid.1992.8.1445 (1992).

230 Werner, G. T. *et al.* Studies on poxvirus infections in irradiated animals. *Arch. Virol.* **64**, 247-256 (1980).

231 Ramirez, J. C. *et al.* Biology of attenuated modified vaccinia virus Ankara recombinant vector in mice: virus fate and activation of B- and T-cell immune responses in comparison with the Western Reserve strain and advantages as a vaccine. *J. Virol.* **74**, 923-933 (2000).

232 Stittelaar, K. J. *et al.* Protective immunity in macaques vaccinated with a modified vaccinia virus Ankara-based measles virus vaccine in the presence of passively acquired antibodies. *J. Virol.* **74**, 4236-4243 (2000).

233 Veits, J. *et al.* Protective efficacy of several vaccines against highly pathogenic H5N1 avian influenza virus under experimental conditions. *Vaccine* **26**, 1688-1696, doi:10.1016/j.vaccine.2008.01.016 (2008).

234 Overton, E. T. *et al.* Safety and Immunogenicity of Modified Vaccinia Ankara-Bavarian Nordic Smallpox Vaccine in Vaccinia-Naive and Experienced Human Immunodeficiency Virus-Infected Individuals: An Open-Label, Controlled Clinical Phase II Trial. *Open Forum Infect. Dis.* **2**, ofv040, doi:10.1093/ofid/ofv040 (2015).

235 Sutter, G. *et al.* A recombinant vector derived from the host range-restricted and highly attenuated MVA strain of vaccinia virus stimulates protective immunity in mice to influenza virus. *Vaccine* **12**, 1032-1040 (1994).

236 Drexler, I. *et al.* Modified vaccinia virus Ankara as antigen delivery system: how can we best use its potential? *Curr. Opin. Biotechnol.* **15**, 506-512, doi:10.1016/j.copbio.2004.09.001 (2004).

237 Carroll, M. W. *et al.* Highly attenuated modified vaccinia virus Ankara (MVA) as an effective recombinant vector: a murine tumor model. *Vaccine* **15**, 387-394 (1997).

238 Hirsch, V. M. *et al.* Patterns of viral replication correlate with outcome in simian immunodeficiency virus (SIV)-infected macaques: effect of prior immunization with a trivalent SIV vaccine in modified vaccinia virus Ankara. *J. Virol.* **70**, 3741-3752 (1996).

239 Forster, R. *et al.* Highly attenuated poxviruses induce functional priming of neutrophils in vitro. *Arch. Virol.* **136**, 219-226 (1994).

240 Buttner, M. *et al.* Interferon induction in peripheral blood mononuclear leukocytes of man and farm animals by poxvirus vector candidates and some poxvirus constructs. *Vet. Immunol. Immunopathol.* **46**, 237-250 (1995).

241 Blanchard, T. J. *et al.* Modified vaccinia virus Ankara undergoes limited replication in human cells and lacks several immunomodulatory proteins: implications for use as a human vaccine. *J. Gen. Virol.* **79 (Pt 5)**, 1159-1167 (1998).

242 Waibler, Z. *et al.* Modified vaccinia virus Ankara induces Toll-like receptor-independent type I interferon responses. *J. Virol.* **81**, 12102-12110, doi:10.1128/JVI.01190-07 (2007).

243 Delaloye, J. *et al.* Innate immune sensing of modified vaccinia virus Ankara (MVA) is mediated by TLR2-TLR6, MDA-5 and the NALP3 inflammasome. *PLoS Pathog.* **5**, e1000480, doi:10.1371/journal.ppat.1000480 (2009).

244 Halle, S. *et al.* Induced bronchus-associated lymphoid tissue serves as a general priming site for T cells and is maintained by dendritic cells. *J. Exp. Med.* **206**, 2593-2601, doi:10.1084/jem.20091472 (2009).

245 Lehmann, M. H. *et al.* Modified vaccinia virus ankara triggers chemotaxis of monocytes and early respiratory immigration of leukocytes by induction of CCL2 expression. *J. Virol.* **83**, 2540-2552, doi:10.1128/JVI.01884-08 (2009).

246 Fleige, H. *et al.* IL-17-induced CXCL12 recruits B cells and induces follicle formation in BALT in the absence of differentiated FDCs. *J. Exp. Med.* **211**, 643-651, doi:10.1084/jem.20131737 (2014).

247 Kremer, M. *et al.* in *Methods Mol. Biol.* Vol. 890 (ed S.N. Isaacs) 59-92 (Humana Press, 2012).

248 Lohr, V. *et al.* New avian suspension cell lines provide production of influenza virus and MVA in serum-free media: studies on growth, metabolism and virus propagation. *Vaccine* **27**, 4975-4982, doi:10.1016/j.vaccine.2009.05.083 (2009).

249 Kreijtz, J. H. *et al.* Poxvirus vectors. *Vaccine* **31**, 4217-4219, doi:10.1016/j.vaccine.2013.06.073 (2013).

250 Ramezanpour, B. *et al.* Vector-based genetically modified vaccines: Exploiting Jenner's legacy. *Vaccine* **34**, doi:10.1016/j.vaccine.2016.06.059 (2016).

251 Hessel, A. *et al.* A pandemic influenza H1N1 live vaccine based on modified vaccinia Ankara is highly immunogenic and protects mice in active and passive immunizations. *PLoS One* **5**, e12217, doi:10.1371/journal.pone.0012217 (2010).

252 Castrucci, M. R. *et al.* Modified vaccinia virus Ankara expressing the hemagglutinin of pandemic (H1N1) 2009 virus induces cross-protective immunity against Eurasian 'avian-like' H1N1 swine viruses in mice. *Influenza Other Respir. Viruses*, doi:10.1111/irv.12221 (2013).

253 Kreijtz, J. H. *et al.* Evaluation of a modified vaccinia virus Ankara (MVA)-based candidate pandemic influenza A/H1N1 vaccine in the ferret model. *J. Gen. Virol.* **91**, 2745-2752, doi:10.1099/vir.0.024885-0 (2010).

254 Florek, N. W. *et al.* Modified vaccinia virus Ankara encoding influenza virus hemagglutinin induces heterosubtypic immunity in macaques. *J. Virol.* **88**, 13418-13428, doi:10.1128/JVI.01219-14 (2014).

255 Rimmelzwaan, G. F. *et al.* Preclinical evaluation of influenza vaccines based on replication-deficient poxvirus vector MVA. *Procedia in Vaccinology* **4**, 5 (2011).

256 Kreijtz, J. H. *et al.* Recombinant modified vaccinia virus Ankara-based vaccine induces protective immunity in mice against infection with influenza virus H5N1. *J. Infect. Dis.* **195**, 1598-1606, doi:10.1086/517614 (2007).

257 Hessel, A. *et al.* Vectors based on modified vaccinia Ankara expressing influenza H5N1 hemagglutinin induce substantial cross-clade protective immunity. *PLoS One* **6**, e16247, doi:10.1371/journal.pone.0016247 (2011).

258 Kreijtz, J. H. *et al.* Preclinical evaluation of a modified vaccinia virus Ankara (MVA)-based vaccine against influenza A/H5N1 viruses. *Vaccine* **27**, 6296-6299, doi:10.1016/j.vaccine.2009.03.020 (2009).

259 Kreijtz, J. H. *et al.* Recombinant modified vaccinia virus Ankara expressing the hemagglutinin gene confers protection against homologous and heterologous H5N1 influenza virus infections in macaques. *J. Infect. Dis.* **199**, 405-413, doi:10.1086/595984 (2009).

260 Kreijtz, J. H. *et al.* Safety and immunogenicity of a modified-vaccinia-virus-Ankara-based influenza A H5N1 vaccine: a randomised, double-blind phase 1/2a clinical trial. *Lancet Infect. Dis.* **14**, 1196-1207, doi:10.1016/S1473-3099(14)70963-6 (2014).

261 de Vries, R. D. *et al.* Induction of influenza (H5N8) antibodies by modified vaccinia virus Ankara H5N1 vaccine. *Emerg. Infect. Dis.* **21**, 1086-1088, doi:10.3201/eid2106.150021 (2015).

262 Kreijtz, J. H. *et al.* MVA-based H5N1 vaccine affords cross-clade protection in mice against influenza A/H5N1 viruses at low doses and after single immunization. *PLoS One* **4**, e7790, doi:10.1371/journal.pone.0007790 (2009).

263 Kamlangdee, A. *et al.* Broad protection against avian influenza virus by using a modified vaccinia Ankara virus expressing a mosaic hemagglutinin gene. *J. Virol.* **88**, 13300-13309, doi:10.1128/JVI.01532-14 (2014).

264 Breathnach, C. C. *et al.* Immunization with recombinant modified vaccinia Ankara (rMVA) constructs encoding the HA or NP gene protects ponies from equine influenza virus challenge. *Vaccine* **24**, 1180-1190, doi:10.1016/j.vaccine.2005.08.091 (2006).

265 Kreijtz, J. H. *et al.* A single immunization with modified vaccinia virus Ankara-based influenza virus H7 vaccine affords protection in the influenza A(H7N9) pneumonia ferret model. *J. Infect. Dis.* **211**, 791-800, doi:10.1093/infdis/jiu528 (2015).

266 Hessel, A. *et al.* MVA vectors expressing conserved influenza proteins protect mice against lethal challenge with H5N1, H9N2 and H7N1 viruses. *PLoS One* **9**, e88340, doi:10.1371/journal.pone.0088340 (2014).

267 Bender, B. S. *et al.* Oral immunization with a replication-deficient recombinant vaccinia virus protects mice against influenza. *J. Virol.* **70**, 6418-6424 (1996).

268 Brewoo, J. N. *et al.* Cross-protective immunity against multiple influenza virus subtypes by a novel modified vaccinia Ankara (MVA) vectored vaccine in mice. *Vaccine* **31**, 1848-1855, doi:10.1016/j.vaccine.2013.01.038 (2013).

269 Berthoud, T. K. *et al.* Potent CD8+ T-cell immunogenicity in humans of a novel heterosubtypic influenza A vaccine, MVA-NP+M1. *Clin. Infect. Dis.* **52**, 1-7, doi:10.1093/cid/ciq015 (2011).

270 Powell, T. J. *et al.* Examination of influenza specific T cell responses after influenza virus challenge in individuals vaccinated with MVA-NP+M1 vaccine. *PLoS One* **8**, e62778, doi:10.1371/journal.pone.0062778 (2013).

271 Antrobus, R. D. *et al.* A T cell-inducing influenza vaccine for the elderly: safety and immunogenicity of MVA-NP+M1 in adults aged over 50 years. *PLoS One* **7**, e48322, doi:10.1371/journal.pone.0048322 (2012).

272 Lillie, P. J. *et al.* Preliminary assessment of the efficacy of a T-cell-based influenza vaccine, MVA-NP+M1, in humans. *Clin. Infect. Dis.* **55**, 19-25, doi:10.1093/cid/cis327 (2012).

273 Lambe, T. *et al.* Immunity against heterosubtypic influenza virus induced by adenovirus and MVA expressing nucleoprotein and matrix protein-1. *Sci. Rep.* **3**, 1443, doi:10.1038/srep01443 (2013).

274 Boyd, A. C. *et al.* Towards a universal vaccine for avian influenza: protective efficacy of modified Vaccinia virus Ankara and Adenovirus vaccines expressing conserved influenza antigens in chickens challenged with low pathogenic avian influenza virus. *Vaccine* **31**, 670-675, doi:10.1016/j.vaccine.2012.11.047 (2013).

275 Mullarkey, C. E. *et al.* Improved adjuvanting of seasonal influenza vaccines: preclinical studies of MVA-NP+M1 coadministration with inactivated influenza vaccine. *Eur. J. Immunol.* **43**, 1940-1952, doi:10.1002/eji.201242922 (2013).

276 Antrobus, R. D. *et al.* Coadministration of seasonal influenza vaccine and MVA-NP+M1 simultaneously achieves potent humoral and cell-mediated responses. *Mol. Ther.* **22**, 233-238, doi:10.1038/mt.2013.162 (2014).

277 Stickl, H. A. Smallpox vaccination and its consequences: first experiences with the highly attenuated smallpox vaccine “MVA”. *Prev. Med.* **3**, 97-101 (1974).

278 Verheust, C. *et al.* Biosafety aspects of modified vaccinia virus Ankara (MVA)-based vectors used for gene therapy or vaccination. *Vaccine* **30**, 2623-2632, doi:10.1016/j.vaccine.2012.02.016 (2012).

279 Stittelaar, K. J. *et al.* Safety of modified vaccinia virus Ankara (MVA) in immune-suppressed macaques. *Vaccine* **19**, 3700-3709 (2001).

280 Altenburg, A. F. *et al.* Modified vaccinia virus ankara (MVA) as production platform for vaccines against influenza and other viral respiratory diseases. *Viruses* **6**, 2735-2761, doi:10.3390/v6072735 (2014).

281 Moss, B. Poxvirus entry and membrane fusion. *Virology* **344**, 48-54, doi:10.1016/j.virol.2005.09.037 (2006).

282 Chahroudi, A. *et al.* Vaccinia virus tropism for primary hematolymphoid cells is determined by restricted expression of a unique virus receptor. *J. Virol.* **79**, 10397-10407, doi:10.1128/JVI.79.16.10397-10407.2005 (2005).

283 Hsiao, J. C. *et al.* Vaccinia virus envelope D8L protein binds to cell surface chondroitin sulfate and mediates the adsorption of intracellular mature virions to cells. *J. Virol.* **73**, 8750-8761 (1999).

284 Lin, C. L. *et al.* Vaccinia virus envelope H3L protein binds to cell surface heparan sulfate and is important for intracellular mature virion morphogenesis and virus infection in vitro and in vivo. *J. Virol.* **74**, 3353-3365 (2000).

285 von Messling, V. *et al.* Tropism illuminated: lymphocyte-based pathways blazed by lethal morbillivirus through the host immune system. *Proc. Natl. Acad. Sci. U. S. A.* **101**, 14216-14221, doi:10.1073/pnas.0403597101 (2004).
286 de Swart, R. L. *et al.* Predominant infection of CD150+ lymphocytes and dendritic cells during measles virus infection of macaques. *PLoS Pathog.* **3**, e178, doi:10.1371/journal.ppat.0030178 (2007).
287 Kobiler, O. *et al.* Herpesviruses carrying a Brainbow cassette reveal replication and expression of limited numbers of incoming genomes. *Nat. Commun.* **1**, 146, doi:10.1038/ncomms1145 (2010).
288 Fukuyama, S. *et al.* Multi-spectral fluorescent reporter influenza viruses (Color-flu) as powerful tools for in vivo studies. *Nat. Commun.* **6**, 6600, doi:10.1038/ncomms7600 (2015).
289 Dominguez, J. *et al.* Green fluorescent protein expressed by a recombinant vaccinia virus permits early detection of infected cells by flow cytometry. *J. Immunol. Methods* **220**, 115-121 (1998).
290 Sanchez-Puig, J. M. *et al.* Susceptibility of different leukocyte cell types to Vaccinia virus infection. *Virol. J.* **1**, 10, doi:10.1186/1743-422X-1-10 (2004).
291 Flechsig, C. *et al.* Uptake of antigens from modified vaccinia Ankara virus-infected leukocytes enhances the immunostimulatory capacity of dendritic cells. *Cytotherapy* **13**, 739-752, doi:10.3109/14653249.2010.549123 (2011).
292 Liu, L. *et al.* Dendritic cells are preferentially targeted among hematolymphocytes by Modified Vaccinia Virus Ankara and play a key role in the induction of virus-specific T cell responses in vivo. *BMC Immunol.* **9**, 15, doi:10.1186/1471-2172-9-15 (2008).
293 Ramirez, J. C. *et al.* Tissue distribution of the Ankara strain of vaccinia virus (MVA) after mucosal or systemic administration. *Arch. Virol.* **148**, 827-839, doi:10.1007/s00705-003-0006-z (2003).
294 Misharin, A. V. *et al.* Flow cytometric analysis of macrophages and dendritic cell subsets in the mouse lung. *Am. J. Respir. Cell Mol. Biol.* **49**, 503-510, doi:10.1165/rcmb.2013-0086MA (2013).
295 Corbett, M. *et al.* Aerosol immunization with NYVAC and MVA vectored vaccines is safe, simple, and immunogenic. *Proc. Natl. Acad. Sci. U. S. A.* **105**, 2046-2051, doi:10.1073/pnas.0705191105 (2008).
296 Lemon, K. *et al.* Early target cells of measles virus after aerosol infection of non-human primates. *PLoS Pathog* **7**, e1001263, doi:10.1371/journal.ppat.1001263 (2011).
297 MacLoughlin, R. J. *et al.* Optimization and Dose Estimation of Aerosol Delivery to Non-Human Primates. *J. Aerosol Med. Pulm. Drug Deliv.* **29**, 281-287, doi:10.1089/jamp.2015.1250 (2016).
298 Volz, A. *et al.* Modified Vaccinia Virus Ankara: History, Value in Basic Research, and Current Perspectives for Vaccine Development. *Adv. Virus Res.* **97**, 187-243, doi:10.1016/bs.aivir.2016.07.001 (2017).
299 Milligan, I. D. *et al.* Safety and Immunogenicity of Novel Adenovirus Type 26- and Modified Vaccinia Ankara-Vectored Ebola Vaccines: A Randomized Clinical Trial. *JAMA* **315**, 1610-1623, doi:10.1001/jama.2016.4218 (2016).
300 Ophorst, O. J. *et al.* An adenoviral type 5 vector carrying a type 35 fiber as a vaccine vehicle: DC targeting, cross neutralization, and immunogenicity. *Vaccine* **22**, 3035-3044, doi:10.1016/j.vaccine.2004.02.011 (2004).
301 Liu, H. *et al.* The route of inoculation determines the tissue tropism of modified vaccinia Tiantan expressing the spike glycoprotein of SARS-CoV in mice. *J. Med. Virol.* **82**, 727-734, doi:10.1002/jmv.21667 (2010).
302 Duffy, D. *et al.* Neutrophils transport antigen from the dermis to the bone marrow, initiating a source of memory CD8+ T cells. *Immunity* **37**, 917-929, doi:10.1016/j.immuni.2012.07.015 (2012).
303 Tonnis, W. F. *et al.* Pulmonary vaccine delivery: a realistic approach? *J. Aerosol Med. Pulm. Drug. Deliv.* **25**, 249-260, doi:10.1089/jamp.2011.0931 (2012).
304 Satti, I. *et al.* Safety and immunogenicity of a candidate tuberculosis vaccine MVA85A delivered by aerosol in BCG-vaccinated healthy adults: a phase 1, double-blind, randomised controlled trial. *Lancet Infect. Dis.* **14**, 939-946, doi:10.1016/S1473-3099(14)70845-X (2014).
305 White, A. D. *et al.* Evaluation of the safety and immunogenicity of a candidate tuberculosis vaccine, MVA85A, delivered by aerosol to the lungs of macaques. *Clin. Vaccine. Immunol.* **20**, 663-672, doi:10.1128/CVI.00690-12 (2013).
306 Lipscomb, M. F. *et al.* Human alveolar macrophages: HLA-DR-positive macrophages that are poor stimulators of a primary mixed leukocyte reaction. *J. Immunol.* **136**, 497-504 (1986).
307 Ettensohn, D. B. *et al.* Human alveolar macrophage regulation of lymphocyte proliferation. *Am. Rev. Respir. Dis.* **133**, 1091-1096, doi:10.1164/arrd.1986.133.6.1091 (1986).

308 Lyons, C. R. *et al.* Inability of human alveolar macrophages to stimulate resting T cells correlates with decreased antigen-specific T cell-macrophage binding. *J. Immunol.* **137**, 1173-1180 (1986).

309 Holt, P. G. *et al.* MHC class II antigen-bearing dendritic cells in pulmonary tissues of the rat. Regulation of antigen presentation activity by endogenous macrophage populations. *J. Exp. Med.* **167**, 262-274 (1988).

310 Braciale, T. J. *et al.* Regulating the adaptive immune response to respiratory virus infection. *Nat. Rev. Immunol.* **12**, 295-305, doi:10.1038/nri3166 (2012).

311 Thiele, F. *et al.* Modified vaccinia virus Ankara-infected dendritic cells present CD4+ T-cell epitopes by endogenous major histocompatibility complex class II presentation pathways. *J. Virol.* **89**, 2698-2709, doi:10.1128/JVI.03244-14 (2015).

312 Nguyen, D. T. *et al.* Paramyxovirus infections in ex vivo lung slice cultures of different host species. *J. Virol. Methods* **193**, 159-165, doi:10.1016/j.jviromet.2013.06.016 (2013).

313 de Vries, R. D. *et al.* In vivo tropism of attenuated and pathogenic measles virus expressing green fluorescent protein in macaques. *J. Virol.* **84**, 4714-4724, doi:10.1128/JVI.02633-09 (2010).

314 Draper, S. J. *et al.* Viruses as vaccine vectors for infectious diseases and cancer. *Nat. Rev. Microbiol.* **8**, 62-73, doi:10.1038/nrmicro2240 (2010).

315 Larocca, C. *et al.* Viral vector-based therapeutic cancer vaccines. *Cancer J.* **17**, 359-371, doi:10.1097/PPO.0b013e3182325e63 (2011).

316 Altenburg, A. F. *et al.* Virus-specific T cells as correlate of (cross-)protective immunity against influenza. *Vaccine* **33**, 500-506, doi:10.1016/j.vaccine.2014.11.054 (2015).

317 Skowronski, D. M. *et al.* Interim estimates of 2014/15 vaccine effectiveness against influenza A(H3N2) from Canada's Sentinel Physician Surveillance Network, January 2015. *Euro. Surveill.* **20** (2015).

318 Pebody, R. G. *et al.* Low effectiveness of seasonal influenza vaccine in preventing laboratory-confirmed influenza in primary care in the United Kingdom: 2014/15 mid-season results. *Euro. Surveill.* **20**, 21025 (2015).

319 Flannery, B. *et al.* Early estimates of seasonal influenza vaccine effectiveness - United States, January 2015. *MMWR. Morb. Mortal. Wkly. Rep.* **64**, 10-15 (2015).

320 World Health Organization. Summary report on first, second and third generation smallpox vaccines. (2013).

321 Hammarlund, E. *et al.* Duration of antiviral immunity after smallpox vaccination. *Nat. Med.* **9**, 1131-1137, doi:10.1038/nm917 (2003).

322 Rooney, J. F. *et al.* Immunization with a vaccinia virus recombinant expressing herpes simplex virus type 1 glycoprotein D: long-term protection and effect of revaccination. *J. Virol.* **62**, 1530-1534 (1988).

323 Swayne, D. E. *et al.* Failure of a recombinant fowl poxvirus vaccine containing an avian influenza hemagglutinin gene to provide consistent protection against influenza in chickens preimmunized with a fowl pox vaccine. *Avian Dis.* **44**, 132-137 (2000).

324 Ramirez, J. C. *et al.* Attenuated modified vaccinia virus Ankara can be used as an immunizing agent under conditions of preexisting immunity to the vector. *J. Virol.* **74**, 7651-7655 (2000).

325 Yang, Z. Y. *et al.* Overcoming immunity to a viral vaccine by DNA priming before vector boosting. *J. Virol.* **77**, 799-803 (2003).

326 Kannanganat, S. *et al.* Preexisting vaccinia virus immunity decreases SIV-specific cellular immunity but does not diminish humoral immunity and efficacy of a DNA/MVA vaccine. *J. Immunol.* **185**, 7262-7273, doi:10.4049/jimmunol.1000751 (2010).

327 Gudmundsdotter, L. *et al.* Recombinant Modified Vaccinia Ankara (MVA) effectively boosts DNA-primed HIV-specific immune responses in humans despite pre-existing vaccinia immunity. *Vaccine* **27**, 4468-4474, doi:10.1016/j.vaccine.2009.05.018 (2009).

328 van der Klis, F. R. *et al.* Second national serum bank for population-based seroprevalence studies in the Netherlands. *Neth. J. Me .* **67**, 301-308 (2009).

329 Hermanson, G. *et al.* Measurement of antibody responses to Modified Vaccinia virus Ankara (MVA) and Dryvax((R)) using proteome microarrays and development of recombinant protein ELISAs. *Vaccine* **30**, 614-625, doi:10.1016/j.vaccine.2011.11.021 (2012).

330 McMichael, A. J. *et al.* The immune response during acute HIV-1 infection: clues for vaccine development. *Nat. Rev. Immunol.* **10**, 11-23, doi:10.1038/nri2674 (2010).

331 Lin, W. H. *et al.* Vaccine-induced measles virus-specific T cells do not prevent infection or disease but facilitate subsequent clearance of viral RNA. *MBio* **5**, e01047, doi:10.1128/mBio.01047-14 (2014).

332 Klenerman, P. *et al.* T cell responses to cytomegalovirus. *Nat. Rev. Immunol.* **16**, 367-377, doi:10.1038/nri.2016.38 (2016).

333 Belyakov, I. M. *et al.* Mucosal vaccination overcomes the barrier to recombinant vaccinia immunization caused by preexisting poxvirus immunity. *Proc. Natl. Acad. Sci. U. S. A.* **96**, 4512-4517 (1999).

334 Sharpe, S. *et al.* Induction of simian immunodeficiency virus (SIV)-specific CTL in rhesus macaques by vaccination with modified vaccinia virus Ankara expressing SIV transgenes: influence of pre-existing anti-vector immunity. *J. Gen. Virol.* **82**, 2215-2223, doi:10.1099/0022-1317-82-9-2215 (2001).

335 La Rosa, C. *et al.* MVA vaccine encoding CMV antigens safely induces durable expansion of CMV-specific T-cells in healthy adults. *Blood*, doi:10.1182/blood-2016-07-729756 (2016).

336 Littaua, R. A. *et al.* Vaccinia virus-specific human CD4+ cytotoxic T-lymphocyte clones. *J. Virol.* **66**, 2274-2280 (1992).

337 Demkowicz, W. E., Jr. *et al.* Vaccinia virus-specific CD8+ cytotoxic T lymphocytes in humans. *J. Virol.* **67**, 1538-1544 (1993).

338 Davies, D. H. *et al.* Profiling the humoral immune response to infection by using proteome microarrays: high-throughput vaccine and diagnostic antigen discovery. *Proc. Natl. Acad. Sci. U. S. A.* **102**, 547-552, doi:10.1073/pnas.0408782102 (2005).

339 Jones-Trower, A. *et al.* Identification and preliminary characterization of vaccinia virus (Dryvax) antigens recognized by vaccinia immune globulin. *Virology* **343**, 128-140, doi:10.1016/j.virol.2005.08.008 (2005).

340 Moss, B. Smallpox vaccines: targets of protective immunity. *Immunol. Rev.* **239**, 8-26, doi:10.1111/j.1600-065X.2010.00975.x (2011).

341 Altenburg, A. F. *et al.* Increased Protein Degradation Improves Influenza Virus Nucleoprotein-Specific CD8+ T Cell Activation In Vitro but Not in C57BL/6 Mice. *J. Virol.* **90**, 10209-10219, doi:10.1128/JVI.01633-16 (2016).

342 Altenburg, A. F. *et al.* Modified Vaccinia Virus Ankara Preferentially Targets Antigen Presenting Cells In Vitro, Ex Vivo and In Vivo. *Sci. Rep.* **7**, 8580, doi:10.1038/s41598-017-08719-y (2017).

343 Rimmelzwaan, G. F. *et al.* Comparison of RNA hybridization, hemagglutination assay, titration of infectious virus and immunofluorescence as methods for monitoring influenza virus replication in vitro. *J. Virol. Methods* **74**, 57-66 (1998).

344 Melamed, S. *et al.* Tail scarification with Vaccinia virus Lister as a model for evaluation of smallpox vaccine potency in mice. *Vaccine* **25**, 7743-7753, doi:10.1016/j.vaccine.2007.09.023 (2007).

345 Altenburg, A. F. *et al.* Protein and modified vaccinia virus Ankara-based influenza virus nucleoprotein vaccines are differentially immunogenic in BALB/c mice. *Clin. Exp. Immunol.* **190**, 19-28, doi:10.1111/cei.13004 (2017).

346 Baas, D. C. *et al.* Detection of influenza A virus homo- and heterosubtype-specific memory B-cells using a novel protein microarray-based analysis tool. *J. Med. Virol.* **85**, 899-909, doi:10.1002/jmv.23535 (2013).

347 Koopmans, M. *et al.* Profiling of humoral immune responses to influenza viruses by using protein microarray. *Clin Microbiol Infect* **18**, 797-807, doi:10.1111/j.1469-0691.2011.03701.x (2012).

348 Palmer D.F., D. W. R., Coleman M.T. and Schild G.C. Advancement laboratory technicals for immunological diagnostics. (Ed U.S. Dept. Health Ed. Welfare) 25-62 (Atlanta, 1975).

349 Ellebedy, A. H. *et al.* Induction of broadly cross-reactive antibody responses to the influenza HA stem region following H5N1 vaccination in humans. *Proc. Natl. Acad. Sci. U. S. A.* **111**, 13133-13138, doi:10.1073/pnas.1414070111 (2014).

350 Townsend, A. R. *et al.* Cytotoxic T cell recognition of the influenza nucleoprotein and hemagglutinin expressed in transfected mouse L cells. *Cell* **39**, 13-25 (1984).

351 Jameson, J. *et al.* Human cytotoxic T-lymphocyte repertoire to influenza A viruses. *J. Virol.* **72**, 8682-8689 (1998).

352 Hillaire, M. L. B. *et al.* Cross-protective immunity against influenza pH1N1 2009 viruses induced by seasonal influenza A (H3N2) virus is mediated by virus-specific T-cells. *J. Gen. Virol.* **92**, 2339-2349, doi:10.1099/vir.0.033076-0 (2011).

353 Kreijtz, J. H. C. M. *et al.* Infection of mice with a human influenza A/H3N2 virus induces protective immunity against lethal infection with influenza A/H5N1 virus. *Vaccine* **27**, 4983-4989, doi:10.1016/j.vaccine.2009.05.079 (2009).
354 Eisfeld, A. J. *et al.* At the centre: influenza A virus ribonucleoproteins. *Nat. Rev. Microbiol.* **13**, 28-41, doi:10.1038/nrmicro3367 (2015).
355 Townsend, A. *et al.* Defective presentation to class I-restricted cytotoxic T lymphocytes in vaccinia-infected cells is overcome by enhanced degradation of antigen. *J. Exp. Med.* **168**, 1211-1224 (1988).
356 Cros, J. F. *et al.* An unconventional NLS is critical for the nuclear import of the influenza A virus nucleoprotein and ribonucleoprotein. *Traffic* **6**, 205-213, doi:10.1111/j.1600-0854.2005.00263.x (2005).
357 Ozawa, M. *et al.* Contributions of two nuclear localization signals of influenza A virus nucleoprotein to viral replication. *J. Virol.* **81**, 30-41, doi:10.1128/JVI.01434-06 (2007).
358 Johnson, E. S. *et al.* Ubiquitin as a degradation signal. *EMBO J.* **11**, 497-505 (1992).
359 Grant, E. P. *et al.* Rate of antigen degradation by the ubiquitin-proteasome pathway influences MHC class I presentation. *J. Immunol.* **155**, 3750-3758 (1995).
360 Tobery, T. W. *et al.* Targeting of HIV-1 antigens for rapid intracellular degradation enhances cytotoxic T lymphocyte (CTL) recognition and the induction of de novo CTL responses in vivo after immunization. *J. Exp. Med.* **185**, 909-920 (1997).
361 Liu, W. J. *et al.* Polynucleotide viral vaccines: codon optimisation and ubiquitin conjugation enhances prophylactic and therapeutic efficacy. *Vaccine* **20**, 862-869 (2001).
362 Qian, S. B. *et al.* Fusion proteins with COOH-terminal ubiquitin are stable and maintain dual functionality in vivo. *J. Biol. Chem.* **277**, 38818-38826, doi:10.1074/jbc.M205547200 (2002).
363 Gasteiger, G. *et al.* Cross-priming of cytotoxic T cells dictates antigen requisites for modified vaccinia virus Ankara vector vaccines. *J. Virol.* **81**, 11925-11936, doi:10.1128/JVI.00903-07 (2007).
364 Schliehe, C. *et al.* Stable antigen is most effective for eliciting CD8+ T-cell responses after DNA vaccination and infection with recombinant vaccinia virus in vivo. *J. Virol.* **86**, 9782-9793, doi:10.1128/JVI.00694-12 (2012).
365 Rimmelzwaan, G. F. *et al.* A randomized, double blind study in young healthy adults comparing cell mediated and humoral immune responses induced by influenza ISCOM vaccines and conventional vaccines. *Vaccine* **19**, 1180-1187 (2000).
366 van de Sandt, C. E. *et al.* Differential Recognition of Influenza A Viruses by M158-66 Epitope-Specific CD8+ T Cells Is Determined by Extraepitopic Amino Acid Residues. *J. Virol.* **90**, 1009-1022, doi:10.1128/JVI.02439-15 (2016).
367 van den Brand, J. M. *et al.* Modification of the ferret model for pneumonia from seasonal human influenza A virus infection. *Vet. Pathol.* **49**, 562-568, doi:10.1177/0300985811429812 (2012).
368 Zhirnov, O. P. *et al.* Two forms of influenza virus nucleoprotein in infected cells and virions. *Virology* **109**, 174-179 (1981).
369 Zhirnov, O. *et al.* Nucleoproteins of animal influenza viruses, in contrast to those of human strains, are not cleaved in infected cells. *J. Gen. Virol.* **65 (Pt 6)**, 1127-1134 (1984).
370 Lipatov, A. S. *et al.* The role of the N-terminal caspase cleavage site in the nucleoprotein of influenza A virus in vitro and in vivo. *Arch. Virol.* **153**, 427-434, doi:10.1007/s00705-007-0003-8 (2008).
371 Betts, M. R. *et al.* Sensitive and viable identification of antigen-specific CD8+ T cells by a flow cytometric assay for degranulation. *J. Immunol. Methods* **281**, 65-78 (2003).
372 Boon, A. C. *et al.* The hypervariable immunodominant NP418-426 epitope from the influenza A virus nucleoprotein is recognized by cytotoxic T lymphocytes with high functional avidity. *J. Virol.* **80**, 6024-6032, doi:10.1128/JVI.00009-06 (2006).
373 Rodriguez, F. *et al.* DNA immunization: ubiquitination of a viral protein enhances cytotoxic T-lymphocyte induction and antiviral protection but abrogates antibody induction. *J. Virol.* **71**, 8497-8503 (1997).
374 Fu, T. M. *et al.* Induction of MHC class I-restricted CTL response by DNA immunization with ubiquitin-influenza virus nucleoprotein fusion antigens. *Vaccine* **16**, 1711-1717 (1998).
375 Andersson, H. A. *et al.* Maximizing antigen targeting to the proteasome for gene-based vaccines. *Mol. Ther.* **10**, 432-446, doi:10.1016/j.ymthe.2004.05.035 (2004).
376 Flynn, K. J. *et al.* Virus-specific CD8+ T cells in primary and secondary influenza pneumonia. *Immunity* **8**, 683-691 (1998).

377 Webby, R. J. *et al.* Protection and compensation in the influenza virus-specific CD8+ T cell response. *Proc. Natl. Acad. Sci. U. S. A.* **100**, 7235-7240, doi:10.1073/pnas.1232449100 (2003).
378 Bodewes, R. *et al.* Redundancy of the influenza A virus-specific cytotoxic T lymphocyte response in HLA-B*2705 transgenic mice limits the impact of a mutation in the immunodominant NP(383-391) epitope on influenza pathogenesis. *Virus Res.* **155**, 123-130, doi:10.1016/j.virusres.2010.09.008 (2011).
379 Yewdell, J. W. Designing CD8+ T cell vaccines: it's not rocket science (yet). *Curr. Opin. Immunol.* **22**, 402-410, doi:10.1016/j.coi.2010.04.002 (2010).
380 Bins, A. D. *et al.* In vivo antigen stability affects DNA vaccine immunogenicity. *J. Immunol.* **179**, 2126-2133 (2007).
381 Ghimire, T. R. *et al.* Alum increases antigen uptake, reduces antigen degradation and sustains antigen presentation by DCs in vitro. *Immunol. Lett.* **147**, 55-62, doi:10.1016/j.imlet.2012.06.002 (2012).
382 World Health Organization. Cumulative number of confirmed human cases for avian influenza A(H5N1) reported to WHO, 2003-2017. (2017).
383 World Health Organization. Human infections with avian influenza A(H5N6) virus. (2016).
384 World Health Organization. Human infection with Avian Influenza A(H7N9) virus in China. (2017).
385 de Vries, R. D. *et al.* Universal influenza vaccines, science fiction or soon reality? *Expert Rev. Vaccines* **14**, 1299-1301, doi:10.1586/14760584.2015.1060860 (2015).
386 de Vries, R. D. *et al.* Universal influenza vaccines: a realistic option? *Clin. Microbiol. Infect.* **22 Suppl 5**, S120-S124, doi:10.1016/j.cmi.2015.12.005 (2016).
387 Krammer, F. *et al.* Advances in universal influenza virus vaccine design and antibody mediated therapies based on conserved regions of the hemagglutinin. *Curr. Top. Microbiol. Immunol.* **386**, 301-321, doi:10.1007/82_2014_408 (2015).
388 Stickl, H. *et al.* [MVA vaccination against smallpox: clinical tests with an attenuated live vaccinia virus strain (MVA) (author's transl)]. *Dtsch. Med. Wochenschr.* **99**, 2386-2392, doi:10.1055/s-0028-1108143 (1974).
389 Ott, G. *et al.* Enhancement of humoral response against human influenza vaccine with the simple submicron oil/water emulsion adjuvant MF59. *Vaccine* **13**, 1557-1562 (1995).
390 Madhun, A. S. *et al.* Intramuscular Matrix-M-adjuvanted virosomal H5N1 vaccine induces high frequencies of multifunctional Th1 CD4+ cells and strong antibody responses in mice. *Vaccine* **27**, 7367-7376, doi:10.1016/j.vaccine.2009.09.044 (2009).
391 Cox, R. J. *et al.* Evaluation of a virosomal H5N1 vaccine formulated with Matrix M adjuvant in a phase I clinical trial. *Vaccine* **29**, 8049-8059, doi:10.1016/j.vaccine.2011.08.042 (2011).
392 Pedersen, G. *et al.* Matrix-M adjuvanted virosomal H5N1 vaccine confers protection against lethal viral challenge in a murine model. *Influenza Other Respir. Viruses* **5**, 426-437, doi:10.1111/j.1750-2659.2011.00256.x (2011).
393 Magnusson, S. E. *et al.* Immune enhancing properties of the novel Matrix-M adjuvant leads to potentiated immune responses to an influenza vaccine in mice. *Vaccine* **31**, 1725-1733, doi:10.1016/j.vaccine.2013.01.039 (2013).
394 Cox, F. *et al.* Protection against H5N1 Influenza Virus Induced by Matrix-M Adjuvanted Seasonal Virosomal Vaccine in Mice Requires Both Antibodies and T Cells. *PLoS One* **10**, e0145243, doi:10.1371/journal.pone.0145243 (2015).
395 Wee, J. L. *et al.* Pulmonary delivery of ISCOMATRIX influenza vaccine induces both systemic and mucosal immunity with antigen dose sparing. *Mucosal Immunol.* **1**, 489-496, doi:10.1038/mi.2008.59 (2008).
396 Mastelic Gavillet, B. *et al.* MF59 Mediates Its B Cell Adjuvanticity by Promoting T Follicular Helper Cells and Thus Germinal Center Responses in Adult and Early Life. *J. Immunol.* **194**, 4836-4845, doi:10.4049/jimmunol.1402071 (2015).
397 Lovgren, K. *et al.* The requirement of lipids for the formation of immunostimulating complexes (iscoms). *Biotechnol. Appl. Biochem.* **10**, 161-172 (1988).
398 Radosevic, K. *et al.* Antibody and T-cell responses to a virosomal adjuvanted H9N2 avian influenza vaccine: impact of distinct additional adjuvants. *Vaccine* **26**, 3640-3646, doi:10.1016/j.vaccine.2008.04.071 (2008).
399 Pedersen, G. K. *et al.* Matrix M(TM) adjuvanted virosomal H5N1 vaccine induces balanced Th1/Th2 CD4(+) T cell responses in man. *Hum. Vaccin. Immunother.* **10**, 2408-2416, doi:10.4161/hv.29583 (2014).

400 Liu, Y. V. *et al.* Recombinant virus-like particles elicit protective immunity against avian influenza A(H7N9) virus infection in ferrets. *Vaccine* **33**, 2152-2158, doi:10.1016/j.vaccine.2015.03.009 (2015).

401 ClinicalTrials.gov Identifier: NCT01444482. Study of Parenterally Administrated Adjuvanted Seasonal Influenza Vaccine in Healthy Elderly Volunteers.

402 ClinicalTrials.gov Identifier: NCT02078674. A(H7N9) VLP Antigen Dose-Ranging Study With Matrix-M1 Adjuvant.

403 Trombetta, C. M. *et al.* Influenza immunology evaluation and correlates of protection: a focus on vaccines. *Expert Rev. Vaccines* **15**, 967-976, doi:10.1586/14760584.2016.1164046 (2016).

404 Cargnelutti, D. E. *et al.* Enhancement of Th1 immune responses to recombinant influenza nucleoprotein by Ribi adjuvant. *New Microbiol.* **36**, 145-151 (2013).

405 Macleod, M. K. *et al.* Influenza nucleoprotein delivered with aluminium salts protects mice from an influenza A virus that expresses an altered nucleoprotein sequence. *PLoS One* **8**, e61775, doi:10.1371/journal.pone.0061775 (2013).

406 Lovgren Bengtsson, K. *et al.* ISCOM technology-based Matrix M adjuvant: success in future vaccines relies on formulation. *Expert Rev. Vaccines* **10**, 401-403, doi:10.1586/erv.11.25 (2011).

407 Luckheeram, R. V. *et al.* CD4(+)T cells: differentiation and functions. *Clin. Dev. Immunol.* **2012**, 925135, doi:10.1155/2012/925135 (2012).

408 Magnusson, S. E. *et al.* Matrix-M adjuvanted envelope protein vaccine protects against lethal lineage 1 and 2 West Nile virus infection in mice. *Vaccine* **32**, 800-808, doi:10.1016/j.vaccine.2013.12.030 (2014).

409 Verstrepen, B. E. *et al.* Vaccine-induced protection of rhesus macaques against plasma viremia after intradermal infection with a European lineage 1 strain of West Nile virus. *PLoS One* **9**, e112568, doi:10.1371/journal.pone.0112568 (2014).

410 Bengtsson, K. L. *et al.* Matrix-M adjuvant enhances antibody, cellular and protective immune responses of a Zaire Ebola/Makona virus glycoprotein (GP) nanoparticle vaccine in mice. *Vaccine* **34**, 1927-1935, doi:10.1016/j.vaccine.2016.02.033 (2016).

411 Lamere, M. W. *et al.* Regulation of antinucleoprotein IgG by systemic vaccination and its effect on influenza virus clearance. *J. Virol.* **85**, 5027-5035, doi:10.1128/JVI.00150-11 (2011).

412 Taylor, P. M. *et al.* Influenza nucleoprotein-specific cytotoxic T-cell clones are protective in vivo. *Immunology* **58**, 417-420 (1986).

413 Price, G. E. *et al.* Vaccination focusing immunity on conserved antigens protects mice and ferrets against virulent H1N1 and H5N1 influenza A viruses. *Vaccine* **27**, 6512-6521, doi:10.1016/j.vaccine.2009.08.053 (2009).

414 Norder, M. *et al.* Modified vaccinia virus Ankara exerts potent immune modulatory activities in a murine model. *PLoS One* **5**, e11400, doi:10.1371/journal.pone.0011400 (2010).

415 Watson, D. L. *et al.* Inflammatory response and antigen localization following immunization with influenza virus ISCOMs. *Inflammation* **13**, 641-649 (1989).

416 Sjolander, A. *et al.* Kinetics, localization and cytokine profile of T cell responses to immune stimulating complexes (iscoms) containing human influenza virus envelope glycoproteins. *Vaccine* **15**, 1030-1038 (1997).

417 Wei, J. *et al.* Varied Role of Ubiquitylation in Generating MHC Class I Peptide Ligands. *J. Immunol.*, doi:10.4049/jimmunol.1602122 (2017).

418 World Health Organization. WHO recommendations on the composition of influenza virus vaccines. http://www.who.int/influenza/vaccines/virus/recommendations/en/. Accessed: 24/09/2017.

419 Parrino, J. *et al.* Safety, immunogenicity and efficacy of modified vaccinia Ankara (MVA) against Dryvax challenge in vaccinia-naive and vaccinia-immune individuals. *Vaccine* **25**, 1513-1525, doi:10.1016/j.vaccine.2006.10.047 (2007).

420 Even-Or, O. *et al.* Adjuvanted influenza vaccines. *Expert Rev. Vaccines* **12**, 1095-1108, doi:10.1586/14760584.2013.825445 (2013).

421 Frey, S. *et al.* Comparison of the safety, tolerability, and immunogenicity of a MF59-adjuvanted influenza vaccine and a non-adjuvanted influenza vaccine in non-elderly adults. *Vaccine* **21**, 4234-4237 (2003).

422 Madan, A. *et al.* Immunogenicity and Safety of an AS03-Adjuvanted H7N9 Pandemic Influenza Vaccine in a Randomized Trial in Healthy Adults. *J. Infect. Dis.* **214**, 1717-1727, doi:10.1093/infdis/jiw414 (2016).

423 Nicholson, K. G. *et al.* Safety and immunogenicity of whole-virus, alum-adjuvanted whole-virus, virosomal, and whole-virus intradermal influenza A/H9N2 vaccine formulations. *Vaccine* **28**, 171-178, doi:10.1016/j.vaccine.2009.09.103 (2009).
424 Chung, K. Y. *et al.* ISCOMATRIX adjuvant promotes epitope spreading and antibody affinity maturation of influenza A H7N9 virus like particle vaccine that correlate with virus neutralization in humans. *Vaccine* **33**, 3953-3962, doi:10.1016/j.vaccine.2015.06.047 (2015).
425 Del Giudice, G. *et al.* Inactivated and adjuvanted influenza vaccines. *Curr. Top. Microbiol. Immunol.* **386**, 151-180, doi:10.1007/82_2014_406 (2015).
426 Osterhaus, A. D. *et al.* Induction of virus-specific immunity by iscoms. *Dev. Biol. Stand.* **92**, 49-58 (1998).
427 Rajput, Z. I. *et al.* Adjuvant effects of saponins on animal immune responses. *J. Zhejiang Univ. Sci. B.* **8**, 153-161, doi:10.1631/jzus.2007.B0153 (2007).
428 Reimer, J. M. *et al.* Matrix-M adjuvant induces local recruitment, activation and maturation of central immune cells in absence of antigen. *PLoS One* **7**, e41451, doi:10.1371/journal.pone.0041451 (2012).
429 Cox, F. *et al.* Matrix-M Adjuvated Seasonal Virosomal Influenza Vaccine Induces Partial Protection in Mice and Ferrets against Avian H5 and H7 Challenge. *PLoS One* **10**, e0135723, doi:10.1371/journal.pone.0135723 (2015).
430 Collins, K. A. *et al.* Enhancing protective immunity to malaria with a highly immunogenic virus-like particle vaccine. *Sci. Rep.* **7**, 46621, doi:10.1038/srep46621 (2017).
431 Warimwe, G. M. *et al.* Immunogenicity and efficacy of a chimpanzee adenovirus-vectored Rift Valley fever vaccine in mice. *Virol. J.* **10**, 349, doi:10.1186/1743-422X-10-349 (2013).
432 Testi, R. *et al.* The CD69 receptor: a multipurpose cell-surface trigger for hematopoietic cells. *Immunol. Today* **15**, 479-483, doi:10.1016/0167-5699(94)90193-7 (1994).
433 Caux, C. *et al.* B70/B7-2 is identical to CD86 and is the major functional ligand for CD28 expressed on human dendritic cells. *J. Exp. Med.* **180**, 1841-1847 (1994).
434 Bengtsson, K. L. *et al.* Matrix-M adjuvant: enhancing immune responses by 'setting the stage' for the antigen. *Expert Rev. Vaccines* **12**, 821-823, doi:10.1586/14760584.2013.814822 (2013).
435 Nimmerjahn, F. *et al.* Divergent immunoglobulin g subclass activity through selective Fc receptor binding. *Science* **310**, 1510-1512, doi:10.1126/science.1118948 (2005).
436 Qu, C. *et al.* Monocyte-derived dendritic cells: targets as potent antigen-presenting cells for the design of vaccines against infectious diseases. *Int. J. Infect. Dis.* **19**, 1-5, doi:10.1016/j.ijid.2013.09.023 (2014).
437 Detienne, S. *et al.* Central Role of CD169+ Lymph Node Resident Macrophages in the Adjuvanticity of the QS-21 Component of AS01. *Sci. Rep.* **6**, 39475, doi:10.1038/srep39475 (2016).
438 Carrasco, Y. R. *et al.* B cells acquire particulate antigen in a macrophage-rich area at the boundary between the follicle and the subcapsular sinus of the lymph node. *Immunity* **27**, 160-171, doi:10.1016/j.immuni.2007.06.007 (2007).
439 Junt, T. *et al.* Subcapsular sinus macrophages in lymph nodes clear lymph-borne viruses and present them to antiviral B cells. *Nature* **450**, 110-114, doi:10.1038/nature06287 (2007).
440 Gray, E. E. *et al.* Lymph node macrophages. *J. Innate Immun.* **4**, 424-436, doi:10.1159/000337007 (2012).
441 Claas, E. C. *et al.* Human influenza A H5N1 virus related to a highly pathogenic avian influenza virus. *Lancet* **351**, 472-477, doi:10.1016/S0140-6736(97)11212-0 (1998).
442 de Jong, J. C. *et al.* A pandemic warning? *Nature* **389**, 554, doi:10.1038/39218 (1997).
443 Subbarao, K. *et al.* Characterization of an avian influenza A (H5N1) virus isolated from a child with a fatal respiratory illness. *Science* **279**, 393-396 (1998).
444 Zhao, G. *et al.* Novel reassortant highly pathogenic H5N2 avian influenza viruses in poultry in China. *PLoS One* **7**, e46183, doi:10.1371/journal.pone.0046183 (2012).
445 Liu, C. G. *et al.* Emerging multiple reassortant H5N5 avian influenza viruses in ducks, China, 2008. *Vet. Microbiol.* **167**, 296-306, doi:10.1016/j.vetmic.2013.09.004 (2013).
446 Zhao, K. *et al.* Characterization of three H5N5 and one H5N8 highly pathogenic avian influenza viruses in China. *Vet. Microbiol.* **163**, 351-357, doi:10.1016/j.vetmic.2012.12.025 (2013).
447 Qi, X. *et al.* Whole-Genome Sequence of a Reassortant H5N6 Avian Influenza Virus Isolated from a Live Poultry Market in China, 2013. *Genome Announc.* **2**, doi:10.1128/genomeA.00706-14 (2014).
448 Wu, H. S. *et al.* Influenza A(H5N2) virus antibodies in humans after contact with infected poultry, Taiwan, 2012. *Emerg. Infect. Dis.* **20**, 857-860, doi:10.3201/eid2005.131393 (2014).

449 European Medicines Agency. Authorization Procedures. http://www.ema.europa.eu/ema/index.jsp?curl=pages/special_topics/q_and_a/q_and_a_detail_000080.jsp Accessed: 17-03-2014.
450 Couch, R. B. *et al.* Evaluations for in vitro correlates of immunogenicity of inactivated influenza a H5, H7 and H9 vaccines in humans. *PLoS One* **7**, e50830, doi:10.1371/journal.pone.0050830 (2012).
451 Smith, G. J. *et al.* Nomenclature updates resulting from the evolution of avian influenza A(H5) virus clades 2.1.3.2a, 2.2.1, and 2.3.4 during 2013-2014. *Influenza Other Respir. Viruses* **9**, 271-276, doi:10.1111/irv.12324 (2015).
452 Paules, C. I. *et al.* The Pathway to a Universal Influenza Vaccine. *Immunity* **47**, 599-603, doi:10.1016/j.immuni.2017.09.007 (2017).
453 McCullers, J. A. *et al.* Recipients of vaccine against the 1976 “swine flu” have enhanced neutralization responses to the 2009 novel H1N1 influenza virus. *Clin. Infect. Dis.* **50**, 1487-1492, doi:10.1086/652441 (2010).
454 de Vries, R. D. *et al.* Influenza virus-specific antibody dependent cellular cytoxicity induced by vaccination or natural infection. *Vaccine* **35**, 238-247, doi:10.1016/j.vaccine.2016.11.082 (2017).
455 de Vries, R. D. *et al.* Primary Human Influenza B Virus Infection Induces Cross-Lineage HA-Stalk-Specific Antibodies Mediating Antibody Dependent Cellular Cytoxicity. *J. Infect. Dis.*, in press (2017).
456 Binyamin, L. *et al.* Blocking NK cell inhibitory self-recognition promotes antibody-dependent cellular cytotoxicity in a model of anti-lymphoma therapy. *J. Immunol.* **180**, 6392-6401 (2008).
457 *MEGA: Molecular Evolutionary Genetics Analysis.* http://www.megasoftware.net/ Accessed: 17-11-2017.
458 Luke, C. J. *et al.* Improving pandemic H5N1 influenza vaccines by combining different vaccine platforms. *Expert Rev. Vaccines* **13**, 873-883, doi:10.1586/14760584.2014.922416 (2014).
459 Hobson, D. *et al.* The role of serum haemagglutination-inhibiting antibody in protection against challenge infection with influenza A2 and B viruses. *J. Hyg. (Lond.)* **70**, 767-777 (1972).
460 Bruhns, P. *et al.* Specificity and affinity of human Fcgamma receptors and their polymorphic variants for human IgG subclasses. *Blood* **113**, 3716-3725, doi:10.1182/blood-2008-09-179754 (2009).
461 He, W. *et al.* Epitope specificity plays a critical role in regulating antibody-dependent cell-mediated cytotoxicity against influenza A virus. *Proc. Natl. Acad. Sci. U. S. A.* **113**, 11931-11936, doi:10.1073/pnas.1609316113 (2016).
462 Cox, F. *et al.* HA Antibody-Mediated FcgammaRIIIa Activity Is Both Dependent on FcR Engagement and Interactions between HA and Sialic Acids. *Front. Immunol.* **7**, 399, doi:10.3389/fimmu.2016.00399 (2016).
463 Leon, P. E. *et al.* Optimal activation of Fc-mediated effector functions by influenza virus hemagglutinin antibodies requires two points of contact. *Proc. Natl. Acad. Sci. U. S. A.* **113**, E5944-E5951, doi:10.1073/pnas.1613225113 (2016).
464 Wiersma, L. C. *et al.* Developing Universal Influenza Vaccines: Hitting the Nail, Not Just on the Head. *Vaccines (Basel)* **3**, 239-262, doi:10.3390/vaccines3020239 (2015).
465 Kastenmuller, W. *et al.* A spatially-organized multicellular innate immune response in lymph nodes limits systemic pathogen spread. *Cell* **150**, 1235-1248, doi:10.1016/j.cell.2012.07.021 (2012).
466 Gorse, G. J. *et al.* DNA and modified vaccinia virus Ankara vaccines encoding multiple cytotoxic and helper T-lymphocyte epitopes of human immunodeficiency virus type 1 (HIV-1) are safe but weakly immunogenic in HIV-1-uninfected, vaccinia virus-naive adults. *Clin. Vaccine Immunol.* **19**, 649-658, doi:10.1128/CVI.00038-12 (2012).
467 Blum, J. S. *et al.* Pathways of antigen processing. *Annu. Rev. Immunol.* **31**, 443-473, doi:10.1146/annurev-immunol-032712-095910 (2013).
468 Gilbert, S. C. Clinical development of Modified Vaccinia virus Ankara vaccines. *Vaccine* **31**, 4241-4246, doi:10.1016/j.vaccine.2013.03.020 (2013).
469 Gomez, C. E. *et al.* Clinical applications of attenuated MVA poxvirus strain. *Expert Rev. Vaccines* **12**, 1395-1416, doi:10.1586/14760584.2013.845531 (2013).
470 European Medicines Agency. Guideline on quality, non-clinical and clinical aspects of live recombinant viral vectored vaccines. (2010).
471 Ohmit, S. E. *et al.* Influenza hemagglutination-inhibition antibody titer as a correlate of vaccine-induced protection. *J. Infect. Dis.* **204**, 1879-1885, doi:10.1093/infdis/jir661 (2011).

Chapter 7

Nederlandse samenvatting

Griep is een luchtweginfectie die wordt veroorzaakt door het influenzavirus. Influenzavirussen behoren tot de familie van orthomyxovirussen en zijn verder onder te verdelen in influenza A-, B-, C- en D-virussen. Influenza A-virussen worden verder gecategoriseerd in zogenaamde subtypes op basis van twee eiwitten op het oppervlak van het viruspartikel: hemagglutinine (HA) en neuraminidase (NA). Momenteel zijn er 18 verschillende HA subtypes (H1-18) en 11 verschillende NA subtypes (N1-11) bekend. De naamgeving van de subtypes van influenza A-virussen is gebaseerd op de HA en NA types op het oppervlak van het viruspartikel, bijvoorbeeld H5N1 (ook wel bekend als vogelgriep).

Influenza A- (H1N1 en H3N2 subtypes) en B-virussen zijn de veroorzakers van de jaarlijkse griepepidemie in de wintermaanden. De Wereldgezondheidsorganisatie (WHO) schat dat het influenzavirus wereldwijd jaarlijks 3-5 miljoen ernstige luchtweginfecties veroorzaakt, waarvan 250.000-500.000 met een dodelijke afloop. Naast de continu circulerende virussen die de seizoensgriep veroorzaken, vinden er sporadisch besmettingen plaats met voor de mens onbekende influenza A-virussen. Deze virussen worden vanuit het dierenrijk, voornamelijk door vogels en varkens, overgedragen op de mens. Als deze nieuwe influenzavirussen zich zo aanpassen dat ze gemakkelijk van mens-op-mens overgedragen kunnen worden, een eigenschap die deze virussen vaak (nog) niet bezitten, is er een kans op een wereldwijde uitbraak (pandemie). Een recent voorbeeld hiervan is de Mexicaanse grieppandemie van 2009, die veroorzaakt werd door een H1N1 influenza A-virus afkomstig uit varkens.

Vaccinatie tegen influenzavirussen

Kwetsbare groepen, zoals ouderen of mensen met luchtwegproblemen, komen in Nederland in aanmerking voor de jaarlijkse 'griepprik'. Dit vaccin tegen de seizoensgriep bestaat uit verzwakte of geïnactiveerde (delen van) influenza A(H1N1)-, A(H3N2)- en B-virussen. Vaccinatie zorgt voornamelijk voor aanmaak van antilichamen die het HA-eiwit op het oppervlakte van een viruspartikel of door influenzavirus geïnfecteerde cellen kunnen herkennen. Wanneer de gastheer daarna in aanraking komt met het influenzavirus, binden deze antilichamen aan het HA-eiwit waardoor wordt voorkomen dat het virus aan gastheercellen kan binden en een infectie kan veroorzaken. Echter, er zijn twee scenario's waarin de jaarlijkse influenzavaccins minder of niet werkzaam zijn. Ten eerste, door mutaties in het HA-eiwit kan het influenzavirus ontsnappen aan herkenning door eerder aangemaakte antilichamen. Het huidige influenzavaccin moet hierdoor bijna jaarlijks aangepast worden om voor de juiste afweer te zorgen tegen de nieuwe influenzavirussen. Om voldoende influenzavaccins te kunnen produceren moet een half jaar voor het griepseizoen worden vastgesteld welke A(H1N1)-, A(H3N2)- en influenza B-virussen er in het vaccin worden opgenomen. Indien er niet goed voorspeld wordt welke virussen er de komende winter zullen circuleren, is er sprake van een *mismatch* tussen het vaccin en de circulerende influenzavirussen. Dit resulteert in verlaagde vaccineffectiviteit: de gevaccineerde mensen hebben grotere kans om toch ziek te worden. Ten tweede beschermt het jaarlijkse influenzavaccin niet tegen pandemische influenzavirussen. In dat geval moet er een geheel nieuw vaccin ontwikkeld worden, wat veel tijd in beslag neemt. Zo kwam tijdens de Mexicaanse grieppandemie het

vaccin in veel landen pas beschikbaar toen de piek van de pandemie al voorbij was. Samengevat: er is een grote behoefte aan nieuwe influenzavaccins die sneller geproduceerd kunnen worden en/of brede(re) bescherming kunnen bieden tegen verschillende subtypes van het influenzavirus.

Brede immuniteit tegen influenzavirussen
Er wordt veel onderzoek gedaan naar de ontwikkeling van nieuwe influenzavaccins die bescherming tegen meerdere influenzavirussen bieden, oftewel die brede immuniteit induceren. Om dit te bereiken wordt er onderzocht of bepaalde vaccins een antilichaamrespons kunnen opwekken die meerdere subtypes van het influenza A-virus herkent. Daarnaast wordt er onderzoek gedaan naar een efficiëntere activatie van influenzavirus-specifieke T-cellen, die door de huidige vaccins niet tot nauwelijks geactiveerd worden. Cytotoxische T-cellen hebben de capaciteit om influenzavirus-geïnfecteerde cellen te lyseren en zo te voorkomen dat een infectie zich kan ontwikkelen en uitbreiden. T-cellen kunnen niet alleen de oppervlakte eiwitten van een virus herkennen, maar ook de eiwitten die in een viruspartikel worden omgeven door een membraan met daarin de oppervlakte eiwitten. In tegenstelling tot HA en NA, zijn deze interne eiwitten een minder variabel onderdeel van de verschillende influenzavirussen en kunnen daarom een sleutelfactor zijn voor het induceren van brede immuniteit.

Andere onderzoeken naar een verbeterde vaccin-geïnduceerde immuunrespons tegen het influenzavirus richten zich op het gebruik van adjuvantia: bestanddelen die aan een vaccin worden toegevoegd om te zorgen dat het immuunsysteem beter op het antigeen (viraal eiwit waartegen de immuunrespons opgewekt moet worden) reageert. Daarnaast worden nieuwe methodes ontwikkeld om een antigeen aan te bieden aan het immuunsysteem zodat zowel antilichamen als T-cellen geactiveerd kunnen worden. Een van die vaccinatiemethodes waar op dit moment zeer veel belangstelling voor bestaat is het gebruik van virale vectoren, zoals de vector *Modified Vaccinia virus Ankara* (MVA). MVA is een verzwakte variant van het vacciniavirus dat tot halverwege de jaren ‘70 is gebruikt om de bevolking tegen het inmiddels uitgeroeide pokkenvirus te beschermen. Het is relatief makkelijk om een recombinant (r)MVA te maken dat een antigeen tot expressie brengt van bijvoorbeeld het influenzavirus. In relatief korte tijd kunnen grote hoeveelheden van een rMVA griepvaccin geproduceerd worden. Bij vaccinatie met rMVA worden gastheercellen geïnfecteerd en vindt er expressie van virale eiwitten, inclusief het influenzavirus antigeen van interesse, plaats. Er is echter geen sprake van actieve virusreplicatie in zoogdiercellen, dus er worden geen nieuwe viruspartikels gevormd. MVA is in ruim 100.000 vrijwilligers getest en altijd veilig gebleken, zelfs bij personen met een gecompromitteerd immuunsysteem. In vele studies met verschillende diermodellen en in klinische trials is aangetoond dat op deze manier efficiënt zowel antilichaamresponsen als T-cellen geïnduceerd kunnen worden tegen het antigeen van interesse.

Dit proefschrift beschrijft onderzoek naar de MVA-vaccinvector en de ontwikkeling van nieuwe influenzavaccins op basis van MVA. Tevens wordt de toevoegde waarde van adjuvantia bij het gebruik van MVA-vaccins onderzocht. In hoofdstuk 1 wordt

een algemene introductie op dit proefschrift gegeven met achtergrondinformatie over influenzavirussen, huidige influenzavaccins, de MVA-vaccinvector en de ontwikkelingen op het gebied van nieuwe influenzavaccins.

MVA als influenzavaccinvector

Hoofdstuk 2 beschrijft twee studies die fundamentele vragen beantwoorden over het gebruik van de MVA-vaccinvector. In hoofdstuk 2.1 is onderzocht welke celtypes er in muizen, fretten en makaken geïnfecteerd worden door MVA. Dit is van belang omdat het antigeen waartegen een immuunrespons opgewekt moet worden door middel van vaccinatie met rMVA tot expressie wordt gebracht in deze cellen. Daarnaast werd in de verschillende diermodellen toediening van MVA door middel van injectie in een spier (de meest gebruikte vaccinatiemethode) vergeleken met toediening aan de luchtwegen. De resultaten lieten zien dat in alle diermodellen via beide toedieningsmethodes voornamelijk antigeen presenterende cellen (APC) zoals dendritische cellen (DC) geïnfecteerd werden door MVA. Dit is een zeer gunstige eigenschap van MVA als vaccinvector aangezien DC een belangrijke rol spelen bij het opwekken en reguleren van immuunresponsen.

In hoofdstuk 2.2 is onderzocht of reeds aanwezige immuniteit tegen de MVA-vaccinvector effect heeft op het induceren van immuunresponsen door vaccinatie met rMVA. Immuniteit tegen de vaccinvector kan geïnduceerd zijn door historische vaccinatiecampagnes tegen de pokken, waarbij gevaccineerd werd met vacciniavirus. Daarnaast kan vaccinvector-specifieke immuniteit opgewekt worden door meerdere keren achter elkaar te vaccineren met een vaccin gebaseerd op MVA. In theorie zou deze pokkenvirus-specifieke immuniteit de werking van rMVA negatief kunnen beïnvloeden. De resultaten van hoofdstuk 2.2 lieten zien dat zowel in muizen als mensen antilichamen tegen de vaccinvector de capaciteit hebben om MVA *in vitro* te neutraliseren. In muizen werd voornamelijk activatie van antigeen-specifieke T-cellen negatief beïnvloed door de bestaande immuunrespons tegen de MVA-vaccinvector. Het effect van de MVA-specifieke immuunrespons op activatie van antigeen-specifieke antilichamen was minimaal en werd alleen gevonden onder 'suboptimale' vaccinatie omstandigheden, zoals bij het gebruik van een lagere vaccindosis. Onder alle geteste omstandigheden waren muizen nog steeds volledig beschermd tegen infectie met het influenzavirus waartegen gevaccineerd werd. De precieze werking van de immuunresponsen tegen de vaccinvector op vaccinatie met een vaccin gebaseerd op MVA in mensen moet nog onderzocht worden. Echter, de studies in muizen suggereren dat het belangrijk is om de vaccindosis en de afweerstatus van een ontvanger van een rMVA-vaccin te beoordelen voordat het vaccin wordt toegediend.

Influenzavaccinkandidaten gebaseerd op MVA

Hoofdstuk 3 richt zich op de ontwikkeling en het testen van nieuwe influenzavaccins gebaseerd op de MVA-vaccinvector. Om T-cellen te activeren worden virale eiwitten die aanwezig zijn in een cel tijdens een infectie afgebroken en de stukjes eiwit die overblijven, zogenaamde peptiden, worden op het oppervlak van de gastheercel gepresenteerd. Cytotoxische T-cellen worden door herkenning van deze peptiden geactiveerd, en kunnen vervolgens de geïnfecteerde cel lyseren en

zo de virusreplicatie reduceren. Door middel van vaccinatie kunnen cytotoxische T-cellen worden getraind om bepaalde virale peptiden te herkennen (immunologisch geheugen), zodat deze bij een daadwerkelijke infectie met het influenzavirus snel kunnen reageren en de geïnfecteerde cellen kunnen opruimen. Hoofdstuk 3.1 beschrijft onderzoek naar optimalisatie van de T-cel respons tegen het interne influenzavirus eiwit nucleoproteïne (NP). Er zijn modificaties aangebracht in het NP-eiwit, dat tot expressie komt door middel van MVA, die erop gericht zijn om het eiwit sneller af te breken. In theorie zijn er dan sneller en/of meer peptiden beschikbaar voor antigeenpresentatie, dus zouden meer T-cellen geactiveerd kunnen worden door vaccinatie. De resultaten lieten zien dat dit *in vitro* inderdaad het geval is, maar dat leidde in muizen niet tot sterkere T-cel responsen of betere bescherming tegen een influenzavirus infectie.

In hoofdstuk 3.2 zijn de resultaten uit hoofdstuk 3.1 bevestigd in een muismodel met een iets andere immuunrespons tegen het influenzavirus. Tevens werd vaccinatie met een op rMVA gebaseerd NP-vaccin vergeleken met NP-eiwit vaccinatie. Over het algemeen hebben eiwitvaccins adjuvantia nodig om een sterke immuunrespons te induceren. In deze studie konden NP-eiwitvaccins inderdaad een sterkere NP-specifieke immuunrespons opwekken wanneer het adjuvans Matrix-M™, een olie-in-water emulsie, werd toegevoegd. Echter, influenza NP-vaccins gebaseerd op MVA induceerden betere cytotoxische T-cel activatie dan vaccins gebaseerd op eiwit, ook als Matrix-M™ aan het eiwitvaccin werd toegevoegd.

Vervolgens is in hoofdstuk 3.3 de immuunrespons na vaccinatie met HA-eiwit of rMVA dat HA tot expressie brengt onderzocht in muizen. Dit vaccin is er voornamelijk op gericht om antilichaamresponsen te induceren. In deze studie wekte het vaccin gebaseerd op MVA een betere immuunrespons op dan het eiwitvaccin. De antilichaamresponsen werden vastgesteld werd door de antilichaamtiter tegen het receptor-bindingsdomein van HA (*hemagglutination inhibition* [HI] titer) te bepalen. Verder is onderzocht wat het effect was van het toevoegen van Matrix-M™ adjuvans aan eiwit of MVA-gebaseerde HA-vaccins. Net als bij NP, werd de immuunrespons tegen HA aanzienlijk verbeterd door het toevoegen van Matrix-M™ aan HA-eiwitvaccins. Over het algemeen wordt aangenomen dat het toevoegen van adjuvantia aan een vaccin gebaseerd op een virale vector niet nodig is, omdat de vaccinvector zelf al voor een verhoogde activatiestatus van het immuunsysteem zorgt. De resultaten lieten zien dat, alhoewel een vaccin gebaseerd op MVA inderdaad meer immunogeen is dan alleen eiwit, het toevoegen van Matrix-M™ adjuvans aan de vaccinmix ook van toegevoegde waarde is voor rMVA-vectorvaccins. De werking van Matrix-M™ adjuvans werd verder onderzocht en leidde zowel bij eiwitvaccins als op MVA gebaseerde HA-vaccins tot meer (geactiveerde) afweercellen in de lymfeknoop die de spier waarin gevaccineerd werd draineert.

Tot slot is in hoofdstuk 4 de immuunrespons in mensen onderzocht na vaccinatie met een rMVA-vectorvaccin dat HA van een H5N1 vogelgriepvirus tot expressie brengt (rMVA-H5). De resultaten lieten zien dat dit vaccin een zeer brede antilichaam respons induceert tegen antigeen verschillende influenzavirussen van het H5 subtype. Deze antilichamen hebben de capaciteit om H5N1 vogelgriepvirussen te neutraliseren,

maar hebben ook niet-neutraliserende capaciteiten zoals *antibody dependent cellular cytotoxicity* (ADCC) activiteit. ADCC is het proces waarbij antilichamen virale eiwitten op het oppervlak van een geïnfecteerde cel herkennen en binden, en vervolgens door middel van activatie van onder andere *natural killer* (NK) cellen lysis van de virus-geïnfecteerde cel induceren. Naast antilichaamresponsen werden er door het rMVA-H5 vaccin ook T-cel responsen geactiveerd die nodig zijn om een efficiënte antilichaamrespons tot stand te brengen. Samenvattend, de resultaten laten zien dat rMVA-H5 een zeer veelbelovende vaccin kandidaat is in het geval van een uitbraak met een vogelgriepvirus van het H5 subtype.

Implicaties van het beschreven onderzoek

De resultaten beschreven in dit proefschrift dragen bij aan de kennis over de werking van MVA als vaccinvector in het algemeen, en specifiek als influenzavaccin. Deze kennis is essentieel voor het verkrijgen van goedkeuring van regulatoire instanties voor het gebruik van vaccins gebaseerd op MVA in mensen. Daarnaast zijn preklinische en klinische studies uitgevoerd met op MVA gebaseerde influenzavaccinkandidaten om de immuunrespons tegen influenzavirussen te optimaliseren en analyseren. Deze studies dragen bij aan de ontwikkeling van een nieuwe generatie influenzavaccins.

Chapter 8

About the author

8.1 *Curriculum Vitae*

Arwen Fieke Altenburg was born 20 June 1990 in Zoelmond and grew up in Culemborg, the Netherlands. In 2008, she obtained her VWO diploma from O.R.S. Lek en Linge (Culemborg) and started the bachelor Biomedical Sciences at Utrecht University. After obtaining the bachelor's degree, Arwen continued with the master programme 'Infection & Immunity' at Utrecht University in 2011. Her first research internship was in the group of Prof. Dr. Linde Meyaard (University Medical Centre, Utrecht) studying the effects of inhibitory immune receptor SIRL-1 on neutrophils. Subsequently, Arwen moved on to Boston for her second internship in the group of Prof. Dr. Hidde Ploegh (Whitehead Institute, MIT, Cambridge, U.S.A.) where she worked on the development and characterization of single-domain antibodies against influenza virus. Arwen obtained her master's degree in 2013 and continued as a PhD student under supervision of Prof. Dr. Guus Rimmelzwaan and Dr. Rory de Vries in the department of Viroscience, Erasmus MC, Rotterdam. Her research focussed on the development of Modified Vaccinia virus Ankara (MVA)-based influenza vaccines that are capable of inducing broadly protective immunity as well as on the validation of the MVA vaccine platform itself. The results of these studies are presented in this thesis.

8.2 PhD portfolio

Name: Arwen Fieke Altenburg
Department: Viroscience, Erasmus MC
Graduate school: Molecular Medicine (MolMed) Post Graduate School
PhD period: 2013-2018
Promotor: Prof. Dr. G.F. Rimmelzwaan
Co-promotor: Dr. R.D. de Vries

Education

2013-2018	PhD programme	Erasmus MC
2011-2013	Master of Science (Infection & Immunity)	Utrecht University
2008-2011	Bachelor of Science (Biomedical Sciences)	Utrecht University

In-depth courses / certificates

2016	Biosafety level 3 training	Dept. Viroscience
2015	Introduction in Graphpad Prism	MolMed
2015	Course in Submandibular Bleeding of Mice	Animal Facility
2014	Course in Virology	MolMed
2014	Course in Systematic Literature Research	MolMed
2014	Course in EndNote	MolMed
2014	*Instellingsgebonden regelgeving stralingshygiëne*	Erasmus MC
2013	Course in Advances in Comparative Pathology	MolMed

Attended meetings / seminars / workshops / journal clubs

2013-2017	Viroscience department seminars	Erasmus MC
2013-2017	Viroscience labmeetings	Erasmus MC
2013-2017	Immunology department seminars	Erasmus MC
2013-2016	T Cell Consortium (TCC) meetings	Erasmus MC
2015-2016	Viroscience journal club	Erasmus MC
2016	PhD day. Workshops: 'Work-life balance' & 'How to give an inspiring presentation'	Erasmus MC
2016	PhD career event. Workshops: 'Personal Leadership' & 'In contact with media'	EUR

Attended symposia / conferences

2017	FLUNIVAC consortium meeting	Den Haag
2017	6th ESWI conference	Riga, Latvia
2017	EDUFLUVAC workshop	Brussels, Belgium
2017	Dutch Society for Immunology (NVVI)	Lunteren
2017	21st MolMed Day	Rotterdam
2017	Dutch Annual Virology Symposium	Amsterdam
2016	FLUNIVAC consortium meeting	Uppsala, Sweden
2016	9th Options for the control of influenza	Chicago, U.S.A.
2016	Dutch Annual Virology Symposium	Amsterdam
2016	20th MolMed Day	Rotterdam
2015	FLUNIVAC consortium meeting	Munich, Germany

2015	7th Orthomyxovirus Research Conference	Toulouse, France
2015	Dutch Society for Immunology (NVVI)	Lunteren
2015	19th MolMed Day	Rotterdam
2015	Dutch Annual Virology Symposium	Amsterdam
2014	FLUNIVAC consortium meeting	Ghent, Belgium
2014	5th ESWI conference	Riga, Latvia
2014	Dutch Annual Virology Symposium	Amsterdam
2014	18th MolMed Day	Rotterdam
2013	Dutch Society for Immunology (NVVI)	Noordwijkerhout
2013	FLUNIVAC consortium kick-off meeting	Rotterdam

Poster presentations

2017	6th ESWI conference	Riga, Latvia
2017	21st MolMed Day	Rotterdam
2016	9th Options for the control of influenza	Chicago, U.S.A.
2016	20th MolMed Day	Rotterdam
2015	19th MolMed Day	Rotterdam
2014	5th ESWI	Riga, Latvia

Oral presentations

2017	FLUNIVAC consortium meeting	Den Haag
2017	European Commission - EDUFLUVAC	Brussels, Belgium
2017	EDUFLUVAC workshop	Brussels, Belgium
2017	Invited speaker group Prof. G.L. Smith	Cambridge, U.K.
2017	Invited speaker group Prof. D.J. Smith	Cambridge, U.K.
2016	FLUNIVAC consortium meeting	Uppsala, Sweden
2016	Dutch Annual Virology Symposium	Amsterdam
2015	FLUNIVAC consortium meeting	Munich, Germany
2015	7th Orthomyxovirus Research Conference	Toulouse, France
2014	FLUNIVAC consortium meeting	Ghent, Belgium

Teaching

2017	Lecturer '*Basisprincipes Immunologie&Vaccinatie'* for Medical Doctors, NSPOH, Rotterdam
2014-2017	Coach & jury member '*Viruskenner'* at different high schools in the Netherlands and Paramaribo, Surinam
2016	Supervision 6-month internship technician in training
2014-2016	Supervision annual labrotations 'Infection & Immunity' master students

Miscellaneous

2017	Reviewer for Viral Immunology
2017	Chair Viroscience labmeeting
2015	Host Viroscience journal club
2015	Visits to Ghent for Pulse-Chase experiments
2014	ESWI Young Scientist travel grant

8.3 List of publications

1. de Vries RD*, **Altenburg AF***, Nieuwkoop NJ, de Bruin E, van Trierum SE, Pronk MR, Lamers MM, Richard M, Nieuwenhuijse DF, Koopmans MPG, Kreijtz JHCM, Fouchier RAM, Osterhaus ADME, Sutter G, Rimmelzwaan GF. Induction of cross-clade antibody and T cell responses by an MVA-based influenza H5N1 vaccine in a randomized phase I/IIa clinical trial. *Manuscript in preparation.*

2. Magnusson SE*, **Altenburg AF***, Bosman F, de Vries RD, Rimmelzwaan GF, Stertman L. Matrix-M™ adjuvant enhances immunogenicity of both protein- and Modified Vaccinia virus Ankara-based influenza vaccines. *Submitted.*

3. **Altenburg AF**, van Trierum SE, de Bruin E, de Meulder D, van de Sandt CE, van der Klis FRM, Fouchier RAM, Koopmans MPG, Rimmelzwaan GF, de Vries RD. Effects of pre-existing orthopoxvirus-specific immunity on the performance of Modified Vaccinia virus Ankara-based influenza vaccines. *Submitted.*

4. **Altenburg AF***, van de Sandt CE*, Li BWS, MacLoughlin R, Fouchier RAM, van Amerongen G, Volz A, Hendriks RW, de Swart RL, Sutter G, Rimmelzwaan GF, de Vries RD. Modified Vaccinia virus Ankara preferentially targets antigen presenting cells *in vitro*, *ex vivo* and *in vivo*. *Scientific Reports, 2017; 7(1)8580: 1-14.*

5. **Altenburg AF***, Magnusson SE*, Bosman F, Stertman L, de Vries RD, Rimmelzwaan GF. Protein- and Modified Vaccinia virus Ankara-based influenza virus nucleoprotein vaccines are differentially immunogenic in BALB/c mice. *Clinical & Experimental Immunology, 2017; 190(1): 19-28.*

6. **Altenburg AF**, van de Sandt CE, van Trierum SE, De Gruyter HL, van Run PR, Fouchier RA, Roose K, Saelens X, Volz A, Sutter G, de Vries RD, Rimmelzwaan GF. Increased protein degradation improves influenza virus nucleoprotein-specific $CD8^+$ T cell activation *in vitro* but not in C57BL/6 mice. *Journal of Virology, 2016; 90(22): 10209-10219.*

7. de Vries RD, **Altenburg AF**, Rimmelzwaan GF. Universal influenza vaccines: a realistic option? *Clinical Microbiology and Infection, 2016; 22: S120-S124.*

8. de Vries RD, **Altenburg AF**, Rimmelzwaan GF. Universal influenza vaccines, science fiction or soon reality? *Expert Review Vaccines, 2015; 14(10): 1299-1301.*

9. **Altenburg AF**, Rimmelzwaan GF, de Vries RD. Virus-specific T cells as correlate of (cross-)protective immunity against influenza. *Vaccine, 2015; 33(4): 500-506.*

10. Ashour J, Schmidt FI, Hanke L, Cragnolini J, Cavallari M, **Altenburg A**, Brewer R, Ingram J, Shoemaker C, Ploegh HL. Intracellular expression of camelid single-domain antibodies specific for influenza virus nucleoprotein uncovers distinct features of its nuclear localization. *Journal of Virology, 2015; 89(5): 2792-2800.*

11. **Altenburg AF**, Kreijtz JH, de Vries RD, Song F, Fux R, Rimmelzwaan GF, Sutter G, Volz A. Modified Vaccinia virus Ankara (MVA) as production platform for vaccines against influenza and other viral respiratory diseases. *Viruses, 2014; 6(7): 2735-2761.*

12. Sanyal S, Ashour J, Maruyama T, **Altenburg AF**, Cragnolini JJ, Bilate A, Avalos AM, Kundrat L, García-Sastre A, Ploegh HL. Type I interferon imposes a TSG101/ISG15 checkpoint at the Golgi for glycoprotein trafficking during influenza virus infection. *Cell Host & Microbe, 2013; 14(5): 510-521.*

13. Dougan SK, Ashour J, Karssemeijer RA, Popp MW, Avalos AM, Barisa M, **Altenburg AF**, Ingram JR, Cragnolini JJ, Guo C, Alt FW, Jaenisch R, Ploegh HL. Antigen-specific B cell receptor sensitizes B cells to infection by influenza virus. *Nature, 2013; 503(7476): 406-409.*

* Authors contributed equally

Dankwoord

Het citaat van stelling 11 heb ik gekozen omdat ik ervan overtuigd ben dat als je iets echt heel graag wil, je het ook echt kunt bereiken. De weg ernaar toe is misschien niet altijd even makkelijk, maar gelukkig hoef je niet altijd alles alleen te doen. Ook bij de totstandkoming van dit proefschrift zijn veel mensen betrokken geweest. Naar goed traditioneel gebruik wil ik aan het eind van dit proefschrift iedereen bedanken voor hun bijdrage en een aantal mensen specifiek noemen.

Guus, bedankt dat ik de afgelopen jaren aan het FLUNIVAC-project heb mogen werken. Je bood veel vrijheid op het lab, maar de deur stond altijd open om even te overleggen en je zorgde ervoor dat de aanpak praktisch en realistisch bleef. Toen ik tijdens mijn sollicitatiegesprek vroeg naar de sfeer op de afdeling zei je al 'work hard, party hard'. Zo heb ik het de afgelopen jaren ook ervaren: het is serieus en hard werken, maar je geeft ook genoeg ruimte aan gezelligheid met onder andere vele enthousiaste verhalen, winter BBQs en een middagje golf (ik denk dat ik maar gewoon blijf wielrennen ☺).

Rory, het wordt straks vast even omschakelen om niet meer dagelijks samen te werken. Je staat altijd voor iedereen klaar en bent altijd bereid mee te denken over experimenten. Ik heb veel kunnen leren van je 'mad-postdoc-lab-skills' (Granny Smith-groen ☺) en de manier waarop je heel efficiënt aan veel verschillende projecten/virussen werkt. Gelukkig begrijp jij als geen ander hoe belangrijk het kan zijn om fanatiek te sporten, zelfs als dat af en toe een uitdaging is naast een drukke baan. Het was superleuk om na het 'Options'-congres nog even naar Boston te gaan en m'n vertrouwde rondje over de bruggen van de Charles hard te lopen!

Ab en **Marion**, bedankt voor alle mogelijkheden die ik heb gekregen tijdens het werken op de afdeling Viroscience.

To all the partners in the FLUNIVAC consortium: thank you for the collaboration and the nice annual meetings! **Gerd** and **Asisa**, thanks for all your expertise and advise on the MVA work in particular. **Xavier** en **Kenny**, bedankt dat ik in Gent de pulse-chase experiment mocht uitvoeren. **Sofia**, too bad we never got to work together in the lab, but I enjoyed our fruitful collaboration!

My Viroscience bestie **Johanna**, thanks for all the coffee breaks and walks in the park. I feel like I can talk about anything with you and I really missed having you in the department last year. Luckily, we are still frequently in touch via FaceTime and I hope we will continue to do so. I am very happy that you wanted to be my paranimf!

Fenne, het begin van onze vriendschap blijft voor mij heel bijzonder; samen een aantal weekendjes naar mooie (en fotogenieke!) plaatsen in Amerika. Na de gedeelde ervaring van een stage in het buitenland, begonnen we allebei aan een PhD in Rotterdam. Ik ben zo blij dat we ook tijdens deze periode ups en downs hebben kunnen delen. Met bemoedigende, zelfverzekerde en attente woorden en advies sta je altijd voor me klaar. Superfijn dat ook jij me als paranimf wil bijstaan bij mijn promotie!

Mijn collega's van de FluI groep: **Stella**, bedankt voor al je hulp op het lab! Dit was onmisbaar bij het groeien van alle MVA-stocks en (grote) experimenten! **Mark**, bedankt voor alle hulp met de ELISA, HI en VN assays. Het was altijd gezellig om samen te werken! **Carolien**, bedankt voor de gedetailleerde protocollen, en dat je een paar keer een dagje bij wou springen op het lab. **Nella**, de ADCC-data zijn een mooi onderdeel van het FLUPLAN-paper! En natuurlijk ook een speciaal bedankje voor **Ruud**, **Joost** & **Heidi** (bedankt voor alle hulp aan het begin van m'n PhD), **Gerrie**, **Tiny** en **Lidewij**.

Mijn kamergenoten van Ee-1771, bedankt voor alle gezelligheid! *Never a dull moment* op de virologie kamer met vele mooie tradities en goede verhalen. De kamer waar het op donderdag maandag is en soms gewoon donderdag, maar waar het uiteindelijk eigenlijk altijd vrijdagmiddag is. Dus naast de roomies die al eerder zijn genoemd, dank je wel **Dennis** (of Dr. de Meuldert na de mailtjes als coauteur ☺) voor al je gezelligheid en hulp bij de experimenten. **Miranda**, trotse winnaar van de eerste Viezerik-award! We hebben een heel aantal keer met tranen in de ogen dubbel gelegen van het lachen als er weer eens iemand in het plakband liep. Ook 's avonds of in het weekend was het zo dus altijd gezellig op de kamer! **Sander**, je hebt me (bijna) van de OCD afgeholpen door alle foto's scheef op te hangen aan de muur ☺. De dansende kip en de hamer zijn zeer waardevolle toevoegingen aan onze kamer, en pim-pam-pet spelen kan nu echt niet meer zonder geluidseffect!

Alle andere collega's van de afdeling Viroscience, bedankt voor jullie hulp, advies, gezellige borrels, labdagen en sinterkerst feesten. **Debby (vR)**, bedankt voor al je advies en dat ik altijd even binnen kon lopen voor serieuze en minder serieuze zaken. **Ron**, bedankt voor je kritische blik op de manuscripten. **Peter (vR)**, altijd leuk om het over wielrennen te hebben en natuurlijk super bedankt voor al je hulp bij maken van histologie coupes! **Mathilde**, thanks for your advice and help with the FLUPLAN-paper. You will get the hang of the Easter egg colour coding ☺. **Theo** en **Monique**, bedankt voor alle hulp en adviezen op het lab! **Oanh**, bedankt voor alle extra kippeneieren en je altijd oprechte vraag over hoe het gaat. **Gijs**, leuk en handig dat we samen konden uitvogelen hoe het afronden van een PhD nou eigenlijk werkt. We gaan er twee mooie feestjes van maken! **Erwin** en **Felicity**, bedankt voor de mooie protein array data en **David (N)** bedankt voor de hulp met het uitwerken hiervan. **Werner** en **Rik**, bedankt dat ik altijd kon aankloppen met vragen of voor reagentia ☺. **Mart**, als ik nog een 'religious album cover' nodig heb, weet ik bij wie ik moet zijn! **Thomas, Jurre, Wesley** & **David (vdV)**, het was superleuk om samen de Tour de Rotterdam te rijden! **Bri**, take care of the old lady Canto! **Laura**, die reis naar Suriname voor viruskenner was echt heel speciaal en leuk dat je een paar keer wou meekijken op het lab. **Chantal** en **Hans**, bedankt voor alle bestellingen. **Robert** en **Peter**, bedankt voor de liters PBS, alle geautoclaveerde materialen en de voorraad schone bekerglazen, maatcilinders etc. die altijd klaarstond. En verder een speciaal bedankje voor **Stefan (vN)**, **Stefan (vdV)**, **Lineke**, **Lonneke**, **Pascal**, **Ramona**, **Judy**, **Josanne**, **Petra**, **Eefje**, **Bernadette**, **Nele**, **Jasmin**, **Samira**, **Sarah** en de mensen van het EDC waaronder **Ingeborg**, **Eva**, **Vincent** en **Vincent**.

Maria, **Loubna** en **Simone**, bedankt voor alle secretariële ondersteuning! **Martine**, bedankt voor al je hulp rondom het FLUNIVAC-project en leuk dat we samen naar de meeting in Brussel konden afgelopen juni. En ook **Anouk** en **Wim**, bedankt voor alle ondersteuning!

Tijdens de dagelijkse bezigheden als PhD student heb ik zeer veel profijt gehad van mijn twee master stages. **Linde**, ik kijk nog steeds met veel plezier op mijn stage terug en vond het heel leuk dat we vorig jaar bij jullie in Amerika langs konden komen! **Hidde**, bedankt voor de uitdagende en zeer leerzame periode op het Whitehead Institute.

Sumana, when things in the lab aren't going the way I want or expect to, I always have to think about what you told me about the Japanese chicken-gender-determining-schools. It always brings a smile to my face and is good motivation to keep going! It was great that you came to visit Rotterdam a couple of times over the last few years. I know, my visit to Hong Kong is long overdue!

BMW chickies **Franka**, **Tonja** en **Melanie**, we leerden samen pipetteren (en werden van de gang weggestuurd tijdens de incubatietijden van een western blot omdat we iets te enthousiast 'saboteur' aan het spelen waren ☺). Vanuit de studietijd dat we elkaar dagelijks zagen, zijn we allemaal wat meer onze eigen weg gegaan. Met onze volle agenda's is het niet altijd makkelijk elkaar regelmatig te zien, maar bijkletsen met jullie voelt altijd weer vertrouwd!

Voor de nodige ontspanning heb ik gelukkig een heel aantal mensen in mijn omgeving met wie ik vele intensieve, uitdagende, relaxte en inspirerende fietskilometers heb kunnen maken. **Hélène**, grappig om te merken dat we met een heel aantal zaken precies hetzelfde in elkaar zitten. Bedankt voor de vele gezamenlijke fietskilometers (al dan niet over kasseien) en alle tips/adviezen zowel qua fietsen als persoonlijk en over werk! **Monica,** ondanks dat we nu wat verder uit elkaar wonen en elkaar wat minder vaak zien, is het toch altijd als vanouds. Onze fietsvakantie in Frankrijk was echt genieten! **Sheila**, met jouw coaching, zowel met trainingsschema's als op persoonlijk vlak, heb je me geholpen om het laatste stukje uit een diep dal te klimmen en weer grip te krijgen op alle (vele) dagelijkse activiteiten. Nu maar opzoek naar een nieuwe serie om te kijken tijdens een SciFi-avondje of op afstand op de tacx! **Hedwich**, onze vakanties de afgelopen paar jaar waren altijd super relaxt. Gewoon lekker fietsen, eten, boekje lezen en natuurlijk niet vergeten om van het uitzicht te genieten (btw WOW!). Ik ben benieuwd wie het nieuwe Rotterdamse prinsesje wordt bij de competitie volgend jaar ☺. **Nelly**, het aanstekelijke enthousiasme waarmee je al 20 jaar zo ontzettend veel organiseert voor het vrouwenwielrennen is echt een inspiratie! De sfeer die je creëert zowel bij de trainingsgroep in Utrecht als bij de landelijke activiteiten is echt heel bijzonder en zorgt ervoor dat ik inmiddels al 10 jaar met heel veel plezier deelneem aan alle activiteiten. Ik kijk uit naar het jubileumjaar 2018! Alle dames van **vrouwenwielrennen Rotterdam**: bedankt voor jullie inzet en enthousiasme. Het organiseren en geven van de trainingen de afgelopen jaren gaf mij altijd een enorme energie boost!

Dit proefschrift wil ik graag afsluiten met een speciaal bedankje voor mijn familie. **Opa Hessel**, bedankt dat u altijd zo meeleeft en altijd interesse heeft voor waar ik mee bezig ben.

Lieve **Nynke**, ik ben echt super trots op jou! Het is op dit moment misschien niet altijd even makkelijk, en daar kan ik me maar al te goed in inleven, maar je toont zo ontzettend veel doorzettingsvermogen! Ik vind het echt heel fijn dat we de laatste tijd weer wat meer contact hebben en hoop dat we dit blijven houden. Superleuk dat we samen de cover van dit boekje hebben kunnen uitwerken!

Lieve **Wiggert**, ik ben benieuwd of ik over vier jaar het dankwoord in jouw proefschrift zit te lezen. Het is nu misschien spannend, maar samen met **Jaimy** vogel je die nieuwe stap wel uit. Welke richting je ook op gaat, ik vind het superleuk dat we eenzelfde studieachtergrond en Boston-ervaring hebben. Keep in mind: ‘Don’t panic and bring a towel’!

Lieve **papa** en **mama**, zonder jullie was ik nooit zo ver gekomen. Mijn schoolcarrière is niet altijd heel makkelijk geweest en ik ben jullie zo ontzettend dankbaar voor alle kansen die jullie voor me gecreëerd hebben. In alles wat ik doe ondersteunen en stimuleren jullie mijn ambities, groot of klein, maar zonder me te pushen. Jullie staan dag en nacht voor me klaar, en dat heb ik een heel aantal keer erg nodig gehad. Dank jullie wel voor alles. Ik hou van jullie.